A study of the role of microRNAs in gastric cancer: the effect of miR-140-5p dysregulation in the expression of MDM2 in p53-dependent gastric cancer subtypes

By

Meng Xie

Cardiff China Medical Research Collaborative

School of Medicine, Cardiff University

Cardiff

May 2019

Thesis submitted to Cardiff University for the degree of Doctor of Medicine

Word Count: 48226

Thesis Summary

Gastric cancer is one of the leading causes of cancer-related death worldwide. Since advanced gastric carcinoma often demonstrates marked architectural and cytological heterogeneity, chemotherapy or targeted agents are seldom effective across all gastric cancer patients. Therefore, there is an urgent need to develop effective biomarkers for identifying patients with highly invasive disease and plan individual treatment decisions for each gastric cancer patient.

In this study, *in Silico* data analysis from TCGA was employed to discover miRNAs which had value in predicting patients' outcome. Among them, miR-140-5p and -3p were chosen to confirm their expression pattern in two independent cohorts with and without neoadjuvant chemotherapy.

miR-140-5p, rather than miR-140-3p, was the dominant miRNA in both gastric tumours and adjacent normal tissues. Reduced expression of miR-140-5p and -3p were found in most gastric tumours compared to matched normal tissues without chemotherapy through online data analysis and qPCR detection. Intestinal-type gastric cancer patients with lower expression of miR-140-5p suffered worse survival. Gastric cancer patients treated with 5-fluorouracil (5FU) based neoadjuvant treatment, both in online data and in independent cohort examination, showed increased expression of miR-140-5p and -3p. Patients without upregulation of neither miR-140-5p nor -3p exhibited the worst survival.

In this study, we explored a new potential target of miR-140-5p, mouse double minute 2 homolog (*MDM2*), which is the principle p53 antagonist in unstressed cells. We also provide evidence, via several functional assays, that enforced miR-140-5p expression inhibits malignant phenotypic characteristics, such as growth, spreading and attachment of gastric cancer cells lines with wild-type p53. However enforced miR-140-5p expression increased the 5FU resistance in these cells, probably due to upregulated p21 and a relatively low proliferation rate. miR-140-5p expression may reflect the activity of p53-dependent apoptosis when tumour cells are treated with 5FU. In this condition, elevated miR-140-5p correlated with higher BAX expression and indicated a highly activated cell apoptosis signaling. The results presented in this study collectively suggest that miR-140-5p and miR-140-3p are involved in controlling the behavior of gastric cancer cells, but their subtype-

specific expression pattern may reflect distinct cell conditions or responses. Several molecular signaling pathways regulated by miR-140-5p or miR-140-3p that may be responsible for these changes. This study found that the expression of miR-140-5p, in particular, could be used as a biomarker for identification of gastric cancer patients with higher malignant potential and for selection of gastric cancer patients who can benefit from the 5FU based treatment, and also may be used for monitoring patients' chemotherapy response.

Contents

List of Figures

List of Tables

Acknowledgments

I am very grateful for the research scholarships from the Doctoral program of Cardiff University and China Scholarships Council (No.201608060223). I would like to thank the many people who contributed to the development and completion of this dissertation. My supervisor, Dr. Alwyn Dart, who always gave me constant support and guidance. I would also like to thank my panel members: Dr. Rachel Hargest who is one of the most well-organized professors I have had; Dr. Yuxin Cui who brings clarity to even the most complex topics, as well as being a most engaging presenter; Dr. You Zhou, who guided my early bioinformatics analysis; and my friend, Dr. Jun Cai, with whom I shared many enjoyable, thought-provoking lunches. Thank you all for your patient observations, suggestions, counsel and, yes, criticisms regarding my often-incoherent ideas. Thanks to Professors Wen Guo Jiang and Jiafu Ji without whom I could not have the chance to study at Cardiff University.

Individual thanks to current and past CCMRC members, each for his/her unique contributions: Malamati, for her encouragement and for putting up with my anxiety; Fiona, the lab mom; Juliet and Hayley for conversations about anything at all; Drs Lin Ye and Sioned Owen for early discussions on the scientific method and reductionism; Dr. Andrew Sanders, a fellow computer expert, Cathy for her indefatigable cheeriness and Channing, the most easy-going guy on the planet; and Dr Tracey Martin, who always makes wonderful and delicious cake. I thank you all for your camaraderie.

Finally, a lifetime of thanks to my family who have been the most supportive and proudest family that I could have ever asked.

To Peng

the best thing that ever happened to me,

whose love, patience and unwavering support

has made every life challenge possible

Publications and presentations arising from this Thesis

Meng Xie, Rachel Hargest, Jiafu Ji, Wenguo Jiang and Alwyn Dart (2018). Relationship of miR-140-5p expression and p53 function and contribution to prognosis prediction and treatment decision of patients with gastric cancer. *Journal of Clinical Oncology* (published conference abstract).

Meng Xie, Alwyn Dart Rachel Hargest, Jiafu Ji and Wenguo Jiang. MicroRNA Signature as a Potential Biomarker for the Identification of Gastric Cancer Progression (submitted conference abstract for International Gastric Cancer Conference 2017).

Glossary of Abbreviations

5'DFUR	5'-deoxy-5-fluorouridine
5FU	5-fluorouracil
ACRG	the Asian Cancer Research Group
AGO	argonaute proteins
AJCC	American Joint Committee on Cancers
AMAG	autoimmune atrophic gastritis
APC	adenomatous polyposis coli
ATM	ataxia telangiectasia mutated
ATR	ataxia telangiectasia-mutated and RAD3-like protein
AUC	area under the ROC curves
BCL-2	B cell leukaemia/lymphoma 2
BAX	BCL2 associated X apoptosis regulator
bp	base pair
BSS	borate buffered saline
CA72-4	carbohydrate antigen 72-4
CCND1	cyclin D1
CDH1	epithelial cadherin
CH2THF	5,10-methylenetetrahydrofolate
CHK1	checkpoint kinase 1
CHK2	cell cycle checkpoint kinase 2
CI	confidence interval
CIMP	extreme high CpG island methylator phenotype
CIN	chromosomal instability
COX-2	cyclooxygenase 2
CSC	cancer stem-like cells
CT	computerized tomography
CTNNA1	α-catenin
CVID	common variable immunodeficiency
DEM	differentially expressed miRNAs
DEPC	diethyl pyrocarbonate
DFS	disease-free survival
DHFU	Dihydrofluorouracil
DMEM	Dulbecco's Modified Eagles' Medium
DMSO	dimethyl sulfoxide
dNTPs	deoxynucleotide triphosphates
DPD	dihydropyrimidine dehydrogenase
dTMP	deoxythymidine monophosphate
DSB	double-strand break
DSS	disease-specific survival
EBV	Epstein–Barr virus

ECM	extracellular matrix
EGF	epidermal growth factor
EGJ	esophagogastric junction
EMAG	environmental metaplastic atrophic gastritis
EMT	epithelial-to-mesenchymal
ES	embryonic stem cells
FAP	familial adenomatous polyposis
FAS	Fas cell surface death receptor
FBS	foetal bovine serum
FGF9	fibroblast growth factor 9
FIGC	familial intestinal gastric cancer
Gadd45	growth arrest and DNA damage-inducible 45
GAPDH	glyceraldehyde 3-phosphate dehydrogenase
GERD	gastroesophageal reflux disease
glm	generalized linear model
GOF	gain of function
GS	genome stable tumours
H. pylori	*Helicobacter pylori*
HDGC	hereditary diffuse gastric cancer
HER2	human epidermal growth factor receptor 2
HNPCC	hereditary non-polyposis colorectal cancer
HR	hazard ratio
IL	interleukin
IM	intestinal metaplasia
IR	ionizing radiation
JNK	Jun-N-terminal Kinase
kb	kilo base pairs
LFS	Li-Fraumeni syndrome
lm	linear model
lncRNAs	long noncoding RNAs
LS	Lynch Syndrome
MAGIC	MRC Adjuvant Gastric Infusional Chemotherapy
MALT	mucosa-associated lymphoid tissue
MDM2	mouse double minute 2
miRNAs	microRNAs
MMP	matrix metalloproteinase
mRNA	messenger RNA
MSI	microsatellite unstable tumours
MSS	microsatellite stable
MTT	3-(4,5-dimethylthiazol-2-yl)-2,5-diphenyl tetrazolium bromide
NACT	Neoadjuvant chemotherapy
NF-κb	nuclear factor-kappa B

NSAID	non-steroidal anti-inflammatory drugs
NSCLC	non-small cell lung cancer
nt	nucleotide
NT	Solid Tissue Normal
ORR	overall response rate
OS	overall survival
PBS	phosphate Buffered Saline
PD-1/L1	programmed cell death 1/ ligand 1
PDX	patient-derived tumour xenografts
PET	positron emission tomography
PFS	progression-free survival
PI3K	phosphoinositide-3-kinas
PJS	Peutz-Jeghers syndrome
PP2A	phosphatase 2A
qPCR	real-time quantitative PCR
RHOA	ras homolog family member A
RISC	RNA-induced silencing complex
RNAPII	RNA polymerase II
ROC	receiver operating characteristic
ROS	reactive oxygen species
rRNA	ribosomal RNA
Runx1t1	runt-related transcription factor 1
SD	standard deviations
SEM	standard error
STAD	Stomach adenocarcinoma
TAK1	TGF-β activated kinase
TCGA	The Cancer Genome Atlas
TGF-β	transforming growth factor beta
TKIs	tyrosine kinase inhibitors
TLRs	toll like receptors
TNM	tumour, node, metastases
TP	Primary Solid Tumor
TP53INP1	tumour protein p53-induced nuclear protein 1
tRNA	transfer RNA
TS	thymidylate synthase
Tween 20	polyoxymethylene (20) sorbitan monolaurate
UTR	untranslated region
VEGFR2	vascular endothelial growth factor receptor-2
WHO	World Health Organization

Chapter 1.

General Introduction

1.1 Gastric cancer

Gastric cancer is the fifth most common cancer worldwide and the third main cause of cancer-related death, accounting for 6.8% of new cancer cases and 13.7% of the total cancer deaths worldwide (Global cancer statistics from the World Health Organization (WHO) in 2012 (Ferlay et al. 2015). Whilst gastric cancer incidence and mortality decreased substantially over the last decades in most countries worldwide, there are differences in the trends and distribution in different areas (Ferro et al. 2014). As the early symptoms of gastric cancer are similar to those of many other conditions, such as gastritis, gastric polyps or gastrointestinal ulcers *et al.*, early detection of gastric cancer mostly depends on opportunistic screening. Nearly half of patients diagnosed with stages T2-T4a (T category defined in the 7th American Joint Committee on Cancers (AJCC) TNM staging system as follows: T1a = mucosa, T1b = submucosa, T2 = muscolaris propria, T3 = subserosa, T4a = perforates the serosa, T4b = infiltration of adjacent structures (Marchet et al. 2011)) develop metastatic disease within two years. Clinical outcomes are poor in metastatic disease, with median survival being around 1 year. For gastric cancer patients diagnosed at a surgically resectable stage, early radical gastrectomy with draining lymph node dissection remains the cornerstone of therapy of muscle-invasive disease. However, cancer-specific survival in patients with extra-gastric extension or lymph node metastases after gastrectomy is relatively only around 25-48% (De Angelis et al. 2014; Ferro et al. 2014; Van Cutsem et al. 2016). In the United Kingdom over the last decade, gastric cancer incidence rates have decreased by more than a quarter while six in ten (4457/6740) gastric cancer patients die from this disease each year (Cancer Research UK 2016a). Approximately half of the world's gastric cancer cases and deaths occur in China, roughly 1364 deaths per day (Zong et al. 2016).

Current treatment options for gastric cancer include surgical intervention, chemotherapy, and radiation therapy or a combination of these options. Surgery for gastric cancer although technically challenging, is still considered the only curative treatment currently. Optimal results are more likely to be achieved with the input of teams of experts from different disciplines through careful tumour staging which is crucial to ensure that appropriate interventions are selected (Coburn et al. 2018). Besides stage-based treatment determination, increased attention has been paid to the molecular classification of gastric cancer. Several histopathological characteristics have a significant prognostic impact on recurrence and

survival rates in gastric cancer and have shown great potential for improvement. Conventional chemotherapy has been successful to some extent; the main drawbacks of chemotherapy are its poor bioavailability, high-dose requirements, adverse side effects, low therapeutic indices, development of multiple drug resistance, and non-specific targeting. Targeted therapies, such as trastuzumab, an antibody against human epidermal growth factor receptor 2 (HER2, also known as ERBB2), the vascular endothelial growth factor receptor-2 (VEGFR-2) antibody ramucirumab, and programmed cell death 1 (PD-1)/ programmed cell death ligand-1(PD-L1) antibody, also show promise. However, the remaining challenge is to find sufficient molecular markers for therapy selection and monitoring.

1.1.1 Epidemiology

According to incidence estimated in the GLOBOCAN 2012 (Torre et al. 2015; Ferlay J 2013), approximately 950 000 new cases are diagnosed annually, of whom 720 000 are expected to die (Ferlay et al. 2015). In 2015 (Fitzmaurice et al. 2017), there were 1.3 million (1.2-1.4 million) incident cases of gastric cancer and 819 000 (95% uncertainty interval, UI: 795 000-844 000) deaths worldwide (Figure 1.1).

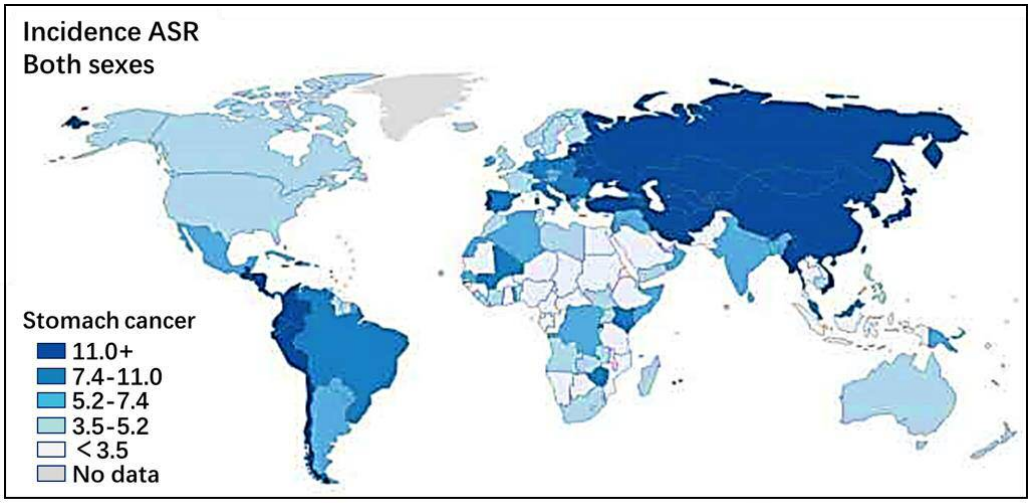

Figure 1.1: Estimated age-standardized incidence rates of gastric cancer (ASR-World) in both sexes per 100,000, IARC GLOBOCAN 2012. Adapted from GLOBOCAN 2012. (Ferlay J 2013; Torre et al. 2015) The highest rates occur in Eastern Asia, South America, and Eastern Europe.

Despite the decline rate, the absolute number of new cases per year is increasing, mainly due to aging in the world population. More than half of gastric cancer patients are over 60 years old and the median age at diagnosis is 70 years (Karimi et al. 2014). Furthermore, the trend toward declining incidence in young patients (younger than 50 years) has halted and replaced

by an upward trend in recent years (Correa 2011; Sonnenberg 2011). Gender, as well as age, plays a crucial role in the incidence of gastric cancer. Age-standardized incidence rates are about twice as high in men as in women, ranging from 3.3 in Western Africa to 35.4 in Eastern Asia for men, and from 2.6 in Western Africa to 13.8 in Eastern Asia for women (Figure 1.2).

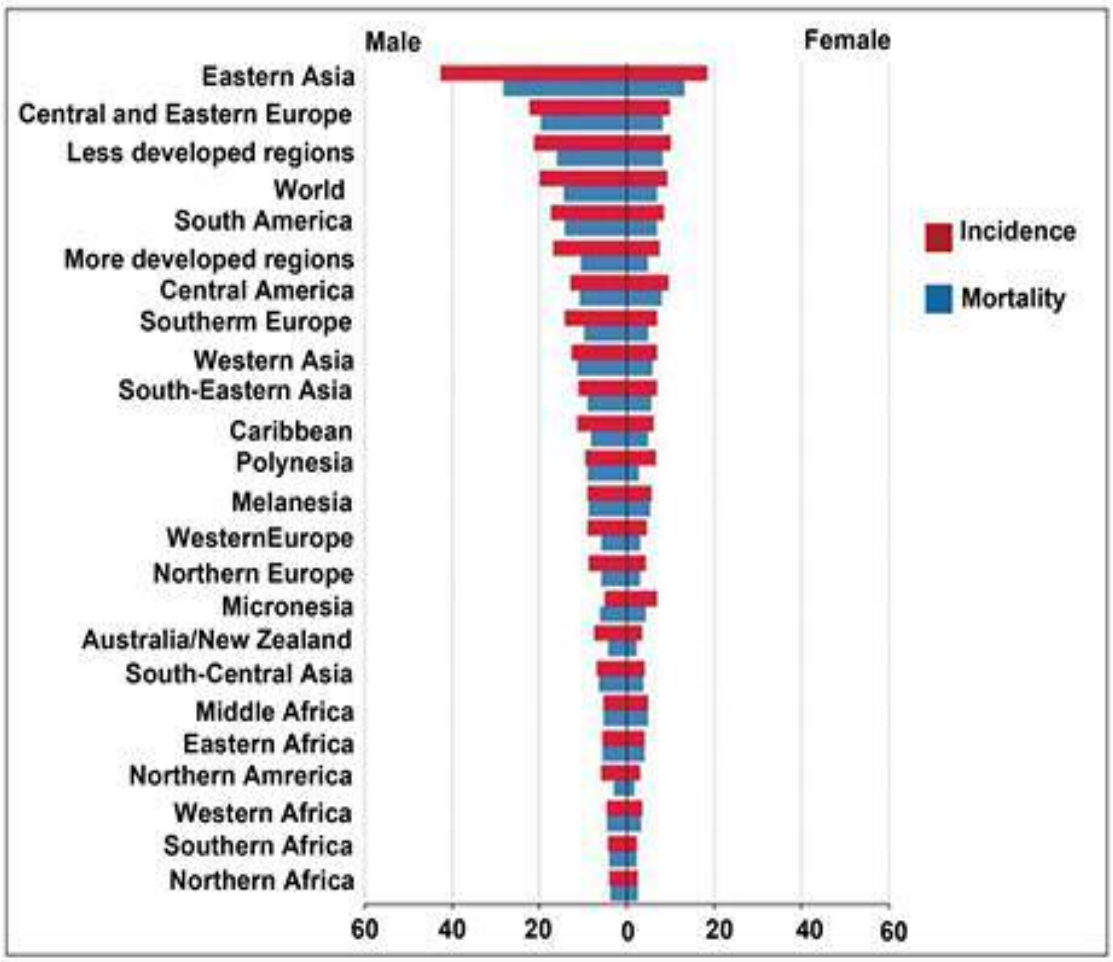

Figure 1.2: Cancer age-standardized incidence and mortality rates of gastric cancer per 100,000 for in both sexes, GLOBOCAN 2012 estimates. Adapted from GLOBOCAN 2012(Torre et al. 2015; Ferlay J 2013).

Among males, incidence rates (cases/100,000) in Japan (Miyagi Prefecture, 66.7) and Korea (64.6) are twice as high as the next highest rates in Iran (Golestan Province, 30.4). Among females, incidence rates in Japan and Korea are 60% higher than the next highest rates in Ecuador and Costa Rica. It was estimated that 1 in 27 men and 1 in 68 women develop gastric cancer before age 79 years (Fitzmaurice et al. 2017). Moreover, globally, gastric cancer incidence shows remarkable international variation and distinct characteristics by two major

topographical subsites, true gastric adenocarcinomas (non-cardia gastric cancers), of which there were 691 000 new cases in 2012, and gastro-oesophageal-junction adenocarcinomas (cardia gastric cancers), of which there were 260 000 new cases in that year(Colquhoun et al. 2015). As a result, the proportion of tumours located in the proximal two-thirds of the stomach now accounts for more than 40 percent of gastric in some reports (Borch et al. 2000).

In Japan, the downward trend was particularly evident in young patients with non-cardia, sporadic, intestinal type of gastric cancer (Kaneko and Yoshimura 2001; Bertuccio et al. 2009). In China, the decline was less dramatic than other countries. Despite an overall decrease in gastric cancer incidence, an increase of non-cardia gastric cancer has been observed in the oldest and the youngest groups, and a less remarkable decline has been observed among women than in men (Jemal et al. 2006; J. Zhang et al. 2018). In the United States, the incidence rate for non-cardia gastric cancer declined among all race and age groups. People aged 65-74 are most frequently diagnosed, and the average age at diagnosis is 69 (National Cancer Institute 2018). About 6/10 patients diagnosed with gastric cancer each year are 65 or older. However, in younger and middle-aged Caucasians (25 to 39 years) the incidence rate for non-cardia gastric cancer significantly increased between 1977 and 2007 (Camargo et al. 2011; Colquhoun et al. 2015; Anderson et al. 2010). Figure 1.3 depicts the global incidence rates of gastric cancer varied by gender; in particular, for cardiac gastric cancer, rates in men were three times the rates in women (Colquhoun et al. 2015).

Histologically, gastric cancer was classified into intestinal and diffuse types by Laurén (Lauren 1965). These two biological entities are different with regard to epidemiology, aetiology, pathogenesis, and behavior (see Chapter 1.15). The intestinal type is more common in males, 2:1 ratio worldwide. Diffuse-type cancers are equally distributed between males and females (Jemal et al. 2011). There has been a worldwide decline in the incidence of the intestinal type in recent decades, which parallels the overall decline in the incidence of gastric cancer. By contrast, the decline in the diffuse type has been more gradual. Hence, the decrease in the intestinal type cancers may partly contribute to the shift from intestinal to diffuse type of gastric cancers (Borch et al. 2000; Kampschoer et al. 1989; Sidoni et al. 1989).

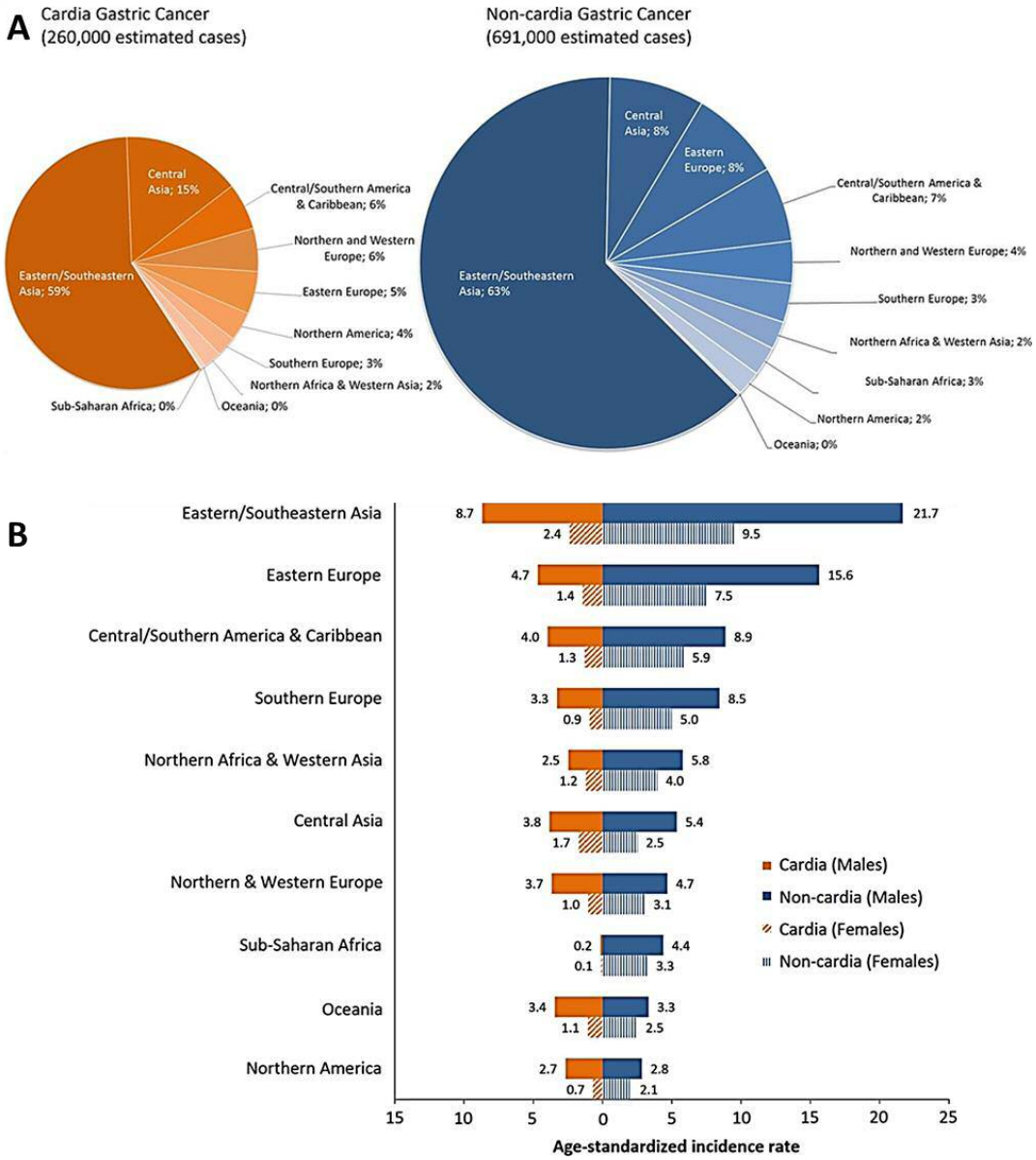

Figure 1.3: Global incidence estimates of cardia and non-cardia gastric cancer by region (A) and Estimated cardia and non-cardia gastric cancer age-standardized incidence rates (per 100 000) by region and sex (B). Source: Global patterns of cardia and non-cardia gastric cancer incidence in 2012 (Colquhoun et al. 2015).

Country	Tracheal, bronchus, and lung cancer	Colon and rectum cancer	Stomach cancer	Liver cancer	Breast cancer	Esophageal cancer	Pancreatic cancer	Prostate cancer	Leukemia	Cervical cancer	Non-Hodgkin lymphoma	Brain and nervous system cancer	Bladder cancer	Ovarian cancer	Acute myeloid leukemia	Lip and oral cavity cancer	Gallbladder and biliary tract cancer	Kidney cancer	Acute lymphoid leukemia	Larynx cancer	Multiple myeloma	Uterine cancer	Other pharynx cancer	Nasopharynx cancer	Chronic lymphoid leukemia	Malignant skin melanoma	Chronic myeloid leukemia	Mesothelioma	Thyroid cancer	Hodgkin lymphoma	Testicular cancer
Global	1	2	3	4	5	6	7	8	9	10	11	12	13	14	15	16	17	18	19	20	21	22	23	24	25	26	27	28	29	30	31
High SDI	1	2	3	6	4	10	5	7	8	18	9	14	11	13	15	20	16	12	26	23	17	21	24	29	22	19	27	25	28	30	31
High-middle SDI	1	4	3	2	6	5	7	8	9	11	12	10	13	15	16	18	14	19	17	20	21	22	24	23	25	26	27	29	28	30	31
Middle SDI	1	4	3	2	6	5	8	10	7	9	12	11	15	17	16	14	19	22	13	20	23	21	24	18	25	28	27	30	26	29	31
Low-middle SDI	1	5	2	4	3	6	11	10	8	7	12	13	15	16	18	9	20	23	17	14	22	19	21	24	26	29	25	31	28	27	30
Low SDI	7	6	3	1	5	4	10	8	9	2	11	12	13	14	17	18	19	21	16	22	20	15	23	25	26	27	24	31	29	28	30
South Asia	1	3	5	8	2	4	10	13	7	9	11	14	15	16	17	6	20	24	19	12	21	22	18	23	27	29	25	31	28	26	30
India	1	4	2	8	5	3	10	11	7	6	13	14	16	15	17	9	20	24	19	12	21	23	18	22	27	29	25	31	28	26	30
Pakistan	2	4	9	6	1	3	14	15	8	19	7	10	12	16	20	5	23	22	18	11	17	13	21	24	28	30	25	31	29	27	26
Bangladesh	1	2	5	9	4	7	10	12	6	8	13	11	17	18	15	3	21	26	16	14	23	22	19	20	27	30	24	31	28	25	29
Nepal	1	6	2	7	3	8	9	13	5	4	12	11	18	16	15	14	20	27	17	10	23	21	19	22	26	29	24	31	28	25	30
East Asia	1	5	3	2	7	4	6	10	8	12	11	9	15	20	18	17	16	21	13	19	23	22	27	14	24	26	30	28	25	29	31
China	1	5	3	2	7	4	6	10	8	12	11	9	15	20	18	17	16	21	13	19	23	22	28	14	24	26	30	27	25	29	31
Southeast Asia	1	3	5	2	4	11	8	10	6	7	12	14	18	13	17	15	16	20	9	22	25	21	23	19	30	29	26	28	24	27	31
Indonesia	5	6	3	2	1	12	8	9	4	7	11	14	16	13	15	22	18	20	10	21	24	19	23	17	30	28	26	29	25	27	31
Philippines	1	3	8	4	2	20	10	6	5	7	13	12	22	14	11	15	24	19	9	21	25	17	26	16	29	27	23	28	18	30	31
Vietnam	1	3	4	2	5	6	7	12	8	11	9	16	17	13	20	10	19	22	15	21	24	23	14	18	31	29	27	28	25	26	30
Thailand	2	3	7	1	5	13	10	12	4	9	18	14	16	17	21	11	8	15	6	19	25	24	22	20	30	29	28	26	23	27	31
Myanmar	1	3	4	6	2	16	8	13	7	5	12	14	18	10	19	11	17	22	9	21	25	15	23	20	28	29	26	30	24	27	31
Malaysia	1	2	6	4	3	14	9	11	5	12	8	16	17	13	18	15	23	19	7	21	20	24	25	10	29	27	26	30	22	28	31
North Africa and Middle East	1	4	2	6	3	13	9	8	5	15	12	7	11	17	10	24	16	19	14	18	21	20	30	25	22	29	23	28	27	26	31
Egypt	2	6	8	1	4	15	10	12	3	19	13	5	7	16	11	22	21	18	9	17	24	20	27	29	14	28	23	25	26	30	31
Iran	2	5	1	9	7	4	11	8	3	20	16	6	14	19	10	22	15	18	13	12	23	26	29	27	21	24	17	30	28	25	31
Turkey	1	2	3	9	6	18	5	7	4	22	11	8	12	13	10	25	19	16	17	15	14	20	31	26	21	24	27	23	28	29	30
Sudan	2	6	1	4	3	13	10	8	5	14	9	7	15	17	11	22	16	21	12	19	23	18	28	27	24	30	20	29	26	25	31
Algeria	1	2	5	9	3	20	6	8	4	10	12	7	14	18	13	25	11	21	15	19	17	22	28	16	23	30	24	29	27	26	31
Iraq	1	7	8	5	2	17	9	13	3	18	12	4	11	15	6	20	23	14	10	22	24	16	26	27	21	28	19	29	25	30	31
Morocco	1	4	3	7	2	17	9	5	6	10	12	8	11	16	14	23	15	22	18	19	20	13	26	24	21	30	25	27	29	28	31
Afghanistan	3	5	1	4	2	9	15	11	6	7	10	8	14	20	17	24	12	23	16	18	25	13	28	27	22	30	21	29	26	19	31
Saudi Arabia	2	1	7	3	4	12	8	10	5	21	9	6	15	16	11	22	18	13	14	20	17	24	27	23	25	29	19	30	26	28	31
Yemen	1	6	2	4	3	13	9	11	5	10	8	7	15	18	14	24	16	22	12	19	25	17	27	28	23	30	20	29	26	21	31
Western Europe	1	2	6	8	3	11	5	4	7	21	10	13	9	12	15	20	17	14	27	24	16	23	25	29	18	19	26	22	28	30	31
Germany	1	2	6	8	3	14	4	5	7	22	10	13	9	12	15	20	16	11	28	25	17	23	21	29	18	19	26	24	27	30	31
France	1	2	8	6	3	10	4	5	7	22	11	15	9	12	16	19	18	14	27	23	13	24	20	28	17	21	26	25	29	30	31
United Kingdom	1	2	8	12	3	6	5	4	7	23	10	13	9	11	14	22	20	15	28	26	16	21	25	27	19	18	24	17	29	30	31
Italy	1	2	4	6	3	18	5	7	8	23	10	12	9	14	15	19	13	11	27	21	16	24	26	29	17	20	25	22	28	30	31
England	1	2	8	12	3	6	5	4	7	23	10	13	9	11	14	22	20	15	28	25	17	21	26	27	19	18	24	16	29	30	31
Spain	1	2	5	8	3	15	6	4	9	23	10	11	7	12	13	19	17	14	27	20	16	21	24	28	18	22	25	26	29	30	31
Western Sub-Saharan Africa	4	7	2	1	6	11	9	5	8	3	10	12	13	18	14	21	17	15	16	22	20	19	23	30	27	26	24	31	29	25	28
Nigeria	3	6	2	1	7	11	9	5	8	4	10	12	16	19	14	21	17	13	15	22	18	20	23	28	27	25	24	31	29	26	30
Ghana	8	10	4	1	2	13	6	3	9	5	7	11	14	18	15	20	19	21	12	22	17	16	23	29	25	26	24	30	28	27	31
Eastern Sub-Saharan Africa	8	4	6	2	5	3	11	7	9	1	10	13	14	12	18	17	22	21	16	20	19	15	24	23	28	25	27	30	26	31	29
Ethiopia	8	3	6	2	5	4	11	7	9	1	10	13	16	12	18	14	20	22	17	21	19	15	24	23	27	26	28	30	25	31	29
Tanzania	8	3	7	2	5	4	11	6	9	1	10	13	14	12	16	19	22	20	15	21	18	17	24	23	28	25	27	29	26	31	30
Kenya	11	4	2	3	5	7	9	6	8	1	13	12	20	10	16	18	21	23	17	14	15	19	24	22	25	28	26	30	27	31	29
Uganda	6	2	8	4	9	1	12	3	10	5	7	13	17	11	19	20	23	18	16	22	15	14	24	21	28	25	27	30	26	31	29
Mozambique	7	5	4	1	6	3	12	9	8	2	10	11	15	14	16	17	22	21	13	20	19	18	23	28	25	26	24	29	27	30	31
High-income North America	1	2	9	8	3	10	4	5	6	20	7	13	11	14	12	21	22	15	26	23	16	19	25	30	18	17	27	24	28	29	31
United States	1	2	14	8	3	9	4	5	6	20	7	12	11	13	10	21	23	15	26	22	16	19	25	30	18	17	27	24	28	29	31
Canada	1	2	6	12	3	10	5	4	8	20	7	11	9	13	15	21	17	14	27	24	16	23	25	29	18	19	26	22	28	30	31
Central Latin America	1	3	2	6	5	17	9	4	7	8	10	12	18	13	16	22	14	15	11	20	19	21	28	30	26	23	25	31	24	27	29
Mexico	1	4	2	6	5	18	9	3	7	8	10	13	17	14	16	21	15	12	11	20	19	22	30	31	27	24	26	29	23	25	28
Colombia	2	3	1	7	4	15	9	5	6	8	10	11	17	14	16	21	13	19	12	20	18	22	28	29	26	23	24	30	25	27	31
Venezuela	1	4	3	9	5	17	8	2	7	6	10	11	18	12	16	22	19	13	14	15	20	21	27	29	26	24	23	31	28	25	30
Eastern Europe	1	2	3	8	4	13	5	6	9	14	18	12	11	7	20	15	22	10	25	17	23	16	21	30	24	19	26	28	27	29	31
Russia	1	2	3	7	4	12	5	6	10	14	18	11	13	9	21	16	22	8	25	17	23	15	20	30	24	19	28	29	26	27	31
Ukraine	1	2	3	14	4	16	5	6	8	10	19	11	9	7	17	15	21	12	26	13	24	22	20	27	31	18	25	23	28	29	30
Tropical Latin America	1	2	3	8	5	7	6	4	10	9	12	11	15	18	17	13	14	19	23	16	21	22	20	30	25	24	26	29	27	28	31
Brazil	1	3	2	8	5	7	6	4	10	9	12	11	15	18	17	13	14	19	23	16	21	22	20	30	25	24	26	29	27	28	31
High-income Asia Pacific	1	3	2	4	7	8	5	10	11	17	9	19	12	15	13	18	6	14	22	25	16	20	21	26	29	27	28	24	23	30	31
Japan	1	3	2	4	7	8	5	10	11	18	9	20	12	15	13	17	6	14	23	25	16	19	21	26	29	27	28	24	22	30	31
South Korea	1	4	3	2	7	10	5	11	8	15	9	13	12	16	17	20	6	14	19	21	18	24	23	26	28	25	27	29	22	30	31
Central Europe	1	2	4	7	3	16	5	6	8	13	15	9	10	12	19	17	14	11	25	18	23	22	20	29	24	21	26	30	27	28	31
Poland	1	2	4	14	3	15	5	6	8	13	16	9	7	11	19	18	12	10	25	17	21	23	24	30	22	20	26	29	27	28	31
Central Sub-Saharan Africa	5	7	3	1	4	6	9	10	8	2	11	12	14	13	16	18	19	21	15	22	20	17	23	26	24	27	25	30	29	28	31
Democratic Republic of the Congo	5	7	3	1	4	6	10	9	8	2	11	12	15	13	16	18	19	21	14	22	20	17	23	26	24	28	25	30	29	27	31
Central Asia	1	5	2	3	4	6	8	11	7	10	16	9	14	12	13	18	20	17	19	15	24	21	22	28	25	23	26	30	29	27	31
Uzbekistan	2	5	1	7	4	3	10	14	6	9	13	8	18	20	11	16	17	19	15	12	22	21	23	28	27	24	25	31	30	26	29
Southern Sub-Saharan Africa	1	5	9	7	4	3	8	6	10	2	13	15	11	12	16	14	22	21	17	19	18	20	26	27	24	23	28	25	29	30	31
South Africa	1	6	9	7	4	3	8	5	10	2	13	18	14	11	15	12	22	21	17	19	16	20	26	27	25	23	28	24	29	30	31
Southern Latin America	1	2	3	11	4	9	6	5	10	8	13	16	14	15	17	21	7	12	23	20	18	19	27	31	24	22	25	29	26	30	28
Argentina	1	2	4	12	3	10	6	5	9	7	13	16	14	15	17	21	8	11	23	18	20	19	28	31	24	22	25	27	26	29	30
Andean Latin America	2	4	1	6	7	18	9	3	8	5	11	12	20	15	13	21	10	17	14	23	19	16	24	31	27	25	26	29	22	28	30
Peru	2	4	1	5	7	19	9	3	8	6	10	12	20	15	13	21	11	16	14	23	18	17	25	31	27	24	26	29	22	28	30
Caribbean	1	3	5	7	4	11	8	2	9	6	10	12	14	18	19	16	21	20	22	15	17	13	24	28	23	26	25	30	29	27	31
Australasia	1	2	8	12	4	10	5	3	6	22	7	11	13	16	15	21	19	14	25	26	17	23	24	27	20	9	28	18	29	30	31
Oceania	1	6	3	4	2	14	10	8	7	5	11	16	22	13	12	15	23	25	19	18	24	9	20	21	31	27	17	29	26	28	30

Figure 1.4: Cancers Ranked by Number of Deaths in Both Sexes, Global, by Region, by Sociodemographic Index (SDI), and in the 50 Most Populous Countries, 2015. The highest rates occur in Eastern Asia, South America, and Eastern Europe (Global Burden of Disease Cancer et al. 2017).

Mortality from gastric cancer has decreased in all countries over the last 50 years, for both men and women, although the rate of decline differs by region (Figure 1.4) (Amiri et al. 2011). The highest estimated mortality rates are in Eastern Asia (24 per 100,000 in men, 9.8 per 100,000 in women), the lowest in Northern America (2.8 and 1.5, respectively). High mortality rates are also present in both sexes in Central and Eastern Europe and in Central and South America (Figure 1.2). Despite the decline in mortality, the 5-year survival rate has improved only by 11% (Figure 1.5) and is still poor in most countries (Collaborators 2016; Danaei et al. 2005; Fontham 2009). Five-year survival rates are as high as 64.6 % in Japan and 74.5% in South Korea (Matsuda et al. 2011). Well-developed, government-sponsored screening programmes for gastric cancer by barium photofluorography or endoscopy are available in these countries (Jung et al. 2017). The 5-year survival rate is 27.4% in China (M. Li et al. 2017) and 20% in the United Kingdom (Cancer Research UK 2016b).

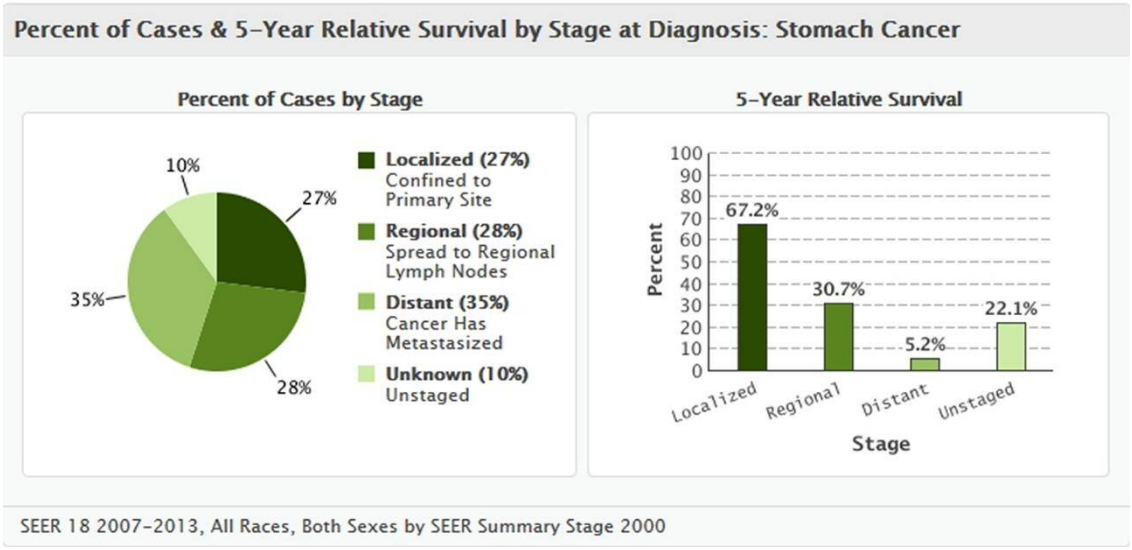

Figure 1.5: Five-year survival rate by gastric cancer stage at diagnosis. Source: Cancer of the Stomach. Surveillance Research Program, Cancer Control, and Population Sciences (National Cancer Institute 2017).

The comparisons of prognosis between women and men are controversial, and the difference is more likely to be tumour stage- and age-dependent (Matsuzaka et al. 2016; Maehara et al. 1992). Mortality rates for gastric cancer are highest in aged people (≥ 70 years) (Liang et al. 2013). For all stages of gastric cancer, the relative 5-year survival is around 20% (Table 1.1) (Cancer Research UK 2016b).

Table 1.1: The 5-year survival rates by stage for gastric cancer treated with surgery. Source: Stomach Cancer. Survival by stage (Cancer Research UK 2016b)

Stage[1]	5 year observed survival
Stage IA	80%
Stage IB	70%
Stage IIA	60%
Stage IIB	40%
Stage IIIA	25%
Stage IIIB	20%
Stage IIIC	10%
Stage IV	5%

[1] TNM classification according to the 6th AJCC staging system.

1.1.2 Risk factors and prevention

A person's risk of developing gastric cancer depends on multiple factors, including age, genetics, and exposure to risk factors (including some potentially avoidable lifestyle factors) (Figure 1.6). Gastric cancer represents a complex and heterogeneous disease. Studies of migrant populations point to the importance of environmental factors in the aetiology of this disease (McCredie et al. 1999).

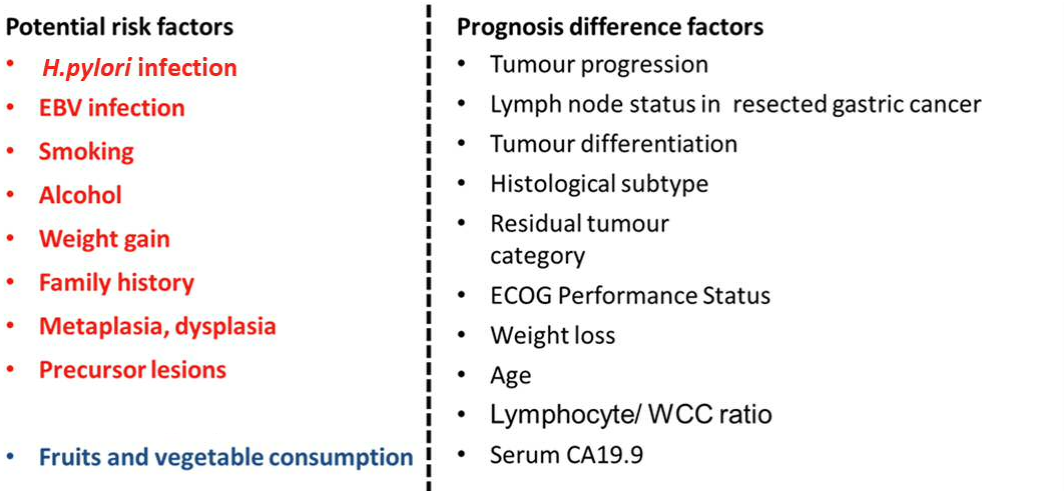

Figure 1.6.: Summary of risk factors and independent prognostic factors in clinical use.
ECOG: The Eastern Cooperative Oncology Group, the ECOG Scale of Performance Status is one such measurement. It describes a patient's level of functioning in terms of their ability to care for themselves, daily activity, and physical ability (walking, working, etc.). **WCC**: the white blood cell count. Factors highlighted in red font represent increased risk, factors highlighted in blue represent reduced risk.

Reactive oxygen species (ROS) is an essential factor in the pathogenesis of gastric cancer (Bhattacharyya et al. 2014). Low and moderate amounts of ROS have beneficial effects on

several physiological processes including killing of invading pathogens, wound healing, and tissue repair processes. Cancer treatment by chemotherapeutic agents and radiotherapy depend largely on ROS generation to destroy malignant cells by inducing apoptosis. However, disproportionate generation of ROS poses a serious problem to bodily homeostasis and causes oxidative tissue damage. Both environmental factors and specific genetic alterations are involved in the deregulation of ROS-mediated gastric cancer (Figure 1.7). It has been suggested that more than 90% of gastric cancer may be determined by environmental rather than genetic causes (Boland and Yurgelun 2017).

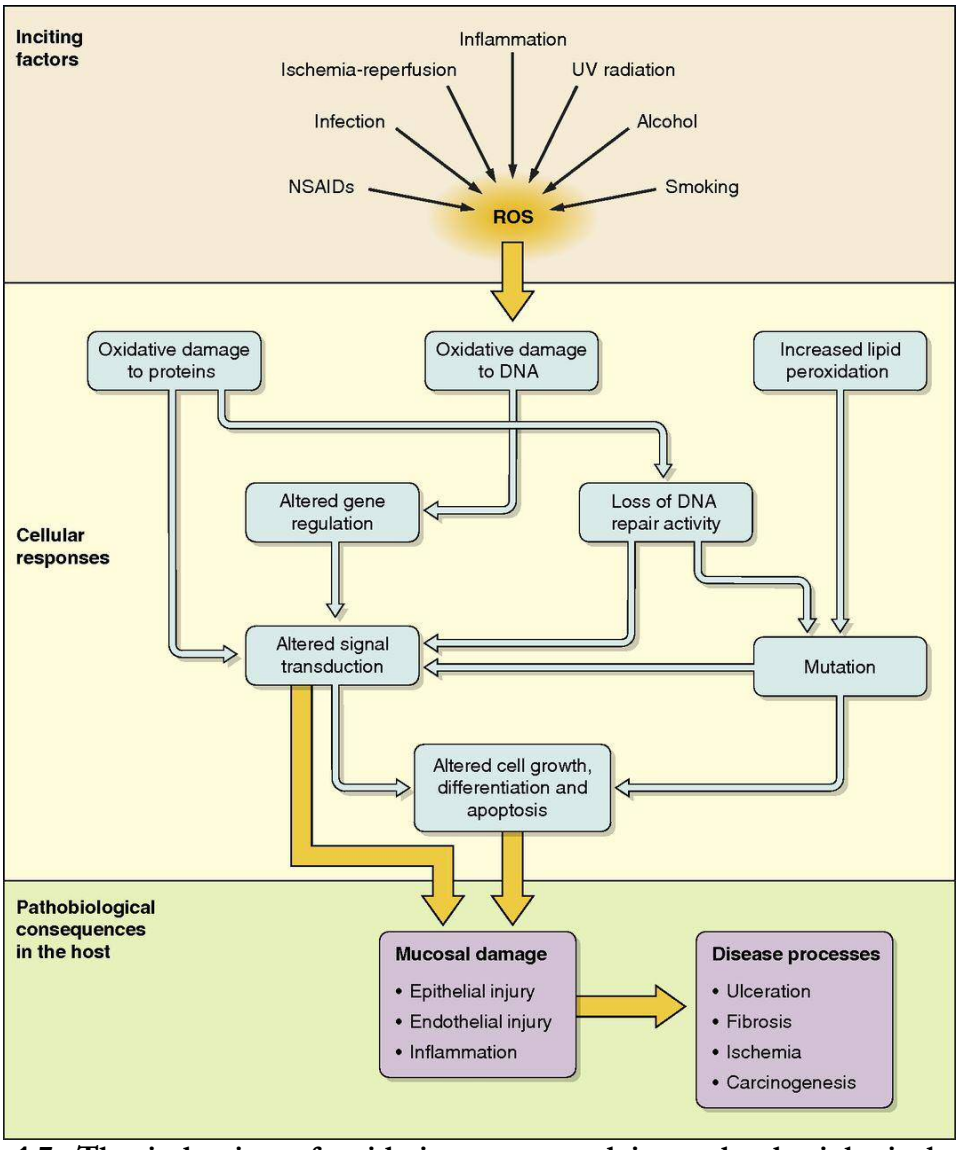

Figure 1.7: The induction of oxidative stress and its pathophysiological effects. Oxidative stress damages internal organs by causing mucosal injury (Bhattacharyya et al. 2014).

1.1.2.1 Infectious and non- infectious environmental risk factors

Helicobacter pylori (H. pylori) is the most important etiologic factor for gastric cancer and is established as a class I carcinogen by the International Agency for Research on gastric cancer in 1994 (International Agency for Research on Cancer. 1994a; Fock et al. 2009). The presence of geographic and familial clusters of gastric cancer presented a conundrum until the most common cause of this disease—chronic infection by *H. pylori*—was discovered by Marshall and Windsor (2005). It is estimated that 89% of non-cardia gastric cancers, which accounts for 78% of gastric cancer cases, are attributed to *H. pylori* infection (International Agency for Research on Cancer 1994b; De Martel et al. 2012). Non-cardia gastric cancer with a high serum anti-*H. pylori* IgG titre was significantly correlated with younger (median age, 55.0 years), a higher proportion of female (45.0%), non-smokers (58.9%) and diffuse-type gastric cancer (Gong et al. 2018). *H. pylori* infection, which infects approximately 50% of the world's population, is a major factor in both the induction of atrophic gastritis and histological progression to gastric cancer (Fox and Wang 2007). Despite the high infection rate, most infected subjects develop no clinical symptoms or peptic ulceration and continue their life with superficial chronic gastritis (Figure 1.8). Approximately 17% of infected subjects will develop peptic ulcers, and 1% will progress to gastric cancer (Salih 2009). A follow-up study of 1526 Japanese patients over a mean period of 7.8 years uncovered that gastric cancer developed in 2.9% of patients infected with *H pylori* but in none of the uninfected patients (Uemura et al. 2001; J. Kang et al. 2002).

H. pylori infection has been associated with an approximately six-fold increase in the risk of distal gastric adenocarcinomas compared to the cardic tumours, including both the intestinal and diffuse types. In terms of histology, *H. pylori* infection may be linked more closely with intestinal-type gastric cancer because it was found in nearly 90% of the noncancerous gastric mucosa in this setting, compared with less than one-third of the diffuse-type cancers (Parsonnet et al. 1991). A modest increase in fasting plasma glucose levels was found to be a risk factor for gastric cancer and that hyperglycaemia could be a possible cofactor increasing the risk posed by *H. pylori* infection (Yamagata et al. 2005).

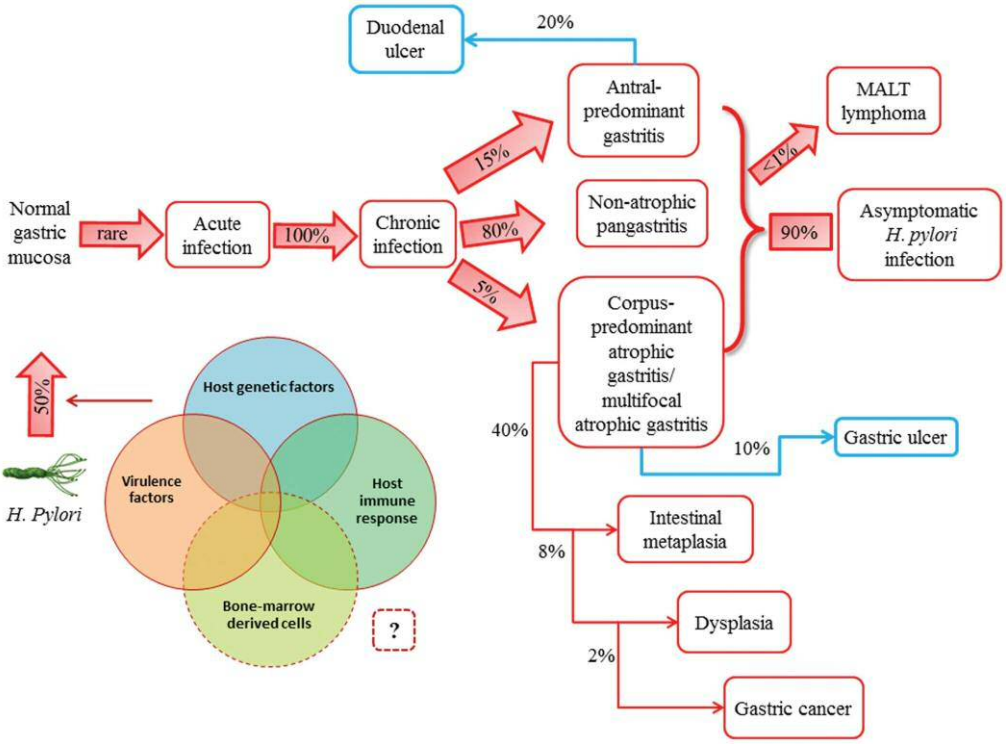

Figure 1.8: Natural history of *H. pylori* infection. The clinical course of *H. pylori* infection is highly variable depending on bacterial and host (genetic and immune) factors. Patients with increased acid secretion are more likely to have antral-predominant gastritis, which predisposes to duodenal ulcers. Patients with low acid secretion will more likely develop gastritis in the body of the stomach and are thus more likely to develop gastric ulcer, leading to gastric atrophy, intestinal metaplasia, dysplasia and, finally, in rare cases, gastric carcinoma. This sequence of events is more frequent in people of advanced age. Source: H. pylori infection and gastric cancer: state of the art (review) (Conteduca et al. 2013).

Long-term exposure to *H. pylori* promotes gastric carcinogenesis mainly through 2 mechanisms: Firstly, *H. pylori* could cause chronic gastric inflammation which may progress to the precancerous changes of atrophic gastritis and intestinal metaplasia. The risk of gastric cancer increases in relation to the severity and extent of those precancerous changes (Naumann and Crabtree 2004); Secondly, chronic *H. pylori* infection can also contribute to gastric mucosal genetic instability by reducing gastric acid secretion (hypochlorhydria), which can promote the growth of gastric microbiome that processes dietary components into carcinogens (Amieva and Peek 2016; Machado et al. 2009). This risk can be even higher in patients with a higher intake of salted foods (Peleteiro et al. 2011).

People who have had mucosa-associated lymphoid tissue (MALT) lymphoma also have an increased risk of getting adenocarcinoma of the stomach. This is probably because MALT lymphoma of the stomach is caused by infection with *H. pylori* bacteria (Sakai et al. 2003)

(Figure 1.9). First-line eradication treatment of *H. pylori* relies on proton pump inhibitors and the combination of two antibiotics such as amoxicillin, clarithromycin, or metronidazole. If the first therapy fails, then the proposed second-line treatment is bismuth salts, proton pump inhibitor, tetracycline, and metronidazole (Malfertheiner et al. 2007). *H. pylori* eradication has been shown to yield 33%-47% reduction in gastric cancer incidence rate (Lee et al. 2016; Pan et al. 2016; Ford et al. 2014). However, more recently it has been reported that a considerable proportion of these individuals continue to progress to gastric cancer even after the eradication of *H. pylori*, it is thought that long-term proton pump inhibitors may have an impact on the development of gastric cancer as well (Cheung et al. 2018). The number of gastric cancer cases that emerge after eradication has continued to increase. Moreover, whether *H. pylori* eradication enables recovery from atrophy and intestinal metaplasia, and eventually prevention for cancer development is not fully understood (Poulsen et al. 2009; Uno et al. 2016; Song et al. 2017).

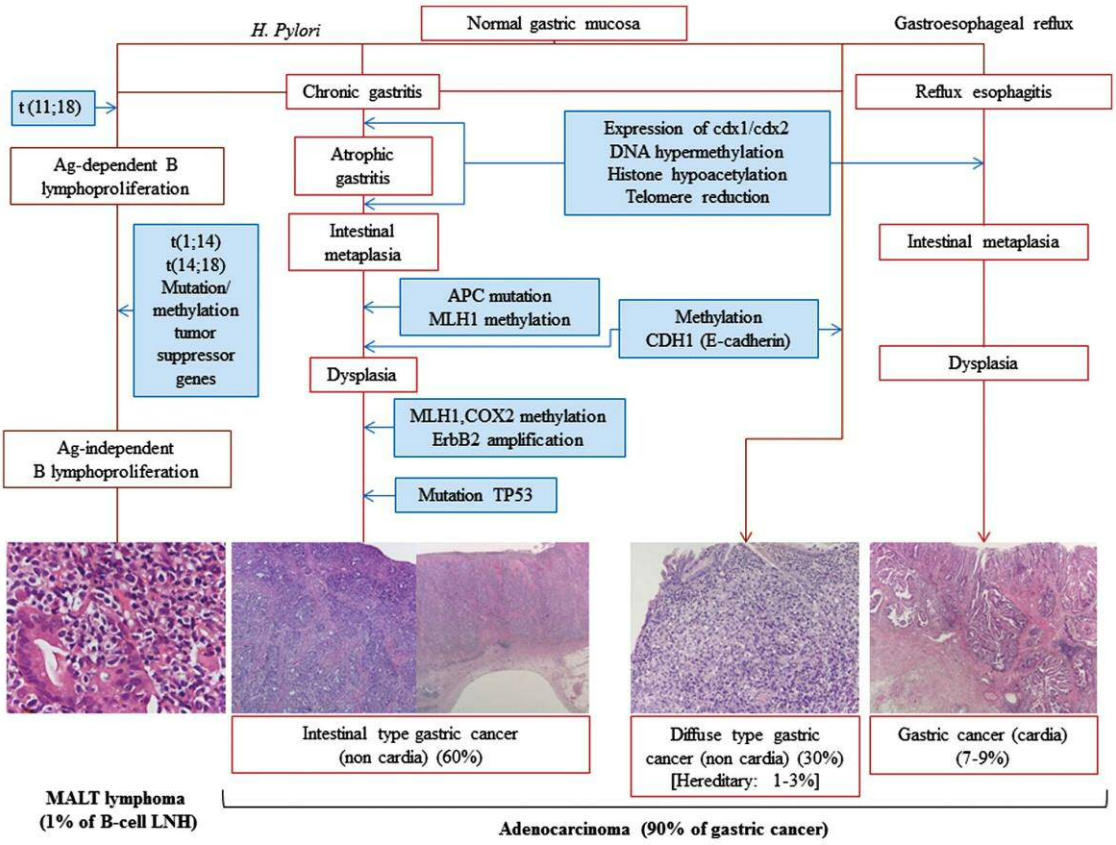

Figure 1.9: Multiple genetic and epigenetic alterations during gastric carcinogenesis and lymphomagenesis and the incidence rates in different types of gastrictumours.
Source: *H. pylori* infection and gastric cancer: state of the art (review) (Conteduca et al. 2013).

Epstein–Barr virus (EBV) is a human herpes virus which latently infects B lymphocytes in the majority of adults. The causal role of EBV in gastric carcinogenesis was suggested in 1994 (Imai et al. 1994). Nowadays, 10% of gastric carcinoma cases harbouring the clonal EBV genome were thought to be Epstein–Barr virus (EBV)-associated throughout the world (Nishikawa et al. 2017). The presence of EBV is observed in 7%–20% of gastric cancers, being slightly more frequent in diffuse-type gastric cancers (Ushijima and Sasako 2004). The highest EBV-positive rates were observed in the cardia and middle gastric cancer (Yamamoto et al. 1994). The association between EBV and carcinogenesis varies from 4% in China, 7.7% in France, 8.1% in Russia, 12.5% in Poland, to 17.9% in Germany (Takada 2000; Czopek et al. 2003). Early studies also demonstrated that EBV infection was absent in preneoplastic gastric lesions (intestinal metaplasia and dysplasia) but present in both intact stomach carcinoma and gastric stump carcinoma suggesting that infection might be a late event in gastric carcinogenesis (Zur Hausen et al. 2004). Intriguingly, EBV is more prevalent in gastric remnant cancers (27.1%) than in an intact stomach. EBV has been shown to extend cell generations of gastric epithelial cells in *in vitro* cell culture, but it cannot immortalize them (Takada 2000). In addition, EBV in carcinoma biopsies indicates a monoclonal proliferation of EBV-infected cells (Iizasa et al. 2012). However, the precise role of EBV in the carcinogenic progress remains to be solved. Methylation of the tumour suppressor genes, such as *p16*, *p73*, and *RUNX3* is a key abnormality in EBV associated gastric cancer (Kang et al. 2002; Nishikawa et al. 2017; Saito et al. 2013). Besides extreme DNA hypermethylation, according to a novel classification system dividing gastric cancer established by The Cancer Genome Atlas (TCGA), EBV associated gastric cancer are characterized by recurrent *PIK3CA* mutations and amplification of *JAK2*, *PD-L1*, and *PD-L2* (Cancer Genome Atlas Research 2014). Mutation of *p53* in gastric cancer was identified independently of EBV infection (Szkaradkiewicz et al. 2006).

Increased age Two-thirds of people who have gastric cancer are over age 65. Especially for intestinal-type gastric cancer, people aged 65-74 are the most frequently diagnosed population (the diffuse type occurs in all age groups with equal gender distribution) (Williams et al. 1988; Zali et al. 2011). Age was also found to be an independent prognostic factor in gastric cancer (Ma et al. 2018). Age-dependent accumulation of DNA demethylation preceding diploidy loss accounted for a significant subset of gastrointestinal cancers (Suzuki

et al. 2006).

Dietary factors including diets, foods, individual nutrients, methods of preparation, and habits of consumption also have been proposed to protect against or increase the risk of gastric carcinogenesis (Abnet et al. 2015). Healthy dietary habits, e.g. high intake of fresh fruits and vegetables, Mediterranean diet, low-sodium diet, salt-preserved food, red and high cured meat, sensible alcohol drinking, and maintaining a proper weight might be associated with a decreased risk of gastric cancer. An evaluation of dose-response found similar levels of association for fruits and vegetables: increase of 100 g of intake/day of fruit was associated with a significant decrease in risk of gastric cancer (summary relative risk, 0.95), and vegetables had a comparable, but not statistically significant association with reduced risk (summary relative risk, 0.96) (Wang et al. 2014). In a large, prospective European study of more than 450,000 people, those with higher fruit and vegetable intakes were less likely to develop any gastric cancer (hazard ratio [HR], 0.77; P for trend=0.02) (Gonzalez et al. 2012). The associations were mainly significant for fresh fruit and diffuse-type gastric cancer (HR, 0.59; P for trend=0.03), for citrus and gastric cardia cancers (HR, 0.61; P for trend=0.01), and for smokers and persons residing in Northern European countries (Gonzalez et al. 2012). In addition to the quantity, the variety of intake may be important. A prospective analysis of a large European cohort containing 475 people who developed gastric or esophageal cancer revealed that increasing variety of the types of fruits and vegetables consumed, independent of total consumption, was inversely associated with the risk of esophageal squamous cell carcinoma, particularly among smokers (Jeurnink et al. 2012). The mechanisms by which fruits and vegetables reduce cancer risk might involve their ability to prevent the development of precancerous conditions, and probably, their high levels of micronutrients (including b-carotene, vitamin C, vitamin E, folate and other antioxidants), which can decrease DNA damage by scavenging for oxygen radicals (Nomura et al. 2003; Abnet et al. 2015).

Smoking The causal relationship between tobacco smoking and gastric cancer had been controversial until 2002 (IARC. IARC monographs. Tobacco smoking and tobacco smoke. Lyon: IARC, 2002) (Gonzalez et al. 2003). The positive correlation between smoking and the risk of gastric cancer was further highlighted by a meta-analysis recently (Ferro et al. 2018a). Frequency, duration, and pack-years of smoking were independently associated with risk of

both gastric cardia adenocarcinoma and non-cardia adenocarcinoma (Steevens et al. 2010). Compared with never smokers, the multivariable-adjusted incidence rate ratio for current smokers was 1.60 for gastric cardia adenocarcinoma (Steevens et al. 2010). Targeting high-risk smokers for serum pepsinogen screening was proposed to be a cost-effective strategy to reduce intestinal-type non-cardia gastric adenocarcinoma mortality (Yeh et al. 2016).

Ethanol was thought to directly and dose-dependently impair the gastric mucosal barrier. Both acidification of the mucosal cells and ethanol itself induce the release of inflammatory and vasoactive substances. Inflammation and vasoconstriction lead to ischemia and mucosal damage. However, an increased risk was only observed in case of patients with chronic atrophic gastritis in Asian alcoholics, who are heterozygous for an inactive aldehyde dehydrogenase (ALDH2) genotype, which has a strong impact on carcinogenic acetaldehyde accumulation after drinking alcohol (Steevens et al. 2010; Testino 2011; Nemati et al. 2012; Ishioka et al. 2018; Choi et al. 2018). In achlorhydric atrophic gastritis, bacterial overgrowth results in the presence of glucose in the formation of minor concentrations of endogenous ethanol and acetaldehyde in gastric juice. After administration of a small amount of alcohol, intragastric acetaldehyde production increases 6.5-fold compared to healthy controls (Testino 2011). For frequent alcohol drinkers (3 or more drinks per week) in US Hispanics, the risk may come from the risk of weight gain (32% vs 26%) (Cokkinides et al. 2012). Meta-analyses of the association between alcohol drinking and gastric cancer additionally indicated that individual participant data pooled analyses yielded more precise estimates for different levels of exposure or cancer subtypes (Ferro et al. 2018b).

Obesity interacts with other mechanisms and results in earlier presentation or more complicate disease. High overall obesity (body mass index (BMI)) (highest (≥35 kg/m^2) *vs.* reference (18.5-<25 kg/m^2) increased the hazard ratio of gastric cardia adenocarcinoma to 3.67, 95% confidence interval, CI 2.00 to 6.71 (O'Doherty et al. 2012). Even in people having no history of reflux, central obesity (large waist circumferences) increased the risk of acid reflux and lengthening of the cardiac mucosa (Robertson et al. 2013; Derakhshan et al. 2015), which was thought to be the cause of the rapid rise in gastroesophageal junction tumours (Quante et al. 2013). Obesity may enhance immature myeloid cell trafficking and TH17 response which may result in accelerating *H pylori*-induced gastric carcinogenesis (Ericksen et al. 2014). A retrospective analysis of 1.79 million men and women from Israel suggested

that adolescent obesity (the body mass index (BMI) ≥ 95th percentile of the baseline) is also associated with an increased risk for non-cardiac gastric cancer (Levi et al. 2018). Leisure-time physical activity has been proven to be associated with lower risk of gastric cardia cancer (Moore et al. 2016; Keum et al. 2016). However, in patients undergoing curative gastric cancer surgery, those who were overweight or mildly-to-moderately obese (BMI 23 to 30 kg/m^2) preoperatively, had better overall survival (OS) and disease-specific survival (DSS) than normal-weight patients (Lee et al. 2018). Therefore, it is suggested that gastroenterologists are uniquely poised to participate in the multidisciplinary management of obesity as physicians caring for people with obesity-related diseases, in addition to their expertise in nutrition and endoscopic interventions (Camilleri et al. 2017).

Others A number of studies report that long-term use of non-steroidal anti-inflammatory drugs (NSAID) such as aspirin is associated with a reduced risk of gastric cancer in a dose-dependent manner. However, such an impact may be more predominantly in intestinal gastric cancer (Lindblad et al. 2005; Wang et al. 2003; Dai and Wang 2006; Huang et al. 2017). The presumed mechanism of chemoprevention is the inhibition of cyclooxygenase (COX)-2. Aspirin exhibits an anti-cancerous effect through several inter-related mechanisms: prostaglandin synthesis and catabolism in epithelial cells, inhibition of Wnt-β-catenin signaling, inactivation of platelets, and the host immune response (Jackson et al. 2000). Previous partial gastrectomy is also a risk factor for gastric cancer even many years later (Offerhaus et al. 1988; Sitarz et al. 2012).

1.1.2.2 Genetic predisposition

Diet and infection with *H. pylori* are probably the prominent risk factors for gastric cancer, however, familial aggregation in a variable but significant proportion of cases suggests the importance of genetic predisposition (Caldas et al. 1999; Oliveira et al. 2015). About 10% of gastric cancer cases show familial clustering (Guilford et al. 1998; Zanghieri et al. 1990; La Vecchia et al. 1992). 1-3% of gastric cancers are linked to inherited gastric cancer predisposition syndromes (Ang and Fock 2014). Earlier studies described a familial component only for diffuse gastric carcinoma, designated hereditary diffuse gastric cancer (HDGC) (Lehtola 1978). Germline mutations in the epithelial cadherin (*CDH1*) gene associated HDGC is characterized by an increased risk for diffuse gastric cancer and lobular

breast cancer (Kaurah et al. 2007). Later research found that intestinal-type adenocarcinoma is the main histological subtype of hereditary gastric cancers (Ang and Fock 2014). The definition of family gastric cancer syndromes was extended to hereditary diffuse gastric cancer, familial intestinal gastric cancer and gastric cancer in other familial cancer syndromes, such as familial adenomatous polyposis (FAP) caused by defects in the adenomatous polyposis coli (APC) gene, Lynch syndrome, an autosomal dominant disease caused by germline mutations in DNA mismatch repair genes (mainly *Hmsh2*, *Hmsh1*, *Hmsh6*, *Hpms*1, *Hpms2*) as well as mutations in the *EPCAM* gene, which inactivates *MSH2* via promoter hypermethylation (Galiatsatos et al. 2017). Li-Fraumeni syndrome (LFS) associated with germline mutations in the TP53 gene, and Peutz-Jeghers syndrome caused by mutations in *STK11* (Van Lier et al. 2011) *et al.*

Other uncommon genetic reasons also include: polymorphisms in inflammatory genes (M. Li et al. 2013; Wen et al. 2014), the variant genotype of folate intaking related enzymes *MTHFR* (Larsson et al. 2006), hypertrophic gastropathy (including Ménétrier's disease) (Tersmette et al. 1990) and even rare inherited cancer syndromes, such as phosphatase and tensin homolog (PTEN) hamartoma tumour (Cowden's) syndrome (Ha et al. 2012). For unknown reasons, people with type A blood have a higher risk of developing gastric cancer (Aird et al. 1953).

1.1.2.3 Precursor lesions

Atrophic gastritis is characterized by the presence of metaplastic epithelial changes. There are two main subtypes, autoimmune (AMAG) and environmental metaplastic atrophic gastritis (EMAG). AMAG is associated with T-cell mediated destruction of the oxyntic mucosa and production of autoantibodies directed against parietal cell antigens and intrinsic factor, resulting in progressive atrophy of the glandular epithelium with loss of parietal and chief cells (Nguyen et al. 2013). The loss of the normal exocrine glands of the gastric mucosa causes hypochlorhydria and a resultant increase in gastric pH. Autoimmune gastritis is increasingly recognized as a contributing aetiology, with or without the presence of *H. pylori* (Coati et al. 2015). Populations with a high prevalence of atrophic gastritis have a high prevalence of gastric cancer, and vice versa. Unlike AMAG, mucosal changes in patients with EMAG affect both the body/fundus and the antrum in a multifocal distribution, but with

the heaviest involvement of the antrum and a relatively preserved gastric acid production. Without the relative protective effect of the accompanying hypochlorhydria, EMAG patients are more likely to develop gastric ulcer disease. It was estimated that atrophic gastritis and other conditions that cause gastric atrophy are associated with an increased risk of both cardia and non-cardia gastric adenocarcinomas, the magnitude of the risk ranges from 3 to 18 times greater than an age-matched population. The crude incidence for cancer was 1.7% for atrophic gastritis during the observation period (Kato et al. 1992; Helicobacter and Cancer Collaborative 2001; De Vries et al. 2008; Cheung 2017).

Metaplasia is thought to be involved in the pathogenesis of gastric cancer, particularly the intestinal type. The estimated odds ratio of gastric cancer adjusted for age and sex, varied from 17.1, for those with baseline diagnoses of superficial intestinal metaplasia (IM), to 29.3, for those with deep IM or mild dysplasia or IM with glandular atrophy and neck hyperplasia, to 104.2, for those with moderate or severe dysplasia, as compared with subjects with superficial gastritis or chronic atrophic gastritis at baseline (You et al. 1999). Most patients diagnosed with high-grade dysplasia of the gastric mucosa either already have or will soon develop gastric cancer. In gastrectomy specimens for gastric cancer, 20-40% of patients have associated dysplasia (Rugge et al. 1994). A report from Sweden which included 405,172 patients with gastric biopsy samples taken for a non-malignant indication between 1979 and 2011, found that the risk of gastric cancer was significantly increased in the presence of intestinal metaplasia (hazard ratio [HR] 6.2, 95% CI 4.7-8.2) and dysplasia (HR 10.9, 95% CI 7.7-15.4). It was estimated that approximately 1 in 39 patients with intestinal metaplasia and 1 in 19 with dysplasia would develop gastric cancer within 20 years (Song et al. 2015).

Gastric polyps are typically found incidentally when upper gastrointestinal endoscopy is performed for an unrelated indication; only rarely do they cause symptoms or other clinical signs. Nevertheless, their discovery can be important since many polyps have malignant potential (Rugge et al. 2016).

Gastric ulcer with benign morphology increased the risk of gastric cancer (incidence ratio 1.8), and this association probably reflects common risk factors (*e.g.*, mainly H. pylori infection) However, the risk were unchanged among patients with prepyloric ulcers, and decreased among those with benign duodenal ulcers (incidence ratio 0.6) (Ihre et al. 1964;

Rollag and Jacobsen 1984; Hansson et al. 1996; Sogaard et al. 2016). A 3.4-year follow-up study involving 1120 Japanese patients with peptic ulcer disease who had *H. pylori* eradication therapy revealed that gastric cancer developed only in patients with a gastric ulcer but not patients with duodenal ulcers. Patients who developed gastric cancer were significantly more likely to have persistent *H. pylori* infection (hazard ratio 3.4). Another follow-up study from the same group showed that, in patients with peptic ulcer disease, the risk of gastric cancer was also significantly increased with a higher grade of baseline gastric mucosal atrophy, and older age (Take et al. 2005; Take et al. 2007).

Besides the above factors, the interactions between host and environmental influences are also worth attention. The best strategy to reduce the mortality for gastric cancer is to schedule appropriate screening and surveillance programs. Currently, endoscopy is generally considered to be the most sensitive and specific diagnostic screening method for gastric cancer. However, mass screening for early detection of gastric cancer is expensive, and the compliance of patients with endoscopy is poor, therefore, national screening programme are only used in regions with high incidences, such as Japan, South Korea, and Singapore. Endoscopic ultrasound is at present available in many centers and, although mainly used to stage previously diagnosed tumours, it might be helpful in identifying early diffuse-type gastric carcinoma lesions. Future studies of these and other methods of examining the stomach in predisposed subjects are needed to draw conclusions on their use in diagnosing early gastric lesions. For now, in the surveillance of those predisposed to gastric cancer development, clinicians are urged to undertake detailed endoscopic mucosal examination with multiple biopsies of even the subtlest of lesions. However, endoscopic surveillance should be performed once or twice a year in patients who are at higher risk of gastric cancer (history of gastric cancer in the family, inherited cancer syndromes) (Kim et al. 2016). Several serum-based tumour markers including carbohydrate antigen (CA) 72-4, CA12-5 and pepsinogenI/II have been widely used in clinical practice for gastric cancer, carcinoembryonic antigen (CEA) and CA19-9 are the two most common markers for following gastric cancer patients with known disease. However, insufficient sensitivity (20%-30%) and specificity of these protein biomarkers limit their utility for early gastric cancer detection. More prospective studies are needed to determine the use of other biomarkers in the early detection of gastric cancer.

1.1.3 Anatomy, Histophysiology and Function of the Stomach

In humans, the stomach is a flattened J-shaped muscular organ located in the upper left part of the abdomen. It extends from the left hypochondriac region into the epigastric region obliquely, starting at the esophagogastric junction (EGJ) and leading to the duodenum via the pylorus (Figure 1.10).

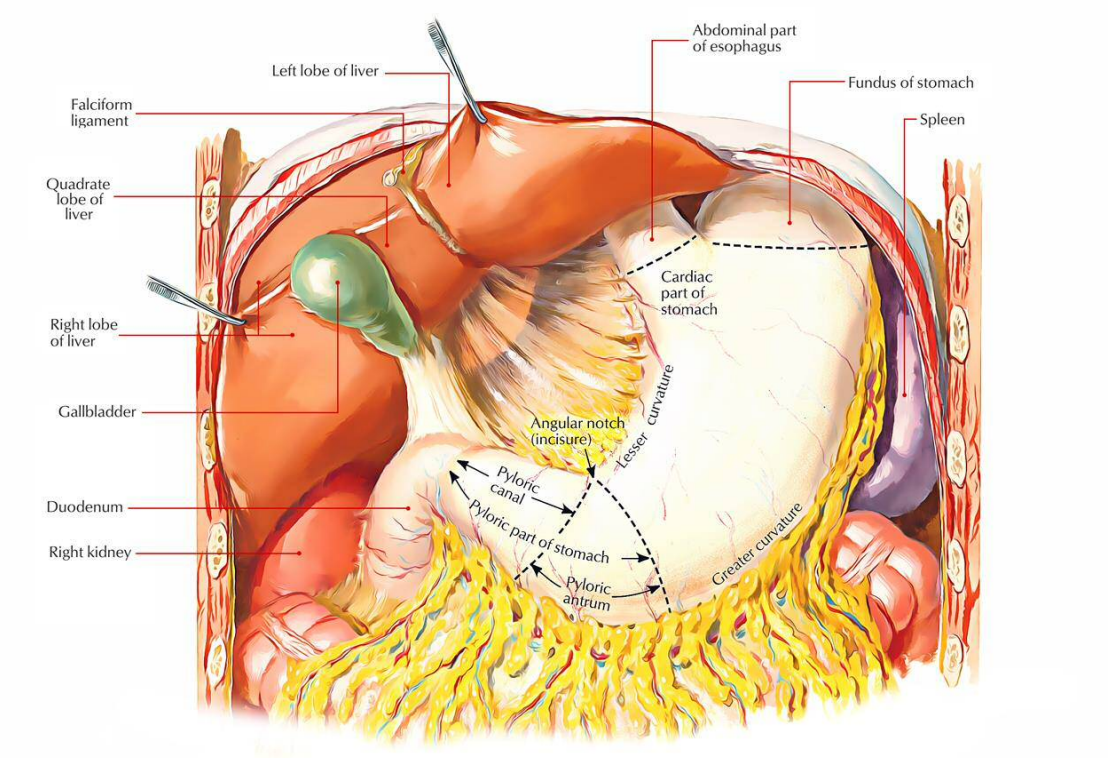

Figure 1.10: Location of the stomach. Source: Anatomy of Stomach, available at https://www.Earthslab.com/anatomy/stomach/

The stomach acts to blend ingested food with gastric secretions to create chyme, a semifluid substance. The stomach controls the speed of delivery of chyme into the small intestine to enable proper digestion and absorption. The gastric glands secret hydrochloric acid which kills bacteria ingested in food. Citadel's Intrinsic Factor within the gastric juice helps in the absorption of vitamin B12 in the small intestine. Thus, the stomach is first and foremost a principal site of digestion. It is the first site of protein break down by the stomach's pepsin enzyme. The capacity of the stomach is variable as the stomach is extremely distensible; At birth the capacity is only 30 mL, at puberty the capacity is 1000 mL and in adults the capacity is 1500 to 2000 mL. The stomach consists of various parts that serve distinct functions. For

the purposes of gross description, four main sections are identified in the stomach: cardia, fundus, corpus (or body), and antrum (pylorus) (Figure 1.10). The superomedial margin is termed the lesser curvature, and the inferolateral margin is termed the greater curvature.

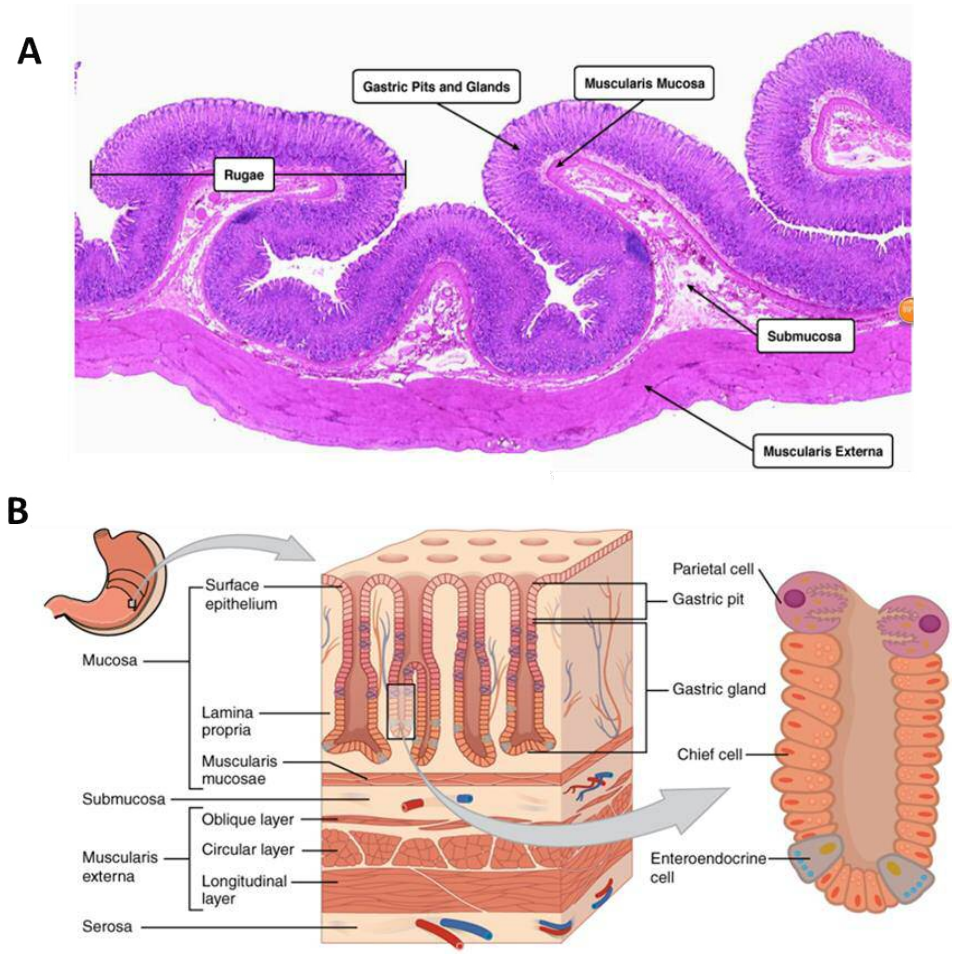

Figure 1.11: The folds of the stomach wall (rugae) lining under the light microscope. A. Haematoxylin and eosin staining show the structure of the stomach lining under the light microscope. The numerous glands invaginate into the lamina propria. The mucosal layer appears with its columnar epithelial cells, narrow lamina propria, and pink-staining muscularis mucosa. The loose connective tissue of the submucosa contains some blood vessels. Adopted from http://medcell.med.yale.edu/ histology/gi_tract_lab/stomach.php. **B. A diagram of the layers of the stomach wall.** Adopted from http://heritance.me/anatomy -of-stomach-wall.

The wall of the stomach has four layers (see Figure 1.11), similar to most of the alimentary canal. From inside outwards, these are mucosa, submucosa, muscularis propria, and subserosa (Mackintosh and Kreel 1977), but the muscularis and mucosa are modified for the special roles of the stomach. Besides the usual circular and longitudinal layers of smooth muscle, the muscularis external has an incomplete innermost layer of smooth muscle fibres which run obliquely. This structure allows the stomach not only to mix, churn, and move

food along the tract, but also to pummel the food, physically breaking it down into smaller fragments and passing it through to the small intestine (Maintenance of the body, Human Anatomy and Physiology, Tenth Edition, Pearson). The mucosa is the most internal layer, it is relatively thick (1.5-2 mm), soft, and velvety. It comprises a single layer of columnar epithelium composed of mucous cells; they produce a cloudy, protective two-layer coat of alkaline mucus in which the surface layer consists of viscous, insoluble mucus that traps a layer of bicarbonate-rich fluid beneath it.

There are three types of glands in the stomach: glands in the cardiac region secrete mucous; glands in the fundus and body include mucous neck cells, which secrete mucus, parietal/oxyntic cells, which secrete hydrochloric acid and gastric intrinsic factor, and chief cells, which secrete pepsinogen; glands in the pyloric region secrete mucus. Endocrine cells in the pyloric mucosa produce the gastrin hormone which increases the secretion of gastric juice. The oxyntic glands in the orad stomach make up 75% of the total number of glands. The remaining 25% are pyloric glands in the antrum and pylorus.

To protect itself from chemical or physical trauma, the stomach mucosa produces a mucosal barrier, by a thick coating of bicarbonate-rich mucus building up on the stomach wall. The epithelial cells of the mucosa are joined together by tight junctions which prevent gastric juice from leaking into underlying tissues layers. Additionally, the damaged epithelial mucosal cells are shed and quickly replaced by division of undifferentiated stem cells that reside where the gastric pits join the gastric glands. The surface epithelial mucous cells are completely renewed every three to six days, but the more sheltered glandular cells deep within the gastric glands have a longer lifespan. Anything that breaches the gel-like mucosal barrier causes inflammation of the stomach wall, a condition called gastritis. Persistent damage to the underlying tissues can promote peptic ulcers.

The next layer, the submucosa is where the nerve bundles locate. Moving outward there are three layers of smooth muscle tissue that form the muscularis external which is responsible for the movements of the stomach, from inner to outer, they are inner oblique layer, circular muscle layer, and longitudinal layer. Finally, the outermost layer is the serosa which encloses the stomach organ and is connected to the lining of the abdominal cavity.

Five arteries supply blood to the stomach. The left gastric artery arises directly from the celiac axis and supplies the cardiac region. The right gastric artery (which supplies the lesser curve) and the right gastroepiploic artery (which supplies the greater curve) arise from the hepatic artery. The left gastroepiploic and the short gastric arteries arise from the splenic artery and also supply the greater curvature. The sympathetic nerve supply to the stomach is derived from the celiac plexus via nerves that follow the gastric and gastroepiploic arteries. Branches also are received from the left and right phrenic nerves. The parasympathetic supply is the vagus nerve via the main anterior and posterior trunks which lie adjacent to the esophagogastric junction.

Recent studies have disproved the former view that lymphatic channels are present at all levels of the lamina propria. By using careful ultrastructural techniques, lymphatics have been demonstrated to be limited to the portion of the lamina propria immediately superficial to the muscularis mucosae. From there, efferents penetrate the muscle and communicate with larger lymphatic channels running in the submucosa. This arrangement implies that an early gastric cancer may have lymphatic metastases, even though the primary tumour is entirely superficial to the muscularis mucosae.

The lymphatic trunks of the stomach generally follow the main arteries and veins. Four areas of drainage can be identified, each with its own group of nodes. The largest area comprises the lower end of the oesophagus and most of the lesser curvature, which drains along the left gastric artery to the left gastric nodes. From the immediate region of the pylorus, on the lesser curvature, drainage is to the right gastric and hepatic nodes. The proximal portion of the greater curvature drains to pancreatic splenic nodes in the hilum of the spleen, and the distal portion of the greater curvature drains to the right gastroepiploic nodes in the greater omentum and to pyloric nodes at the head of the pancreas. Efferents from all four groups ultimately pass to celiac nodes around the main celiac axis (Human Anatomy and Physiology, Tenth Edition, Pearson).

1.1.4 Classification of gastric cancer

Carcinomas of the stomach are morphologically heterogeneous. This heterogeneity is reflected in the diversity of histopathological classifications available which are based on different approaches, such as histological profile, degree of differentiation, pattern of growth,

and histogenesis. Several pathohistological classification systems proposed for the diagnosis of gastric cancer based on macroscopic and/or microscopic feature. It is still controversial as to which classification system imparts the most reliable information, and therefore, the choice of system is varied in clinical routine. (Surgical Pathology criteria, Stanford Medicine, Available at http://surgpathcriteria.stanford.edu/gitumours/ gastric-adenocarcinoma/). Clinically, TNM (tumour, node, metastases) staging is far more important for prediction of survival than any of these classifications.

1.1.4.1 Early and advanced gastric cancer

Early gastric cancer is defined as invasive cancer confined to mucosa and/or submucosa, with or without lymph node metastases, irrespective of the tumour size (Hamilton R, Aatonen LA. Tumours of Digestive System. Lyon: IARC; 2000:39-52). Most early gastric carcinomas are small, measuring 2 to 5 cm in size, and often located at lesser curvature near the angularis. Some early gastric carcinomas can be multifocal, often indicative of a worse prognosis. 10% of early gastric cancer presents with lymph node metastases (Hu et al. 2012).

Early gastric carcinoma is divided into Type I for tumours with exophytic growth, Type II with superficial growth, Type III with excavating growth, and Type IV for infiltrating growth with lateral spreading (Figure 1.12) (Hu et al. 2012). Type II tumours are further divided into IIa (elevated), IIb (flat) and IIc (depressed), as proposed by the Japanese Endoscopic Society (Japanese Gastric Cancer 2011). A Paris classification has endorsed three gross patterns for superficial neoplastic lesions in the gastrointestinal tract. Grossly and endoscopically, tumours are classified as Type 0-I for polypoid growth (which is subcategorized to 0-Ip for pedunculated growth and 0-Is for sessile growth), Type 0-II for nonpolypoid growth (which is subcategorized into Type 0-IIa for slightly elevated growth, Type 0-IIb for flat growth, and Type 0-IIc for slightly depressed growth), and Type 0-III for excavated growth.

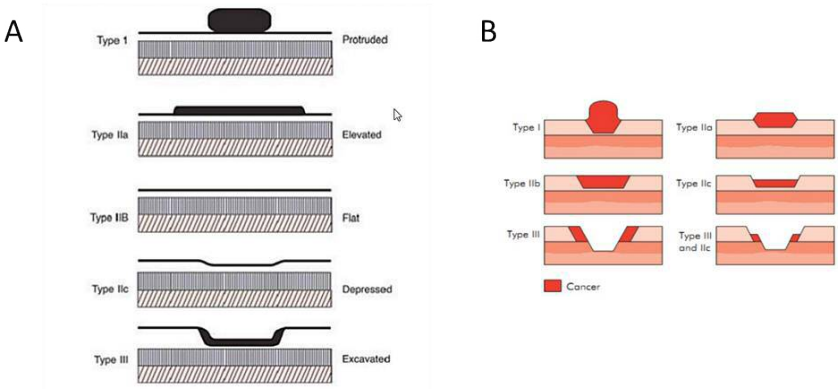

Figure 1.12: Pathological types of early gastric cancer. A. Paris classification. B. Japanese classification.

Histologically, approximately 50-70% early gastric cancers are well differentiated, 10-30% are poorly differentiated (Green and O"Toole 1982; Q. Huang et al. 2015). Tubular and papillary architecture are the most common forms of well-differentiated early gastric cancer (Hu et al. 2012). The distinction between well-differentiated carcinoma and high-grade dysplasia or carcinoma-in-situ can be challenging when only mucosal tissue is available for histologic assessment (Hu et al. 2012). Intramucosal invasion may not be as easily confirmed as an invasive carcinoma into submucosa where stromal desmoplasia is usually evident (Hu et al. 2012). The distinction between intramucosal carcinoma and carcinoma-in-situ or high-grade dysplasia is important, as the intramucosal carcinoma of stomach, unlike the intramucosal carcinoma in the colon, does metastasize (Hu et al. 2012). Generally, the useful histologic features of intramucosal invasion are single tumour cell in the lamina propria and significantly fused neoplastic glands of various sizes (Hu et al. 2012). Through adequate tumour section and lymphadenectomy, the prognosis of early gastric carcinoma can reach ever greater than 90% (Onodera et al. 2004; Suzuki et al. 2016).

Advanced gastric cancer, defined as carcinoma with muscularis propria invasion or beyond, carries a much worse prognosis, with a 5 years survival rate at less than 60% (Hu et al. 2012). Gastric cancer patients classified as stages II-IV (the 7th AJCC cancer staging system) demonstrated high recurrence rates ranging from 25%-40% in an adjuvant setting, with metastatic cases not amenable to re-resection (Cristescu et al. 2015). The distinction between early and advanced gastric carcinoma before resection is clinically important because it helps to decide if a neoadjuvant (pre-operative) therapy, which has shown to improve disease-free survival (DFS) and OS, is warranted (Cunningham et al. 2006; Ychou et al. 2011). While the

macroscopic appearance is informative, the most accurate pre-operative staging information is generally obtained with endoscopic ultrasonography (EUS) and computerised tomography (CT) (Hwang et al. 2010).

1.1.4.2 Borrmann's classification

The appearance of advanced gastric carcinomas can be exophytic, ulcerated, infiltrative or combined (Hu et al. 2012). Endoscopic classification of advanced gastric cancer is well known and was introduced by Borrmann in 1926 (Borrmann 1926) including 4 types: type I for polypoid growth, type II for fungating growth, type III for ulcerating growth, and type IV for diffusely infiltrating growth which is also referred to as linitis plastica-a signet ring cell carcinoma involving most of gastric wall by infiltrating tumour cells. Histologically, advanced gastric carcinoma often demonstrates marked architectural and cytological heterogeneity, with several co-existing histologic growth patterns (Hu et al. 2012).

1.1.4.3 Cardia gastric cancer and Non-cardia gastric cancer

Anatomically, gastric cancers are classified into true gastric (non-cardia) and gastro-oesophageal-junction cancers (cardia). Due to their differences in incidence, geographical distribution, causes and clinical disease course, treatments for them also differ. The Siewert classification (Figure 1.13) based on the epicentre location of tumour is widely used to category the gastro-oesophageal-junction cancers into three types (Siewert and Stein 1998). However, the biology difference between Siewert type II and type III gastric cancer is unclear. The classification is also criticized by the non-specific definition of gastro-oesophageal-junction adenocarcinoma (Demicco et al. 2011). TNM classification introduced a more simplified categorization to aid correct anatomical classification, in which both the epicentre and the tumour extension margin (within or beyond the gastro-oesophageal junction) are included.

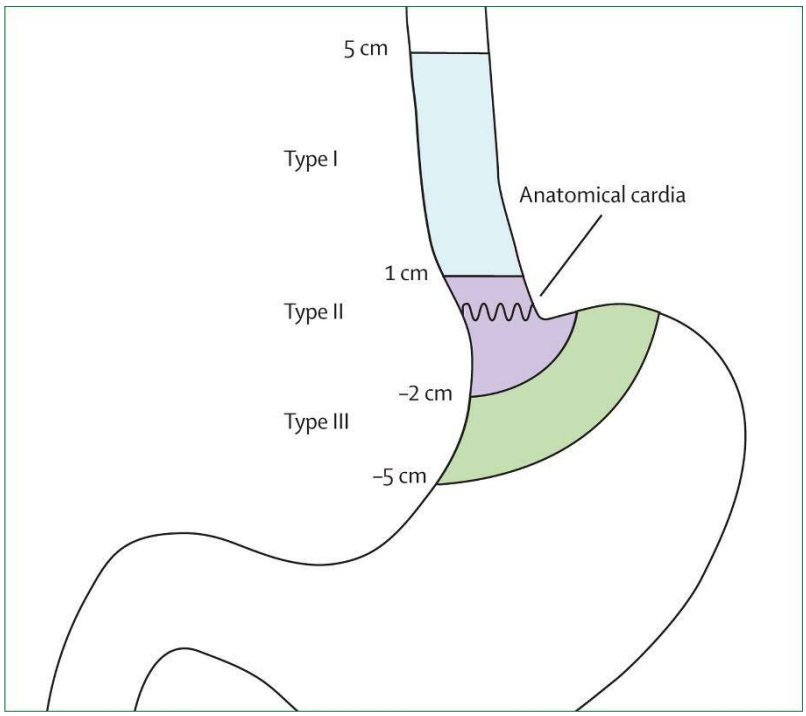

Figure 1.13: Schematic illustration of the modified Siewert's classification. The distance of the center of a tumour from anatomical cardia determines tumour type. Source: Oesophagogastric junction adenocarcinoma: which therapeutic approach (Mariette et al. 2011).

1.1.4.4 Laurén classification

Some national guidelines for the treatment of gastric cancer refer to the Laurén or the WHO classifications regarding therapeutic decision-making (Okines et al. 2010), which underlines the importance of a reliable classification system for gastric cancer. Currently, Laurén (Lauren 1965) and WHO [FT Bosman, F Carneiro, RH Hruban, ND Thiese (Eds.), WHO classification of tumours of the digestive system (4th ed.), IARC, Lyon (2010), pp. 44-58] schemes are the most commonly used (Table 1.2).

Table 1.2: Laurén and WHO classification. Source: Pathohistological classification systems in gastric cancer: Diagnostic relevance and prognostic value (Berlth et al. 2014).

Laurén classificatio	WHO classification
Intestinal type	Papillary adenocarcinoma
	Tubular adenocarcinoma
	Mucinous adenocarcinoma
Diffuse type	Signet-ring cell carcinoma and other poorly cohesive carcinomas
Indeterminate type	Mixed carcinoma
	Adenosquamous Carcinoma

	Squamous cell carcinoma
	Hepatoid adenocarcinoma
	Carcinoma with lymphoid stroma
	Choriocarcinoma
	Carcinosarcoma
	Parietal cell carcinoma
	Malignant rhabdoid tumour
	Mucoepidermoid carcinoma
	Paneth cell carcinoma
	Undifferentiated carcinoma
	Mixed adeno-neuroendocrine carcinoma
	Endodermal sinus tumour
	Embryonal carcinoma
	Pure gastric yolk sac tumour
	Oncocytic adenocarcinoma

According to the Laurén classification, gastric carcinomas are separated into intestinal and diffuse two main histological types presenting differences in not only in histomorphology but also in clinical and epidemiological characteristics. Cohesiveness and glandular differentiated malignant epithelial cells infiltrating the stroma characterize intestinal carcinomas. Tumour cells may display varying degrees of nuclear atypia and may present tubular, trabecular, papillary or tubular-papillary structures (Figure 1.14 A-C). According to cellular and architectural criteria, gastric adenocarcinomas are classified as well, moderately and poorly differentiated. A small percentage of adenocarcinomas are mixed, presenting features of both types. Cytologically, cells are large and display cytoplasmic as well as nuclear pleomorphism. In intestinal-type carcinoma, mitoses are frequently seen, as are polymorphous inflammatory infiltrates.

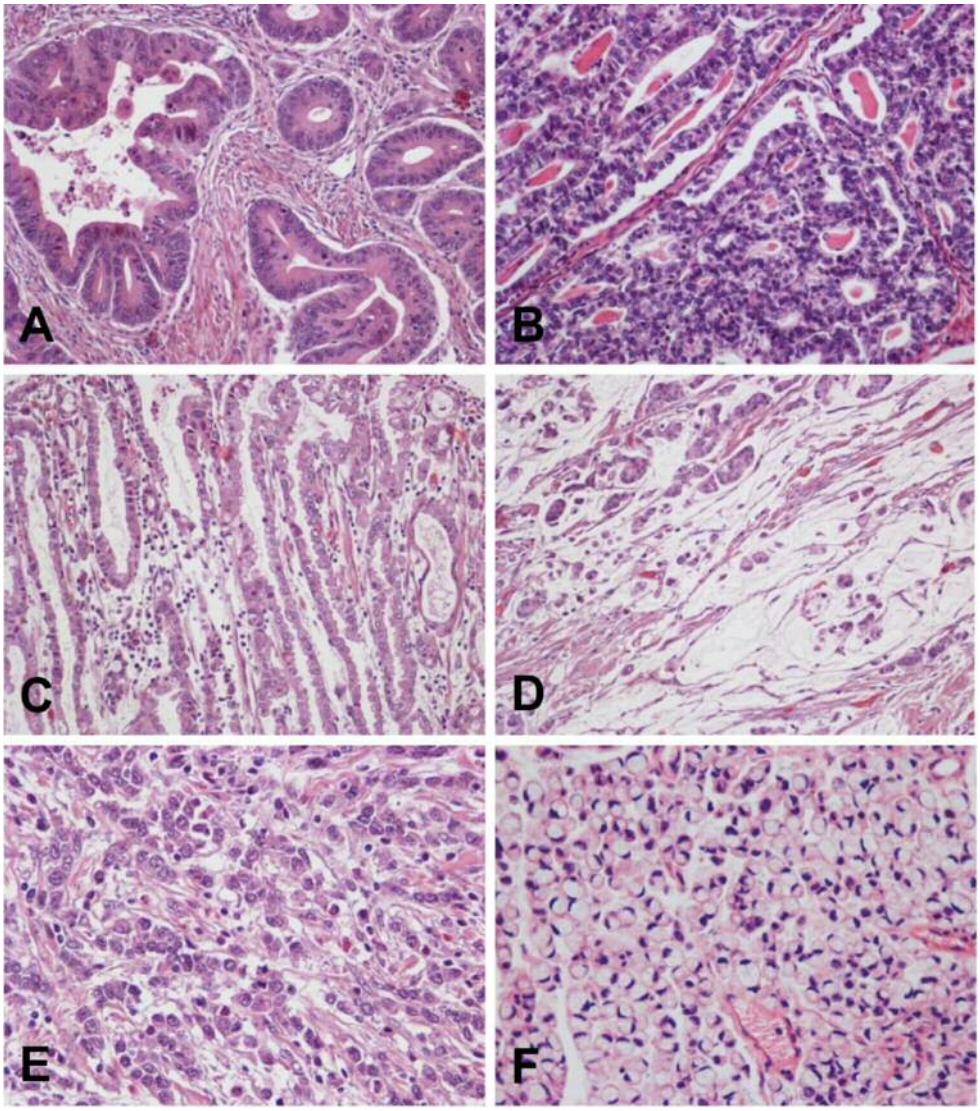

Figure 1.14: Haematoxylin-eosin staining for Laurén classification of gastric cancer. **A-C**, Intestinal-type. Three different tumours are shown with the formation of irregular glands, tubules, and papillae. **D**, Mucinous adenocarcinoma, with small groups of tumour cells floating in pools of mucin. **E, F**, Diffuse type. Two different tumours are shown composed of non-cohesive individual cells infiltrating the stroma. Signet ring cell carcinoma (**F**) is formed by cells with abundant intracytoplasmic mucin and nuclei displaced to the periphery. This morphology is characteristic of this tumour type. Source: Gastric cancer: Overview, available from http://colombiamedica.univalle. Edu.co/index.php/comedica /article/view/1263/2150

In contrast, diffuse carcinomas are composed of discohesive cells that infiltrate the stroma individually or in small groups (Figure 1.14 E-F). In some cases, the tumour may form solid masses, but even in these cases the cells appear to be loose, with little cohesiveness and do not form epithelial cords. Occasionally, tiny glandular lumens can be observed, formed by cells that have no polarity and are surrounded by a diffuse infiltration of isolated tumour cells. Infiltration of malignant cells with indistinct cytoplasm and pyknotic nuclei often

produces a connective tissue proliferation and a chronic, lymphocytic type of inflammation. A variant of the diffuse histological type is the signet ring cell adenocarcinoma. By definition, it must be predominantly composed (>50%) of signet ring cells. These cells are characterized by abundant cytoplasmic mucin that displaces the nucleus to the periphery (Figure 1.14 F) (Parsonnet et al. 1991).

Mucinous (colloid) adenocarcinomas may originate in adenocarcinomas of either intestinal or diffuse types (Lauren 1965). They are rare histological subtype of undifferentiated gastric carcinoma, accounting for approximately 2.6–6.6% of all gastric cancer cases (Kunisaki et al. 2006; Huszno et al. 2012). Mucinous gastric cancer exhibits a poorer prognosis compared to non-mucinous gastric cancer, partly due to a more frequent incidence of advanced-stage disease at diagnosis (Isobe et al. 2015). These tumours are composed of malignant epithelial cells floating loose or in small groups in large mucinous areas (Figure 1.14 D). In some cases, signet ring cells may be observed. By definition, the extracellular mucinous pools constitute at least 50% of the tumour.

Despite its high clinical relevance, the prognosis value of Laurén's classification remained controversial (Goseki et al. 1992; Qiu et al. 2013). A recent systematic review and meta-analysis which included 61,468 patients from 73 published studies, revealed that gastric cancer patients with diffuse-type histology have a worse prognosis than those with intestinal subgroup in all studies (HR 1.23; 95% CI, 1.17–1.29; P<0.0001). This applies to both loco-regional confined (HR 1.21; 95% CI, 1.12–1.30; P<0.0001) and advanced disease (HR 1.25; 95% CI, 1.046–1.50; p=0.014), in both Asiatic (HR 1.2; 95% CI, 1.14–1.27; P<0.0001) and Western patients (HR 1.3; 95% CI, 1.19–1.41; P<0.0001). Furthermore, both in those not exposed (HR 1.15; 95% CI, 1.07–1.24; P<0.0001) or exposed (HR 1.27; 95% CI, 1.17–1.37; P<0.0001) to (neo) adjuvant therapy. This provides important evidence for the use of classification systems for stratification purposes in future clinical trials (Petrelli et al. 2017).

Similarly, a study enrolling 3071 patients evaluating the prognostic significance of Lauren's classification in gastric cancer also showed with intestinal-type gastric cancer (57.7%) had a better 5-year OS than diffuse type (45.6%) and mixed type (43.4%, $p < 0.001$). Besides, gastric cancer patients with intestinal type were older ($p < 0.001$), male predominant ($p < 0.001$), smaller tumour size ($p < 0.001$), distal stomach predominant ($p < 0.001$),

relatively well differentiated ($p < 0.001$), less advanced Borrmann type ($p < 0.001$), less scirrhous type stromal reaction($p < 0.001$), less infiltrating type of Ming's histology type (refer to 1.1.4.6)($p < 0.001$), less tumour invasion depth and less lymphovascular invasion ($p < 0.001$). Lauren's classification is an independent prognostic factor in gastric cancer patients undergoing gastrectomy (Chen et al. 2016).

1.1.4.5 WHO classification

WHO classification includes not only adenocarcinoma of the stomach but also all other types of gastric tumours of lower frequency (Table 1.2). The most common type of gastric cancer is tubular adenocarcinoma, followed by papillary and mucinous types. Signet ring cell carcinoma accounts for approximately 10% of gastric cancers and is defined by the presence of signet ring cells in over 50% of the tumour. Patients with papillary adenocarcinoma, mucinous adenocarcinoma were reported to experience unfavorable prognosis (Yasuda et al. 2000; Zheng et al. 2010; Kawamura et al. 2001). The Japanese classification system further divides tubular adenocarcinoma into well-differentiated and moderately differentiated adenocarcinoma (Japanese Gastric Cancer Association 2011).

1.1.4.6 Goseki classification (microscopic) and Ming classification (microscopic)

Prognostic-related but less common classification systems were demonstrated to correlate with the pre-existing classification systems. Goseki *et al.* grading system (Goseki et al. 1992), based on tubular differentiation and mucin secretion, was described to divide gastric cancer into four groups, as presented in Table 1.3. Ming described the growth pattern of the lesion and recognized two main growth patterns: the expanding growth pattern and the infiltrating growth pattern (Table 1.4) (Ming 1977).

Table 1.3: Goseki classification. Source: Pathohistological classification systems in gastric cancer: Diagnostic relevance and prognostic value (Berlth et al. 2014).

Type	Tubules	Intracytoplasmic Mucin
I	Well-differentiated	Poor
II	Well-differentiated	Rich
III	Poorly differentiated	Poor
IV	Poorly differentiated	Rich

Table 1.4: Ming classification. Source: (Surgical Pathology criteria, Stanford Medicine. (Available at http://surgpathcriteria.stanford.edu/gitumours/gastric-adenocarcinoma/).

Type	Description
Expanding type	Infiltrating cohesive cell aggregates
Infiltrating type	Diffuse permeative infiltration by single noncohesive cells or individual glands
Unclassified	

In conclusion, the histotype-based classification system for gastric cancers demonstrated a potential role as an effective tool for distinguishing patients in different clinical settings and with distinct outcomes. However, due to the limited advantages of any one particular classification, there's no international consensus for research purposes. The difficulty of assessing the prognosis of gastric cancer using histological methods is widely accepted and this is also reflected in the essentially descriptive character of presently used classifications. Several histotypes exhibited lower malignant potential have been identified, including lymphocyte-rich cancer, muconodular cancer, very-well-differentiated tubular cancer with an intestinal or gastric phenotype, and a low-grade subtype of diffuse desmoplastic cancer. Other types of gastric cancer with poor outcome have also been identified from poorly differentiated neuroendocrine carcinoma to anaplastic diffuse cancer or hepatoid, chorioncarcinomatous and adenosquamous carcinoma. The different behaviour of these histotypes led to a development of a histological grading system for prognostic evaluation, in which low-grade or grade 1 (G1) was defined as muconodular, well-differentiated tubular, diffuse desmoplastic and high lymphoid response (HLR); high-grade or grade 3 (G3) was anaplastic and mucinous invasive and intermediate-grade or grade 2 (G2) was described as ordinary cohesive, diffuse and mucinous cancers. This grading system was highly predictive of patient outcome when applied to a large tumour series (Solcia et al. 2009; Chiaravalli et al. 2012). While for the evaluation of grade 2 ordinary cancers, which form a very large, histologically heterogeneous group with a wide prognostic spectrum, carefully assessed stage, other common histological parameters (invasive pattern, proliferative rate, structural or cytological atypia, tumour cell phenotype) or a variety of promising molecular tools are crucial for appropriate clinical decisions (Chiaravalli et al. 2012).

1.1.4.7 Molecular classification

1.1.4.7.1 The classification system proposed by TCGA

The latest results from gastric cancer molecular subtype studies indicate that it might be useful to integrate genomic and proteomic-based features of gastric cancer into the classification systems to establish prognostic relevance (Berlth et al. 2014; Wong et al. 2014).

Several whole genome projects were carried out to develop a biologic classification scheme helping guide patient therapy. TCGA research network published the results of full genomic profiling of 295 primary gastric adenocarcinomas in 2014 (Cancer Genome Atlas Research 2014), which ushered in an era of precision medicine of gastric cancer with strong genetic–clinical association.

Through complex statistical analyses, four tumour subgroups were identified: positive for Epstein-Barr virus (EBV, 9%), microsatellite unstable tumours (MSI, 22%), genomically stable tumours (GS, 20%), and chromosomally instability tumours (CIN, 50%). Correlation with histological characteristics revealed enrichment of the diffuse subtype in the genomically stable group (73%) (Figure 1.15). The frequency of chromosomally unstable tumours was increased in gastro-oesophageal-junction adenocarcinomas, and most tumours positive for Epstein-Barr virus were located in the fundus or body of the stomach. Finally, tumours positive for this virus were mostly found in men (81%), but the predominance of microsatellite unstable tumours slightly favored women (56%) (Figure 1.16).

EBV subtype Deregulated pathways and candidate drivers of each distinct classes of gastric cancer were identified underlining the possibility of customized treatment and determination of prognosis. EBV-positive tumours harbor a high CpG island methylator phenotype CIMP) and exhibit a strong predilection for *PIK3CA* mutations and *ARID1A* mutations. All EBV-positive tumours assayed displayed *CDKN2A* ($p16^{INK4A}$) promoter hypermethylation but lacked the *MLH1* hypermethylation characteristic of (MSI-associated tumours in line with previous studies (Bernal et al. 2012). EBV-positive tumours also show amplification of immune stimuli related kinase *JAK2*, and immunosuppressant proteins: PD-L1 and PD-L2, suggesting that PD-L1/2 antagonists and JAK2 inhibitors be tested in this subgroup (Cancer Genome Atlas Research 2014).

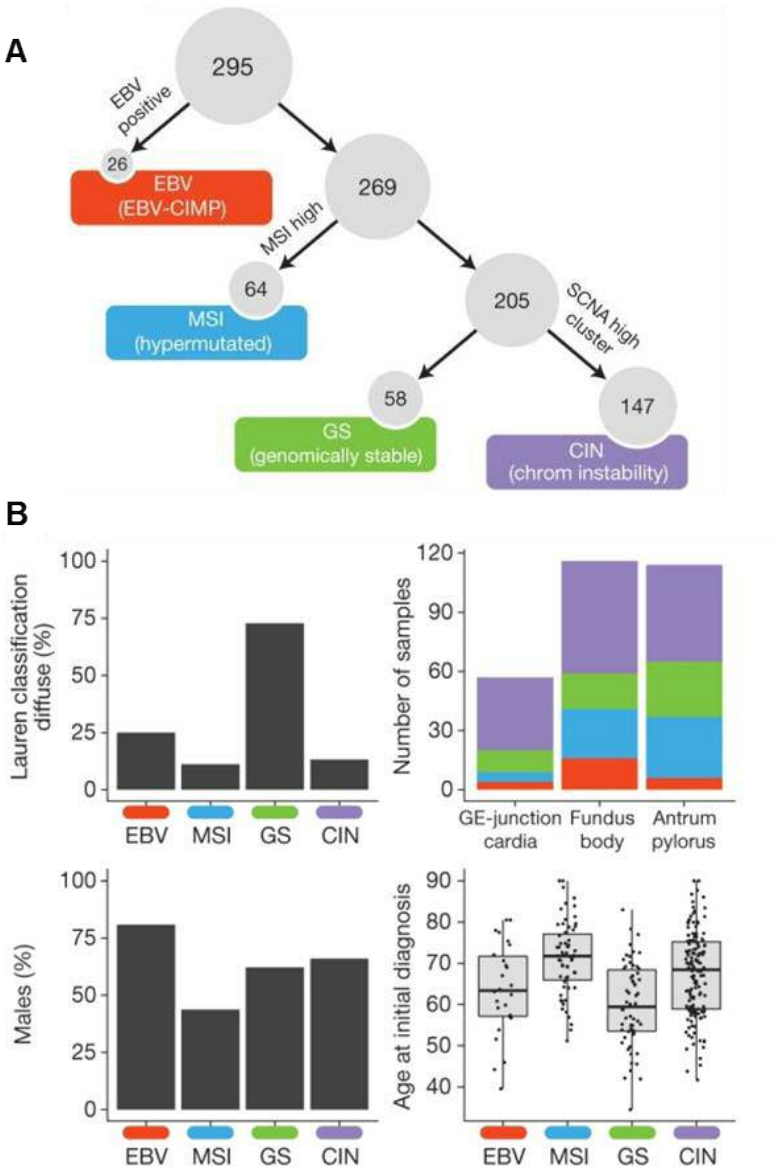

Figure 1.15: Differences in clinical and histological characteristics among subtypes. **A** Flowchart outlines how tumours were classified into molecular subtypes. **B,** Epstein–Barr virus (EBV)-positive (red), microsatellite instability (MSI, blue), genomically stable (GS, green) and chromosomal instability (CIN, light purple) and ordered by mutation rate. The plot of patient age at initial diagnosis shows the median, 25th, and 75th percentile values (horizontal bar, bottom and top bounds of the box), and the highest and lowest values within 1.5 times the interquartile range (top and bottom whiskers, respectively). GE, gastroesophageal. Source: Comprehensive molecular characterization of gastric adenocarcinoma (Cancer Genome Atlas Research 2014).

MSI subtype tumours showed elevated mutation rates and hypermethylation (including hypermethylation at the *MLH1* promoter). Mutations in the top ten significantly mutated genes, including *TP53*, *KRAS*, *ARID1A*, *PIK3CA*, *ERBB3*, *PTEN, HLA-B, RNF43, B2M,* and *NF1*. *B2M* resulted in loss of expression of HLA class 1 complexes (Bernal et al. 2012),

suggesting an impair in reducing antigen presentation to the immune system (Cancer Genome Atlas Research 2014).

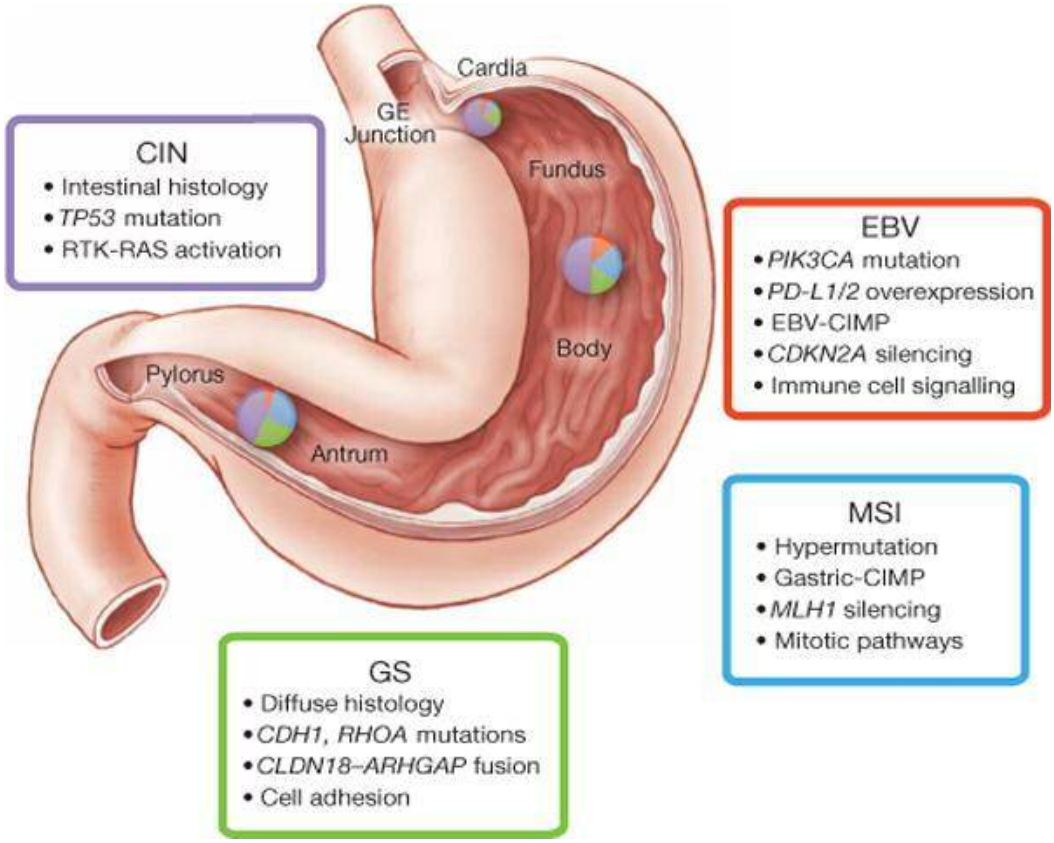

Figure 1.16: Key features of gastric cancer molecular subtypes. As proposed by TCGA. This schematic lists some of the salient features associated with each of the four molecular subtypes of gastric cancer. Distribution of molecular subtypes in tumours obtained from distinct regions of the stomach is represented by inset charts. Epstein–Barr virus (EBV)-positive (red), microsatellite instability (MSI, blue), genomically stable (GS, green) and chromosomal instability (CIN, light purple) (Cancer Genome Atlas Research 2014).

CIN subtype Phosphorylation of EGFR (Py1068) was significantly elevated in the CIN subtype, consistent with amplification of *EGFR* within that subtype. Elevated expression of p53 was also consistent with frequent *TP53* mutation and aneuploidy in the CIN subtype (Cancer Genome Atlas Research 2014). Suppressed cytokines such as IL1B, IL2, IL3, IL21, IL27, and INFG were found in CIN suggesting that high copy-number alteration may play roles in cancer immunity by suppressing activation of immune cells (Sohn et al. 2017).

GS subtype *CDH1* somatic mutations (37% of cases) and ras homolog family member A *(RHOA)* mutations were almost exclusively enriched in the genome stable subtype. Analysis

of base changes' patterns within gastric cancer revealed elevated rates of C to T transitions at CpG dinucleotides and A to C transversions at the 3' adenine of AA dinucleotides, especially at AAG trinucleotides. In agreement with a prior study, the A to C transversions were prominent in CIN, EBV and genome stable gastric cancers, not in MSI tumours (Dulak et al. 2013).

The clinical utility of molecular classification has been reported recently. The EBV subtype was associated with the best prognosis, for both DFS (P=0.006 by the log-rank test) and OS. The genomically stable (GS) subtype was associated with the worst prognosis. Patients with the MSI and CIN subtypes had a moderate prognosis. Patients with the CIN subtype exhibited the greatest benefit from adjuvant chemotherapy (either single-agent 5-fluorouracil (5FU) or a combination of 5FU and cisplatin/oxaliplatin, doxorubicin, or paclitaxel), as evidenced by significantly increased DFS rates. The 3-year DFS rate was 58.7% for those who received chemotherapy, compared with 33.5% for those who did not. The hazard ratio (HR) for recurrence among those who received adjuvant chemotherapy was 0.39 (95% CI, 0.16–0.94, p=0.03). However, no benefit from adjuvant chemotherapy was observed among patients with the GS subtype. Activated transcription regulator NUPR1 may be blamed for chemoresistance (Vincent et al. 2012; Chowdhury et al. 2009). Patients with the MSI subtype showed only moderate benefit from adjuvant chemotherapy. The benefit of adjuvant chemotherapy could not be assessed for patients with the EBV subtype because all patients received chemotherapy (Sohn et al. 2017).

1.1.4.7.2 The classification system proposed by ACRG

Similarly, the Asian Cancer Research Group (ACRG) (Cristescu et al. 2015) also proposed a four-subgroup classification system associated with distinct genomic alterations, disease progression, and prognosis across multiple gastric cancer cohorts, including microsatellite stable with epithelial-to-mesenchymal transition features (MSS/EMT), MSS with mutant type of TP53 (MSS/TP53+), and MSS with wild-type TP53 (MSS/TP53–).

MSI tumours (22.7%), with a parallel distribution ratio as the analysis from TCGA (22%), were hyper-mutated intestinal-subtype tumours (>60%) predominantly occurring in the antrum; diagnosed at clinical stage I/II (>50%). MSI tumours had the best prognosis; their

recurrence rate (22%) after surgical resection of primary GC was the lowest among all 4 subtypes.

MSS/EMT subtype The MSS/EMT (15.3%) and MSI distribution outliers exhibited a mutually exclusive pattern. MSS/EMT subtype occurred at a significantly younger age than did other subtypes. The majority (>80%) of the subjects in this subtype were diagnosed with diffuse-type at stage III/IV. The MSS/EMT subtype also had the worst prognosis and the highest recurrence rate (63%), with recurrences located mostly in the peritoneal cavity. *CDH1* mutations were highly prevalent (37%) in the TCGA Genome Stable (GS) subtype but were infrequent in the ACRG MSS/EMT subtype (2.8%).

For the remaining tumours, a two-gene (CDKN1A [also known as p21] and MDM2) p53-activity signature was applied to reflect p53-activity. The signature shows a high score in tumours with intact p53 activity (26.3%) and a low score in tumours with the p53 functional loss (35.7%). Further analysis revealed a significant association between the p53 activity signature and *p53* mutation status. The MSS/*p53*− subtype showed the highest prevalence of *p53* mutations (60%), with recurrent focal amplifications in *ERBB2*, *EGFR*, Cyclin E1 (*CCNE1)*, Cyclin D1 (*CCND1)*, *MDM2* and *MYC* and a corresponding increased mRNA and protein levels of EGFR and ERBB2; By contrast the MSS/*p53*+ subtype showed a relatively higher prevalence (compared to MSS/*p53*−) of mutations in *APC*, *ARID1A*, *KRAS*, *PIK3CA,* and *SMAD4*. MSS/*p53*+tumours which were found to be correlated with EBV infection and had the second-best prognosis, followed by MSS/*p53*-tumours. Whereas the *p53* signature is associated with survival in the MSS non-EMT subtype, neither *p53* mutation status nor tumour proliferation signature alone significantly predicts survival. A more recent project from Japan, employing ACRG classification to categorize patients with gastric cancer using *p53* tumour-specific single nucleotide mutation, found that the patients were significantly younger in EMT. The undifferentiated type was significantly dominant in MSI. There was no statistically significant difference in tumour depth, lymph node metastasis, or tumour stage among the groups. Two-year cause-specific survival (CSS) rates were 95.5% in MSI, 49.9% in EMT, 65.5% in *p53*+, and 78.5% in *p53*- (P=0.048). Although the follow-up period was insufficient, CSS was worse in *p53*+ than in *p53*-tumours (Ahn et al. 2017). These two newly classification system delineated the molecular signatures associated with distinct clinical outcomes and potential therapeutic implications. Currently, the antitumour

efficacy of a molecularly targeted agent is tested in all gastric cancer types regardless of molecular subtypes both in preclinical and clinical trials. Molecular screening and therapeutic development according to gastric cancer molecular classifications may help to stratify patients. (Cancer Genome Atlas Research 2014).

1.1.5 Pathology of gastric cancer

The morphological heterogeneity of gastric carcinomas is also reflected by the frequent occurrence of two or more distinct components in individual cases (Caldas et al. 1999). The classical classification system Laurén's criteria, introduced in 1965, and remains currently widely accepted and employed, since it constitutes a simple and robust classification approach (Lauren 1965). As discussed in the previous section, intestinal and diffuse gastric cancers exhibit a number of distinct clinical and molecular characteristics, including histogenesis, cell differentiation, epidemiology, aetiology, carcinogenesis, biological behaviours, and prognosis.

Carcinogenesis of intestinal gastric cancer

It is believed that a multistep cascade model for the development of intestinal-type gastric adenocarcinoma consists of a sequential precancerous process of with the following well-recognized steps progression from chronic superficial (non-atrophic) gastritis (chronic active inflammation), to chronic atrophic gastritis (gland loss) to intestinal metaplasia, followed by dysplasia and finally, gastric adenocarcinoma （Figure 1.17） (Lauren 1965; Correa 1992). It is generally recognized that the process starts during childhood, triggered by the infection with *H. pylori*, and advances slowly through the years, eventually leading in a few patients, after several decades, to invasive carcinoma (Correa and Piazuelo 2011). This chronic inflammation could induce higher levels of inducible nitric oxide synthase and spermine oxidase, enzymes involved in nitrosative and oxidative stress that permanently alter the DNA molecules of the gastric epithelial cells, such as *p53* mutation and deficiency in mismatch repair genes. Another hypothesis postulates that host innate immune response such as bone marrow-derived cells contribute to the development of gastric cancer in the Helicobacter-infected gastric mucosa. Experiments in mice reconstituted with labeled bone marrow and infected with *H. felis* (the mouse-adapted *Helicobacter* species) demonstrated that bone marrow-derived cells travel to, and engraft in, gastric mucosa with chronic inflammation and

progress to adenocarcinoma (Peek et al. 2010). At the same time, the host genetic susceptibility cannot be ignored. Important advances include investigations of polymorphisms in genes associated with the immune response to *H. pylori* infection, mainly in IL-1B, IL1RN, TNF, and IL10. IL-1β is a proinflammatory cytokine and a potent inhibitor of gastric acid secretion (El-Omar 2001). It has been hypothesized that profound suppression of acid secretion promotes dissemination of *H. pylori* proximally to the corpus, leading to a more extensive and severe gastritis that may favor the development of atrophy and subsequently cancer (El-Omar 2001).

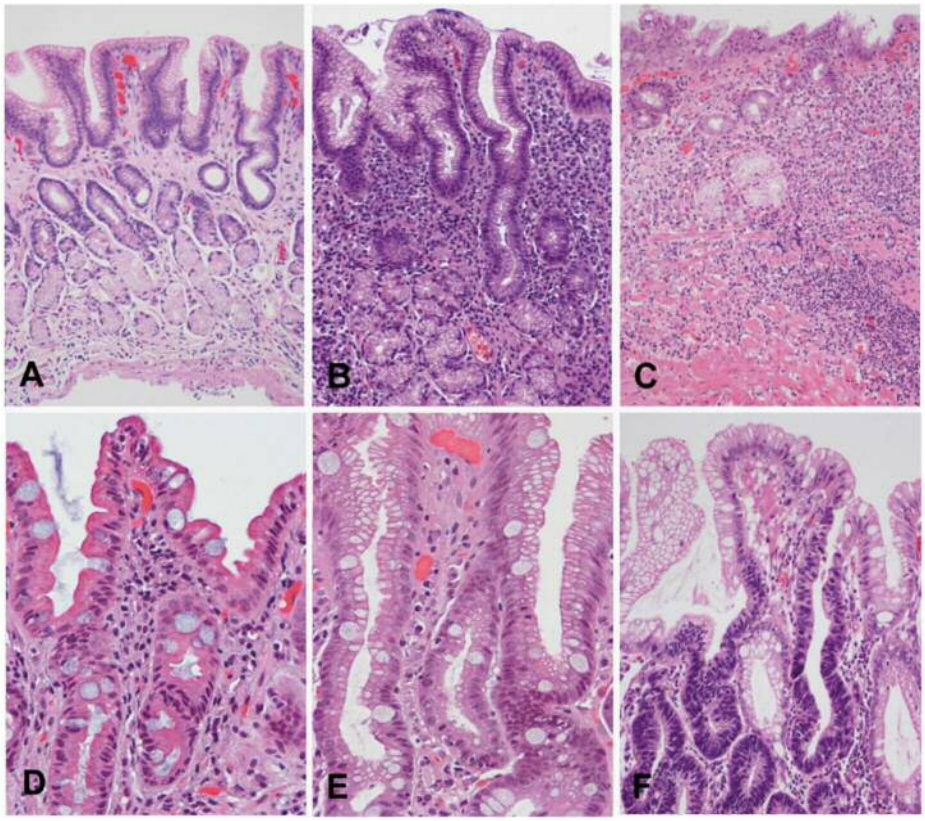

Figure 1.17: Haematoxylin-eosin staining for Correa's precancerous cascade in gastric cancer. A, Normal gastric mucosa. **B**, Non-atrophic chronic gastritis. The abundant inflammatory infiltrates in lamina propria with well-preserved glands observed in the deeper half of the mucosa. **C**, Multifocal atrophic gastritis without intestinal metaplasia. Marked loss of glands, with a prominent inflammatory, infiltrate and proliferation of fibrous tissue in the lamina propria. **D**, Intestinal metaplasia, complete type. Goblet cells alternating with absorptive enterocytes that present well-developed brush border. E, Intestinal metaplasia, incomplete type. Goblet cells alternating with columnar cells that contain mucin droplets of variable sizes. **F**, Dysplasia. Epithelium with high-grade dysplasia (lower half of the photograph) occurring in a background of incomplete metaplasia (observed in the foveolar superficial epithelium). (H&E; original magnification: A-C x100; D-F x200). Source: Gastric Cancer: Overview, available from http://colombiamedica.univalle.edu.co/index.php/comedica/article/view/1263/2150

Carcinogenesis of diffuse gastric cancer

Diffuse-type adenocarcinomas do not show gender predominance, tend to develop in younger subjects, have a poorer prognosis than the intestinal-type tumours, and are more frequently located in the proximal stomach than in the distal stomach. Although environmental factors seem to play a less important role than in the intestinal-type tumours, *H. pylori* infection is also associated with the development of diffuse-type adenocarcinomas (Gong et al. 2018; Kwak et al. 2014; Correa and Piazuelo 2012; Watanabe et al. 2012; Tatemichi et al. 2008; Parsonnet et al. 1991; Marshall and Warren 1984). *H. pylori*-induced inflammation activity has been shown to be well correlated with serum Hp-IgG or pepsinogen II levels (Biasco et al. 1993; Plebani et al. 1996; Tu et al. 2014; Hsu et al. 1997; Tatemichi et al. 2008). In a recent study, the proportion of diffuse-type gastric cancers increased with higher Hp-IgG titre groups only among the non-smokers, and more patients with intestinal-type gastric cancer had histories of smoking than those with diffuse-type gastric cancer (Kwak et al. 2014). This could be partly explained by the hypothesis that intestinal-type gastric cancer is more likely related to environmental factors than diffuse-type gastric cancer (Chen et al. 2016). (Table 1.5)

Table 1.5: The comparison between the intestinal and diffuse type of gastric cancer. Summarized from the review: Laurén classification and individualized chemotherapy in gastric cancer (Ma et al. 2016).

Characteristics	Laurén classification type	
	Intestinal gastric cancer	**Diffuse gastric cancer**
Clinical	commonly in elderly male patients	commonly in younger female patients
	usually affects the gastric antrum	usually affects the stomach body
	exhibits a longer course and better prognosis	presents shorter duration and worse prognosis
Pathological	with exitence of adhesion	lacking adhesion and infiltrate the stroma as single cells or small subgroups, leading to a population of non-cohesive, scattered tumour cells
	arranged in tubular or glandular formations	Intracellular mucus may push the nucleus of the cell aside to form signet-ring cell carcinoma.
	Associated with intestinal metaplasia	without easily recognized precursor lesions
	associated with lymphatic or vascular invasion	Peritoneal metastasis of diffuse gastric cancer

	lesions are scattered in distant positions	
Epidemiological Etiology and Pathogenesis	more prevalent in high-risk areas associated with environmental factors share common dietary and environmental risk factors atrophic gastritis, intestinal metaplasia involves DNA methylation (such as *CDH1*), histone modifications and chromosome recombination (Yamamoto et al. 2011)	more prevalent in low-risk areas presents a genetic etiology gastritis
Genetic factors	*CTNNB1* (the gene encoding β-catenin) mutation 17-27% *K-ras* mutation 0-18% in both histological types Amplifications of the *ERBB2* *p53* mutations (36-43%)	*p53* mutations (0-21%) Somatic mutations of E-cadherin (in 33-50% sporadic diffuse-type gastric cancer)

Laurén's classification has, nevertheless, several drawbacks. The first concerns the existence of a fairly large group of tumours which do not fit within the two major types. This group of "unclassified" or "indeterminate" gastric cancer includes undifferentiated (solid) carcinomas, as well as carcinomas exhibiting a dual pattern of differentiation (mixed intestinal and diffuse). The solid carcinomas display a clinicopathological profile similar to that of glandular (intestinal) carcinomas, thus supporting the assumption that they could be considered as a solid variant of intestinal carcinoma. Another drawback to Laurén's classification concerns the confusion linked to the term "intestinal". This led to the proposal of a modification of Laurén's classification which recognizes four main types of gastric cancer: glandular, isolated cell type, solid, and mixed carcinoma (Caldas et al. 1999). The importance of distinguishing two main histopathological types of gastric cancer, one with a diffuse component (isolated cell and mixed types) and one without a diffuse component (glandular/intestinal and solid types), is highlighted by finding somatic E-cadherin mutations exclusively in the first group (Muta et al. 1996; Tamura et al. 1996; Machado et al. 1999).

Features of gastric mucosa at the periphery of sporadic gastric carcinomas are in keeping with these two histogenetic pathways. Chronic atrophic gastritis and intestinal metaplasia are significantly more frequent at the periphery of glandular (intestinal) carcinomas and there is a higher prevalence of foveolar hyperplasia at the mucosa overlying or at the periphery of isolated cell type (diffuse) carcinomas (Carneiro et al. 1994).

Mixed stomach carcinomas, regardless of displaying a predominantly intestinal (glandular), or a predominantly diffuse (isolated cell) pattern, do carry, in a multivariate analysis, a significantly worse prognosis than the main types of Laurén's classification (intestinal, diffuse and unclassified/solid types) (Carneiro et al. 1995).

1.1.6 Diagnosis and staging of gastric cancer

Diagnosing gastric cancer in its early stages is a difficult task. Symptoms do not appear until the lesion reaches late stages of development and are generally non-specific (Caldas et al. 1999). When the diagnosis of gastric carcinoma is established, it is at an incurable advanced stage (stage III or IV) in over two-thirds of cases in non-endemic regions. In endemic regions such as Japan, which use mass screening protocols, a higher rate of diagnosis of early-stage gastric cancers has been observed for the past two decades (Yoshida and Saito 1996). Survival after early gastric cancer is much better than advanced lesions, so identifying these lesions at the earliest of stages is imperative for optimal survival. There are several conditions/lesions of the stomach, such as chronic atrophic gastritis, intestinal metaplasia, dysplasia/intraepithelial neoplasia, generally recognized as precancerous with varying degrees of risk but, excluding dysplasia, routine interval surveillance examinations such as endoscopy are not routinely performed in these conditions (The American Society for Gastrointestinal Endoscopy 1988, Dinis-Ribeiro et al. 2012).

The most common symptoms at diagnosis of gastric cancer are anorexia, dyspepsia, weight loss, and abdominal pain. Patients with tumours at the gastro-oesophageal junction or proximal stomach may also present with dysphagia.

The diagnosis of gastric cancer relies on endoscopy and biopsy. For locally advanced gastric cancer, EUS and CT of the chest and abdomen are currently the primary means of staging. Laparoscopy is used to exclude small-volume peritoneal metastatic disease. A meta-analysis

showed that the sensitivity and specificity of EUS could discriminate between T1–T2 (superficial) and T3–T4 (advanced) gastric carcinomas, with a sensitivity of 86% (95% CI 81%-90%). The sensitivity values for diagnosis of superficial tumours (T1a vs T1b) and lymph node status (positive vs negative) were 87% (81%-92%) and 83% (79%-87%), respectively (Mocellin and Pasquali 2015).

EUS is useful in the preoperative diagnosis of T stage for selecting limited treatments, such as laparoscopic proximal gastrectomy (LPG), which lacks the ability to palpate the tumour. The tumour size may be underestimated if tumours are located in the upper third of the stomach and are more histologically diffuse, scirrhous, with infiltrative growth, and more frequent lymphatic and venous invasion. It is suggested that gastric cancer in the upper third of the stomach with diffuse-type histology and >20 mm needs particular attention when considering the application of LPG (Van Cutsem et al. 2016).

PET-CT (positron emission tomography [PET]) and MRI are not routinely used for staging in gastric cancer, although growing evidence suggests that PET-CT could improve staging through increased detection of involved lymph nodes and metastatic disease. These tests, however, are not always informative, especially in patients with mucinous tumours, as they might under stage the disease (Van Cutsem et al. 2016; Altini et al. 2015; Waddell et al. 2014). A role for MRI also seems to be emerging, especially for the detection of peritoneal metastases. Intraperitoneal metastases are common in people with gastric or gastro-oesophageal-junction carcinomas and are difficult to diagnose with conventional imaging methods.

Laparoscopic staging, with or without peritoneal lavage for malignant cells, remains controversial, but expert groups recommend this approach in patients with potentially curable gastric or gastro-oesophageal-junction carcinomas (Waddell et al. 2014; Van Cutsem et al. 2008). Peritoneal lavage showing positive cytology, in the absence of macroscopic peritoneal metastases, is associated with poor survival and is defined as metastatic disease (Mezhir et al. 2011). Serosal infiltration is a strong indicator of peritoneal carcinomatosis, which develops in up to 60% of patients with gastric cancer (Nakamura et al. 1992).

The staging system most often used for gastric cancer is the AJCC TNM system, which is

based on tumour size (T), number of lymph node involved (N), metastasis to distant sites (M). TNM classification and the corresponding staging is crucial to ensure that appropriate interventions are selected, and for monitoring outcomes. According to guidelines from the American Cancer Society, pathologic stage (pStage, also called the surgical stage) is determined by examining tissue removed during an operation. If surgery is not possible, the cancer will be given a clinical stage (cStage) instead, which is based on the results of a physical exam, biopsy, and imaging tests. The clinical stage will be used to help plan treatment, but it may not predict the patient's outlook as accurately as a pathologic stage, due to the difficulty in accurately staging tumour thickness and nodal status.

Staging and TNM classification of gastric cancer according to the most recent American Joint Committee on Cancer (AJCC) system 8th edition of the guidelines and staging manual is listed in Table 1.6 (Gastric cancer Stages, available at https://www.cancer.org/cancer/stomach-cancer/detection-diagnosis-staging/staging.html).

With the development of neoadjuvant chemotherapy in gastric cancer (see details below), a new concept of post neoadjuvant pathological stage (ypTNM or ypStage) is introduced. ypStage represents the combination of tumour status and its response to preoperative therapy; pStage does not incorporate tumour treatment response. This new ypStage system was created based on the National Cancer Database (NCDB), which included a relatively small number of patients treated with preoperative therapy (<700) with a short median follow-up (23 months); therefore, additional studies from more cancer centers that utilize preoperative therapy are needed (Ikoma et al. 2018).

Table 1.6: Pathologic stage. It is determined by examining tissue removed during an operation. Source: Gastric cancer Stages, American Cancer Society, available at https://www.cancer.org /cancer/stomach-cancer/detection-diagnosis-staging/staging.html. The T categories are described in the table below, except for TX: the main tumour cannot be assessed due to lack of information. T0: No evidence of a primary tumour. The N categories are described in the table below, except for NX: Regional lymph nodes cannot be assessed due to lack of information.

AJCC Stage	Stage grouping	Stage description
0	Tis N0 M0	There is high-grade dysplasia (very abnormal-looking cells) in the stomach lining OR there are cancer cells only in the top layer of cells of the mucosa (innermost layer of the stomach) and have not grown into deeper layers of tissue such as the lamina propria (Tis). This stage is also known as carcinoma in situ (Tis). It has not spread to nearby lymph nodes (N0) or distant sites (M0).
IA	T1 N0 M0	The tumour has grown from the top layer of cells of the

		mucosa into the next layers below such as the lamina propria, the muscularis mucosa, or submucosa (T1). It has not spread to nearby lymph nodes (N0) or to distant sites (M0).
IB	T1 N1 M0	The cancer has grown from the top layer of cells of the mucosa into the next layers below such as the lamina propria, the muscularis mucosa, or submucosa (T1) AND it has spread to 1 to 2 nearby lymph nodes (N1). It has not spread to distant sites (M0).
	T2 N0 M0	The cancer is growing into the muscularis propria layer (T2). It has not spread to nearby lymph nodes (N0) or to distant sites (M0).
IIA	T1 N2 M0	The cancer has grown from the top layer of cells of the mucosa into the next layers below such as the lamina propria, the muscularis mucosa, or submucosa (T1) AND it has spread to 3 to 6 nearby lymph nodes (N2). It has not spread to distant sites (M0).
	T2 N1 M0	The cancer is growing into the muscularis propria layer (T2) and it has spread to 1 to 2 nearby lymph nodes (N1) but not to distant sites (M0).
	T3 N0 M0	The cancer is growing into the subserosa layer (T3). It has not spread to nearby lymph nodes (N0) or to distant sites (M0).
IIB	T1 N3a M0	The cancer has grown from the top layer of cells of the mucosa into the next layers below such as the lamina propria, the muscularis mucosa, or submucosa (T1) and it has spread to 7 to 15 nearby lymph nodes (N3a). It has not spread to distant sites (M0).
	T2 N2 M0	The cancer is growing into the muscularis propria layer (T2) and it has spread to 3 to 6 nearby lymph nodes (N2). It has not spread to distant sites (M0).
	T3 N1 M0	The cancer is growing into the subserosa layer (T3) and it has spread to 1 to 2 nearby lymph nodes (N1) but not to distant sites (M0).
	T4a N0 M0	The tumour has grown through the stomach wall into the serosa, but the cancer hasn't grown into any of the nearby organs or structures (T4a). It has not spread to nearby lymph nodes (N0) or to distant sites (M0).
IIIA	T2 N3a M0	The cancer is growing into the muscularis propria layer (T2) AND it has spread to 7 to 15 nearby lymph nodes (N3a). It has not spread to distant sites (M0).
	T3 N2 M0	The cancer is growing into the subserosa layer (T3) and it has spread to 3 to 6 nearby lymph nodes (N2). It has not spread to distant sites (M0).
	T4a N1 M0	The cancer has grown through the stomach wall into the serosa, but it has not grown into any of the nearby organs or structures (T4a). It has spread to 1 to 2 nearby lymph nodes (N1) but not to distant sites (M0).
	T4a N2 M0	The cancer has grown through the stomach wall into the serosa, but it has not grown into any of the nearby organs or structures (T4a). It has spread to 3 to 6 nearby lymph

		nodes (N1) but not to distant sites (M0).
	T4b N0 M0	The cancer has grown through the stomach wall and into nearby organs or structures (T4b). It has not spread to nearby lymph nodes (N0) or to distant sites (M0).
IIIB	T1 N3b M0	The cancer has grown from the top layer of cells of the mucosa into the next layers below such as the lamina propria, the muscularis mucosa, or submucosa (T1) and it has spread to 16 or more nearby lymph nodes (N3b). It has not spread to distant sites (M0).
	T2 N3b M0	The cancer is growing into the muscularis propria layer (T2) and it has spread to 16 or more nearby lymph nodes (N3b). It has not spread to distant sites (M0).
	T3 N3a M0	The cancer is growing into the subserosa layer (T3) and it has spread to 7 to 15 nearby lymph nodes (N3a). It has not spread to distant sites (M0).
	T4a N3a M0	The cancer has grown through the stomach wall into the serosa, but it has not grown into any of the nearby organs or structures (T4a) and it has spread to 7 to 15 nearby lymph nodes (N3a). It has not spread to distant sites (M0).
	T4b N1 M0	The cancer has grown through the stomach wall and into nearby organs or structures (T4b). It has spread to 1 to 2 nearby lymph nodes (N1) but not to distant sites (M0).
	T4b N2 M0	The cancer has grown through the stomach wall and into nearby organs or structures (T4b). It has spread to 3 to 6 nearby lymph nodes (N1) but not to distant sites (M0).
IIIC	T3 N3b M0	The cancer is growing into the subserosa layer (T3) and it has spread to 16 or more nearby lymph nodes (N3b). It has not spread to distant sites (M0).
	T4a N3b M0	The cancer has grown through the stomach wall into the serosa, but it has not grown into any of the nearby organs or structures (T4a) and it has spread to 16 or more nearby lymph nodes (N3b). It has not spread to distant sites (M0).
	T4b N3a M0	The cancer has grown through the stomach wall and into nearby organs or structures (T4b) and it has spread to 7 to 15 nearby lymph nodes (N3a). It has not spread to distant sites (M0).
	T4b N3b M0	The cancer has grown through the stomach wall and into nearby organs or structures (T4b) and it has spread to 16 or more nearby lymph nodes (N3b). It has not spread to distant sites (M0).
IV	Any T Any N M1	The cancer can grow into any layers (Any T) and might or might not have spread to nearby lymph nodes (Any N). It has spread to distant organs such as the liver, lungs, brain, or the peritoneum (the lining of the space around the digestive organs) (M1).

1.1.7 Treatment of gastric cancer

Treatment of gastric cancer depends on the TNM classification and staging which reflect both the primary site of cancer started and its pattern of growth and metastasis. Despite

invading the wall of the stomach and nearby organs, the stomach has a very rich network of lymph vessels and nodes, and the biological factors determine that gastric cancers spread easily through the lymph vessels and nearby lymph nodes. As gastric cancer becomes more advanced, it can travel through the bloodstream and metastasize to organs such as the liver, lungs, and bones, which make it harder to treat.

1.1.7.1 Surgery

Adequate surgical resection is the only therapeutic option with an intention to cure for gastric cancer (Ikoma et al. 2018). Endoscopic resection might be suitable as an alternative to surgery for small well-differentiated early-stage tumours (T1a). The extent of surgery is determined by tumour stage, diameter, location, and histological type. Adequate surgery in the stomach is defined as complete resection of primary cancer with tumour-free surgical margins of at least 4 cm and adequate lymphadenectomy (Van Cutsem et al. 2016). These requirements correspond to total gastrectomy for gastric cancers with signet-ring cells (linitis plastica), and those located in the upper third of the stomach or with atrophic gastritis. Cancer in the lower two-thirds of the stomach can often be treated with subtotal gastrectomy. At least 16 lymph nodes should be removed to enable adequate tumour staging and ensure optimum surgical resection (Van Cutsem et al. 2016). Although there is no worldwide consensus on the degree of lymphadenectomy, the D2 lymphadenectomy (perigastric [D1] plus coeliac artery and its branches) is generally recommended if the associated postoperative morbidity and mortality rates are acceptably low—for instance, in high-volume hospitals with experienced surgeons (Songun et al. 2010; Van Cutsem et al. 2016). This approach, together with the improved methods for staging, increased use of adjuvant and neoadjuvant therapies, and centralization of surgery has contributed to improved cure rates in various registries and studies, from 30% to up to 55% in the past decade.

Transabdominal total gastrectomy is the standard surgical approach to treat patients with Siewert type II or III cancer of the gastro-oesophageal junction. This procedure is extended with a transhiatal resection of the distal esophagus and lymphadenectomy of the lower mediastinum and the abdominal D2 nodal compartment. A thoracoabdominal approach in these patients can increase the risk of morbidity without improving survival and, therefore, is not usually recommended to treat cardia (type II) or subcardia (type III) gastric cancers

(Van Cutsem et al. 2016; Sasako et al. 2006).

Early gastric cancer is limited to the mucosa or submucosa (pathologically staged as T1 or lower), regardless of nodal status. Even in early gastric cancer, use of a multidisciplinary approach to determine the best therapeutic strategy (*i.e.*, endoscopic or surgical resection) is mandatory because lymph-node metastases occur in up to 20% of patients and correlate well with tumour penetration of the stomach wall and large tumour diameter (Dinis-Ribeiro et al. 2012; Wang et al. 2014).

Endoscopic versus surgical management of early gastric cancer has not been studied in randomized clinical trials, but surgical resection is viewed as the gold standard and is associated with 5-year recurrence-free survival of up to 98% (Youn et al. 2010). For mucosal gastric carcinoma (T1a), endoscopic resection is deemed sufficient in all European guidelines because the incidence of the lymph-node metastatic disease is very low. For patients with the early disease but suspected or histologically proven lymph-node metastasis, endoscopic resection should not be attempted, If the histopathological findings confirm a submucosal carcinoma (T1b) after endoscopic resection, surgical resection that includes systematic lymphadenectomy is recommended, because lymph-node involvement is seen in up to 20% of these patients. Endoscopic resection of early gastric cancer should be done as a complete en-bloc resection to allow full histological assessment of the lateral and basal margins (Van Cutsem et al. 2008; Moehler et al. 2015). Patients who have endoscopic resection should be monitored frequently by endoscopic surveillance.

Most patients with locally advanced gastric cancer, which invades the muscularis propria and beyond (pathologically staged as T2 or higher), present with metastases in lymph nodes, distant organs, or both. Locally advanced gastric cancer may need total resection of involved structures. Prophylactic splenectomy is discouraged because it increases the risk of operative morbidity and mortality without any survival benefit but might be necessary if the spleen or its hilar lymph nodes are affected. Only patients without metastatic disease are potential candidates for surgical management with curative intent, although selected patients with peritoneal carcinomatosis or positive peritoneal cytology might benefit from aggressive surgery in expert centers (Sano et al. 2004). Cytoreductive surgery with hyperthermic intraperitoneal chemotherapy for prevention and treatment of peritoneal carcinomatosis

from gastric cancer was reported to be associated with improved OS at 1, 2, and 3 years, but not at 5 years in a meta-analysis (Coccolini et al. 2014). However, better designed randomized clinical trials with robust methods are needed to confirm the potential benefits of this approach (Van Cutsem et al. 2016).

Minimally invasive surgery by laparoscopy has been gradually accepted in surgical oncology over the past decade. Laparoscopic distal gastrectomy compared with open surgery was associated with similar lymph-node dissection and long-term survival and with reduced intraoperative blood loss, postoperative complications, analgesic consumption, and length of hospital stay (Zeng et al. 2012). Well-designed randomized clinical trials with robust methods, a precision evaluation of preoperative stage and a comprehensive understanding of the biological behavior of gastric cancer may be required for better selection of adequate patients who can benefit from laparoscopic gastrectomy.

1.1.7.2 Radiotherapy

Ionizing radiation (IR) introduces overwhelming genetic lesions in the DNA of irradiated cells, causing cell death. Currently, adjuvant radio-chemotherapy is recommended in patients with loco-regionally advanced carcinoma of the gastro-oesophageal junction (T2N1-3M0 or T3N0-3M0) (Zeng et al. 2012). For patients with ⩾Stage IB gastric cancer who have undergone surgery without administration of preoperative chemotherapy (e.g. due to understaging before the initial decision for upfront surgery), postoperative chemoradiotherapy (CRT) or adjuvant chemotherapy is recommended (Smyth et al. 2016). Although, radiotherapy is proven to be tolerated, improves the resectability of the tumour, and does not increase the frequency of surgical complications. Off-target effects remain a serious burden on patients receiving radiation therapy. The lungs are one of the most sensitive organs to radiation, and chest radiation has a high chance of leading to radiation-induced lung injury. For unresectable gastric cancer, radiotherapy is justified in cases with anaemia, and/or in the cases with pyloric or cardiac obstruction (Sitarz et al. 2018). A recent meta-analysis demonstrated that more than two-thirds of patients receiving palliative radiotherapy would have a clinical benefit. Low biological equivalent dose (<39Gy regimens) can be adequate for symptom palliation, such as diminishing bleeding and/or improving the food passage. Toxicity rates appear acceptable for patients treated with palliative radiotherapy

alone. The optimal dose fractionation regimen for symptom palliation remains unclear. The effect is usually short (3–6 months), but it is an easy therapeutic option. Prospective studies to determine the effects of palliative gastric palliative radiotherapy on health-related quality of life outcomes are still warranted (Tey et al. 2017).

1.1.7.3 Chemotherapy

No further treatment is usually needed after surgery for stage 0, or IA gastric cancer. However, for management of locally advanced disease, especially for patients with T3, T4, or node-positive tumours, adjuvant and neoadjuvant therapies are recommended. There is improved DFS and OS in patients who have undergone adequate complete surgical resection (R0) of locally advanced gastric cancer by eradicating microscopic disease locoregionally and at a distance from the primary tumour (Lutz et al. 2012; Van Cutsem et al. 2011; Cunningham et al. 2006).

Single-agent activity of many classical drugs was tested in advanced gastric cancer before the 1980s. Complete responses with single-agent therapy are uncommon, and partial responses ranged from 10-20%, followed by a short time period to disease progression (Table 1.7).

Table 1.7: Single-agent activity in advanced gastric cancer. Agents that have obtained more than 10% response rate. Source: Chemotherapy for gastric cancer (Sastre et al. 2006).

Agents	Response rate (%)
Mitomycin C	30
Doxorubicin	17
Epirubicin	19
Cisplatin	19
BCNU	18
5FU	21
Etoposide (oral)	21
Hydroxyurea	19
UFT	27
Capecitabine	19
S-1	45
Paclitaxel	17-23
Docetaxel	17-29
CPT-11	18

Chemotherapy regimens for gastric cancer have varied considerably since the 1980s. There were no analyses supporting the regular use of adjuvant chemotherapy for gastric cancer until 1993. Combination regimens of Platinum compounds, 5FU, taxanes or irinotecan were developed to improve overall response rate and survival (Table 1.8).

Table 1.8: Combination therapy for advanced gastric cancer. FAM fluorouracil-doxorubicin-mitomycin C, **FAMTX** methotrexate-leucovo-5FU-adriamycin, **FEMTX** adriamycin was substituted by its analogue 4-epi-doxorubicin, **ELF** 5FU-leucovorin -intravenous etoposide, **modified-EFL** oral etoposide, oral leucovorin and either 5FU continuous infusion or tegafur, **ECF** continuous 5FU infusion, cisplatin and epirubicin, **PF** cisplatin and 5FU, **EAP** cisplatin-etoposide-doxorubicin, **FLEP** 5FU modulated by folinic acid (FA)- epirubicin-cisplatin, **ECC** epirubicin-cisplatin-capecitabine, **P-S-1** cisplatin- S-1 (oral fluoropyrimidine derivative analogue), **MCF** mitomycin C, cisplatin and fluorouracil, **DP** docetaxel-cisplatin, **DCF** docetaxel-cisplatin-5FU, **EOF** epirubicin-oxaliplatin-5FU, **ECX** epirubicin-cisplatin-capecitabine, **EOX** epirubicin-oxaliplatin-capecitabine

	Response rate (%)	Median survival (months)
5FU-based combinations		
FAM	30-42	6-9
FAMTX	33-63	6
ELF	53	11
Modified-ELF	16-42	6-9.5
Cisplatin-5FU CI synergism		
PF	40	9-10
ECF	59-71	8.7
P-5FU 48-h CI	50	9.3
P-5FU 24-h CI	58	11
Cisplatin-based combinations		
EAP	33-64	9
FLEP	35	8
FLEP-type	39	11
LV5FU2-P	27	13.3
Combinations including new drugs		
P-CPT11	41-58	9-12
LOHP-CPT11	50	8.5
CPT11-bolus 5FU	22	7.6
CPT11- 5FU CI	20	7
P-Xeloda	54.8	10.1
ECC	59	9.6
P-S-1	73-74	12
TPFU/LV	50	11-14
DP	37-56	9-11
DCF	51	9.3

It is now well recognized that combination chemotherapy regimens improve patient outcomes, but there is no accepted global standard regimen. In the daily clinical practice, several drugs such as fluorouracil, capecitabine, cisplatin, oxaliplatin docetaxel, epirubicin, paclitaxel, and irinotecan are major components of conventional regimens. 5FU given as a continuous infusion in combination with cisplatin (FP) has consistently demonstrated superiority in terms of response rate and time to disease progression, compared with 5FU monotherapy and other combination regimens, although it has not shown a significant survival advantage in phase III clinical trial (Koizumi et al. 2008; Van Cutsem et al. 2006; Al-Batran et al. 2008; Boku et al. 2009; Cunningham et al. 2008). A small but clinically relevant 1-month mean average survival benefit of combination chemotherapy was shown to be statistically significant (p=0.001) compared to monotherapy in a meta-analysis of several clinical trials (Wagner et al. 2006). The combination of cisplatin, 5FU +/- epirubicin is the mostly commonly recommended first-line treatment for advanced gastric cancer (Bittoni et al. 2015). There are some regional variations in chemotherapy regimens. In the UK, the most popular chemotherapy is epirubicin plus cisplatin plus 5FU or epirubicin plus oxaliplatin plus capecitabine (Cunningham et al. 2008). In Europe, the most commonly used regimen is docetaxel plus cisplatin plus 5FU (DCF) or 5FU, leucovorin, and oxaliplatin (FOLFOX) (Van Cutsem et al. 2006). Cisplatin plus 5FU or DCF is the commonest scenario in the United States, while in Eastern countries, two drugs combination S-1 plus cisplatin in Japan, or capecitabine and oxaliplatin in South Korea are the most commonly administered therapy (Noh et al. 2014; Koizumi et al. 2008). The overall response rate for sequential treatment with epirubicin, oxaliplatin and 5FU (EOF) followed by docetaxel, oxaliplatin and 5FU (DOF) in a single-institution from Italy was 51.1 % (95 % CI 35.7-66.2 %) and 93.3 % of patients were progression-free 6 months after the onset of chemotherapy. A similar response rate (61.7%) was shown in the TCOG 3211 Clinical Trial conducted in Taipei, where the median progression-free survival and OS were 8.6 and 11.0 months, respectively (M. H. Chen et al. 2016). A recent Cochrane meta-analysis (Wagner et al. 2017) confirmed that chemotherapy improves gastric cancer patients' survival (by approximately 6.7 months) and quality of life in comparison to best supportive care alone. Furthermore, First-line combination chemotherapy improves survival (by one month) compared to single-agent 5FU. People with locally advanced disease or age<65 might benefit from a three-drug regimen including 5FU, docetaxel, and oxaliplatin as compared to a two-drug combination of 5FU

and oxaliplatin. However, the OS benefit from treatment with adjuvant chemotherapy is estimated to be approximately 4%, with the greatest benefit in patients with node-positive disease. A meta-analysis (GASTRIC [Global Advanced/Adjuvant Stomach Tumour Research International Collaboration] Group 2013) from Global Advanced/Adjuvant Stomach Tumour Research International Collaboration in 2013 collected individual treatment information from 4245 patients of 22 clinical trials and demonstrated the benefits of the experimental treatments over their corresponding controls which hazard reductions of 13% for OS (HR = 0.87, P < 0.0001,) and 21% for PFS (HR = 0.79, P < 0.0001,). Although these overall relative risk reductions translate into only modest absolute improvements in median OS and PFS, they nevertheless confirm the benefit of chemotherapy for advanced gastric cancer and justify further efforts at improving current regimens.

Given the relatively minor benefits of adjuvant chemotherapy seen in these early analyses, the high rate of local relapse continued to stimulate interest in adjunctive treatment modalities, resulting in two different but beneficial approaches. The first was postoperative chemoradiotherapy, which was tested in a US Southwest Oncology Group/Intergroup study (SWOG 9008/INT 0116, Figure 1.18A) (Macdonald et al. 2001), and the second was perioperative chemotherapy, tested in a UK Medical Research Council (MRC) randomized trial (the MRC Adjuvant Gastric Infusional Chemotherapy [MAGIC] trial, Figure 1.18B) (Cunningham et al. 2006). These trials demonstrated clinically and statistically significant survival benefits that have changed practice with two different treatment options in resectable gastric cancer. As the patient populations studied were different, the results are not directly comparable, but they do suggest treatment options for patients at different points in their care.

Based on experience from adjuvant chemotherapy, most patients, currently receive fluoropyrimidine- and platinum-based neoadjuvant therapy before initial surgery. This approach is preferred especially for patients with a high likelihood of developing distant metastases (*i.e.*, those with bulky T3/T4tumours, visible perigastric nodes by preoperative imaging studies, a linitis plastica appearance, or positive peritoneal cytology in the absence of visible peritoneal disease). However, there are no randomized trials demonstrating better

outcomes from neoadjuvant therapy versus initial surgery followed by any form of adjuvant therapy. Pragmatically there is a greater chance of delivering therapy in the preoperative setting, and patients who are at high risk of developing distant metastases may be spared the morbidity of unnecessary gastrectomy if evidence of distant metastases emerges after chemotherapy. Currently, upfront surgery still remains an accepted approach, especially for patients with clinically staged, non-bulky, T2 or T3 tumours with no visible perigastric nodes. Clinical studies for choosing the best chemotherapy regimen are still ongoing (Cunningham et al. 2006; Al-Batran et al. 2016; Xiong et al. 2014; Ronellenfitsch et al. 2013).

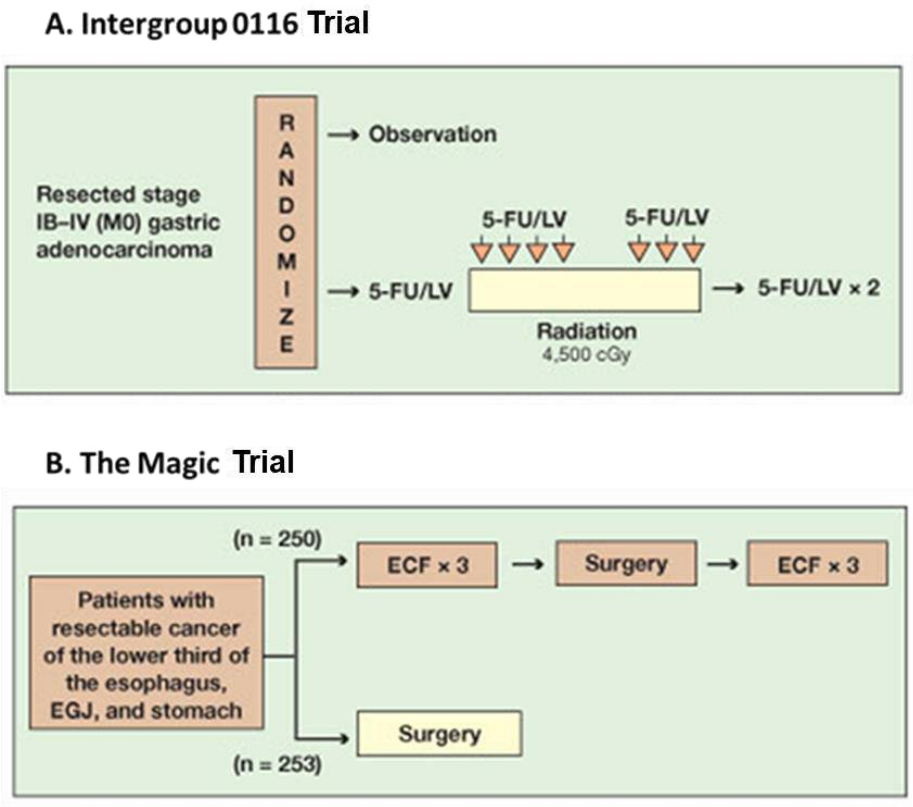

Figure 1.18: Designs of the Intergroup 0116 Trial and of the UK Medical Research Council's MAGIC Trial. A. A trial of postoperative chemoradiotherapy in stage IB-IV gastric cancer. 5FU stands for fluorouracil; LV stands for leucovorin. **B.** A trial of perioperative chemotherapy in patients with operable gastric cancer. ECF= epirubicin/cisplatin/fluorouracil; Source: Therapeutic Options in Gastric Cancer (Jackson et al. 2007).

The outlook for patients with metastatic gastric cancer is very poor, with median survival ranging from 4 months when treated only with best supportive care, to around 12 months when treated with combination cytotoxic chemotherapy. The most frequently used standard first-line chemotherapy regimen in metastatic gastric cancer is a combination of a

fluoropyrimidine with a platinum, although triple regimens including docetaxel might be useful in otherwise healthy patients with a high tumour burden. Median survival does usually not exceed 1 year. In patients with good performance status and organ function, second-line treatment with agents that were not used in first-line treatments (*i.e.*, taxanes or irinotecan) can lead to slight survival benefits (Ford et al. 2014; Kang et al. 2012; Bolke et al. 2008; Van Cutsem et al. 2006).

Generally, treatment regimens selection, dosing, administration, and the management of related adverse events for gastric cancer can be a complex process that should be handled by an experienced healthcare team. Clinicians must choose and verify treatment options based on the individual patient. Drug dose modifications and supportive care interventions should be administered accordingly. The cancer treatment regimens in Appendix 6 includes both U.S. Food and Drug Administration-approved and unapproved indications/regimens. These regimens are provided only to supplement the latest treatment strategies. The guidelines are a work in progress that may be refined when new significant data becomes available.

1.1.7.4 Target therapy

The pivotal ToGA trial was the first randomized, prospective, multicentre phase 3 trial to study the efficacy of targeted therapy with first line trastuzumab (a monoclonal antibody against HER2) in patients with HER2-positive advanced gastric or gastro-oesophageal-junction cancer (Bang et al. 2010). Up to 20% of gastric tumours overexpress the HER2 receptor, mostly because of *HER2* amplification. 584 patients were enrolled and received study treatment at least once. Median OS was 13.8 months (95% CI 12-16) in the trastuzumab group, compared with 11.1 months in the chemotherapy group (10–13) (hazard ratio 0·74; 95% CI 0·60-0·91; p=0·0046). The longest survival (median 16.0 months) was seen in patients with high HER2 protein overexpression and *HER2* amplification. On the basis of this study, trastuzumab in combination with cisplatin and a fluoropyrimidine has been approved for first-line treatment of advanced HER2-positive gastric and gastro-oesophageal-junction adenocarcinomas (Van Cutsem et al. 2015; Jorgensen 2010).

Randomised trials have included assessments of antibodies against EGFR (Waddell et al. 2013; Lordick et al. 2013), and VEGFR2 (Wilke et al. 2014; Fuchs et al. 2014) in combination

with chemotherapy, but results have generally shown no or limited benefit, partly due to the inappropriate selection of patients (Lordick et al. 2014; Tan et al. 2011). Several other biological targeted agents are being, or have been, investigated. Hepatocyte growth factor (HGF) and its receptor, the transmembrane tyrosine kinase cMET, as well as fibroblast growth factor receptor (FGFR) are among the candidate targets for new agents in advanced gastric cancer. Additionally, in view of the new data from the Cancer Genome Atlas research network, PD-1 and PD-L1 may serve as emerging targets for treatment, and initial promising results have been reported with pembrolizumab.

There is increasing recognition that for gastric cancer and other malignancies, that besides the tumour stage, the intrinsic subtypes of GC, based on distinct patterns of expression, may influence patient survival and response to chemotherapy. Distinct patterns of genomic alteration or protein expression may provide clues for management and improvement of patients' clinical outcomes.

1.1.8 Precision medicine for gastric cancer

Identifying specific signaling pathways in individual patients might improve treatment outcomes, for example, the use of anti-human epidermal growth factor receptor-2 monoclonal antibody, trastuzumab (Bang et al. 2010), anti-vascular endothelial growth factor receptor-2 monoclonal antibody, ramucirumab (Fuchs et al. 2014), and has shifted the previous histopathologic paradigm to incorporate new genetic and molecular features (Figure 1.19). However, equally importantly, tailoring individualized cytotoxic therapy for the treatment of gastric cancer is warranted (Ma et al. 2016).

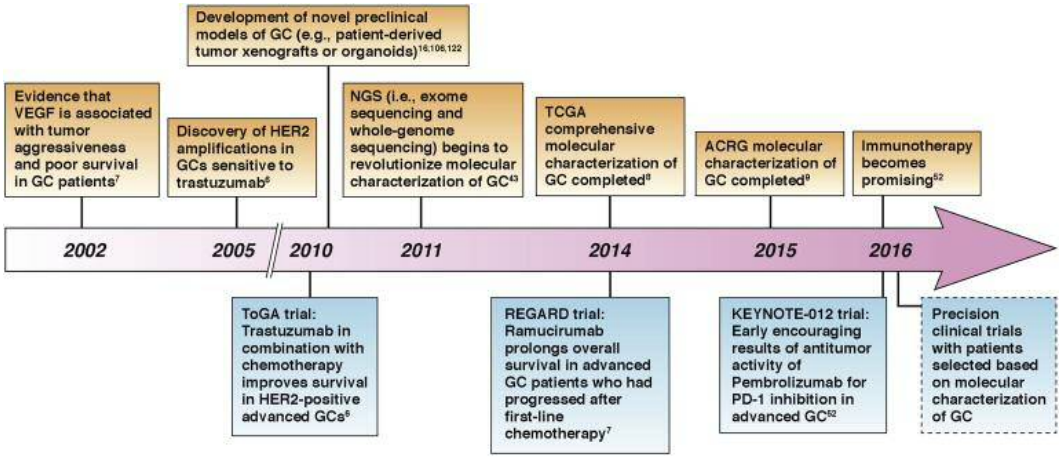

Figure 1.19: Timeline of selected major developments in gastric cancer (above arrow)

and related clinical trials (below arrow) in recent years. Source: Gastric Cancer in the Era of Precision Medicine. (Liu and Meltzer 2017)

1.1.8.1 Cytotoxic drugs sensitivity in gastric cancer according to Laurén classification

Evidence of different response to treatment between gastric cancer subtypes has been reported not only in patients with advanced disease but also in the adjuvant setting. In particular, in an updated analysis of the INT-0116 study, evaluating post-operative chemo-radiotherapy in patients with resected gastric cancer, it has been shown that the benefit of adjuvant treatment is minimal in patients with diffuse histology while is significant in all the other subsets (Smalley et al. 2012). Similar findings have been observed also in the ITACA-S trial, a multicentre phase III trial comparing 5FU and leucovorin versus a sequential regimen including irinotecan and 5FU followed by cisplatin and docetaxel in the adjuvant treatment of resected gastric cancer patients. In a subgroups analysis of the trial, which could not demonstrate any benefit for the intensive treatment versus the fluorouracil monotherapy, the authors compared the outcome of patients according to disease histopathologic and anatomic criteria-diffuse gastric cancer presented a worse outcome in terms of OS compared to distal non-diffuse gastric cancer (HR=1.35; 95% CI 1.06–1.72, p=0.016) while no significant difference in terms of prognosis was found between distal or proximal non-diffuse gastric cancer. None of the three subtypes showed a benefit for the experimental arm versus the 5FU arm.

It has been observed that the overall response rate to first-line chemotherapy (two drugs fluoropyrimidine-based chemotherapy regimen or three drugs regimen as first-line combination chemotherapy, including a platinum derivate, a fluoropyrimidine, and a third drug) was 29.6%. The response rate for diffuse gastric cancer is about 20.4%, while in patients with proximal non-diffuse gastric cancer or distal non-diffuse gastric cancer, the response rate is higher, 46.1% and 34.3% respectively. Diffuse type gastric cancer patients also presented a shorter PFS compared to other subgroups with a median PFS of 4.2 months compared to 7.2 months for proximal non-diffuse gastric cancer patients and 5.9 months for distal non-diffuse gastric cancer patients. These differences translated into statistically significant differences in OS (Shah et al. 2011).

Interestingly, in these studies, gastroesophageal tumours, usually considered more aggressive and presenting a worse prognosis compared to tumours arising from the rest of the stomach (Kattan et al. 2003; Sakaguchi et al. 1998), had a greater benefit from the treatment. A subset analysis of a phase II trial evaluating bevacizumab with a modified DCF regimen (docetaxel, cisplatin, 5FU) in advanced gastric cancer patients diffused type of gastric cancer was shown to have significantly worse PFS and OS compared to other subtypes. Diffuse tumours also presented the worse response rate with 38% compared to 56% of distal/body diffuse gastric cancer and 85% of proximal non-diffuse gastric cancer (Shah et al. 2011).

A subset analysis comparing the efficiency of trastuzumab in intestinal and diffuse type gastric cancers showed that the addition of trastuzumab to chemotherapy showed that diffuse type gastric cancer patients with 2% *HER2* amplification had no effect on survival with an HR for OS of 1.07 (0.56-2.05) versus an HR of 0.69 (0.54-0.88) for intestinal type gastric cancer patients with 21.5% *HER2* amplification (Bang et al. 2010; Tanner et al. 2005).

A multicentre study with more than 1000 HER2 negative gastric cancers undergoing chemotherapy containing 2-3 drugs, sought to evaluate whether Laurén type influences the efficacy of various chemotherapies and on patient OS. The ORR was found decreased when tumours presenting a diffuse component. Anthracycline- or docetaxel-containing schedules increased ORR only in the intestinal type. The diffuse type displayed increased mortality with HR of 1.201 (95% CI, 1.054-1.368), Patients receiving chemotherapy with docetaxel had no increase in OS for the subset having a diffuse component but exhibited increased OS in the intestinal type: HR 0.65 (95% CI, 0.49-0.87). There was a similar significant difference for the PFS analysis. These results further proved the clinical application utility of Laurén classification in survival prediction and also to guide in chemotherapy selection (Jimenez Fonseca et al. 2017).

1.1.8.2 Chemotherapy-associated genes in gastric cancer

Innate and acquired chemoresistance is multi-factorial and involves multiple key molecules and accounts for the majority of relapse cases in cancer patients. Untailored treatment may result in side effects and great economic burden without actual benefit.

Cell kinetic differences in normal and malignant tissues could significantly influence the

survival response of mammalian cells to most anti-tumour agents (Meyn et al. 1980). This has been demonstrated by a quantitative assay for assessing the sensitivity of resting normal bone marrow stem cells and rapidly dividing clonogenic AKR lymphoma cells to a variety of cytotoxic agents. These agents are classified into 3 classes according to their activities during certain phases of the cell cycle and on resting cells. For Class I agents there was no difference in the toxicity exerted in rapidly proliferating or resting cells. Agents in this class (e.g. X-irradiation) were said to be non-specific. In Class II the agents were more toxic to proliferating cells than to the resting cells, with increasing doses killing a greater number of cells until a plateau was reached, after which there was no further increase in cell kill. This second class of agents is called phase-specific because proliferating cells were killed during a specific part of the cell cycle. Resting (G0) cells do not appear to be affected by these agents provided the exposure time is kept short (24 hours). For Class III agents, the survival curves were exponential, but there was a great variance between the slopes. For equivalent doses, some compounds exerted greater specificity against the tumour cells. These agents were termed cycle specific, since although they damaged both proliferating and resting cells, dividing cells were more sensitive than G0 cells and were killed throughout the cell cycle (Figure 1.20).

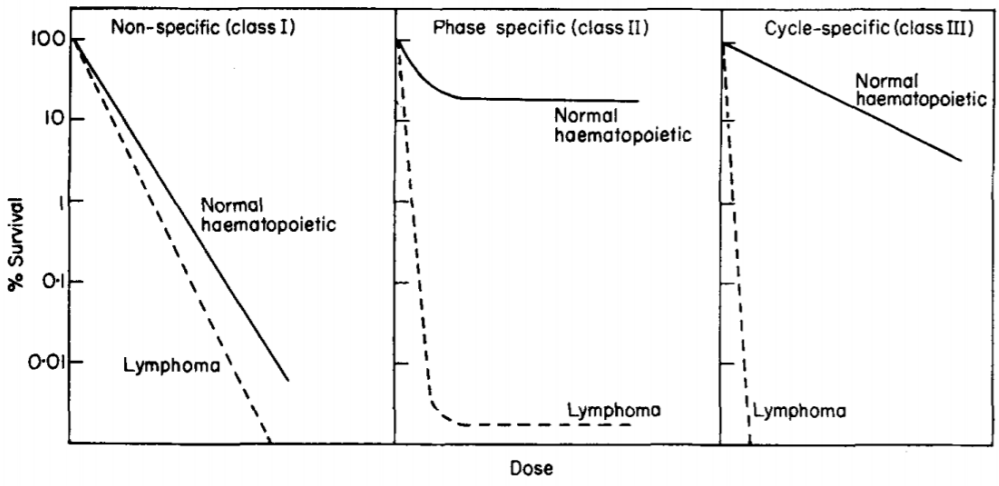

Figure 1.20: Dose-survival curves for both normal hematopoietic and transplanted lymphoma colony forming units. Normal or tumour-bearing mice were given different doses of various agents and their femoral bone marrows were assayed 24 hours later for their content of colony-forming units. Source: The cell cycle and its significance for cancer treatment (Hill and Baserga 1975).

When mice were treated with short courses of phase-specific or cycle-specific agents there was a much greater loss of malignant as opposed to normal stem cells. Subsequent studies

have confirmed that prolonged exposure to cycle specific agents resulted in an increased sensitivity of normal stem cells, whereas tumour cells appeared less sensitive as treatment continued. Similarly, if mice were treated after the previous injury to the marrow when hematopoietic stem cells were proliferating to repair the damage, the specificity of these agents for malignant cells was lost. Owing to these earlier studies relevant to the mode of action, indications, and scheduling of cell cycle-specific and cell cycle-nonspecific drugs, information on cell and population kinetics of cancer cells explain, in part, the limited effectiveness of most available anticancer drugs. Also, the kinetic classification of antitumour drugs is well-documented and aid the establishment of principles for agents' administration in clinical practice (Hill and Baserga 1975). Conventional chemotherapeutic agents are falling into these two major classes (Table 1.9). A schematic summary of cell cycle kinetics is presented in Figure 1.21.

Table 1.9: Cell cycle effects of major classes of anti-cancer drugs. Source: https:// basicmedicalkey .com /cancer-chemotherapy/

Cell cycle-Specific (CSS) Agents	Cell cycle-Nonspecific (CCNS) Agents
Antimetabolites (S phase)	**Alkylating agents**
Capecitabine	Altretamine
Cladribine	Bendamustine
Clofarabine (ara-C)	Busulfan
Fludarabine	Carmustine
5FU	Chlorambucil
Gemcitabine	Cyclophosphamide
Methortrexate (MTX)	Dacarbazine
Nelarabine	Lomustine
Pralatrexate	Mechlorethamine
6-Thioguanine (6-TG)	Melphalan
Topoisomerase II inhibitor (G1-S phase)	Temzolomide
Etoposide	Thiotepa
Topoisomerase I inhibitor (G2-M phase)	**Antitumour antibiotics**
Irinotecan	Dactinomycin
Topotecan	Mitomycin
Taxanes (M phase)	**Platinum analogues**
Albumin-bound paclitaxel	Carboplatin
Cabazitaxel	Cisplatin
Docetaxel	Oxaliplatin
Paclitaxel	**Anthracyclines**
Vinca alkaloids (M phase)	Daunorubicin
Vinblastine	Doxorubicin
Vincristine	Epirubin

Vinorelbine	Idarubicin
Antimicrotubule inhibitor (M phase)	Mitoxantrone
Ixabepilone	
Eribulin	
Antitumour antibiotics (G2-M phase)	
Bleomycin	

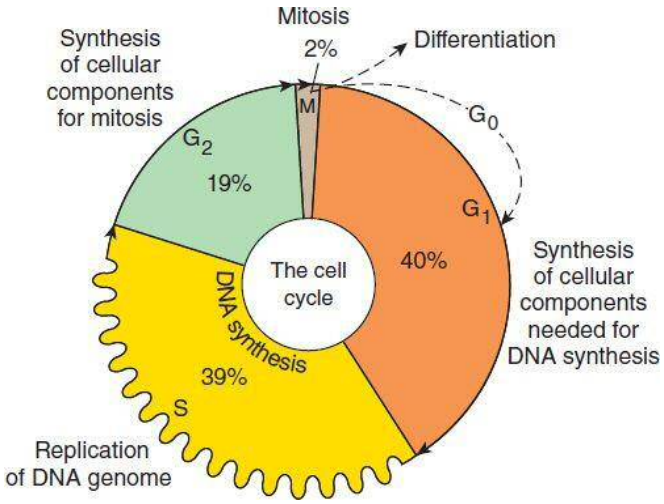

Figure 1.21: The different phases of the cell cycle. The cell cycle includes four distinct phases: G1 (gap phase 1), S (DNA synthesis), G2 (gap phase 2), and M (mitosis). In the first phase (G1) the cell grows. When it has reached a certain size, it enters the phase of DNA-synthesis (S) where the chromosomes are duplicated. During the next phase (G2) the cell prepares itself for division. During mitosis (M) the chromosomes are separated and segregated to the daughter cells, which thereby get exactly the same chromosome set up. The cells are then back in G1 and the cell cycle is completed. G0 is the resting phase when the cell does not undergo division. Source: https://basicmedicalkey.com/cancer-chemotherapy/

5FU is a remarkable drug that has been available in the past half-century and has become the mainstay of chemotherapy for gastrointestinal cancer. 5FU is an analogue of uracil with a fluorine atom at the C-5 position in place of hydrogen (Wohlhueter et al. 1980). It rapidly enters cells using the same facilitated transport mechanism as uracil. 5FU has converted intracellularly to several active metabolites: fluorodeoxyuridine monophosphate (FdUMP), fluorodeoxyuridine triphosphate (FdUTP) and fluorouridine triphosphate (FUTP). These active metabolites disrupt RNA synthesis and the action of thymidylate synthase (TS). The rate-limiting enzyme in 5FU catabolism is dihydropyrimidine dehydrogenase (DPD), which converts 5FU to dihydrofluorouracil (DHFU). More than 80% of administered 5FU is normally catabolized primarily in the liver, where DPD is abundantly expressed (Diasio and Harris 1989). TS catalyzes the reductive methylation of deoxyuridine monophosphate

(dUMP) to deoxythymidine monophosphate (dTMP), with reduced 5,10-methylenetetrahydrofolate (CH2THF) as the methyl donor. This reaction provides the sole *de novo* source of thymidylate, which is necessary for DNA replication and repair. The 36-kDa TS protein functions as a dimer, both subunits of which contain a nucleotide-binding site and a binding site for CH2THF. The 5FU metabolite FdUMP binds to the nucleotide-binding site of TS, forming a stable ternary complex with the enzyme and CH2THF, thereby blocking binding of the normal substrate dUMP and inhibiting dTMP synthesis (Rennert and Anker 1963; Sommer and Santi 1974). The exact molecular mechanisms that mediate events downstream of TS inhibition have not been fully elucidated. Deoxynucleotide pool imbalances (in particular, the dATP/dTTP ratio) are thought to severely disrupt DNA synthesis and repair, resulting in lethal DNA damage (Yoshioka et al. 1987; Houghton et al. 1995). In addition, TS inhibition results in the accumulation of dUMP, which might subsequently lead to increased levels of deoxyuridine triphosphate (dUTP). Both dUTP and the 5FU metabolite FdUTP can be misincorporated into DNA. Repair of uracil and 5FU-containing DNA by the nucleotide excision repair enzyme uracil-DNA-glycosylase (UDG) is futile in the presence of high (F) dUTP/dTTP ratios and only results in further false-nucleotide incorporation (Lindahl 1974). These futile cycles of misincorporation, excision, and repair eventually lead to DNA strand breaks and cell death. DNA damage due to dUTP misincorporation is highly dependent on the levels of the pyrophosphatase dUTPase, which limits the intracellular accumulation of dUTP (Ladner 2001; Webley et al. 2000).

The 5FU metabolite FUTP is extensively incorporated into RNA, disrupting normal RNA processing and function. Significant correlations between 5FU misincorporation into RNA and loss of clonogenic potential have been shown in human colon and breast cancer cell lines (Glazer and Lloyd 1982; Kufe and Major 1981). A number of *in vitro* studies indicated that 5FU misincorporation can potentially disrupt many aspects of RNA processing, leading to profound effects on cellular metabolism and viability.

To inhibit DPD-mediated degradation of 5FU. The UFT (uracil/Ftorafur) formulation uses a 4:1 combination of uracil with the 5FU pro-drug Ftorafur, which improves 5FU bioavailability by saturating DPD with its natural substrate (Adjei 1999). On this basis, further optimization was made in a novel oral DPD inhibitory fluoropyrimidine S-1 containing tegafur and two types of enzyme inhibitors, 5-chloro-2,4-dihydroxypyridine and potassium

oxonate in a molar ratio of 1:0.4:1 (Maehara 2003). Another approach has been to design 5FU pro-drugs that avoid DPD-mediated degradation in the liver. Capecitabine is an oral fluoropyrimidine that is absorbed unchanged through the gastrointestinal wall and is converted to 5'-deoxy-5-fluorouridine (5'DFUR) in the liver by the sequential action of carboxylesterase and cytidine deaminase (Johnston and Kaye 2001). 5'DFUR is then converted to 5FU by thymidine phosphorylase (TP) and/or uridine phosphorylase (Cao et al. 2002; Miwa et al. 1998), both of which have been reported to be significantly more active in tumour tissue than in normal tissue.

1.1.8.2.1 Metabolic related genes

Several studies have been set up to characterize the biological factors which correlate with response to 5FU-based chemotherapy in order to define those patients who are most likely to benefit of these drugs. Preclinical studies have demonstrated that TS expression is a key determinant of 5FU sensitivity. Gene amplification of TS with consequent increases in TS mRNA and protein has been observed in cell lines which are resistant to 5FU and fluorodeoxyuridine (FUDR) (Copur et al. 1995; Cao et al. 2002). The TS gene promoter is polymorphic and usually has either two (TSER*2) or three (TSER*3) 28-base-pair tandem-repeat sequences (Horie et al. 1995). Preliminary studies indicate that TSER*3/TSER*3 homozygous patients are less likely to respond to 5FU-based chemotherapy than TSER*2/TSER*2 homozygous and TSER*2/TSER*3 heterozygous patients (Pullarkat et al. 2001; Marsh et al. 2001). Treatment with 5FU has been shown to acutely induce TS expression in both cell lines and tumours (Swain et al. 1989; Chu et al. 1993). The thymidylate synthase (TS) gene, which is induced at the G1–S transition in growth stimulated cells, encodes an enzyme that is essential for DNA replication and cell survival. A study by Kamoshida et *al* assessed the expression of TS, DPD, and TP levels in different tumour types, including intestinal-type and diffuse-type gastric adenocarcinoma. The authors found a high level of expression of TS, which may be associated with poor response to 5FU based chemotherapy, in diffuse GC while TS was not overexpressed in intestinal type gastric cancer (Kamoshida et al. 2005).

1.1.8.2.2 Cancer stem cells and epithelial-to-mesenchymal transition

The cancer stem cell theory postulates that cancers harbour a subset of cells which share

characteristics of normal stem cells, with a capacity for self-renewal and differentiation (Rocco et al. 2012). Numerous studies have demonstrated that purported cancer stem-like cells (CSC) are more resistant to chemotherapy than non-CSCs (Alison et al. 2012). Acquired resistance is driven, in part, by intratumoural heterogeneity, that is, the phenotypic diversity of cancer cells co-inhabiting a single tumour mass. This concept, taken together with the identification of the EMT programme as a critical regulator of the CSC phenotype, offers an opportunity to investigate the nature of intratumoural heterogeneity and a possible mechanistic basis for anticancer drug resistance. Accumulating evidence has indicated that conventional therapies often fail to eradicate carcinoma cells which have entered the CSC state via activation of the EMT programme, thereby permitting CSC-mediated clinical relapse (Shibue and Weinberg 2017). Diffuse gastric cancer was demonstrated to be enriched in genome stable subtype in TCGA classification and in MSS-EMT subtype in ACRG classification. Certain relevant genes correlated to the EMT process may contribute to drug resistance in diffuse gastric cancers.

Two studies in Nature Genetics further confirmed a ranging mutation from 14.3%- 25.3% of *RHOA* in diffuse gastric cancers (Kakiuchi et al. 2014; Kumar et al. 2016). Higher activity of RhoA by its mutation in spheroids growth was proven *in vitro* and negatively correlated with 5FU and cisplatin efficiency *in vivo*. Inhibition of RhoA could synergetically improve tumour suppression with cisplatin by more than 70%.

BMI1, belonging to a polycomb group family, was found enriched in a CD44+ subgroup of gastric cancer cells and was identified as a CSC biomarker in many malignancies. High BMI1 levels in gastric cancer cells increased resistance to 5FU, whereas BMI1 silencing enhanced 5FU antitumour activity (Xu et al. 2015).

1.1.8.2.3 Cell cycle-related genes

As mentioned above, slowly proliferating or quiescent cells are more resistant to DNA damaging agent treatments such as 5FU acting in S phase of the cell cycle to cause DNA damage. Cancer stem-like cells exhibit a low rate of division and proliferation in their niche that helps them to avoid chemotherapy and radiation (Zou 2008). Usually, cells take a range of actions to respond to the cytotoxic agents and involve a number of downstream sensors, mediators, transducers and final effectors of the DNA damage response.

If a DNA lesion cannot be repaired quickly, apoptosis is initiated to eliminate the damaged cell before it can undergo malignant transformation. p53 plays a crucial role in double-strand break (DSB)-induced apoptosis. In response to DSBs, transcriptional activation of proapoptotic factors such as Fas cell surface death receptor (FAS), B cell leukaemia/lymphoma 2 (BCL2) associated X apoptosis regulator (BAX) and BCL2 binding component 3 (BBC3, also known as PUMA), and is induced by ataxia telangiectasia mutated (ATM)/ cell cycle checkpoint kinase 2 (CHK2) and ataxia telangiectasia-mutated and RAD3-like protein (ATR)/ checkpoint kinase 1 (CHK1), phosphorylating and stabilizing p53. CHK1 and CHK2 also stimulate the expression of E2F1 and p73 to support the action of p53. This, in turn, transcribes BAX, PUMA, and phorbol-12-myristate-13-acetate-induced protein 1 (Pmaip1, also known as NOXA).

In addition to cell apoptosis, p53 is also an important anticipator in the major pathway controlling the DNA damage-induced G1/S-phase checkpoint and triggering G1-phase arrest, *i.e.* the ATM/ATR-CHK2/CHK1-p53/MDM2-p21 pathway. DSBs and single-strand breaks activate ATM/CHK2 and ATR/CHK1, which mediates MDM2 phosphorylation and subsequent degradation through a self-catalytic mechanism, thereby stabilizing p53 expression and inducing p21 expression, which inhibits the activity of CCNE/CDK2 and CCND/CDK4/6 complexes. This signalling cascade leads to cell-cycle arrest at G1 phase. The cell-cycle arrest may also be induced via activation of CHK1/CHK2 and inactivation of the CDC25A phosphatase. It consequently inhibits expression of the CCNE/CDK2 and cyclin A/CDK2 complexes and delays the cell cycle at the G1/S transition (Kastenhuber and Lowe 2017).

Thus, one important mechanism leading to chemoresistance is the dysfunction or loss of p53-mediated apoptotic pathways typically triggered by DNA damage. For example, the loss of the tumour suppressor protein p53 due to deregulated expression of its regulators (MDM2 [de Rozieres et al. 2000]) leads to abnormal downstream targets such as p21, and growth arrest and DNA damage-inducible 45 (Gadd45) (Brady et al. 2011).

As the most frequently mutated gene in human tumours (Kandoth et al. 2013), *p53* mutations were reported to induce resistance for a variety of standard chemotherapies in previous studies. The primary alterations in *p53* resulting from most tumour-associated mutations

could be only a single amino acid substitution in the 393-amino-acid protein, most of which are within the central DNA-binding domain and can be any amino acid in this region. There are a number of hotspots, including R175, G245, R248, R249, R273, and R282. Besides the loss of tumour suppressor function and acquisition of the ability to suppress the function of the remaining wild-type *p53* allele via a dominant-negative mechanism, *p53* mutations can also demonstrate an abnormal gain of function (GOF) to facilitate oncogenesis, metastasis and chemoresistance. This phenomenon has been widely demonstrated by many *in vivo* and *in vitro* experiments. The most compelling evidence of mutant *p53* (mut*p53*) GOF comes from mice engineered to harbour tumour-associated hot spot *p53* mutations. Knock-in mice exhibited a broader tumour spectrum with a more invasive and metastatic phenotype than *p53*–/– or *p53*+/– mice (Donehower 2014). Major mechanisms of mut*p53*-induced chemoresistance include enhanced drug efflux and metabolism, promoting cell survival, inhibiting apoptosis, upregulating DNA repair, suppressing autophagy, elevating microenvironmental resistance and inducing a stem-like phenotype. However, mut*p*53 has also been identified as a good predictor of chemoresistance in some clinical studies (Young et al. 2008; Perrone et al. 2010; Kandoth et al. 2013; Yamasaki et al. 2010; Dawson et al. 2009).

The transcriptional activation function of p53 is fundamental for both cell cycle arrest and apoptosis pathways. The p53 protein consists of two N-terminal transactivation domains followed by a conserved proline-rich domain, a central DNA binding domain, and a C terminus encoding its nuclear localization signals and an oligomerization domain needed for transcriptional activity. p53 contains two distinct transcriptional activation domains (comprising residues 1–40 and 40–83, respectively). Different p53 transcriptional activation requirements, associated with different target gene expression programs, are important in the settings of acute genotoxic stress and oncogenic stimuli. A functional assay using an allelic series of p53 transactivation domain mutant knock-in mice suggested that p53 may trigger multiple sub-programs which cooperate to promote tumour suppression, in response to acute DNA damage or senescence, and by regulating actin dynamics or cell migration, and DNA repair (Brady et al. 2011). p53 responses to acute DNA damage in primary cells rely on an intact first transcriptional activation domain of p53 as the L25Q; W26S mutations within this domain severely impair transactivation of most classical p53 targets including p21,

NOXA, and PUMA, and abrogate activity in both DNA damage-induced G1 arrest and apoptosis(Brady et al. 2011). Consistent with the importance of p53-mediated transcription in tumour suppression, the vast majority of tumour-derived *p53* mutations occur in the region encoding p53's DNA binding domain. In normal cells, p53 protein is maintained at low levels by a series of regulators including MDM2, which functions as a p53 ubiquitin ligase to facilitate its degradation. DNA damage and replication stress produced by deregulated oncogenes will activate p53 by promoting p53 phosphorylation, phosphorylation or by inducing the ARF tumour suppressor to inhibit MDM2 (Xu and El-Gewely 2001).

Recently, advances in next-generation sequencing (NGS) technologies have defined the genomic landscape of gastric cancer; studies of miRNAs and long noncoding RNAs (lncRNAs), as well as novel preclinical models (such as patient-derived tumour xenografts (PDX) and patient-derived organoids), have largely filled the gap between cancer genetics and phenotype. These advances have made it possible to integrate traditional, genome-based and phenotype-based diagnostic and therapeutic methods with application to individual gastric cancer patients in the era of precision medicine (Liu and Meltzer 2017).

1.2 microRNAs (miRNAs)

MicroRNAs, a class of short RNAs; together with a variety of long ncRNAs (lncRNAs), such as lincRNAs, antisense RNAs, pseudogenes, and circular RNAs (Figure 1.22) are collectively known as the noncoding RNAs (ncRNAs). They constitute the majority of the transcribed genome, of which only 1–2% code for proteins (Djebali et al. 2012; Carninci et al. 2005), hinting that higher eukaryotes increased their complexity not by increasing the number of genes but through more sophisticated regulation in which the ncRNAs are also involved. Interest in this field has seen numerous studies delineating the coding-independent functions of this novel class of RNAs, to decipher their roles and corresponding mechanism in biological processes in different diseases, including in cancer development (Chan and Tay 2018).

miRNAs regulate post-transcriptional gene expression and may be exported from cells via exosomes or in partnership with RNA-binding proteins. miRNAs in body fluids can act in a hormone-like manner and play important roles in disease initiation and progression. Hence,

miRNAs are promising candidates for biomarkers (Pacholewska et al. 2017).

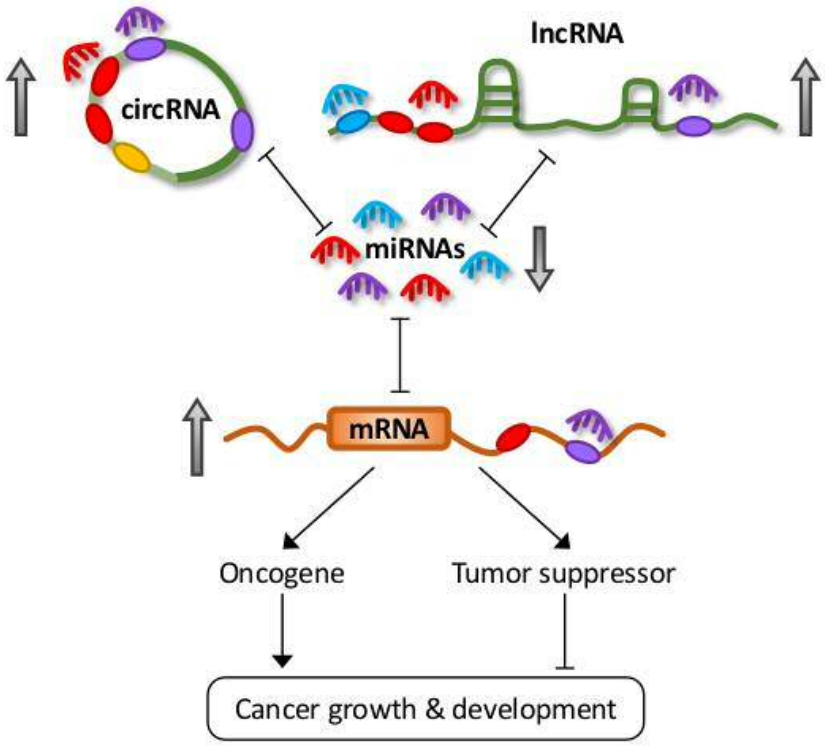

Figure 1.22: Noncoding RNA Regulatory Networks in Cancer. Noncoding RNAs (ncRNAs) constitute the majority of the human transcribed genome. The different subclasses of ncRNAs include microRNAs, a class of short ncRNAs; and a variety of long ncRNAs (lncRNAs), such as lincRNAs, antisense RNAs, pseudogenes, and circular RNAs (circRNA). Many studies have demonstrated the involvement of these ncRNAs in competitive regulatory interactions, known as competing endogenous RNA (ceRNA) networks, whereby lncRNAs can act as microRNA decoys to modulate gene expression. These interactions are often interconnected, thus aberrant expression of any network component could derail the complex regulatory circuitry, culminating in cancer development and progression. (Chan and Tay 2018).

1.2.1 Discovery of miRNAs

Six decades ago, Francis Crick proposed the 'central dogma', asserting that genetic information travels from DNA through RNA towards protein synthesis (Crick 1970). Since then RNAs have been mainly characterized as intermediaries in the process of protein production, principally as temporary copies of genetic information (mRNA), components of the ribosome (ribosomal RNAs [rRNAs]) or translators of codon sequence (tRNAs). For many years, proteins represented the primary functional end product of genetic information, though the genes that encode them account for less than 2% of the genome. Twenty years ago, the first small temporal RNAs, lineage defective 4 (lin-4)4 and lethal 7 (let-7), were

discovered in *Caenorhabditis elegans,* demonstrating that some RNAs, despite lacking protein-coding regions, are conserved functional molecules required for development. These two important findings demonstrated a new post-transcriptional gene regulation mechanism. Approximately seven years later, the importance of miRNAs was realized when Ruvkun and Horvitz identified another miRNA in C. elegans (Reinhart et al. 2000). Later, small interfering RNA (siRNA) was described -another short-chain RNA involved in the process of RNA interference and related phenomena in plants and animals. In 2001, three research groups from different countries all identified 21–22 nucleotide (nt) non-coding small RNA molecules in C. elegans, Drosophila and humans (Hutvagner et al. 2001). These single-stranded small RNA molecules with spatial and temporal expression were different from the previously reported siRNA detected in the interference pathway (RNA interference; RNAi) and were subsequently named miRNA (Xu et al. 2013).

miRNAs, together with the transcribed ultra-conserved regions and circular RNAs (circRNAs) belongs to the highly conserved functional products encoded by the genome and represent an important class of regulators in many crucial biological processes in developmental and differentiation processes and play key roles in many diseases.

It is estimated that miRNAs constitute nearly 1% of all predicted genes in mammalian genomes, and approximately >60% of all mammalian protein-coding genes can be regulated by miRNAs (Bartel 2009). To date, 2656 human miRNAs have been found according to miRbase (version 22; University of Manchester, Manchester, UK; http://www.mirbase.org/). These follow nomenclature rules outlined in Table 1.10 (Desvignes et al. 2015).

Table 1.10: Nomenclature rules for miRNAs.

Example miRNA: hsa-miR-133a-1-5p	
hsa	*Homo sapiens*. The first three letters signify the organism.
miR/mir	The capitalization of the "R" infers that the miRNA is the mature sequence, opposed to "r" which refers to the miRNA precursor, the genomic locus, the primary transcript, or the extended hairpin that includes the precursor.
133	Named sequentially. The same number is used for miRNA of different species that are orthologous but conveys no information about functionality.
a	Paralogous miRNAs that differ in 1 or 2 nt.
1	miRNAs with identical sequences are transcribed from distinct precursor sequences and genomic loci.
-5p/-3p	the same mature miRs originate from opposite arms of the same pre-miRNA
*	Previously, one of the duplex mature miRs was believed to be degraded has been conventionally named with an asterix suffix, but now suffixes -3p and -5p were adopted

1.2.2 miRNA Biosynthesis and Mechanisms of Action

miRNA biogenesis consists of multiple steps of processing involving both nuclear and cytoplasmic compartments (Figure 1.23). The canonical miRNA processing pathway starts with encoding of primary miRNA transcript (pri-miRNA) from different regions of the genome typically by RNA polymerase II (RNAPII). The majority of miRNA genes are intergenic.

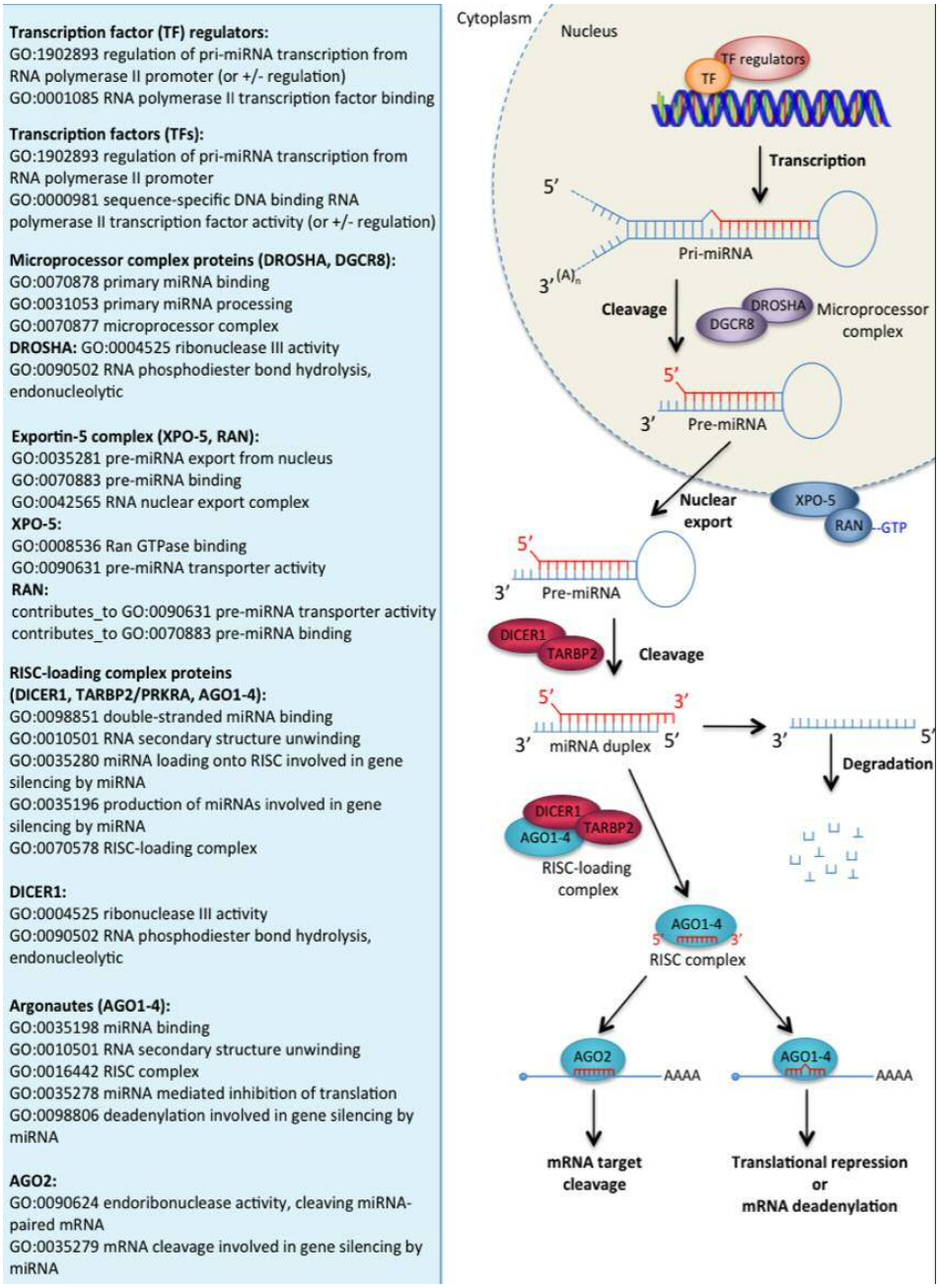

Figure 1.23: microRNA Biosynthesis. Source: Noncoding RNA: RNA Regulatory Networks in Cancer (Chan and Tay 2018).

However, about 20-40% of human miRNA genes originate in the introns of protein and non-protein genes, or the exons of long protein-coding transcripts and are therefore transcribed and regulated along with their host genes (Aravin et al. 2003; Ambros et al. 2003). For miRNA genes organized in clusters, the pri-miRNA can be monocistronic or polycistronic (Desvignes et al. 2015). Pri-miRNAs are subsequently cleaved by the microprocessor complex DROSHA–DGCR8 resulting in a precursor hairpin. The pre-miRNA is then exported from the nucleus by RAN: GTP: XPO5. Approximately 70 bp pre-miRNA hairpin structures in the nucleus are subsequently exported to the cytoplasm by an Exportin-5-mediated mechanism where they are further processed by the Dicer–TRBP complex to form the mature 22 nt miRNA duplexes. In the cytoplasm, the miRNA duplex is unwound, and the passenger strand is released and discarded. The mature single-stranded miRNA is then incorporated into the miRNA-containing RNA-induced silencing complex (miRISC) resulting in a precursor hairpin-the pre-miRNA, which is exported from the nucleus by RAN: GTP: XPO5. Once in the cytoplasm, DICER1 ribonuclease, in complex with one of the double-stranded RNA-binding proteins, TARBP2 or PRKRA (PACT), cleaves the pre-miRNA hairpin to its mature double-stranded length of around 22 nucleotides. The RNA-induced silencing complex (RISC)-loading complex, comprising of DICER1, TARBP2 (or PRKRA) and one of the Argonaute proteins (AGO1-4), loads the functional strand of the mature miRNA into the RISC and the passenger strand is degraded. DICER1 and TARBP2/PRKRA then dissociate leaving the mature RISC consisting of AGO1-4 and miRNA. The miRNA then guides the RISC to silence target mRNAs through mRNA cleavage, translational repression or deadenylation. (Figure 1.24). Special cases of miRNA-like sequences from non-canonical biogenesis pathways including DROSHA-independent miRNAs (e.g. miRtrons), Dicer-independent miRNAs (e.g. miR-451), and pathways from other non-coding RNA genes (e.g. snoRNA or lncRNA) could be accepted as miRNAs (Desvignes et al. 2015).

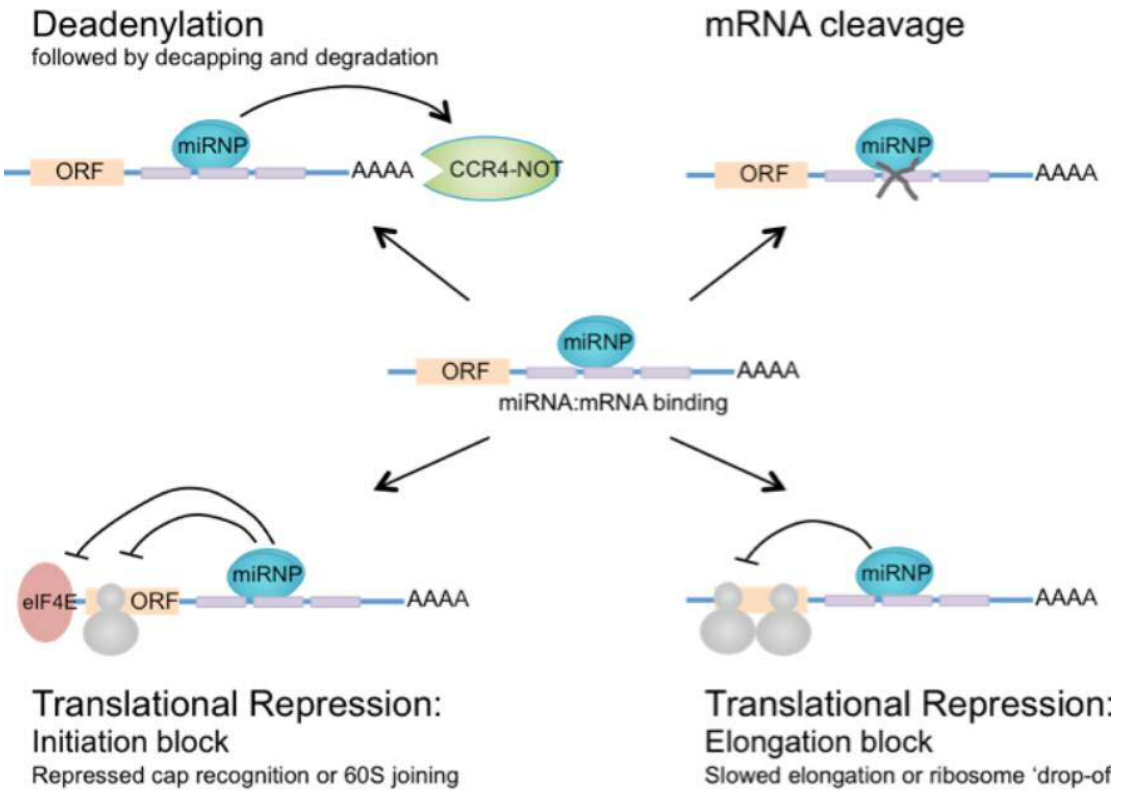

Figure 1.24: Post-transcriptional modes of miRNA action. miRNAs may promote degradation of mRNA via deadenylation and decapping or mRNA cleavage as well as repress translation of mRNAs by initiation or elongation block (Chan and Tay 2018).

miRNAs were primarily introduced to exert negative regulatory effects on genes via the interaction between a miRNA-containing RISC complex and the 3'UTR of its target mRNA, causing either mRNA cleavage, translational repression (initiation or elongation block) or mRNA deadenylation followed by decapping and degradation of the mRNA. In addition to 3'UTR targeting, miRNAs were reported to be involved in gene activation which can also enhance protein translation during amino acid starvation by targeting 5'UTR of mRNAs encoding ribosomal proteins. As another nonclassical example, miR-483-5p, embedded within the IGF2 gene, induces the transcription of its host gene by binding to the 5'UTR region. Understanding of the mechanisms of action of miRNAs has significantly expanded in the last few years, with discoveries demonstrating unexpected complexities of their regulative manner, such as promoter binding, protein binding, or direct interaction with other ncRNAs, or even relocalization in the nucleus. This localization supports the already proven hypothesis that miRNAs can alternatively regulate transcriptional processes at a DNA level. For example, human miR-373 binds to the E-cadherin (*CDH1*) promoter, thereby inducing

its expression (Ambros 2003). miRNAs have also been found to favour protein expression (in addition to downregulating it) (Vasudevan et al. 2007). Finally, besides mRNAs, miRNAs can target different types of ncRNAs, some of them being highly conserved among species such as the ultra-conserved genes or poorly conserved such as the pseudogenes (Salmena et al. 2011; Calin et al. 2007).

miRNAs also work as secreted molecules that trigger a receptor-mediated response in a different cell or tissue. They have the ability to be released into the extracellular environment within exosomes (cell-derived vesicles originated by the inward budding in the plasma membrane generating multivesicular bodies) which are present in many and perhaps all biological fluids. In this way, they can act as "hormones" (Cortez et al. 2011). Similarly, exosomes have been shown to modulate tumour microenvironments by releasing miRNAs in a coordinated manner. miR-21 and miR-29a can be transported through exosomes and can act as direct agonists of Toll-like receptors (TLRs). By binding as ligands to receptors of the TLR family in immune cells, these miRNAs were shown to trigger a TLR-mediated prometastatic inflammatory response (such as secretion of interleukins) which could favour tumour growth and metastasis (Lehmann et al. 2012; Fabbri et al. 2012). A better understanding of the diversity of mechanism of miRNA's action may provide solutions for intervention in the future.

1.2.3 miRNAs involved in gastric cancer progression

The number of animal miRNAs gradually expanded during long-term evolution, their expression pattern changed in various species, tissue or cell settings. Recent studies have identified a number of miRNAs with aberrant expression in gastric cancer (Xie et al. 2018) (Appendix 7). For example, the comparison of miRNAs deregulated in gastric cancer revealed a significant increase of several tumour-associated miRNAs such as miR-21, -25 and -106a and miRNAs from the miR-17-92 cluster (Link et al. 2012). Eight miRNAs (including miR-100, -143 and −145) were upregulated specifically in diffuse-type, while four miRNAs (miR-202, -373, -494 and −498) in intestinal-type gastric cancer (Song et al. 2012). Comparison between diffuse-type gastric cancers compared with intestinal-type gastric cancers, uncovered largely downregulations of hsa-let7d*, hsa-miR-328, hsa-miR-32*, hsa-

miR-1227, hsa-miR-206, hsa-miR-1229, hsa-miR-595, and hsa-miR-631.

Some miRNAs are significantly enriched in clusters in discrete genomic regions. The clustering patterns suggest that miRNAs in the same cluster might be transcribed in a polycistronic manner, and miRNAs in the same cluster were hypothesized to regulate functionally related genes. There is accumulating evidence suggesting that epigenetic and genetic defects in noncoding RNAs play crucial roles in tumour initiation, progression, invasion, and metastasis. For miRNAs, extensive studies explored their deregulation, function and underlining mechanisms and correlated these with progression and prognosis of gastric cancer, using miRNAs' microarray and bioinformatics analysis together with *in vitro* or *in vivo* experiments. Overexpressed oncogenic microRNAs that target tumour suppressor genes or reduction of tumour suppressor miRNAs *versus* targeting oncogenes could synergistically promote progression, resist apoptotic signals, and promote cell invasion and tumour metastasis (Ueda et al. 2010; Song and Meltzer 2012). Among these high-throughput studies, several clusters of miRNAs exhibited consistent deregulation, highlighting their significant roles in fine tuning the transcriptome during distinct status setting or response to specific stimuli promoting gastric cancer progression.

miRNAs are exported from cells both within and outside the exosomes (Iguchi et al. 2010). Exosomes act as mediators of cell cell communication (Rani et al. 2011; Ahmed and Xiang 2011) and are carriers for functional miRNA delivery (M. Yang et al. 2011; Pegtel et al. 2010). There is considerable interest in using exosomes in clinical applications as biomarkers and/or as potential therapeutic tools (Bobrie et al. 2011; Zomer et al. 2010).

More recently, circular RNAs, characterized by the formation of a covalently closed continuous RNA loop, are drawing renewed attention in cancer research. Moreover, noncoding RNAs are stable in bodily fluids such as serum, plasma, gastric juice, and even in exosomes, making them promising non- or less invasive gastric cancer biomarkers.

1.2.4 Diagnostic potential of microRNAs in gastric cancer

Over the past decade, the emergence of miRNA research has firmly established this molecular family as a key component in cells. Expression levels of certain miRNAs are altered in many diseases. Identification of tumour-specific genetic alterations in the miRNA

processing machinery, such as in the genes encoding TARBP2, AGO2, Dicer, and Exportin-5 (XPO5) provide strong evidence of deregulated miRNAs being relevant in cellular transformation processes (Abelson et al. 2005). Exploiting their roles as potential biomarkers to predict, diagnose or monitor disease including cancer has become a focus for researchers around the globe. This is being driven by the importance of early cancer diagnosis and the need to be able to distinguish between different forms of cancer. Alongside altered expression under different disease states, miRNAs have other features that make them ideally suited as biomarkers. miRNAs are present in biofluids including blood, urine, and saliva, allowing relatively non-invasive sample collection. In addition to their accessibility, miRNAs are highly stable in biofluids and in collected samples making miRNAs relatively easy to work with and assay via a range of different methods.

Discovering miRNA expression patterns that are unique to a particular cancer is an important first step in identifying biomarker signatures which will be effective in its detection. A particular problem with cancer is the difficulty of determining whether the cancer is an aggressive form that requires immediate treatment or low-grade cancer. In gastric cancer, studies on miRNA profiling of cancer versus normal tissues showed significant changes and defined commonly altered miRNAs. Profiling of miRNAs by various methods has allowed for the identification of signatures associated with the diagnosis, staging, disease progression, prognosis, and response to treatment of gastric cancer. For example, a five-microRNA signature in plasma (consistently elevated miR-1, miR-20a, miR-27a, miR-34 and miR-423-5p) was established by comparing 160 cancer-free controls, 124 patients with gastric non-cardia adenocarcinoma (GNCA) and 36 patients diagnosed gastric cardia adenocarcinoma (GCA). For GNCA, an area under the receiver operating characteristic (ROC) curves (AUCs) ranged from 0.850 to 0.925 and 0.694 to 0.790 in the training and validation phases, respectively (Abelson et al. 2005). Masahiro *et al.* reported that plasma miR-18a concentrations were significantly higher in gastric cancer patients than in healthy controls. Furthermore, plasma miR-18a levels were significantly reduced in postoperative samples compared to in preoperative samples (Tsujiura et al. 2015). A similar study indicated that plasma miRNA-199a-3p could be novel a potential diagnostic biomarker for early gastric cancer (Li et al. 2013).

Significant analytical challenges using miRNAs in cancer and disease diagnostics remains, such as identification of robust, reproducible and economic methods of detecting expression of miRNAs, and selection of reference genes. There is no currently known extracellular reference RNA for cell free miRNA analysis. Moreover, the assessment of sample quantity and quality is more challenging for miRNAs than for message RNAs, for which the sizes and relative abundance of ribosomal RNAs can be used to check RNA integrity. In conclusion, validation of specific miRNA signatures as biomarkers could be a critical milestone in diagnostics.

1.2.5 Therapeutic potential of microRNAs in cancer

By blocking the function of targeted mRNAs in specific cell types or microenvironment conditions, miRNAs could represent a valid option for treating patients with certain cancers in the future.

The advantages of using miRNAs (compared with other gene-silencing therapies) includes the fact that it is an innate product and can be metabolised in human cells and likewise. miRNAs can target multiple genes from the same pathway and therefore their action can occur at multiple levels in the same pathway, thereby significantly reducing the development of resistance. For example, miR-17-5p and miR-20, both of which have increased expression in gastric cancer patients, have 2 anti-proliferative targets: p21 and TP53INP1 (Wang et al. 2013). Therefore, a personalized therapy based on the identification of patients with upregulated miR-17-5p/miR-20a cluster expression and p21 and TP53INP1 protein reduction in gastric cancer patients can be envisioned. These types of therapies are very specific for patients having these molecular characteristics in the same cells. Patients with high levels of miR-17-5p/miR-20a but normal levels of p21 and TP53INP1 or conversely with normal levels of miRNAs but abnormal levels of these anti-proliferative tumour suppressors should be excluded from clinical trials targeting miR-17-5p/ miR-20a. Strategies for miRNA targeting are based on either restoring miRNA levels or blocking miRNA function with oligonucleotide-based strategies. A targeted approach to replenish the expression levels of particular miRNAs is restoring the level and function of one or a limited number of miRNAs, usually located within a cluster (such as miR-15a and miR-16-1 at 13q14.3), either with miRNA mimics or with miRNAs encoded in expression vectors.

miRNA mimic molecules are double-stranded sequences with 100% similarity to the endogenous miRNA, which can be delivered by nanoparticles and thereby are expressed in the cells. This approach is particularly attractive because nanoparticles can be coated with antibodies that recognize tumour-specific antigens, therefore allowing a tumour-specific delivery of the miRNA of interest Recently, a clinical trial of MRX34 (Mirna Therapeutics, TX, USA) constructed a miR-34 mimetic using nanoparticles coated with a neuroblastoma-specific antidisialoganglioside GD2 antibody to restore miR-34 expression in cancer cells. The agent was used to treat liver cancer and liver metastasis of other cancers in phase I clinical trial. The therapy has proved to be effective in the inhibition of neuroblastoma tumour growth in a murine orthotopic xenograft model (Tivnan et al. 2012). Moreover, MRX34, a liposome-formulated mimic of the tumour suppressor miR-34, has been developed in a clinical phase 1 trial for patients with advanced or metastatic liver cancer. Preclinical studies have already shown that tail vein injection of MRX34 reduced tumour growth and significantly enhanced survival with a favourable safety profile in orthotopic mouse models of hepatocellular carcinoma (Bader 2012). In a pre-clinical study of non-small cell lung cancer (NSCLC), MRX34 treatment significantly reduced the expression of the checkpoint signal PD-L1 and increased infiltrating CD8+ cells in tumour tissues (Cortez et al. 2016). However, the MRX34 clinical trial was stopped in 2016 since multiple serious immune-related side effects were observed in patients. So, the safety of MRX34 still requires further research (Beg et al. 2017).

Current strategies for inhibitory targeting of microRNAs are mainly based on antisense oligonucleotides (so-called anti-miRNAs), comprised of locked nucleic acids (LNA) along with tiny LNA anti-miRNA constructs, antagomirs, and miRNA sponges. Miravirsen (SPC3649), an LNA against miR-122, is the first miRNA target therapy tested in a clinical trial for the treatment of hepatitis C virus infection. This recently completed phase 2a trial showed that SPC3649 exhibited robust antiviral activity in a dose-dependent manner (Lindow and Kauppinen 2012). More impressively, 4 of 9 patients treated at the highest dose (7 mg/kg) with SPC3649 reached undetectable levels of hepatitis C virus RNA (consequently decreasing the possibility of developing hepatocellular carcinoma) (Janssen et al. 2013). The effectiveness of antimiR-122 treatment proved the plausibility of LNA-based therapeutics and encourages the development of other specific miRNA-targeting therapeutic strategies

(Berindan-Neagoe et al. 2014).

Conversely, miRNA also plays critical roles in drug resistance. An increasing number of studies have demonstrated that miRNA can significantly influence drug transporters, drug-metabolizing enzymes, transcription factor and nuclear receptors. Wang and colleagues determined that exosomes serving as nanoparticles could deliver anti-miR-214 to reverse chemoresistance to cisplatin in gastric cancer (Wang et al. 2018). Related miRNAs may also include miR-21, whose reduction was also proved to have a significant impact on increasing the anti-proliferative effects and apoptosis induced by Cisplatin (Yang et al. 2013). Meanwhile, miR-200c inhibits transforming growth factor-β (TGF-β)-induced-EMT to restore trastuzumab sensitivity by targeting ZEB1 and ZEB2 in gastric cancer.

Nevertheless, non-specific cytotoxicity, poor biocompatibility, low delivery efficacy and unexpected off-target effect have remained as challenges for carrying miRNAs *in vivo*. Thus, treatment based on miRNA therapy should be explored with better specificity (Hao et al. 2017).

1.3 miR-140-5p and miR-140-3p

The human mir-140 primary transcript, located at 16q22.1, is an intron-retained RNA co-expressed with a Wwp2-C isoform. Two mature miRNAs, miR-140-5p and miR-140-3p, were processed and produced with different seed sequences, and were predicted to target different genes. As shown in Figure 1.25, miR-140-5p originates from the 5-prime arm of the hairpin of the precursor, while miR-140-3p comes from the 3-prime arm. Like many other miRNAs, the abundance of the miR-140-5p and miR-140-3p stands are different according to tissues type or species (Kenyon et al. 2019; Gibson and Asahara 2013; Griffiths-Jones et al. 2006; Ambros et al. 2003). The mechanism of strand selection is still unknown. It has been verified in both a bone matrix gelatine (BMG) rat model and Genome-Wide MicroRNA and Gene Analysis of mesenchymal stem cell chondrogenesis, that miR-140-5p might have more important functions than miR-140-3p (Barter et al. 2015; Min et al. 2015).

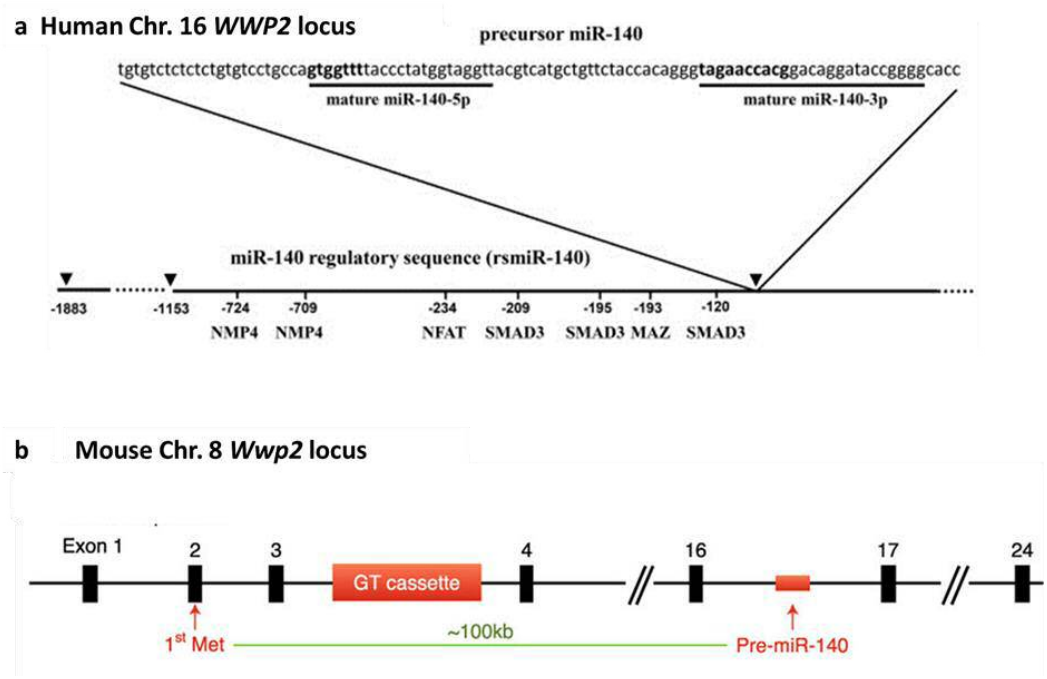

Figure 1.25: miR-140 sequence in human and mouse. A. In human, sequence of the miR-140 precursor (pre-miR-140) stem-loop located in intron 16 of the WWP2 gene. Seed sequence is represented in bold format. **B**. A schematic illustration demonstrating Wwp2 and pre-miR-140 loci are on mouse chromosome 8. Black boxes indicate exons of Wwp2, and the red box indicates the pre-miR-140 gene. (Adapted from previous publication (Inui et al. 2018; Tardif et al. 2013))

Previous reports have shown that miR-140-5p and miR-140-3p are almost exclusively specific to chondrocytes and have been a focus of cartilage miRNA research to date. The mir-140-deficient mice manifested a mild skeletal phenotype, with short stature and low body weight, as well as craniofacial deformities characterized by a short snout and domed skull, supporting the notion that mir-140 is a tissue-specific miRNA important in cartilage development. Furthermore, mir-140-deficient mice showed age-related osteoarthritis (OA)-like changes characterized by proteoglycan loss and fibrillation of articular cartilage. However, transgenic mice overexpressing miR-140 in cartilage were resistant to antigen-induced arthritis (Papaioannou et al. 2015; Araldi and Schipani 2010; Miyaki et al. 2010). Several studies have also clarified that miR-140-5p exhibited the largest expression difference between human articular chondrocytes and mesenchymal stem cells (Karlsen et al. 2014; Miyaki et al. 2010; Miyaki et al. 2009). Gene Ontology (GO) analysis on the transcriptome data with input lists of statistically significant up- or downregulated genes after either stable miR-140-5p inhibition in differentiating mesenchymal stem cells or transient miR-140-5p overexpression in dedifferentiating articular chondrocytes showed that miR-140-5p

negatively regulated genes involved in cytoskeleton remodelling and cell division, but positively regulated genes related to extracellular regions and the extracellular matrix (Karlsen et al. 2014). Additionally, miRNA-140-5p inhibits MSCs proliferation by targeting CXCL12 during TGF-β3-induced chondrogenic differentiation. TGF-β3 induced significant elevation of miR-140-5p followed by markedly decreased CXCL12 inhibited mesenchymal stem cell's viability. It is worth noting that miR-140-5p was also significantly upregulated during cellular senescence in mesenchymal stem cells (Yoo et al. 2014).

Furthermore, miR-140-5p is among the candidate miRNAs which can function *in vivo* to suppress Fibroblast Growth Factor 9 (FGF9) as lung development progresses from pseudoglandular to canalicular stages. Disruption of this progress or lack of epithelial Dicer1 increased FGF9 expression in pulmonary mesenchymal hyperplasia and a multicystic architecture which is histologically and molecularly indistinguishable from Type I Pleuropulmonary Blastoma (PPB) (Yin et al. 2015). In addition, downregulation of miR-140-5p could have a role during pancreatic development. It may enhance OASIS expression and activation in modulating extracellular matrix production, such as extracellular sulfated proteoglycans, which regulate pancreatic endocrine differentiation during development by inhibiting endocrine cell (β and α cell) development (Zertal-Zidani et al. 2007) and provide help for the developing pancreas against physiological endoplasmic reticulum (ER) stress (Vellanki et al. 2010). A similar phenomenon was shown in toxicity studies where OASIS protects pancreatic β-cell lines and the C6 glioma line from tunicamycin and thapsigargin (Vellanki et al. 2010) and protect astrocytes from kainic acid toxicity (Chihara et al. 2009), which all are known to induce ER stress.

miR-140-3p demonstrates highest expression in human primary articular chondrocytes at early passages compared with their dedifferentiated counterparts (Yan et al. 2011; Crowe et al. 2016). miR-140-3p was also the most highly expressed microRNA in osteoarthritic cartilage, playing a protective role against inflammation in chondrocytes (Crowe et al. 2016). Corresponding targets of miR-140-3p included ADAMTS-5 and runt-related transcription factor 2 (RUNX-2) (Le et al. 2013). Differential expression of miR-140-3p was found in hematopoietic lineages and may be associated with platelet production and activation (Collares et al. 2013).

Research on understanding inflammation has suggested that miR-140-5p and miR-140-3p may play critical roles in the adaptive and innate immunity (O'Neill et al. 2011; Shimokawa et al. 1998; Davidson-Moncada et al. 2010). They have also been reported as key components in T cell differentiation, modulating the inflammatory response and activating toll-like receptor pathways in macrophages (O'Neill et al. 2011; Shimokawa et al. 1998). Toll-like receptors (TLRs) are pattern recognition receptors which regulate innate immunity and defend against invading microorganisms (Sabroe et al. 2003). TLRs also mediate autoimmunity. Upon stimulation, TLRs initiate downstream signalling pathways and lead to the secretion of inflammatory chemokines and cytokines (Liu et al. 2014). miR-140-5p downregulated TLR22 may be associated with or trigger a Th2 type immune response (Valenzuela-Munoz et al. 2017). Lipopolysaccharides (LPS) treatment suppressed miR-140-5p expression thus induced the high expression of TLR4 resulting in dramatically increasing the number of the Th17 cells as well as the release of IL-6, IL-17 and IL-22 (Dileepan et al. 2016; Newcomb and Peebles 2013; Sethi et al. 2013; Kowalski et al. 2008). After an injury such as radiation-treatment, miR-140-5p played a key role in maintaining this balance by regulating macrophage polarization towards M1 macrophages, and antagonizing TGF-β1 activation, which promoted normal tissue repair and prevented the development of fibrosis. In the absence of miR-140, M2 macrophages prevail and with constant wound healing of lung tissue, scar tissue accumulated and contributed to the development of fibrosis (Duru et al. 2016).

miR-140-3p negatively regulates nuclear factor-κB (NF-κB) inflammatory signaling by regulating the expression of nuclear receptor coactivator 1 (NCOA1) and nuclear receptor-interacting protein 1 (NRIP1), both of which are NF-κB co-activators (Takata et al. 2011). NF-κB and AP-1 activated TNF-α which further augmented CD38 expression in human airway smooth muscle (ASM) cells. CD38 is a cell-surface protein expressed in human ASM cells, generating calcium-mobilizing second messenger molecules such as cyclic ADP-ribose, contributing to airway hyper-responsiveness and the process of Asthma (Guedes et al. 2015). Inflammation also plays a key role in coronary artery disease (CAD) and other manifestations of atherosclerosis (Hansson 2005). To identify differentially regulated miRNAs in whole blood in patients with coronary artery disease, a microarray study was conducted in 12

patients with CAD and 12 healthy control subjects. miR-140-3p, showed a rising trend, accompanied by significantly reduced expression of target genes associated with mitochondrial dysfunction and oxidative phosphorylation (Taurino et al. 2010). Upregulation of miR-140-3p was also discovered in the coronary sinus blood of acute coronary syndrome (ACS) patients, and this elevation was likely mainly derived from peripheral blood mononuclear cells, including monocytes, circulating endothelial cells (CECs) and lymphocytes (Li et al. 2017), which was, however, related to higher death rates in ACS of CAD patients (Karakas et al. 2017). Ellagic acid and breviscapine inhibited cell apoptosis and decreased fibrosis area and infarct area after acute myocardial infarction (AMI) by up-regulating miR-140-3p and inhibiting MKK6 and subsequent TLR4 pathway (Wei et al. 2017).

In other respects, miR-140-5p was found to be upregulated in inhibition of biological pathways associated with anabolic metabolisms, such as adipogenesis, cholesterol biosynthesis, triacylglycerol synthesis, and insulin signaling (Craig et al. 2014). A marked increase of circulating miR-140-5p was shown in morbidly obese patients; while surgery-induced weight loss and food restriction led to a decrease of miR-140-5p (Gat-Yablonski et al. 2013). Pioglitazone can decrease miR-140-5p expression and increase HDAC7 expression in insulin resistance and adiposity patients (Liu et al. 2016).

Emerging evidence also revealed an altered expression of miR-140-5p and miR-140-3p in different malignancies. Downregulation of miR-140-5p was reported in NSCLC, primary breast cancer, colon cancer, hepatocellular carcinoma (HCC), osteosarcoma, chordomas and lymphoma et al. Overexpression of miR-140-5p was reported to inhibit cell proliferation, and cell cycle arrest in both colon cancer cell lines and a cancer stem cell line (Song et al. 2009). Mosakhani *et al.* (2012) found that upregulation of miR-140-5p was significantly associated with poorer OS in metastatic colon cancer patients with wild-type KRAS/BRAF. TGFβ signaling regulates tumour progression by a tumour cell-autonomous mechanism or through a tumour–stroma interaction and has either a tumour-suppressing or tumour-promoting function depending on cellular context (Ikushima and Miyazono 2010). miR-140-5p could suppress the TGFβ pathway through targeting Smad3 (Butz et al. 2011; Pais et al. 2010). TGFβ receptor 1 (TGFBR1) and FGF9 are also direct targets for miR-140-5p. Silencing TGFBR1 and FGF9 by small interfering RNA (siRNA) resembled the phenotype resulting from the ectopic miR-140-5p expression, while overexpression of TGFBR1 and

FGF9 attenuated the effect of miR-140-5p on HCC growth and metastasis (H. Yang et al. 2013). An increasing body of evidence supports a stepwise model for the progression of breast cancer from ductal carcinoma in situ (DCIS) to invasive ductal carcinoma (IDC). Cancer stem cells (CSCs) are thought to be already programmed in pre-malignant DCIS lesions and these tumour-initiating cells may determine the phenotype of DCIS. miRNA profiling of normal mammary stem cells and cancer stem-like cells from DCIS tumours revealed that miR-140-5p is significantly downregulated in cancer stem-like cells (basal-like DCIS) compared with normal stem cells, linking miR-140 and dysregulated stem cell circuitry. Targets of miR-140-5p, SOX9 and ALDH1, were the most significantly activated stem-cell factors in DCIS stem-like cells (Li et al. 2014b; Wolfson et al. 2014; Yan et al. 2008). Targeted therapies (tamoxifen) are only able to reduce DCIS risk in patients with oestrogen receptor α (ERα)-positive disease (Li et al. 2014b). These may link to the restoration of miR-140-5p after release from the suppression by ERα. Exosomal levels of miR-140-5p from stem cell populations can be rescued by treatment with sulforaphane (Li et al. 2014b). In gastric cancer, Cha *et al.* (2018) and Wu *et al.* (2019) have successively reported decreased miR-140-5p expression in gastric cancer tissues, and its positive correlation with advanced stage and poor clinical overcome. WNT1-mediated Wnt-β-catenin and THY1-mediated Notch signalling pathway were identified to be responsible for lower miR-140-5p induced increased proliferation, migration, invasion and impaired apoptosis of GC. Besides, Yu et al. (2019) discussed miR-140-5p participated in regulation of NDRG3 and contributed to 5-fluorouracil resistance in gastric cancer. However, it was reported that miR-140 exhibited significantly higher expression levels in post-neoadjuvant chemotherapy specimens compared with pre-neoadjuvant chemotherapy biopsies in breast cancer, and exhibited significantly even higher expression levels in the ineffective group compared to the effective group after neoadjuvant chemotherapy which indicated a poorer survival in breast cancer patients (Chen et al. 2016). Retinoblastoma (Rb) depletion or inactivation in soft tissue sarcoma cells exhibited slower proliferation and less efficient BrdU incorporation. However, much higher spherogenic activity and aggressive behavior both *in vitro* and *vivo.* miR-140-5p appeared to be positively controlled by Rb and to antagonize the effect of Rb depletion through targeting IL-6 (Yoshida et al. 2017). The induction of IL-6 secretion and subsequent autocrine/paracrine activation of STAT3 signalling supports the self-renewal activity of not only cancer cells (Sansone et al. 2007; Korkaya et al. 2012; Marotta et al. 2011) but also

embryonic stem cells or induced pluripotent stem cells (Takahashi and Yamanaka 2016; Brady et al. 2013). Furthermore, the promoting role of miR-140-5p to chemotherapy-induced autophagy was determined by in osteosarcoma cells. miR-140-5p expression was highly induced during chemotherapy of osteosarcoma cells, and this was accompanied by up-regulated autophagy. The increased miR-140-5p expression levels up-regulated anticancer drug-induced autophagy in osteosarcoma cells and ameliorated anticancer drug-induced cell proliferation and decreased viability decrease (Wei et al. 2016).

Significant upregulation of miR-140-3p was found in metastatic nodal tissues compared to nonmetastatic oral squamous cell carcinoma, and its expression had a strong negative correlation with their DNA copy numbers and a negative correlation with their target genes. Ingenuity Pathway Analysis on the expression of its target genes revealed a network associated with cell cycle, connective tissue development, and cellular function and maintenance. The central regulators in this pathway are p53, NF-κB, and HDAC1 (Serrano et al. 2012). In line with this study, highly expressed miR-140-3p has been demonstrated to control stemness of breast cancer cells as well. Contrary to the effect of the canonical hsa-miR-140-3p, overexpression of the 5'isomiR-140-3p led to a decrease in cell viability. The latter observation was supported by cell cycle analysis, where the 5'isomiR-140-3p but not the hsa-miR-140-3p caused cell cycle arrest in G0/G1-phase. Additionally, 5'ismoiR-140-3p overexpression was found to cause a decrease in cell migration (Salem et al. 2016). Up-regulated miR-140-3p was shown in metastatic renal cell carcinoma comparing to localized renal cell carcinoma (Zhu et al. 2016). Overexpression of miR-140-3p likewise correlated with recurrence and tumour invasion in patients with spinal chordoma (Gulluoglu et al. 2016; Zou et al. 2014). However, one controversial paper reported that increased expression of miR-140-3p predicted improved breast cancer survival (Chang et al. 2016).

1.4 Aims and objectives of this study

The aims of the present study are:

1) To examine the expression of deregulated miRNAs and prognostic related miRNAs in gastric cancer and their implication in the subtype classification of gastric cancer subtypes;

2) To select and clarify the role(s) of one or two miRNA(s) in gastric tissues and evaluate its or their potential as clinically relevant prognostic biomarker(s).

3) To determine its or their impact on the functions of gastric cancer cells via an *in vitro* cell model, which may contribute to its/their role(s) in the disease;

4) To discuss possible underlying molecular mechanism in its deregulation of gastric cancer.

Objective 1: Determination of miRNAs expression pattern in gastric cancer and their clinical relevance. The expression analysis of miRNAs sequencing data from the TCGA cohort (n=436) of gastric cancer tissue samples will be performed.

Objective 2: Expression of miR-140-5p and miR-140-3p will be determined using real-time quantitative PCR in two independent gastric cancer patients' cohorts with or without neoadjuvant chemotherapy, respectively. The association with histopathological and clinical characteristics will be evaluated accordingly. Additional analyses will be performed on relevant public gene expression array data to further validate our findings.

Objective 3: Function of miR-140-5p and miR-140-3p on gastric cancer cells.

This will be achieved initially by studying the behavior, in particular proliferation, migration, invasion and drug response of different gastric cell lines in response to transfection with miRNA overexpression miRNA mimics or inhibitors.

Objective 4: Molecular mechanisms.

According to the Gene Set Enrichment Analysis (GSEA) analysis, a computational method that determines whether an a priori defined set of transcriptome shows statistically significant, concordant differences between two biological states (a specific miRNA

upregulation and suppression) from TCGA, combining with the clinical relevance analysis and related cell behaviour alteration, cell cycle-related molecular mechanism will be investigated by determining expression and activation of candidate molecules.

Chapter 2.

Materials and Methods

2.1 Clinical cohort study

2.1.1 Gastric cancer cohort patient selection and tissue collection

Pairs of primary human gastric cancer tissue and corresponding normal gastric tissue (>5 cm away from tumour margin) were collected from surgical specimens of informed, consenting patients in 2 independent clinical cohorts. The first one included 70 gastric cancer patients who did not receive any pre-treatment before surgery from the Beijing Cancer Hospital from January 2004 to December 2010, and the second cohort contained 87 gastric cancer patients (diagnosed and histologically confirmed with stage IIIA, IIIB, or IV [M0]) attending the Beijing Cancer Hospital neoadjuvant chemotherapy clinic trial from January 2002 to December 2006. This study was conducted according to the principles of the Declaration of Helsinki and was approved by the Ethics Committee of The Beijing Cancer Hospital. After gastrostomy, resected specimens were processed routinely for macroscopic pathological assessment, then tissue samples sectioned at 20 μm thickness for RNA extraction, reverse transcription and transcript expression analysis using quantitative polymerase chain reaction (qPCR) were placed in labelled cryo vials, frozen in liquid nitrogen and stored in the research laboratory at -80°C until required for processing and analysis. The remaining surgical specimen was fixed in formalin for further wax blocking and section examination; the subsequent report was obtained for data stratification. Gastric cancer stage was classified according to the 2010 TNM classification recommended by the AJCC (7th edition). Patient records were reviewed in the context of clinicopathological and follow-up information. The median follow-up period was 21.7 months.

2.1.2 Preparation of tissue samples

Multiple sections of frozen tissue samples from the same patient sample biopsy were ground using a Leica CM1900 Cryostat (Leica Biosystems, Newcastle Upon Tyne, UK). 100 mg of homogenized sections were mixed thoroughly in 1 mL ice-cold TRI reagent (Sigma-Aldrich, Poole, UK) using a handheld homogenizer (Cole Palmer, London, UK). RNA was subsequently extracted according to the manufacturer's instructions. Following extraction, RNA was resuspended in diethyl pyrocarbonate (DEPC) water and quantified using a spectrophotometer (WPA UV 1101, Biotech, Cambridge, UK). Five micrograms of RNA samples were prepared for miRNA assay analysis, the remaining samples were subsequently

standardized before undertaking the reverse transcription reaction using an iScript cDNA synthesis kit (Bio-Rad Laboratories, Hemel Hemstead, UK) to generate cDNA.

2.1.3 General compounds

The general compounds used in this study and their sources are listed in Appendix 2.

2.1.4 General plastic consumables, hardware and software

The general plastic consumables, hardware, and software used in this study and their sources are listed in Appendix 3.

2.2 Cell lines

Six gastric cancer cell lines and a pair of colon cancer cell lines were used for the study. MKN7, MKN74, MKN45 and NUGC4 which have differing p53 status and established from gastric carcinomas, were purchased from RIKEN BioResource Centre CELL BANK (Ibaraki-ken, 305-0074 Japan); AGS and HGC27 were purchased from the American Type Culture Collection (ATTC, Rockville, Maryland, USA). The HCT116 p53 Wild type cell line and HCT116 p53 Knock-out cell line were provided by Professor M.C. Bibby (Cancer Research Unit, University of Bradford, UK) and routinely maintained in our lab. All information regarding these cell lines is listed in Table 2.1.

Table 2.1: Cell Lines, Origin and Additional Information. [1]WT: Wild Type, [2]stable: Microsatellite

Cell lines	Derived from	Morphology					Culture Properties	Donor	
		Lauren type	Original	Differentiation	p53	Others		age	gend
Gastric Cancer Cell Lines									
AGS	Primary cancer	Intestinal	Epithelial	Poorly	WT[1]	Stable[2]	Adherent	54	Fem
NUGC4	Primary cancer	Diffuse	Signet ring cell	Poorly	WT	Stable[2]	Adherent	35	Fem
MKN7	Metastatic site（lymph nodes）	Intestinal	Tubular adenocarcinoma	Well	Missense mutation (278)	HER-2 positive	Adherent	39	Ma
MKN74	Metastatic site（liver）	Intestinal	Tubular adenocarcinoma	Moderately	Missense mutation (251)	?	Adherent	37	Ma
MKN45	Metastatic site（liver）	Diffuse	Epithelial	?	p53 Missense mutation (110)	CEA highly producing	Adherent	62	Fem
HGC27	Metastatic site（lymph nodes）	?	?	Undifferentiated	p53 frameshift (152)	Stable[2]	Adherent	?	?
Colon Cancer Cell Lines									
HCT116 p53 WT	Metastatic site	?	Epithelial		WT	Unstable (MSI-high), CEA highly producing	Adherent	48	Ma
HCT116 p53 KO					Deleted of the exon2				

Table 2.2: Primers used in the current study to quantify gene expression

Gene	Primer	The sequence of Primer (5'->3')	size (bp)	Tm (°C)
CCND1	F1	AATGACCCCGCACGATTTC	191	59
	ZR1	ACTGAACCTGACCGTACATCAGGTTCAGGCCTTGCAC		
	F8	TGTGCTGCGAAGTGGAAACC	405	61
	R8	CCATTTGCAGCAGCTCCTCG		
DNMT1	F1	CGTGGTGGTGGATGACAAG	150	60
	ZR1	ACTGAACCTGACCGTACAGGCTCCCCGTTGTAGGAGAT		
	F8	GTGGGGGACTGTGTCTCTGT	676	59
	R8	TGCTGCCTTTGATGTAGTCG		
MDM2	F1	GTTATCTCAGTGCCTTTTGC	101	58
	ZR1	ACTGAACCTGACCGTACAAACAGACACATGTTCTACCC		
	F8	CCTTCGTGAGAATTGGCTTC	462	57
	R8	CATACTGGGCAGGGCTTATTC		
p21	F1	CTGGAGACTCTCAGGGTCGAA	66	60
	ZR1	ACTGAACCTGACCGTACAGCGTTTGGAGTGGTAGAAATCT		
	F8	GCGATGGAACTTCGACTTTG	352	58
	R8	GGGCTTCCTCTTGGAGAAGAT		
p53	F1	CTGTCATCTTCTGTCCCTTC	172	60
	ZR1	ACTGAACCTGATGGAATCAACCCACAGCTGCA		
	F8	AGACCCAGGTCCAGATGAAG	484	59
	R8	CACCACACTATGTCGAAAAGTGT		
GAPDH	F1	AAGGTCATCCATGACAACTT	87	55
	ZR1	ACTGAACCTGACCGTACAGCCATCCACAGTCTTCTG		
	F8	GGCTGCTTTTAACTCTGGTA	475	55
	R8	GACTGTGGTCATGAGTCCTT		

2.4 Antibodies

Primary antibodies used in this study are shown in Table 2.3

Table 2.3: Primary antibodies used in Western Blot. Secondary antibodies used were either horseradish peroxidase (HR
rabbit (A0545) IgG antibodies from Sigma-Aldrich (Poole, Dorset, UK), in a dilution of 1 in 2000.

Antibody	The molecular weight (kDa)	Target	Species	
MDM2	90	Raised against amino acids 154-167 of MDM2 of human origin for detection of MDM2, MDM2 p60 cleavage product and p53-MDM2 complexes by WB	mouse monoclonal	
p53	53	Specifically recognizes the N-terminal epitope mapping between amino acid residues 11-25 of p53 of human origin, which could be used for detection of wild-type and mutant p53 under denaturing and non-denaturing conditions of human origin by WB.	mouse monoclonal	
p21	21	Specific for an epitope mapping between amino acids 124-164 at the C-terminus of p21 of human origin	mouse monoclonal	
BAX	23	Amino acids 1-171 of Baxα	rabbit monoclonal	
GAPDH	37	GAPDH purified from rabbit muscle. recommended for detection of GAPDH of human origin by WB	Mouse monoclonal	B

2.5 Mimics and inhibitors

The ready-to-use MISSION miRNAs (Sigma-Aldrich, Poole, Dorset, UK): hsa-miR-140-5p (HMI0214), hsa-miR-140-3p (HMI0215) and the negative control mimic (HMC0003, sequence from *Caenorhabditis elegans* with no homology to human gene sequences) mimics were diluted in DEPC water to produce a stock concentration of 20 μM and used at a working concentration of 20 nM. MISSION® Synthetic microRNA inhibitors: miR-140-5p (HSTUD0214), hsa-miR-140-3p (HSTUD0215), and negative control inhibitor (cel-miR-243-3p, NCSTUD002) were diluted in DEPC water to produce a stock concentration of 10 μM and used at a working concentration of 10 nM.

2.6 Preparation for standard reagents and solutions

2.6.1 General laboratory used materials

Phosphate buffered saline (PBS)

One PBS tablet (Sigma-Aldrich) was dissolved in 200 mL of purified water to make a working concentration (containing 137 mM NaCl, 2.7 mM KCl, 10 mM Na_2HPO_4, 1.8 mM KH_2PO_4, pH 7.20 - 7.60). This was then autoclaved and aliquoted accordingly.

2.6.2 Materials for cell culture use

0.25% Trypsin-EDTA

A 10X stock of Trypsin-EDTA (Sigma-Aldrich) was diluted to a 1X solution with PBS. This was aliquoted and stored at -20℃ until use.

Antibiotics

Five millimolars of 100X antibiotics containing 10,000 U/mL penicillin, 10 mg/mL streptomycin, 25 μg/mL amphotericin was added to 500 mL growth media to make a final working concentration at 100 U/mL, 0.1 g/mL, streptomycin and 0.25 μg/mL amphotericin.

2.6.3 Materials for molecular biology

0.05% DEPC water (Diethyl pyrocarbonate)

A working solution of 0.05% DEPC water was prepared by dissolving 250 µL of DEPC was added to 500 mL of distilled water, left for 24 hrs and then autoclaved.

2.6.4 Materials for bacterial transformation

LB broth

LB broth was made by dissolving 10 g tryptone, 10 g NaCl and 5 g yeast extract in 1 liter of distilled water. After being adjusted pH to 7.0, the media was autoclaved prior to storage at 4°C until use. Appropriate antibiotics for colony selection were added prior to use.

LB Agar

LB agar was prepared by dissolving 10 g tryptone, 5 g yeast extract, 15 g agar and 10 g NaCl in 1 liter of distilled water. The pH was adjusted to 7.0 and the media was autoclaved and solid at room temperature. To prepare LB agar dishes, the agar was melted by heating in a microwave to reach a liquid state. And when it cooled to approximately 65°C, the appropriate antibiotic for colony selection was added, then poured into 10cm^2 Petri dishes. Once solidified, the plates were kept at 4°C until use.

2.6.5 Materials for western blot

Lysis buffer

The 100 mL lysis buffer containing NaCl 150 mM (0.87 g), TRIS base 50 mM (0.61 g), EGTA 5 mM (0.19 g), Triton X-100 1% (1 mL) was purchased from Melford Laboratories, UK. A protease inhibitor cocktail tablet (Roche) was added and the solution was aliquoted and stored at -20°C until use.

10% Ammonium Persulphate (APS)

One gram of APS (Melford Laboratories Ltd, UK) was dissolved in 10 mL of distilled water and stored at 4°C until use for up to 2 weeks.

10% Sodium dodecyl sulfate (SDS)

Ten grams of SDS (Sigma-Aldrich) was dissolved in 100 mL of distilled water and was stored at room temperature.

Running Buffer

One liter of 10X Tris-Glycine SDS buffer (Sigma-Aldrich) was added to 9 L of distilled water.

Transfer Buffer

One liter of 10X Tris-Glycine concentrate buffer (Sigma-Aldrich) was added to 7 L of distilled water and 2 L of methanol (Fisher Chemical, Leicestershire).

0.01% TBS-Tween (TBS-T)

For the washing solution, 500 µL of Tween20 (Melford Laboratories Ltd, UK) was added to 500 mL of 1X TBS and mixed thoroughly.

Blocking buffer

Non-fat dried milk (Marvel) was dissolved in 1X TBS-T to a final concentration of 5% (weight /volume) used for blocking membranes.

2.7 Cell culture, maintenance, and storage

2.7.1 Growth media

AGS, HGC27, HCT116 cell lines are cultured in Dulbecco's Modified Eagle's Medium (Sigma-Aldrich, Dorset, UK), supplemented with 10% fetal calf serum (FCS) (Sigma-Aldrich, Dorset, England, UK) and 1 × penicillin/streptomycin antibiotics (Sigma-Aldrich, Dorset, UK). The other cell lines are maintained in RPMI-1640 Medium (Sigma-Aldrich, Dorset, UK) and supplemented with FCS and antibiotics.

2.7.2 Cell maintenance

Cells were grown in culture flasks and incubated at 37°C and 5% CO_2 in a humidified incubator. Cells were cultured in 6-well-plates, 25cm^2 or 75cm^2 tissue culture flasks (Greiner Bio-One Ltd, Gloucestershire, UK) with loosely fitted caps. Mycoplasma contamination in cell cultures was estimated using EZ-PCR Mycoplasma Test Kit (Biological Industries, Israel). Cell medium was changed every 2-3 days and sub-cultured once they reached a confluence of approximately 85-90%. All cell work was carried out aseptically, using a Class II Laminar Flow Cabinet with sterile and autoclaved equipment and

consumables.

2.7.3 Trypsinisation of adherent cells and cell counting

Cell medium was aspirated, and the cells were briefly rinsed with sterile PBS before detaching adherent cells. Depending on the amount and characteristics of cells were cultured, 0.5-2 ml of Trypsin/EDTA (0.01% trypsin, 0.05% EDTA in borate buffered saline, BSS) was used to detach adherent cells and they were incubated at 37 °C for 2-5 minutes. Once disassociated, cells were collected in the appropriate medium containing FBS to stop the trypsinization reaction and transferred to 20 ml universal containers (Greiner Bio-One Ltd, Gloucestershire, UK) before being centrifuged at 1200 rpm for 5 minutes. The supernatant was then aspirated, and the cell pellet was resuspended in an appropriate amount of medium. Cells were either split and transferred to fresh tissue culture flasks for re-culturing or counted using Counter II FL Automated Cell Counter (Thermo Fisher Scientific, Waltham, MA USA) and then seeded at an appropriate concentration of cells for experimental requirements.

2.7.4 Frozen storage of cell stocks

Cells were trypsinized as previously described (section 2.7.3) and resuspended in medium containing 10% Dimethyl sulphoxide (DMSO; Sigma-Aldrich, Dorset, UK) at a cell density of about 10^6 cells/ml. The cell suspension was then divided into 1 mL aliquots and transferred into cryo-vials (Grenier Bio-One, Germany) pre-labelled with cell names, date of storing, owner's name and was then wrapped in protective tissue paper or loaded into frozen storage box containing isopropanol, before being stored at -80 °C or in liquid nitrogen tanks for long-term preservation.

2.7.5 Resuscitation of cells

After being removed from frozen storage, cryo-vials were thawed immediately in a 37 °C water bath. Once melting, cells are transferred into a universal container containing 9 mL of normal culture medium and being centrifuged at 1000 rpm for 5 minutes. The supernatant was then aspirated to remove the traces of DMSO from the cells. The cell pellet was resuspended in 5 mL of the medium before being transferred to a fresh 25 cm^2 tissue culture flask left overnight in normal culture conditions. After 24 hours, the revived cells were examined under the microscope to visually assess the viability of the adherent cells. The medium was aspirated and replaced with fresh medium. The flask was returned to the

incubator and the previous standard subculture techniques were carried out when necessary.

2.8 Methods for isolation and quantification of genetic material

2.8.1 RNA Extraction

The TRI Reagent® (Sigma-Aldrich, Poole, Dorset, England, UK), containing phenol and guanidine isothiocyanate which can break the protein-protein interactions and combine with the inactivation of cellular nucleases, was employed for RNA extraction. According to the manufacturer's instructions, cell medium was replaced with TRIzol® Reagent (1 mL for 5-10×10^5 cells). After addition of the reagent, this homogenate was passed several times through pipetting to form a homogenous lysate and then transferred in a 1.5 mL Eppendorf. Samples were left for 5 minutes at room temperature to ensure complete dissociation of nucleoprotein complexes. This was followed by the addition of 100 µL of 1-Bromo-3-chloropropane (Sigma-Aldrich, Poole, Dorset, England, UK), vigorous shaking for 15 seconds and incubation at room temperature for 15 min. The resulting homogenate was then centrifuged at 12,000 x g for 15 minutes at 4 °C. Under these acidic conditions, Centrifugation separates the homogenate into 3 phases: a pink organic phase (containing protein), a white interphase (containing DNA), and a colourless upper aqueous phase (containing RNA). This aqueous phase, which should constitute around 40-50% of the total volume, was then carefully removed and transferred into a fresh tube, before adding 0.5 mL of isopropanol (Sigma-Aldrich, Inc., Poole, Dorset, England, UK), and incubating for 10 minutes at room temperature. After centrifuging the samples at 12, 000 x g for 10 minutes at 4 °C, the RNA precipitate forms as a white pellet could be seen on the side and bottom of the tube. The supernatant was then aspirated, and the RNA pellet was washed by vortexing it with 1 mL of 75% ethanol (3:1 ratio of pure ethanol and diethylpyrocarbonate, DEPC, water) and subsequently vortexing and centrifuging the samples at 7, 500 x g for 5 minutes at 4 °C. After the ethanol was aspirated, the pellets were further air-dried at room temperature for 5 mins to remove any remaining traces of ethanol. DEPC water was pre-warmed at 55 °C in a Techne, Hybridiser HB-1D drying oven (Wolf Laboratories, York, UK), then dissolve the RNA pellet in 20-50 µL (depending on pellet size) in pre-warmed DEPC water by repeated pipetting for a short while.

2.8.2 Genomic DNA extraction

In order to assess the status of miR-140 in different cell lines used in this study, again, the TRI-reagent was applied for this procedure. Cells were lysed and separated into three different phases as elucidated previously. The aqueous RNA phase overlaying the DNA interphase was carefully removed to improve the quality of the DNA isolated. The DNA was precipitated from the interphase and organic phase by adding 0.3 mL of 100% ethanol per 1 mL of TRI-Reagent used and mixing by inversion. The mix was allowed to stand for 2-3 minutes at room temperature before being centrifuged at 2, 000 x g for 5 minutes at 4 °C. The supernatant was discarded, and the DNA pellet was washed twice in 1 mL of 0.1 M trisodium citrate, 10% ethanol solution for every 1 mL of TRI-reagent used to remove phenol from the DNA. During each wash, DNA pellet was allowed to stand for at least 30 minutes. With occasional mixing. Samples were centrifuged again at 2, 000 x g for 5 minutes at 4 °C and the DNA pellet was resuspended in 1.5 mL of 75% ethanol per 1 mL of TRI-reagent and left to stand for 20 minutes at room temperature. The DNA pellet was air-dried for 5-10 minutes and dissolved by repeated slow pipetting with a micropipette in 8 mM NaOH (0.1 mL to the DNA isolated from fully confluent 25 cm^2 flask).

2.8.3 Spectrophotometric quantification of RNA and DNA

Once isolation was completed, the concentration and purity of the RNA and DNA were measured by a NanoPhotometer (Implen, München, Germany). The absorbance measure unit is the wavelength (λ) and some typical values are reported below:

λ = 230 nm: the wavelength of absorption of complex carbohydrates and phenols;

λ = 280 nm: the wavelength of absorption of proteins;

λ = 260 nm: the wavelength of absorption of nucleic acids;

λ = 320 nm: the wavelength of absorption of other contaminants.

Two μL sample was used to detect single-stranded RNA (μg/μL) at the wavelength of 260 nm, using DEPC water as a blank. The purity of RNA is evaluated by the ratio of the readings at 260 nm and 280 nm (A260 / A280) and at 260 nm and 230 nm (A260 / A230). The A260 / A280 ratio provides an estimate of the purity of RNA with respect to contamination by protein and its value must be higher than 1.7. The A260 / A230 ratio provides an estimate of the purity of RNA with respect to contamination by solvent (phenol, salts) and its value must not be fewer than 2.2. Contaminations may decrease the efficiency

of the following reactions, mainly by the inhibition of the enzymes. DNA was also measured using the NanoPhotometer, set to measure double-stranded DNA at 260 nm. After the purification and quantification, the RNA samples are ready to be used immediately or they can be stored at -80^{o}C for later use.

2.8.4 Reverse transcription (RT) of mRNA

To measure genes expression at transcription level, 500 ng of RNA (cDNA synthesis, as measured by real-time PCR, has a linear relationship to the input RNA across this range.) was converted into complementary DNA (cDNA) using the GoScript™ Reverse Transcription System (Promega Corporation, Madison, USA), following the protocol outlined below.

The required volume of isolated RNA containing the desired quantity of RNA was made up to 9 µL with PCR water in a thin walled 0.2 mL PCR tube. 1 µL of RT primer was added and the resultant mixture was heated at 70°C for 5 minutes to denature the secondary structure of RNA allowing more effective reverse transcription.

Table 2.4.1: Reverse transcription PCR preparation 1

Component	1 reaction (µL)
RNA template (up to 2 µg)	X
RT primer	1.0
RNAse/DNAse free water	X
Final volume	5

Oligo-dT primers which bind to the polyA tail of messenger RNA were preferentially used in this process. Following this incubation period, the PCR tube was immediately placed on ice. The RT mix was made up using the following components:

Table 2.4.2: Reverse transcription PCR preparation 2

Component	1 reaction (µL)
GoScript™ 5X Reaction Buffer	4.0
$MgCl_2$ (final concentration 25 mM)	2.0
dNTP mix 10 mM	1.0
RNAse/DNAse free water	7.0
GoScript™ Reverse Transcriptase	1.0
Final volume	15.0

10 μL of the above RT mix was added to each of the samples on ice. After briefly cortex and a pulse spin, the resultant mixture was incubated at 25°C for 5 minutes, 42°C for 60 minutes and 75°C for 20 minutes. The cDNA was diluted in nuclease-free water in the ratio 1:8. cDNA Samples were added to PCR or qPCR amplification or stored at -20°C until use.

2.8.5 General polymerase chain reaction (PCR)

General PCR was performed using GoTaq Green Master Mix (Promega, Madison, USA) and specific primers designed for the identification of the gene targets, which were synthesized by Sigma (Sigma-Aldrich, Dorset, UK). Reactions for each sample were set up in 0.2 mL PCR tube or a 96 well plate, as shown below:

Table 2.5: General PCR preparation

Component	1 reaction (μL)
2X GoTaq Green Master Mix	8.0
Forward primer (10 pmol)	1.0
Reverse primer (10 pmol)	1.0
Nuclease-free water	5.0
cDNA template	1.0
Final volume	16.0

Once set up, the prepared reactions were briefly mixed and centrifuged. All reactions were run alongside a negative control, which consisted of using nuclease-free water instead of the cDNA template to ensure there was no contamination of the master mix. A loading control probing for *GAPDH* expression was also run for each sample to confirm similar cDNA quantities in each reaction prepared.

The PCR tubes or 96 well plates were placed in a 2720 Thermal Cycler (Applied Biosystems, Paisley, UK). PCR conditions for *MDM2* and *GAPDH* primers were optimized as:

Step 1 – Initial denaturation at 94 ˚C for 5 minutes

Followed by 25-42 cycles of:

Step 2 – Denaturing step at 94 ˚C for 30 seconds

Step 3 – Annealing step at 55 ˚C for 30 seconds

Step 4 – Extension step at 72 ˚C for 1.5 minutes

And finally:

Step 5 – Final extension at 72 ˚C for 10 minutes

2.8.6 Agarose gel electrophoresis and visualization

Samples were loaded onto 0.8% to 2.5% agarose gels (Melford Chemicals, Suffolk, UK), depending on the predicted size of the DNA products. Weigh out the appropriate mass of agarose into an Erlenmeyer flask, UK), and add the appropriate volume of 1X Tris-borate-EDTA (TBE) buffer. Melt the agarose/buffer mixture by heating in a microwave, at 30 s intervals, remove the flask and swirl the contents to mix well. Repeat until the agarose has completely dissolved. SYBR Safe Gel Stain (Invitrogen, Paisley, UK) was then added at a ratio of 1:10000. The agarose was left to cool slightly before being poured into the removable gel tray and it was allowed to place an appropriate comb into the gel mold to create the wells. Once set, the gel was submerged in 1X TBE buffer and the comb was removed. 10 μL of the PCR samples were loaded in each well, alongside 5 μL of a 100 bp or 1 Kb DNA ladder (Genscript, Piscataway, USA). Attach the leads of the gel box to the power supply, double checking the cathode (black leads) should be closer the wells than the anode (red leads). The samples were subjected to electrophoresis using a power pack (Gibco, Paisley, UK) at 100 V, 90 mA, 50 W for 30 minutes (or until the dye has migrated to an appropriate distance). Gels were visualized and imaged using a U: Genius gel doc system (Syngene, Cambridge, UK).

2.8.7 Real-time quantitative polymerase chain reaction (RT-qPCR)

Quantitative PCR with a heat stable DNA polymerase could detect the products of the reaction from the first cycle in which the amplified target becomes detectable (threshold cycle, Ct) and thus generate a more accurate and reproducible result than the traditional end-point PCR. The Ct value is inversely correlated with the starting amount of target genes. In the current study, qPCR was performed using the Amplifluor ™ Universal Detection System (Intergen®, New York, USA). This system is based on molecular energy transfer from an excited fluorophore (fluorescein) to an acceptor moiety [4-(4'-dimethylaminophenylazo) sulfonic acid (DABSYL)] that quenches the fluorescence emission. The fluorophore and acceptor are tethered together via an oligonucleotide primer called UniPrimer™. Amplifluor™ UniPrimer™ hairpin primers are designed in such a way that a fluorescent

signal is only generated when the primer is unfolded during its incorporation into an amplification product.

Contained within the UniPrimer™ is a 3'-18 base oligonucleotides of tail called a Z sequence, which acts as a universal PCR primer. The fluorophore and acceptor are located at the 5' end. In order to use the UniPrimer™, the Z sequence is added to the 5' end of a target-specific primer. The UniPrimer™ can then anneal to the Z' sequence in an amplicon generated in the initial cycles of the PCR reaction. As the UniPrimer™ is incorporated, the hairpin becomes unfolded, quenching can no longer occur and then a fluorescence signal that directly correlates to the amount of amplified DNA is produced. An illustration showing how the Amplifluor™ Universal detection system using the UniPrimer™ detection system works is shown in Appendix 4.

The components of each qPCR reaction are shown in Table. 2.6 Each sample was loaded into a 96 well plate (Applied Biosystems™, Life Technologies Ltd, Paisley, UK), covered with MicroAmp® Optical Adhesive film (ThermoFisher Scientific, Life Technologies Ltd, Paisley, UK) and run alongside a podoplanin (PDPL) standard of a known transcript number (ranging from 101 to 108). PDPL is a lymphangiogenesis marker, which acted as a reference control gene to ensure any differences observed were not due to technical errors and allowed normalization of results from different plates. GAPDH is an enzyme of ~37kDa that catalyses the sixth step of glycolysis and thus serves to break down glucose for energy and carbon molecules. Because the *GAPDH* gene is often stably and constitutively expressed at a high level in most tissues and cells, it is considered a housekeeping gene and is commonly used as a reference point for the analysis of expression levels of other genes. The 96 well plate was placed in an iCycler Thermal Cycler which uses a light source to excite the fluorescent molecules in the wells and an image intensifier and a 350,000-pixel charge-coupled device (CCD) detector to image all 96 wells every second and detect fluorescent light.

An example of the amplification plot and standard curve produced using qPCR is shown in Appendix 5.

Each cDNA sample was diluted 1:8 with ddH_2O. RT-qPCR performed using TaqMan® Universal PCR Master Mix (Applied Biosystems, Paisley, UK) and Universal Primer

(Intergen®, New York, USA), with forward and fluorescent tagged reverse primers designed for target gene amplification. Reactions for each sample were loaded in a 96 well plate with triplicates, as shown in Table 2.6.

Table 2.6: qPCR preparation

Component	1 reaction (µL)
2X IQ Master Mix	5.0
Forward primer (10 pmol)	0.3
Reverse primer (1 pmol)	0.3
Universal primer (10 pmol)	0.3
cDNA template	1.0
ddH2O	3.1
Final volume	10.0

The plate was covered with optically clear Microseal® (BioRad Laboratories, California, USA) and placed in a StepOnePlus™ Real-Time PCR System (Thermo Fisher Scientific, Waltham, MA USA) at the following parameters: initial denaturation for 10 minutes at 95 ˚C; followed by 85 cycles of denaturation at 95 ˚C for 10 seconds, annealing at 55 ˚C for 30 seconds and elongation at 72°C for 10 seconds. Results were analyzed using ΔΔCT normalization to the housekeeping gene, GAPDH.

2.8.8 miRNA reverse Transcription and real-time PCR

The reverse transcription for mature miRNA quantification was performed using TaqMan™ Advanced miRNA cDNA Synthesis Kit (Applied Biosystems, UK). Each reaction containing 5 ng RNA sample was set up in a 0.2 mL PCR tube (ABgene, Surrey, UK) and the manufacturer's protocol was adjusted as follow:

Perform the poly (A) tailing reaction, to modify mature miRNA by adding a 3' adenosine tail to the miRNA.

Table 2.7.1: miRNA reverse transcription PCR preparation

Component	1 reaction (µL)
10X Poly (A) Buffer	0.5
ATP	0.5
Poly (A) Enzyme	0.3
RNase-free water	1.7
RNA sample (5 ng)	2.0
Final volume	5.0

The reaction plate or tubes are placed into a 2720 Thermal Cycler (Applied Biosystems, Paisley, UK), then incubate using the following settings and standard cycling: polyadenylation at 37 ˚C for 45 minutes, 65 ˚C for 10 minutes and Hold at 4°C, then proceed to Ligation Reaction, which allows the miRNA with poly(A) tail undergoes adaptor ligation at the 5' end and the adaptor could act as the forward-primer binding site for the following miR-Amp reaction .

Table 2.7.2: miRNA reverse transcription PCR preparation.

Component	1 reaction (µL)
5X DNA Ligase Buffer	3.0
50% PEG 8000	4.5
25X Ligation Adaptor	0.6
RNA Ligase	1.5
RNase-free water	0.4
Poly(A) tailing reaction product.	5.0
Final volume	15.0

Samples were incubated in a thermal cycler using the following settings and standard cycling: ligation at 16 ˚C for 60 minutes, following setting up and mixing with the reverse transcription (RT) reaction immediately as below:

Table 2.7.3: miRNA reverse transcription PCR preparation

Component	1 reaction (µL)
5X RT Buffer	6.0
dNTP Mix (25 mM each)	1.2
20X Universal RT Primer	1.5
10X RT Enzyme Mix	3.0
RNase-free water	3.3
Adaptor ligation reaction product	15.0
Final volume	30.0

The reaction plate or tubes are placed into a thermal cycler, then incubated using the following settings and standard cycling: reverse transcription at 42 ˚C for 15 mins, stop reaction at 85 ˚C for 5 minutes; In this step, a Universal RT primer binds to the 3' poly(A) tail and the miRNA is reverse transcribed. The resulting cDNA will be suitable for all TaqMan® Advanced miRNA Assays. The last step is preparing the miR-Amp reaction to improve detection of miRNA targets.

Table 2.7.4: miRNA reverse transcription PCR preparation

Component	1 reaction (μL)
2X miR-Amp Master Mix	25.0
20X miR-Amp Primer Mix	2.5
RNase-free water	17.5
RT reaction products	5.0
Final volume	45.0

PCR amplification was performed following parameters: enzyme activation for 5 minutes at 95°C; followed by 14 cycles of denature at 95 °C for 3 seconds, annealing and extending at 60°C for 30 seconds, finally stop the reaction at 99 °C for 10 minutes. The undiluted miR-Amp reaction products were proceeded to performing the real-time PCR or stored at –20 °C for up to 2 months.

Before performing real-time PCR, cDNA templates were diluted 1:10 with ddH_2O. Each reaction was performed as follows:

Table 2.8: qPCR preparation

Component	1 reaction (μL)
TaqMan® Fast Advanced Master Mix (2X)	10.0
TaqMan® Advanced miRNA Assay (20X)	1.0
RNase-free water	4.0
Diluted cDNA template	5.0
Final volume	20.0

The reaction plate was loaded in the StepOnePlus™ instrument (Thermo Fisher Scientific, Waltham, MA USA), at the following conditions: enzyme activation at 95°C for 20 seconds, following 40 cycles denature at 95 °C for 1 second and anneal/extend at 60°C for 20 seconds. Results were transformed by $2^{-\Delta\Delta Ct}$, where: ΔCt = target gene Ct – housekeeping gene, Ct ΔΔCT = ΔCt experimental group – ΔCt mean of the negative control group. Our examination of hsa-miR-423-5p verified it was relatively consistent and moderately abundant across stomach tissues and gastric cancer cell lines. Thus hsa-miR-423-5p was chosen as an endogenous control for normalization.

Table 2.9: miRNA assay information

Assay name	Target Sequence
hsa-miR-423-5p	5'-UGAGGGGCAGAGAGCGAGACUUU-3'

hsa-miR-140-5p	5'-CAGUGGUUUUACCCUAUGGUAG-3'
hsa-miR-140-3p	5'-UACCACAGGGUAGAACCACGG-3'

2.9 Methods for protein extraction and detection

2.9.1 Protein extraction

Cells were seeded into 6-well-plates. Upon reaching sufficient confluency, cells were washed with ice-cold PBS twice and scraped with 80 uL cell lysis buffer on ice. The cell suspension was transferred to a 2 mL Eppendorf tube and followed by being placed on a Labinoco rotating wheel (Wolf Laboratories, York, UK) for 1 hour rolling at 25 rpm. The lysates were then centrifuged at maximum speed (15,000 x g) in a benchtop Eppendorf microcentrifuge for 30 minutes at 4 °C. The supernatant was then transferred to a new 1.5 mL microcentrifuge tube for determination of protein quantification.

2.9.2 Determination of protein concentration

For a typical protein assay, a chemical reagent is added to the protein sample, producing a colour change in the sample solution. This colour change is quantitated with a spectrophotometer or microplate reader and compared to a standard curve of known concentrations of protein versus their absorbance after reaction with the reagent. The amount of protein in the unknown sample is determined by interpolation, reading the concentration of protein on the standard curve that corresponds to its absorbance.

2.9.2.1 Preparation of diluted albumin (BSA) standards

A standard curve was made by preparation of diluted bovine serum albumin (BSA) standards. Dilute the contents of 1mL of 10 mg/mL BSA into several clean vials, as shown in Table 2.10.

Table 2.10: Preparation of diluted BSA Standards

Vial	Volume of Diluent (µL)	Volume and Source of BSA (µL)	Final BSA Concentration (µg/mL)
1	0	300 of Stock	10,000
2	100	400 of Stock	8,000
3	325	325 of Stock	5000
4	325	325 of Vial 2	4000
5	325	325 of Vial 3	2500

6	325	325 of Vial 4	2000
7	325	325 of Vial 6	1000
8	400	100 of Vial 5	500
9	400	100 of Vial 7	200
10	375	375 of Vial 9	100
11	400	100 of Vial 10	25
12	400	0	Blank = 0

2.9.2.2 Preparation of the working reagent

The colorimetric Bio-Rad Detergent Compatible Protein Assay Kit was used to determine protein concentration. These assay solutions include the Reagent A (alkaline copper tartrate solution), Reagent S (surfactant solution), and Reagent B (Folin reagent). Prepare working reagent by mixing 50 parts of Reagent A with 1 part of Reagent S (50:1, Reagent A: S).

The following formula was used to determine the total volume of Bio-Rad required: (# standards + # unknowns) × (# replicates) × (25 μL per sample) = total volume working reagent required

Five microliters of standards and unknown samples in triplicate were pipetted into 96-well -plate. 25 μL of working reagent was added to each well and gently mixed. 200 μL of Reagent B was subsequently added into each well. The samples were mixed thoroughly using a microplate mixer and incubated at room temperature for 15 mins. Then the absorbance was measured at 630 nm (available at 405-750 nm) using the ELx800 plate reading spectrophotometer (Bio-Tek, WolfLaboratories, York, UK). After calculating the concentration by comparing the reading to BSA standard curve, samples were diluted into the same concentration (4 μg/μL) with lysis buffer, and aliquoted into several 0.5 mL Eppendorf tubes. One of them was further mixed with 2X SDS Laemmli Buffer (Sigma-Aldrich) at a ratio of 1:1. The samples were then denatured at 100 °C for 5 minutes and spun down briefly before loading onto the SDS-PAGE gel. The remaining aliquots were stored at -80°C for up to one month.

2.9.3 SDS Polyacrylamide gel electrophoresis (SDS-PAGE) for protein separation

The percentage of the gel used was dependent on the molecular weight (MW) of the desired protein to be detected. As shown in Table 2.11.

Table 2.11: Protein size and gel percentage selection

Protein MW range (kDa)	Recommended gel (%)
10-80	14%
20-150	12%
30-200	10%
40-250	8%
60-300	6%

For a 10% resolving gel, Table 2.12 depicts the components and volumes used. For the 5% stacking gel, Table 2.13 depicts the components and volumes used.

Table 2.12: Components and volumes for a 10% resolving gel

Solution	Component volume (mL)
H_2O	5.9
30% acrylamide mix (Sigma-Aldrich, St Louis, USA)	5.0
1.5 M Tris-HCl (pH 8.8)	3.0
10% SDS	0.15
10% Ammonium persulfate	0.15
N, N, N′ , N′ -tetramethylelthylenediamine (TEMED, Sigma- Aldrich St Louis, USA)	0.006

Table 2.13: Components and volumes for a 5% stacking gel

Solution	Component volume (mL)
H_2O	3.4
30% acrylamide mix (Sigma-Aldrich, St Louis, USA)	0.83
0.5 M Tris-HCl (pH 6.8)	0.63
10% SDS	0.05
10% Ammonium persulfate	0.05
TEMED (Sigma- Aldrich St Louis, USA)	0.005

The resolving gel was added between two glass plates held in place by a loading cassette up to 1.5 cm below the top edge of the plate. To produce a smooth level surface, the gel was coved by water and allow to polymerize at room temperature. Once the resolving gel had set totally, the overlaid water was poured out and the excess was removed by using a piece of filter paper. The stacking gel was prepared according to Table 2.13 and added above the resolving gel. A well-forming Teflon comb was then inserted, and the gel was allowed to polymerize at room temperature. The cassette was then placed into a gel electrophoresis apparatus filled with running buffer before removing the wells' comb. 5 µL of a protein MW marker (BLUeye Prestained Protein Ladder, 10-250 kDa, GeneDireX, Belgium) and 20 µg

pre-heated protein sample were loaded. The gel was run at a constant voltage of 80 V for 100 minutes (until the blue indicator strip reached the end).

2.9.4 Transfer of proteins to polyvinylidene fluoride membrane and membrane blocking

Once the SDS-PAGE was completed, the protein samples were transferred to an Immobilon® PVDF membrane (Merck Millipore, MA, USA) using a SemiDry system. A piece of PVDF membrane cut to the same size as the resolving gel was activated in methanol for 5 minutes. Simultaneously, six pieces of similarly sized filter papers were soaked in 1X transfer buffer. Three of these sheets were placed one at a time onto the bottom graphite base electrode of an SD20 SemiDry Maxi System blotting unit (SemiDry, Wolf Laboratories, York, UK). The SDS-PAGE gel cassette was removed from the tank and the glass plates gently pried using a scalpel and the resolving gel was carefully transferred on top of the PVDF membrane, alongside the remaining three sheets of filter paper. Following removing air bubbles between each layer by rolling a roller over the top filter paper, electroblotting was carried out at a constant current of 500 mA (approximately 15 V) for 90-120 minutes. (Figure 2.1 from Nature Protocol Exchange: https:// www.nature.com/ protocol exchange/ protocols/ 2925)

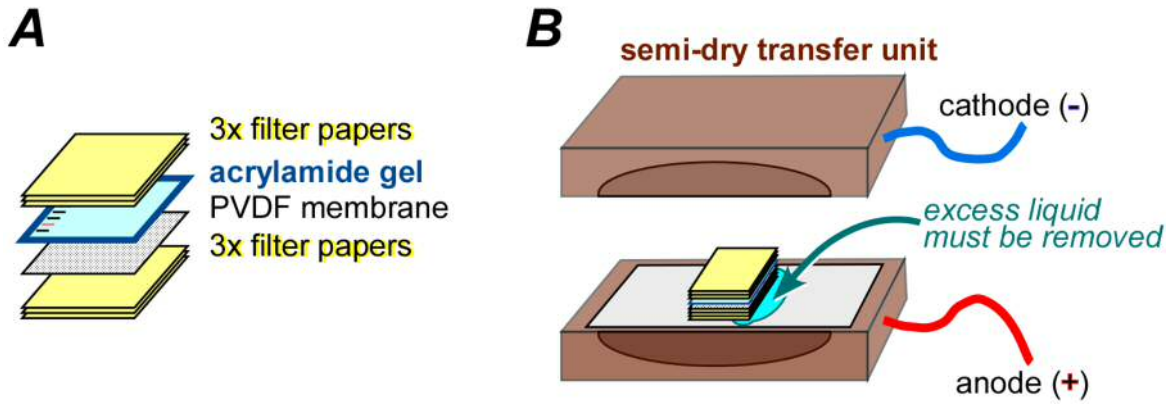

Figure 2.1: The arrangement of paper, gel and nitrocellulose membrane. A. The membrane is oriented nearest to the positive electrode while the gel is situated towards the negative electrode. B. Representative diagrams of the transfer sandwitch setup for semi-dry transfer. The SDS-bound negatively charged proteins with thus migrate out of the gel and onto the membrane. Source: https://protocolexchange.researchsquare.com/article/nprot-2925/v1

Once the transfer was completed, membranes were transferred into a universal container and incubated in 5% (w/v) blocking buffer (5 g of fat-free milk powder (Marvel) in 100 mL of

0.1% TBS-Tween) for at least one hour to ensure non-specific binding of the primary antibody. The universals were kept on a rolling platform (Wolf Laboratories, York, UK).

2.9.5 Immuno-blotting of proteins

Primary antibodies were diluted in TBS-T according to Table 2.3. After the blocking, the membrane was incubated with the primary antibody at 4°C overnight with constant rotation. Membranes were then washed three times (5 minutes each) using 0.1% TBS-Tween with constant rotation. The secondary antibody was chosen according to the source of the primary antibody. 2.5 µL of HRP-conjugated secondary antibody was diluted 5 mL 0.1% TBS-Tween. The membrane was then incubated in the secondary antibody for 1 hour at room temperature with constant rotation.

Chemiluminescence was performed using a luminol/ peroxide based enhanced chemiluminescence (ECL) reagent (Supersignal™ West Pico, Thermo Fisher Scientific, Waltham, MA USA). The ECL reagent enables low picogram or high femtogram detection of antigen by oxidizing luminol in the presence of HRP and peroxide. This reaction produces a prolonged chemiluminescence that can be visualized on X-ray film or an imaging system. According to the manufacturer's instruction, 100 µL of ECL reagent was required to per cm^2 of membrane area. After 5 minutes of incubation, the chemiluminescent signal from the HRP-conjugated antibody was detected using G: Box (Syngene, Cambridge, UK), composed of an illuminator and a camera connected to a computer. Briefly, the membrane was placed on the black Chemiluminescence Exposure Screen. The imager calculates and displays the exposure time with maximum dynamic range and minimum pixel saturation. Images were captured and further analyzed by Image J software (National Institute of Health, NY, USA, https://imagej.nih.gov/ij/, 1997-2016) for band quantification.

2.10 Methods for cell functional assays

2.10.1 Transfection of miRNA mimic/ inhibitor into Cell Lines

Following seeding of 3 x 10^5 cells/well in 6-well-plate, cells were incubated until adherent. 20 pmol of MISSION miRNA-140-5p, miRNA-140-3p or Negative Control mimic (Sigma, St. Louis, USA) was transfected the cell line using 7.5 µL Lipofectamine® 3000 reagent per well with Opti-MEM, according to manufacturer's instructions (Invitrogen, Thermo Fisher,

UK).

2.10.2 Proliferation assay using thiazolyl blue tetrazolium bromide (MTT)

Cell proliferation in response to treatment with miRNA mimics was measured using MTT (Sigma-Aldrich, St. Louis, MO, USA) assay. The MTT assay involves the conversion of the water-soluble MTT (3-(4, 5-dimethylthiazol-2-yl)-2, 5-diphenyltetrazolium bromide) to an insoluble formazan. The formazan is then solubilized, and the concentration determined by optical density at 570 nm. MTT solution was made by diluting 100 mg of MTT in 20 mL of PBS and was filter sterilized through a 0.2 μm sterile filter (Sartorius AG, Göttingen, Germany) to produce a working concentration of 5 mg/mL. Following 12 hours of treatment of cells with mimics or inhibitors, cells were harvested, pelleted and resuspended. Using 96-well-plate, 3000 cells in 100 μL of complete media were plated per well of six 96 well plates using at least six repeats for each cell line and a negative control. The plates were incubated at 37 °C and 5% CO_2 for a period of 12, 24, 36, 48 and 64 hours respectively. At each time point, 10 μL of MTT solution was added directly to the well. Following a 4-hour incubation period at 37°C, the media was poured out gently and blotted the excess liquid with a piece of tissue paper. To solubilize formazan crystals, lysis buffer was mixed by 10 g SDS in 100 mL H_2O with 83 μL of 37% HCl under the fume hood. 100 μL of the SDS-HCl lysis solution was added to each well and mixed thoroughly using the pipette. Absorbance was read at 570 nm (Bio-Rad 550 microplate reader; Bio-Rad Laboratories Inc., Hercules, CA, USA).

2.10.3 Scratch assay for migration

Migration reflects cell motility in a 2D pattern such as a basal membrane, extracellular matrix or on plastic plates. Via wound healing assay, the speed of wound closure and cell migration can be quantified by taking snapshot pictures with a regular inverted microscope at several time intervals.

Sufficient cells ($1x10^6$/well) were seeded into a 6-well plate and allowed to adherent overnight to form a confluent monolayer in the incubator. The scratch wound was made in a linear fashion with a sharp sterile pipette tip and washed twice with PBS to remove floating cells. The cells were re-cultured in 2 mL of new media and cell migratory behaviour was documented every 1 hour using the EVOS® Cell Imaging time-lapse microscopy system

(Life Technologies, Paisley, UK). The size of the wounds was subsequently measured with ImageJ software.

2.10.4 Transwell invasion assay

Invasive migration is a fundamental function underlying cellular processes such as angiogenesis, immune response, metastasis, and invasion of cancer cells. Cell invasion assays monitor cell movement penetrating a barrier which consists of basement membrane components. Matrigel® (BD Biosciences, NJ USA) was used to mimic extracellular matrices (Figure 2.2).

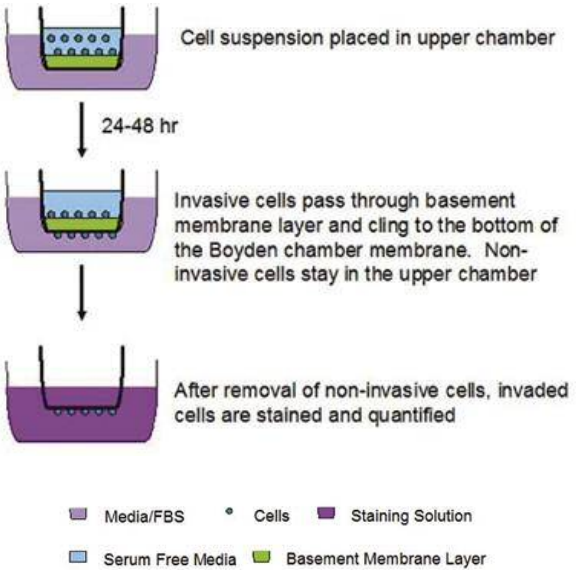

Figure 2.2: In vitro Matrigel® invasion assay. Cells seeded at the top chamber and chemoattractant or different cell line in the bottom chamber – outcome: number of cells migrated to the bottom chamber, compared to controls. Source: Adapted from http://cellomaticsbio.com/molecule-testing.php

2.10.5 Flow cytometry cell cycle assay

Flow cytometry was carried out for cell cycle analysis by quantitation of DNA content. Propidium iodide (PI), one of the DNA-binding dyes, is used in this analysis. Cells must be fixed or permeabilized to allow entry of the dye which is otherwise actively pumped out by living cells. Alcohol is a dehydrating fixative which also permeabilizes. This will allow easy access of the dye to the DNA and gives good profiles (low coefficient of variation, CV). With fixed cells, samples may be accumulated, stained and analyzed at the conclusion of an experiment. Alcohol-fixed cells are stable for several weeks at 4°C.

When the cells were grown to 80% confluent, cell medium and PBS used to wash cells were collected in labeled 20 mL universal containers (Greiner Bio-One Ltd, Gloucestershire, UK); Meanwhile, cells were trypsinized and plated in the incubator until disassociation. Then, cells are harvested into universals using pre-collected cell medium and PBS to neutralize trypsinization reaction. The suspension was centrifuged at 1500 × rpm for 5 minutes. The cell pellet was fixed in 10 mL iced 70% ethanol. Samples were pipetted thoroughly to ensure fixation of all cells and minimize clumping and stored at 4 ˚C for 30 min or until analysis. Spin at 850 g in a centrifuge and spinning out of ethanol carefully to avoid cell loss when discarding the supernatant. 50 μL of a 100 μg/ml sock of RNase was added to ensure only DNA, not RNA, will be stained. 200 μL PI (from 50 μg/ml stock solution) was added before cell cycle measurement. Flow cytometry analysis was performed on a Cyflow® flow cytometer (Partec, New Jersey, USA). Data were analyzed using FCS Express 4 Flow Research Edition (De Novo Software, California, USA).

Gating for live cells was carried out using forward scatter area (FCS-A) and side scatters area (SSC-A). FCS-A measures the size whereas the SSC-A measures the cell granularity. Next gating for single cells was performed using the FSC-A and forward scatter height (FSC-W) to eliminate doublet cells (Figure 2.3) From this gate the cell cycle histogram was made using fluorochrome channel PerCP-CY5-5-A against cell count. From here the percentage of cells in G1, S and G2 phase could be calculated (Figure 2.4).

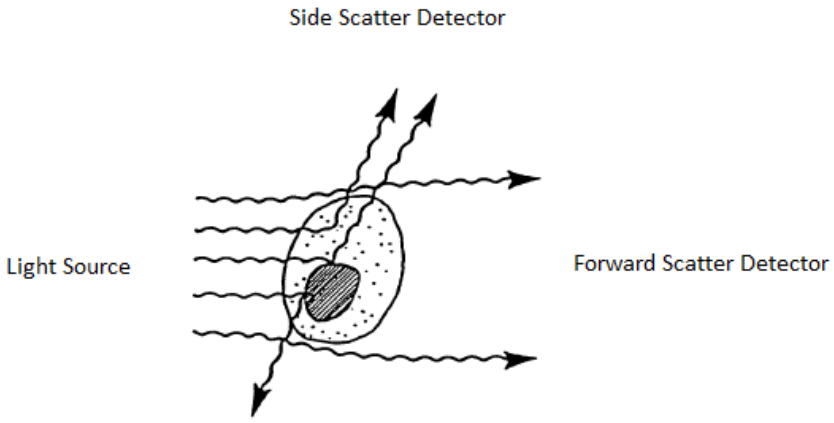

Figure 2.3: Scattering system in FACS. Forward and side scatter data can be used to classify samples by size (FSC) and by internal complexity (SSC). Source: Flowcytometrynet https://www.flowcytometry net.com/

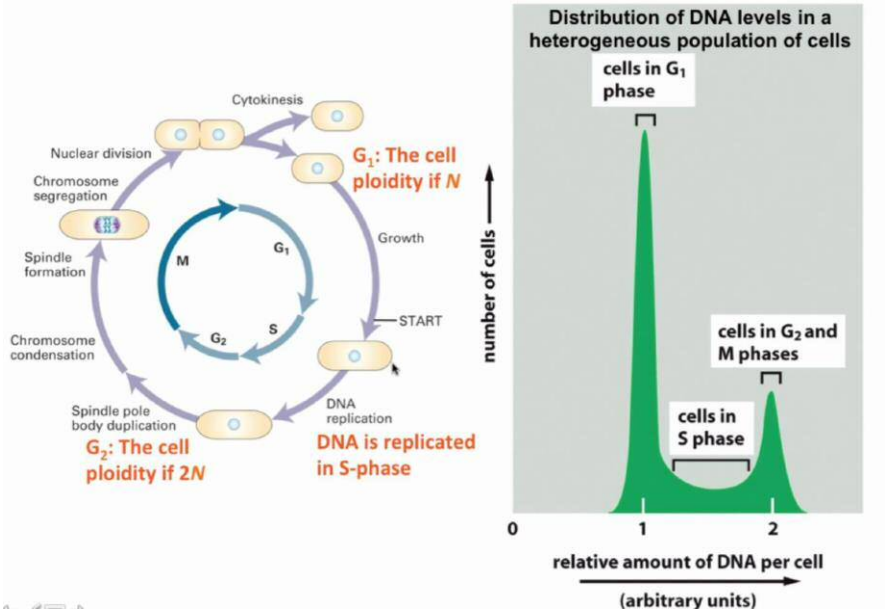

Figure 2.4: Relationship between the cell cycle and the DNA histogram. Source: http://flowbook.denovosoftware.com/ chapter-6-DNA-analysis

2.10.6 Cytotoxicity assays using MTT

To determine the effects of 5FU and cisplatin on cell proliferation, growth assay based on the enzymatic reduction of the tetrazolium salt MTT by metabolically active cells. Cell growth was determined as described previously, with a few modifications. Briefly, 10^4 cells were seeded per well of 96-well plates, in 100 µL of steroid-stripped medium (without additions). Cells were allowed to attach for 24 hrs, after which 8 wells were assayed immediately to establish time 0 (t0). To the remaining wells, 100 µL of culture medium were added either alone or supplemented with increasing concentrations of 5FU (ranging from 1.2 µM to 153.6 µM) or Cisplatin (0.78 µM to 100 µM); Cells were then incubated for 2 days at 37 °C in the incubator. At the end of the incubations, 10 µL of 5 mg /mL MTT were added to each well and cells were further incubated for 4 hr. at 37 °C. After carefully removing the medium, 100 µL of the SDS-HCl lysis solution was added to each well and mixed thoroughly using the pipette. Absorbance was read at 570 nm (Bio-Rad 550 microplate reader; Bio-Rad Laboratories Inc., Hercules, CA, USA). Wells containing medium alone served as blanks. The results were expressed as the mean ±standard error of the mean (SEM) of at least 3 independent experiments, each with 6 replicate wells per cell line per cytotoxic condition.

2.11 Statistical analysis

Transcript levels from qPCR experiments are reported as mean ± SEM unless otherwise stated in results. Other data are presented as mean ± standard deviation (SD). The Mann-Whitney test was used to analyze data where medians are presented, students t-test was used to analyze data where means are presented. Each experiment was conducted at least 3 times unless otherwise stated, and representative examples are shown. Unpaired t-tests and 2-way ANOVA tests were used to statistically analyze differences between treated and control groups. Differences from 3 independent repeats of an experiment were considered to be statistically significant at $p<0.05$.

Chapter 3.

The miRNAs Profiling of Gastric Cancer Progression

3.1 Chapter Introduction

Chapter 1 described the importance of miRNAs as critical regulators of global mRNA expression in tumourigenesis and cancer progression. Recent miRNA expression profiling studies suggested the clinical use of miRNAs as potential prognostic biomarkers in various malignancies. Among 2588 identified human miRNAs, 352 have been shown to be either increased or decreased in gastric cancer tissues compared with non-tumour adjacent mucosa, with 120 miRNAs reported in 2 or more of the studies (Kuo et al. 2015; Shrestha et al. 2014). Upregulation of miR-21, miR-25, miR-92, miR-223 and downregulation of miR-375 and miR-148a were some of the most consistently altered microRNAs in gastric cancer despite marked variability in study designs and specimen types (Shrestha et al. 2014).

Thus far, dysregulation of miRNAs in gastric cancer has been reported to be associated with histology, Epstein-Barr virus infection, chemotherapy response, progression and metastasis (Huang et al. 2015; Li et al. 2018; Kim et al. 2011; Treece et al. 2016; Katada et al. 2009).

A number of miRNAs were further proposed to be potential prognostic biomarkers for gastric cancer patients, such as miR-1, miR-20b, miR-150, miR-214, miR-375, let-7g, miR-125-5p, miR-146a, miR-218, miR-433, miR-451 and miR-200b/c (Katada et al. 2009). Moreover, a seven-miRNA signature (miR-10b, miR-21, miR-223, miR-338, let-7a, miR-30a-5p, and miR-126) has recently been identified as an independent predictor for relapse-free survival among patients with gastric cancer (Li et al. 2010).

The possible drawback of these studies, however, is that a limited number of around 300 microRNAs have been chosen for the custom microarrays. This is merely 10% of the total number of human microRNAs registered on miRbase. As well as limitations in the dynamic range, sensitivity, and specificity of the microarray data themselves, different technological detection platforms, small sample size, different sample origins, and various methods employed for data processing and analysis may result in significant variations (Ding et al. 2017).

With the growing power and reducing cost of next-generation sequencing and bioinformatics, the launch of TCGA, as well as other large-scale cancer genome projects, have provided a comprehensive and multi-dimensional database of the key genomic and

epigenomic changes in cancer which are readily achieved and accessed. Bioinformatic analysis of TCGA datasets has been shown to be an outstanding tool in identifying genetic and epigenetic changes related to clinical outcomes.

The aim of this chapter was to identify potential therapeutic target miRNAs in gastric cancer. In order to reduce the variables, the present study only investigated the expression RNA sequencing data of gastric tissues. The miRNA dataset deposited by TCGA was used to identify differentially expressed miRNAs (DEMs). Then prognosis related miRNAs were selected according to both a generalized linear model (glm) and linear model (lm) analysis and further confirmed via Kaplan-Meier method and log-rank test.

3.2 Materials and methods

3.2.1 miRNA, mRNA expression profiles, and clinical information

The Illumina HiSeq profile dataset of 1881 miRNA (436 tumour samples and 41 non-tumour samples), mRNA expression (375 tumour samples and 32 non-tumour samples) and corresponding clinical dataset from 443 cases were downloaded from the TCGA database (https://portal.gdc.cancer.gov/projects/TCGA) up to June 2017. A customized R script to match patients' tumour and normal samples in the same case was applied to generate four tabular data files (tumour and normal each for miRNA and mRNA expression profiles) for gastric cancer patients.

3.2.2 Differentially expressed miRNAs (DEMs) screening

Only those mature miRNAs that had expression values in 90% of samples were further evaluated. This led to a subsequent analysis of 377 mature miRNAs. The differentially expressed miRNAs were screened out between patient and control samples applying linear model fitting and eBays approach. Briefly, eBayes function uses linear fitting of individual genes to build a hierarchical Bayes model, which estimates the probability of their differential expressions. It uses data-defined global priors to shrink the sample variances toward a common value and, therefore, enhance the statistical power and accuracy. Differential expression analysis was performed by three approaches. At first, raw reads were analyzed using R package *DESeq2*. In order to circumvent the multiple testing problems, which may induce false-positive results, the Benjamin-Hochberg procedure was used to control the false

discovery rate (FDR) by adjusting the raw *P*-values (Benjamini et al. 1995). miRNAs with Log2 fold change <-1 or >1 (P<0.05, after FDR adjusted) were considered as differentially expressed miRNAs and were selected. Secondly, student's test was performed to further compare the difference of miRNAs expression by measuring RPKM (reads per kilobase of exon model per million reads) between primary tumour samples (TP) and tissue normal samples (NT) in both paired manner (41 TP vs 41 NT) and unpaired manner (436 TP vs 41 NT). The DEMs for further prognostic analysis were those in the overlap of the three groups.

3.2.3 Prognosis-related DEMs determination

Both a generalized linear model (glm) and linear model (lm) analysis were performed between the miRNA HiSeq dataset and OS. The miRNAs with FDR less than 0.05 and those possessing matching directionalities to survival in both the glm and lm analyses were overlapped. Finally, the miRNAs with the lowest FDR values in both analyses were chosen as miRNAs of interest. The Kaplan-Meier method and log-rank test were also applied to further assess the clinical relevance of 16 miRNAs of interest. Comparisons between patients with low and high miRNA expression were made by separating patients into low and high expression group based on the median value of each miRNA's expression. Survival analysis was performed using GraphPad Prime v 6.0 (GraphPad Software, San Diego, CA). Log-rank P < 0.05 was considered statistically significant.

3.3 Results

3.3.1 Demographics study

A total of 443 gastric cancer patients were enrolled in this study. 41 had paired tissues examined in TCGA, while 402 had only tumour samples available. The characteristics of the subsets of 41 paired cancer tissues with adjacent normal mucosa or 402 cancer tissues without matched normal mucosa are listed in Table 3.1. No significant differences were observed between these two groups in the distribution of age (P=0.73, Fisher's exact test) and gender (P=0.1, Fisher's exact test). TCGA is comprised of a multi-race population. More than half of the samples obtained were White, 20% were Asian and the remainder were Black or African and native Hawaiian or other Pacific Islanders (P=0.61, Fisher's exact test). All gastric cancer cases in this study were adenocarcinomas. However, the distribution of tumour stage and the primary treatment response rate differed between the two groups. The

percentage of stage II patients in the paired and unpaired group are 46.34% and 27.61%, respectively; In contrast, the stage III patients in the first and second group are 19.51% and 43.53%, respectively. Similarly, the percentage of patients presenting stable disease in paired group is 29.27%, compared to 13.18% in the unpaired group. We thus further performed three different algorithms including paired and unpaired analyses.

Table 3.1: Patients' demographics: characteristics of gastric cancer patient with paired tumour tissues and normal samples or with only tumour tissues. NA, not available. P values were calculated by Fisher's exact test.

Variable	Gastric cancer patients with paired tissues (n = 41), n (%)	Gastric cancer patients with only tumour tissue (n = 402), n (%)	P value
Gender			0.73
Male	25 (60.98)	260 (64.68)	
Female	16 (39.02)	142 (35.32)	
Age (years)			0.51
≥65	26 (63.41)	227 (56.47)	
< 65	15 (36.59)	170 (42.29)	
NA		5 (1.24)	
Race			0.61
Asian	10 (24.39)	79 (19.65)	
Black or African	1 (2.44)	12 (2.99)	
White	22 (53.66)	255 (63.43)	
NA	8 (19.51)	56 (13.68)	
***H. pylori* infection**			0.20
Yes	1 (2.44)	19 (4.73)	
No	11 (26.83)	157 (39.05)	
NA	29 (70.73)	226 (56.22)	
Histology			0.63
Intestinal	15 (36.59)	176 (43.79)	
Diffuse	8 (19.51)	77(19.15)	
NA	18 (43.90)	149 (39.07)	
TNM stage			**0.01**
I	9 (21.95)	50 (12.44)	
II	19 (46.34)	111 (27.61)	
III	8 (19.51)	175 (43.53)	
IV	4 (9.76)	40 (9.95)	
NA	1 (2.44)	26 (6.47)	
Lymph-node status			0.36
No metastasis	16 (39.02)	116 (28.86)	
Metastasis	24 (58.54)	268 (66.67)	
NA	1 (2.44)	18 (4.47)	
Primary therapy outcome			**0.04**
Complete remission	20 (48.78)	221 (54.98)	
Partial Remission	0 (0.0)	6 (1.49)	
Stable or progressive	12 (29.27)	53 (13.18)	

NA	9 (21.95)	122 (30.35)	
Recurrence			0.10
Yes	5 (12.20)	107 (26.62)	
NO	26 (63.41)	234 (58.21)	
NA	10 (24.39)	61(15.17)	

3.3.2 Screening of DEMs

We evaluated samples by cluster analysis and searched for miRNAs with altered expression in primary tumour samples (TP) and tissue normal samples (NT) using different expression analyses. At first, we conducted one-way hierarchical clustering analysis using Principal Component Analysis to verify correct segregation of patients' and control samples (Figure 3.1) and observed that libraries of three normal tissues clustered with tumour samples, however, several tumour samples clustered with normal samples. The linear fitting model assuming the common dispersion for all the miRNAs revealed that not only one cluster distributed in either tumour samples or neighbouring normal tissues (Figure 3.2). Generally, the miRNAs exhibited heterogeneous between tumours and normal tissues and harboured homogeneity among tumours or normal tissues.

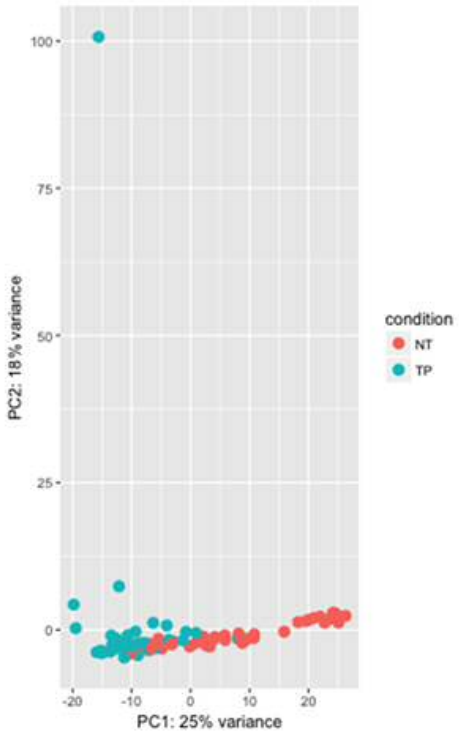

Figure 3.1: Cluster analysis. One-way hierarchical clustering using Principal Component Analysis (PCA) to verify the correct segregation of patients' and control samples in the miRNA-Seq analysis. PCA summarizes the major variation that is contained in many dimensions into a reduced number of uncorrelated dimensions. Two principal components which identified those variables that express a large

amount of variation (25% and 18% respectively) were chosen to represent the difference between TP and NT. The plot on the first 2 principal components shows an interesting separation of the NT group along the first component. PC1 denotes principal component 1, PC2 denotes principal component 2.

Next, we employed three differential expression analyses with both raw data and normalized data to identify miRNAs with altered expression between gastric cancer tissues and non-cancerous tissues. We used the DESeq2 package which bases the estimation of the dispersion on calculated mean-variance relationships in the dataset provided. It is thought to be a powerful method for analysing RNA-Seq data (Bencurova et al. 2017). DESeq2 identified 288 differentially expressed miRNAs. Paired t-test and unpaired t-test identified 321 and 304 deregulated miRNAs respectively (Figure 3.3). The overlap analysis generated 207 differentially expressed miRNAs, among which 65 miRNAs were downregulated and 142 miRNAs were upregulated (Appendix 8). These candidate miRNAs are chosen to study further.

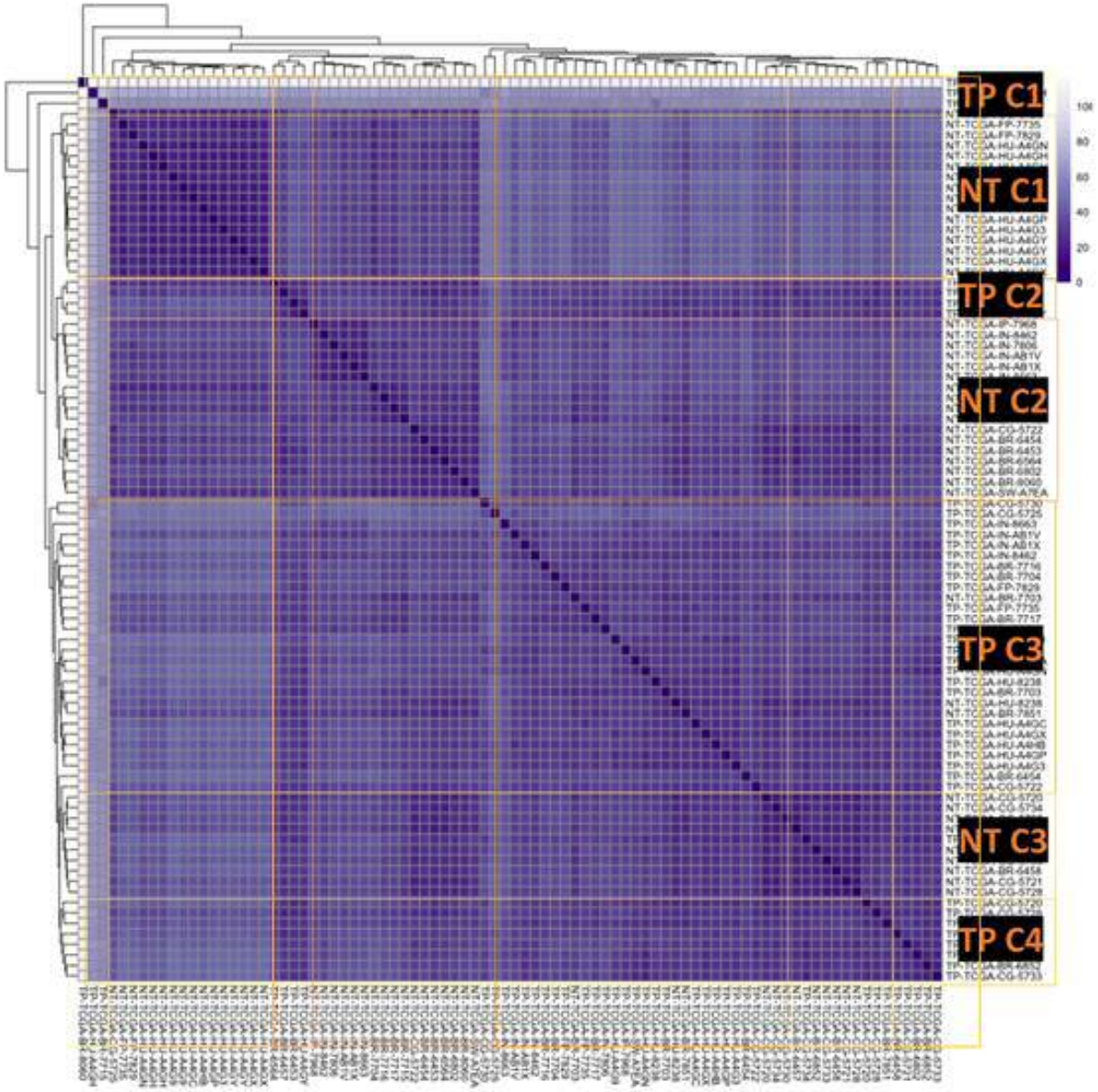

Figure 3.2: Differences comparison based on miRNAs and Correlations. The differentially expressed miRNA pattern in paired tissue samples was further demonstrated in an eBayes based linear model. The labels adjacent to the heatmap far right column and bottom row were used to denote a label for each sample. In this plot the distance between labels (samples) corresponded exactly to the colours of the dendrogram clusters. The darker the square was, the closer the compared samples were. Four TP patterns and three NT patterns were subgrouped according to their general distances for all miRNAs examined. .

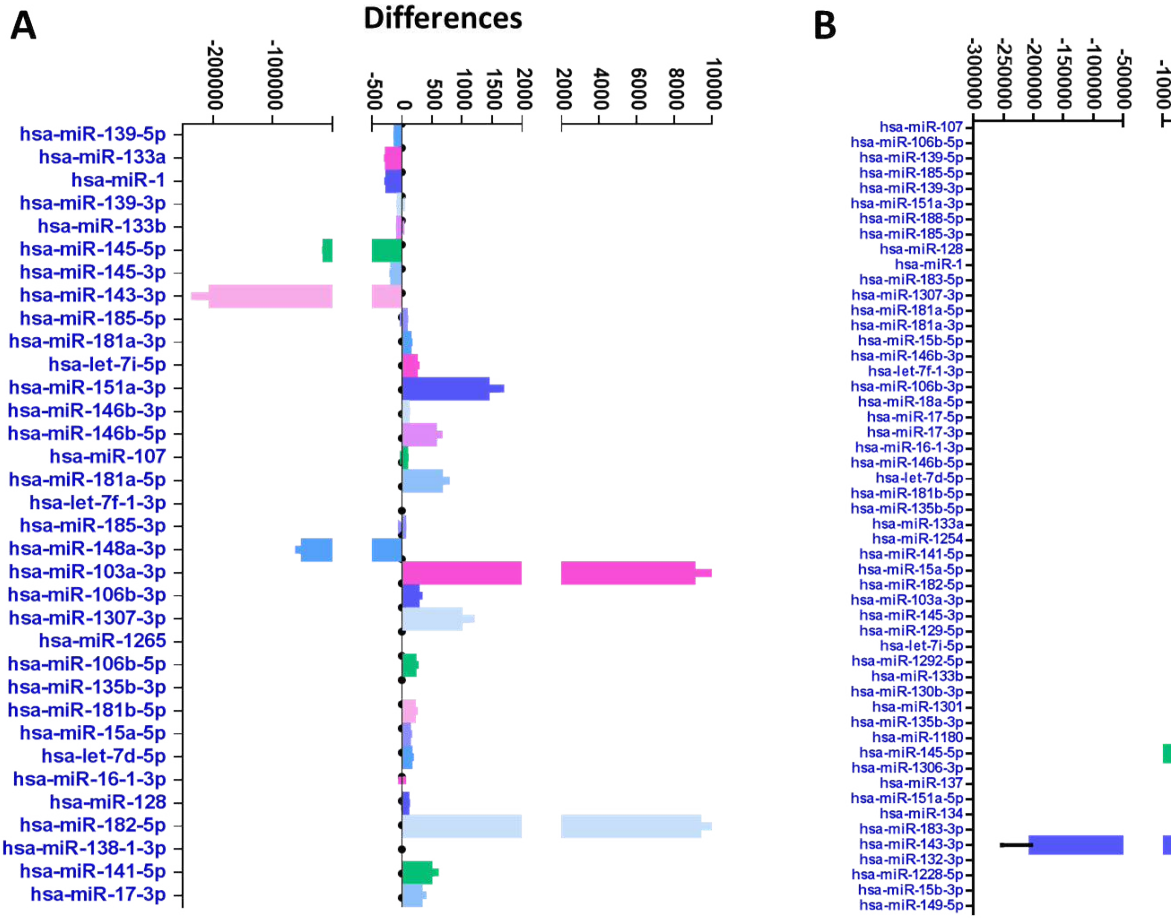

Figure 3.3: Significantly deregulated miRNAs in student's t-tests (P＜0.00001). A. Unpaired t-test analysis betv
matched normal stomach tissues. **B**. Paired t-test analysis. Error bars represent standard error.

3.3.3 DEMs associated with Overall Survival of gastric cancer patients

Prediction of survival is one of the main functions of prognostic biomarkers. Both the glm and lm function of R was applied to identify prognostically relevant miRNAs in gastric cancer. In the glm analysis, the expression revealed 37 mature miRNAs were correlated with gastric cancer patient's survival (FDR<0.05). The lm analysis revealed 18 such miRNAs. The directionality of the two lists of miRNAs was compared and overlapped to yield 16 common miRNAs (Table 3.2). High expression of 10 miRNAs (hsa-mir-549a, hsa-mir-514a-1, hsa-mir-21, hsa-mir-514a-3, hsa-mir-4326, hsa-mir-493, hsa-mir-34b, hsa-mir-1255a, hsa-mir-455 and hsa-mir-671) were correlated with poor prognosis. Six miRNAs (hsa-mir-140, hsa-mir-328, hsa-mir-193a, hsa-mir-28, hsa-mir-129-2 and hsa-mir-5683) were positively associated with better OS rate. Furthermore, we performed an unpaired t-test for each miRNA to compare their expression in different stage tumours, and we found miR-21, miR-140, miR-193a and miR-4326 showed significant correlation with gastric cancer progression (Figure 3.4).

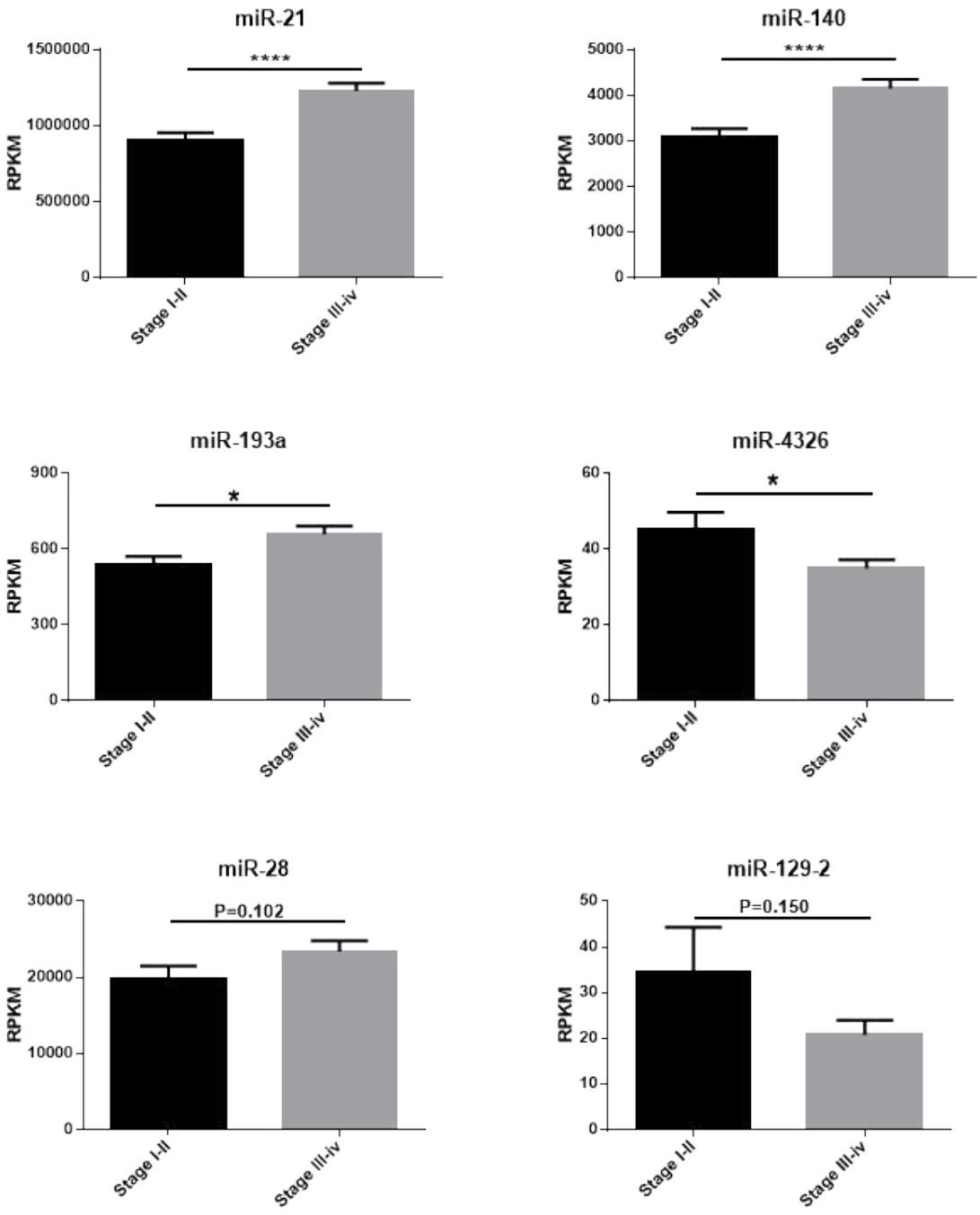

Figure 3.4: Stage-related miRNAs in student's t-tests. Statistical analysis compared the miRNAs' expression between stage I-II and stage III-IV, the results revealed miR-21 and miR-140 are both significantly and positively correlated with gastric cancer stage. Shown are representative results of unpaired t-test analysis. Error bars represent standard error. **** represent $p<0.0001$ and * represents $p<0.05$.

Table 3.2: Prognostic related miRNAs. Information on 16 miRNAs associated with OS of gastric cancer patients. Derived
lm analysis.

miRNAs	Mean	Log2 fold change	Expression comparison P v
hsa-mir-549a	2.297475	2.954531	6.19E-13
hsa-mir-514a-1	1.900981	2.093362	2.99E-06
hsa-mir-21	974536.9	1.878363	8.95E-74
hsa-mir-514a-3	1.897514	1.752371	7.48E-05
hsa-mir-4326	33.39163	1.278167	1.28E-07
hsa-mir-493	49.48034	0.874156	3.09E-10
hsa-mir-34b	3.388662	0.869264	0.000187
hsa-mir-1255a	1.896506	0.860887	0.005471
hsa-mir-455	874.2628	0.779891	3.41E-05
hsa-mir-671	24.5909	0.708348	1.21E-08
hsa-mir-140	3622.466	-0.9567	4.58E-19
hsa-mir-328	66.30372	-0.99735	2.41E-11
hsa-mir-193a	624.3456	-1.14638	1.28E-19
hsa-mir-28	21953.87	-1.17633	2.77E-23
hsa-mir-129-2	20.10709	-1.60691	7.94E-08
hsa-mir-5683	16.02191	-2.88421	6.49E-19

3.4 Discussion

The data presented here, and previous literature have suggested miRNAs are deregulated in gastric cancer and even indicate distant or progressive disease. In this study, comparisons between gastric cancer samples and normal stomach tissues from TCGA dataset generated 207 differentially expressed miRNAs in line with the studies from Ding *et al.* (Ding et al. 2017) and Shrestha *et al.* (Shrestha et al. 2014). (Table 3.3).

Table 3.3: Consistently deregulated miRNAs in three independent studies. This table shows the 12 deregulated miRNAs which feature in all three studies. Dark grey= those miRNAs which were downregulated in at least two of three studies. Light grey= those miRNAs were upregulated in two of three studies. No colour= those miRNAs showed contrary expression patterns in the systematic review comparing to those in the other 2 studies. FC stands for fold change.

Current study		**Ding *et al.***		**Shrestha *et al.***	
miRNA	**log2 FC**	**miRNA**	**logFC**	**hsa-miRNA**	**Median FC**
hsa-mir-490	-3.3	hsa-mir-490	-4.8	hsa-mir-133b	-2.40
hsa-mir-133b	-2.8	hsa-mir-133b	-3.4	hsa-mir-139	-1.84
hsa-mir-139	-2.3	hsa-mir-139	-2.6	hsa-mir-490	-1.51
hsa-mir-29c	-1.8	hsa-mir-100	-1.5	hsa-mir-29c	-1.32
hsa-mir-100	-1.3	hsa-mir-29c	-1.5	hsa-mir-188	-
hsa-mir-200b	1.2	hsa-mir-19a	1.2	hsa-mir-135b	0.67
hsa-mir-188	1.5	hsa-mir-335	1.2	hsa-mir-100	1.09
hsa-mir-19a	1.6	hsa-mir-200b	1.5	hsa-mir-18a	1.18
hsa-mir-335	1.6	hsa-mir-21	1.5	hsa-mir-200b	1.31
hsa-mir-21	1.9	hsa-mir-188	1.6	hsa-mir-335	1.97
hsa-mir-18a	2.1	hsa-mir-18a	1.8	hsa-mir-19a	2.00
hsa-mir-135b	3.3	hsa-mir-135b	3.2	hsa-mir-21	2.02

We found that miR-490 was the most pronounced downregulated miRNAs followed by miR-1/-133 family, miR-139 and miR-383. The miR-196 family and miR-21 were the most commonly and significantly upregulated miRNAs in gastric cancer. miR-490 and miR-1/133 family were found to be involved in the multistage cascade of gastric carcinogenesis (Shen et al. 2015). Upregulated miR-196a in gastric cancer promoted cell proliferation by downregulating p27(kip1) (Sun et al. 2012). In addition, increased circulating miR-196a in patient serum was associated with gastric cancer disease status and relapse (Tsai et al. 2012). Co-activation of miR-196b and HOXA10 characterized a poor-prognosis subgroup of patients with gastric cancer (Lim et al. 2013), in which miR-196b decreased levels of E-cadherin, but drastically induced vimentin, MMP2, and MMP9, implying activation of EMT (Liao et al. 2012). miR-21 has been identified as the best hit in a number of medium-scale

and high-scale profiling experiments designed for the detection of miRNAs dysregulated in cancer (Chan et al. 2005). In a large-scale profiling of miRNA expression in 540 human samples derived from 363 specimens representing six types of solid tumours and 177 respective normal control tissues, miR-21 was the only miRNA up-regulated in all types of the analysed tumours, including breast, colon, lung, pancreas, prostate, and stomach(Volinia et al. 2006). Generally, miR-21 expression levels are also very high in most cancer cell lines of various origins, and in some lines, it accounts up for 15-25% of the cellular miRNA content (Landgraf et al. 2007). Therefore, abundant miR-21 may be a general, albeit not universal, feature of tumour cells.

Based on these deregulated miRNAs, we further explored which of them were significantly correlated with patients' survival. The analysis revealed 16 miRNAs among which miR-140-5p, miR-328, miR-193a, miR-28 miR-129-2 and miR-5683 potentially acted as tumour suppressors and were positively correlated with better survival. Although their downregulation has been demonstrated in gastric cancer (Kim et al. 2011, Huo 2017), their roles in disease progression and prognosis remained to be defined by more evidence from *in vitro* and *in vivo* studies. Since miR-21 and miR-140 showed significant differences in expression between early and advanced gastric cancer, and miR-21 has been widely examined and demonstrated in various disease, including gastric cancer, we selected miR-140-5p for further analysis. It is worth noting that though miR-140-5p was downregulated in tumour tissues compared to normal samples, its downregulation correlated with gastric cancer progression but only reached a boundary statistic value. However, a higher level of miR-140-5p was more likely to appear in advanced gastric cancer tissues, reflecting its multiple identities in gastric cancer progression. Moreover, Kim et al. demonstrated that higher miR-140-5p in tumour samples from chemo-treated gastric cancer patients were correlated with chemosensitivity (Kim et al. 2011). miR-140-5p is well established to have decreased expression in many forms of cancer including; lung, breast, and colon *et al.* Most of the functional pathways influenced by miR-140-5p have so far implicated it in tumour-suppressing, these included SOX9 and ALDH1, which were significantly activated in CSCs. miR-140-5p could also target IL-6, which activates STAT3 signalling supports the self-renewal activity of cancer cells. The role of miR-140-5p in gastric cancer is yet to be established. To define the role of miR-140-5p in gastric cancer, the next step is to perform quantitive analysis of miR-140-5p expression level on independent human gastric cancer

cohort with a view to identifying whether miR-140-5p are deregulated in gastric cancer and its correlation with clinicopathological features.

Chapter 4.
Expression of miR-140-5p and miR-140-3p in Gastric cancer and Their Clinical Relevance

4.1 Chapter Introduction

The human mir-140 primary transcript generates two mature miRNAs, miR-140-5p and miR-140-3p. Initially reported in zebrafish, miR-140-5p and miR-140-3p are evolutionarily conserved among vertebrates suggesting that these miRNAs occupy an important biological role. Their expression in chondrocyte differentiation and cartilage tissue homeostasis is well documented (Hong and Reddi 2013). Generally, the precursor microRNAs are designated mir (lower case r) as in mir-140, whereas the mature microRNAs are designated miR (upper case R). When relative expression levels are known the microRNA with low expression (i.e., the degraded strand) is designated by an asterisk, as in miR-140*, which in this case is the same as miR-140-3p. However, miR-140-5p and miR-140-3p like many other miRNAs, the abundance of the -5p and -3p stands are different according to tissues type or species (Ambros et al. 2003; Griffiths-Jones et al. 2006; Gibson and Asahara 2013; Kenyon et al. 2019). Although miR-140-5p and miR-140-3p have identical seed sequences, the roles of miR-140-5p and miR-140-3p are complementary to one another in chondroplasia (Kenyon et al. 2019; Tao et al. 2017), in the development of Rheumatoid Arthritis and other autoimmune disease (Peng et al. 2016; Li et al. 2017) and in cancer progression as well (Flamini et al. 2017; Kong et al. 2015; Li and He 2014). We thus tried to explore the expression pattern of both miR-140-5p and miR-140-3p in the current study. It has been reported that miR-140-5p and -3p appear to function as either tumour-suppressing or tumour-promoting factors in cancer progression. It is clear that a large number of cellular context-dependent factors contribute to the dynamic regulatory roles of miR-140-5p/3p. Against this background, the rest part of this study aimed to examine the role of miR-140-5p and 3p in gastric cancer. The first objective was set to determine their deregulation pattern by comparing tumour samples and adjacent non-tumour tissues in an independent cohort. In this chapter, we aimed to explore the expression and association of miR-140-5p and miR-140-3p using *in Silico* analysis and qPCR detection in an independent cohort and to associate such expression with the clinical pathological characteristics of gastric cancer patients.

4.2 Materials and methods

4.2.1 Tissue samples from two independent gastric cancer patients' cohorts.

The collection of tissue samples has been described in Chapter 2. The first cohort (n=70),

composed of gastric cancer patients who did not receive any treatment before sample collection, were used to compare miR-140-5p and -3p expression between stomach tumour and non-tumour samples, and their association with disease progression such as tumour size, metastasis status and patients' OS. The second cohort was made of 87 patients who received 5FU based neoadjuvant chemotherapy, the comparison would be mainly between patients' tumour samples with chemoresponse and those without response from chemotherapy.

4.2.2 RNA extraction and miR-140-5p/3p detection

RNA was extracted using TRI Reagent® See 2.8.1; The reverse transcription for mature miRNA quantification was performed using TaqMan™ Advanced miRNA cDNA Synthesis Kit and qPCR was performed using miR-140-5p and miR-140-3p assay with triplicate reactions for each sample. miR-423-5p was used as the endogenous control. See 2.8.8.

4.2.3 Statistical analysis

Associations between miR-140-5p/3p expression and clinical characteristics were assessed with either the Student's t-test, One-way ANOVA or Mann-Whitney test. The predicted probability of survival with gastric cancer was used as a surrogate marker to establish the ROC curve. The Kaplan-Meier method and log-rank test were used for describing the survival curve. The area under the curve (AUC) was used as an accuracy index for evaluating the predictive performance of the selected miRNA signature. Univariate Cox regression analysis was used to evaluate the hazard ratio (HR) of miRNA and clinical variables for patient survival. Multivariate Cox regression analysis was conducted to test for independent prognostic factors of OS, which was defined as the time from the operation date to the date of death or final follow-up. Student's t-test, One-way ANOVA or Mann-Whitney test were performed using the statistical software Prism 6.0 (GraphPad Software, San Diego, CA Software, La Jolla, CA), and all the other statistical tests were performed with SPSS version 23.0. Statistical significance was defined as $p<0.05$.

4.3 Results

4.3.1 *In Silico* analysis of miR-140-5p expression in gastric cancer

Using the normalized data from RNAseq in TCGA cohort (released June 2017), in which only miR-140-5p was available, the expression of miR-140-5p in gastric cancer was first

evaluated by determining its levels based on the comparison between gastric cancer (n=435) and the paired adjacent non-tumour gastric tissues (n=41). Clinical and pathological information together with average miR-140-5p expression level is shown in Table 4.1. Compared to adjacent normal tissues miR-140-5p reduced in gastric tumours (P=0.048) (Table 4.1 and Figure 4.1).

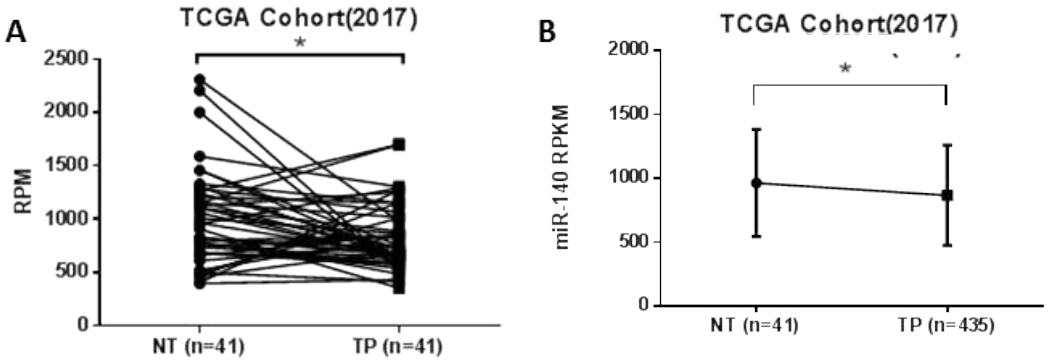

Figure 4.1: The miRNA-140-5p expression between NT and TP. A. Paired analysis showed a significant decrease trend in primary tumour tissue compared to adjacent normal sample. **B.** Unpaired analysis between gastric cancer and normal tissues showed a general decline of miR-140-5p in gastric cancer tissues as well.

Compared to diffuse type gastric cancers, a lower level of miR-140-5p was shown in intestinal type gastric cancer tissue samples (P=0.11), and it could be even lower in poorer differentiated intestinal gastric cancers (P=0.14) or gastric cancers with metastasis (P=0.03). A relatively higher expression of miR-140-5p was observed in tumours from younger patients (P=0.16), and higher miR-140-5p was correlated with advanced tumour stage in the whole patient group and those with tumour metastases in the intestinal type of gastric cancer (Table 4.1).

Table 4.1: miR-140 expression in gastric cancer cohort from TCGA.

	Whole (n=435)			Intestinal type (n=186)			
	N	**Mean ± SEM**	**P value**	**N**	**Mean ± SEM**	**P value**	**N**
			0.048			0.232	
Tumour	435	865.5 ± 14.86		186	873.1 ± 28.41		72
Normal	41	962.5 ± 22.61		15	999.0 ± 112.8		3
Gender			0.701			0.401	
Male	280	870.8 ± 23.83		124	890.3 ± 37.95		42
Female	155	855.7 ± 30.87		62	839.5 ± 38.94		30
Age			0.161			0.792	
⩾65	247	839.4 ± 24.73		115	876.7 ± 38.78		28
<65	183	893.3 ± 29.53		68	860.9 ± 41.70		44
Differentiation			0.163			0.135	
High-Moderate	107	794.8 ± 86.94		101	940.4 ± 45.24		2
Poor	280	887.8 ± 24.37		81	850.6 ± 35.74		70
Histology			0.224				
Intestinal	186	873.3 ± 28.41					
Diffuse	72	965.2 ± 53.81	0.106				
Signet ring type	11	968.0 ± 78.44	0.984				
TNM staging			**0.048**			0.436	
1-2	185	837.0 ± 24.81		70	847.7 ± 37.78		28
3-4	223	914.3 ± 29.00		113	893.4 ± 39.62		40
Node status			0.927			0.738	
Node negative	128	878.6 ± 36.31		49	892.4 ± 55.86		9
Node positive	288	874.8 ± 22.80		131	870.6 ± 33.90		33
Metastasis			0.099			**0.032**	
Yes	30	981.7 ± 85.90		14	1086 ± 154.4		8
No	402	858.8 ± 19.30		172	856.0 ± 27.83		64
Clinical outcomes			0.885			0.703	
Alive	264	863.2 ± 24.81		115	864.8 ± 38.11		44
Dead	171	868.8 ± 28.96		71	887.2 ± 41.95		28
Primary therapy response			0.912			0.858	
Complete/ Partial Remission	244	910.9 ± 26.33		105	908.7 ± 40.92		38
Stable / Progressive Disease	89	905.3 ± 40.47		41	921.9 ± 54.68		22

We then analyzed the association of miR-140-5p expression level with OS in gastric cancer patients. Since adjacent normal samples' transcriptional levels likely provided complementary information on patient survival, the expression level changes of miRNAs between tumour and paired nontumour samples may be more correlated with cancer relapse and survival than absolute expression levels in tumour samples alone (Huang et al. 2016). Receiver operating characteristic (ROC) curves were further employed to calculate the optimal cut-off value for miR-140-5p in discriminating tumour tissues from non-tumour samples. The areas under the curve (AUC) were 0.576 (95% confidence interval (CI): 0.484 to 0.668, p=0.108). According to the analysis result, > 964.3 was set as cut off value for miR-140-5p overexpression, the other way around was set as miR-140 low expression (Figure 4.2).

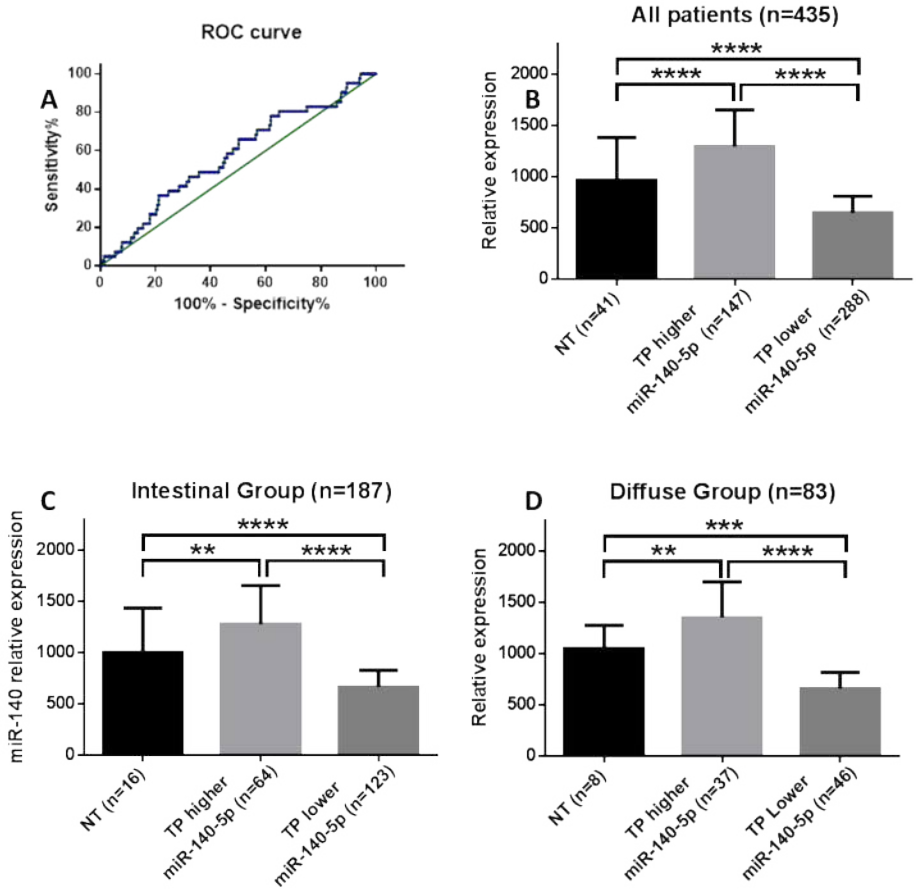

Figure 4.2: miR-140-5p expression in gastric cancer. A ROC curve of miR-140-5p as discriminators between gastric cancer and normal tissues**. B.C.D.** Comparisons of miR-140-5p expression in whole patients and patients' different subtypes of gastric cancer.

Prognosis differed between patients with low miR-140-5p expression and those with high miR-140-5p expression. Kaplan-Meier curve and log-rank analysis showed that low miR-140-5p expression positively correlated with poor gastric cancer patients' survival (OS: HR,

1.42; 95% CI, 1.01 to 1.91; P < 0.001 Figure 4.3 A; DFS: HR, 1.456; 95% CI, 0.9918 to 2.081; P=0.056 Figure 4.4 A). This observation was also shown in the intestinal subtype of gastric cancer (OS: HR, 1.70; 95% CI, 0.9958 to 2.901; P=0.121 Figure 4.3 B; DFS: HR, 1.418; 95% CI, 0.8000 to 2.480; P=0.24 Figure 4.4 B), but not in those with diffuse subtype (Figure 4.3 C, 4.4 C).

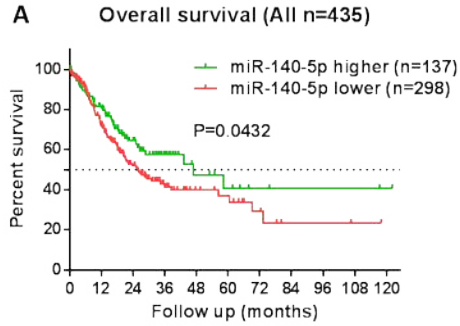

Log-rank (Mantel-Cox) test		
Chi square	4.087	
df	1	
P value	0.0432	
Median survival		
miR-140-5p lower (n=298)	26.08	
miR-140-5p higher (n=137)	46.90	
Hazard Ratio (log-rank)		
Ratio (and its reciprocal)	0.5561	1.798
95% CI of ratio	0.3961 to 0.7806	1.281 to 2.524

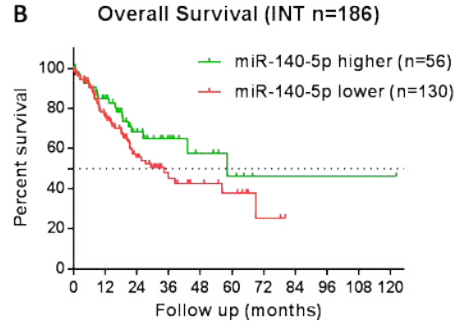

Log-rank (Mantel-Cox) test		
Chi square	2.398	
df	1	
P value	0.1215	
Median survival		
miR-140-5p lower (n=130)	34.26	
miR-140-5p higher (n=56)	58.23	
Hazard Ratio (log-rank)		
Ratio (and its reciprocal)	0.5883	1.700
95% CI of ratio	0.3447 to 1.004	0.9958 to 2.901

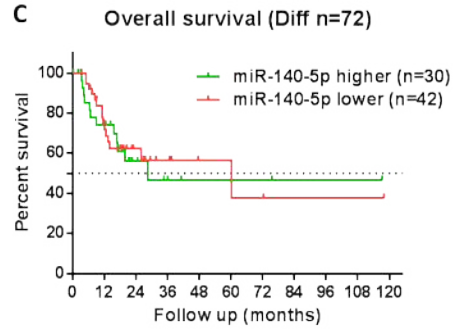

Log-rank (Mantel-Cox) test		
Chi square	0.09249	
df	1	
P value	0.7610	
Median survival		
miR-140-5p lower(n=42)	60.37	
miR-140-5p higher(n=30)	28.55	
Hazard Ratio (log-rank)		
Ratio (and its reciprocal)	2.114	0.4729
95% CI of ratio	0.9897 to 4.517	0.2214 to 1.010

Figure 4.3: Kaplan–Meier OS analysis for patients with miR-140-5p high or miR-140-5p low gastric cancer tissues. A. In the analysis included total patients, patients with high miR-140-5p expression (median survival 46.9 months) showed better OS versus low miR-140-5p expression in gastric cancer tissues (median survival 26.08 months). **B.** The analysis for patients with the intestinal type of gastric cancer showed a similar trend, a better clinical outcome for patients with higher miR-140-5p expression (median survival 58.23 months) compared to those with miR-140-5p lower expression (median survival 34.26 months). **C.** For patients with the diffuse type of gastric cancer, there is no significant difference between patients with higher miR-140-5p and those with lower miR-140-5p. **Abbreviations:** INT, intestinal type of gastric cancer; Diff, diffuse type of gastric cancer.

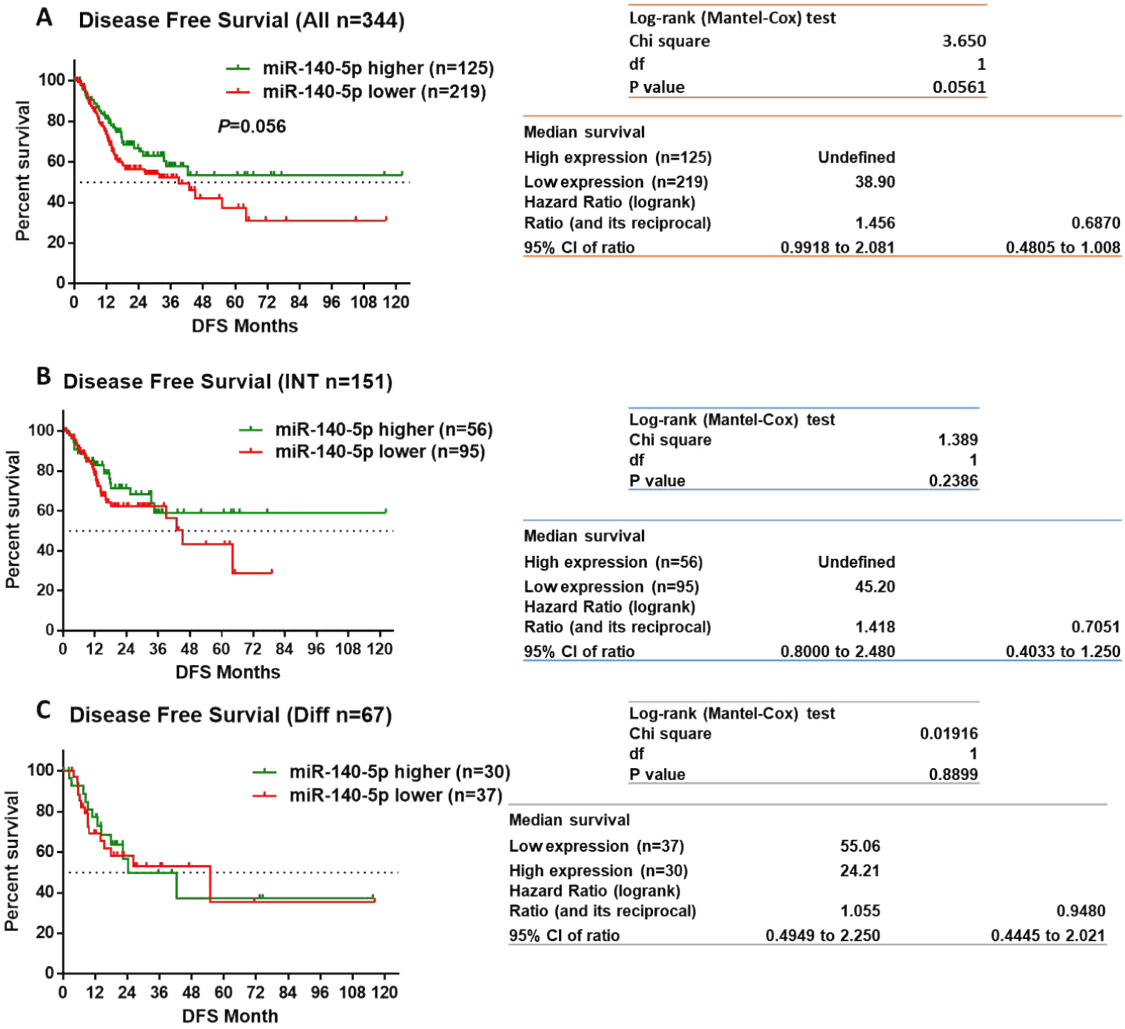

Figure 4.4: Kaplan–Meier DFS analysis for patients with miR-140-5p high or miR-140-5p low gastric cancer tissues. A. The analysis included total patients, with almost approached significance, patients with high miR-140-5p expression (undefined) tended to show better DFS versus low miR-140-5p expression in gastric cancer tissues (median survival 38.9 months). **B.** The analysis for patients with the intestinal type of gastric cancer showed a similar trend, a better clinical outcome for patients with higher miR-140-5p expression (undefined) compared to those with miR-140-5p lower expression (median survival 45.2 months). **C.** For patients with the diffuse type of gastric cancer, higher miR-140-5p (median survival 24.21 months), however, indicated shorter DFS; Those patients with lower miR-140-5p exhibited a longer DFS (median survival 55.06 months). **Abbreviations:** INT, intestinal type of gastric cancer; Diff, diffuse type of gastric cancer.

We further compared the OS for two different histological groups of patients-there was no statistically significant difference in OS between patients with the diffuse type or with the intestinal type of gastric cancer (Figure 4.5 A). However, when we combined the discrimination of miR-140-5p expression, patients with intestinal type and higher miR-140-5p expression showed the best OS, whereas patients with intestinal type and lower miR-140-5p expression showed a worse OS (Figure 4.5 B).

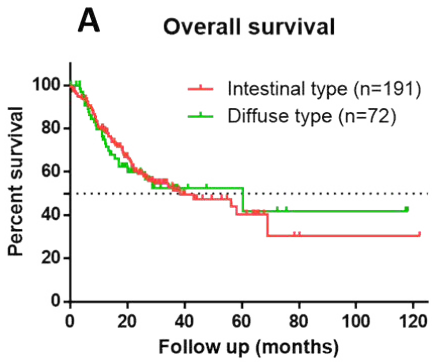

Log-rank (Mantel-Cox) test	
Chi square	0.04
df	1
P value	0.8382

Median survival		
Low expression (n=130)	38.43	
High expression (n=56)	60.37	
Hazard Ratio (log-rank)		
Ratio (and its reciprocal)	0.9546	1.048
95% CI of ratio	0.6108 to 1.492	0.6703 to 1.637

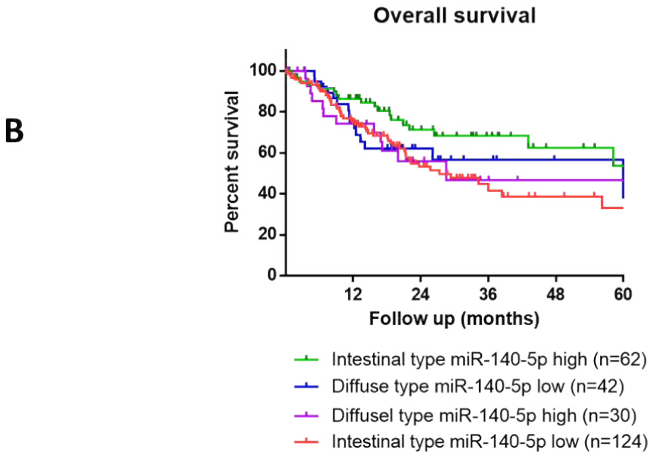

	INT+miR-140H	Diff+miR-140L	Diff+miR-140H	INT+miR-140L
Median survival	Undefined	60.37	28.55	27.33
Log-rank (Mantel-Cox) test				
Chi square	5.86			
df	3			
P value	0.12			
Log-rank (Mantel-Cox) test				
	---	0.20	0.14	0.014
		---	0.76	0.50
			---	0.77

Figure 4.5: Kaplan–Meier survival analysis for patients with different histological types and different miR-140-5p expression. A. The comparison between gastric cancer patients with intestinal subtype or with diffuse subtype showed no significant differences statistically. **B.** Although the comparison did not statistical significantly difference, gastric cancer patients with intestinal subtype and high miR-140-5p expression showed the best survival with undefined median survival. Individuals with diffuse type but high miR-140-5p expression showed a poor OS.

The multivariate Cox regression forward stepwise likelihood ratio (LR) analysis for the whole patients showed TNM stage, age, tumour differentiation, miR-140-5p expression and primary treatment response provided independent prognostic information (Table 4.2).

Table 4.2: Cox regression analysis for comparison of gastric cancer patients OS. Abbreviations: HR, hazard ratio; EGJ, esophagogastric junction.

Parameters	Univariate analysis			Multi variate analysis		
	HR	**95% CI**	**P**	**HR**	**95% CI**	**P**
Stage			**0.01**			**0.02**
Stage I	0.23	0.08-0.64	0.01	0.24	0.08-0.69	0.01
Stage II	0.36	0.17-0.76	0.01	0.34	0.15-0.74	0.01
Stage III	0.60	0.33-1.11	0.10	0.47	0.24-0.91	0.03
Stage IV		reference				
Age			**0.09**			**0.01**
< 65	0.68	0.43-1.07		0.54	0.34-0.85	
≥ 65		reference				
Differentiation			**0.06**			**0.01**
Well to moderate	0.66	0.41-1.02		0.49	0.30-0.81	
Poor		reference				
Primary treatment			**<0.001**			**<0.001**
Non-response	3.661	2.352-5.699		3.57	2.26-5.64	
Response		reference				
miR-140-5p			**0.07**			**0.02**
High expression	0.65	0.41-1.03		0.58	0.31-0.83	
Low expression		reference				
Gender			0.52			
Male	1.16	0.74-1.83				
Female		reference				
Histology			0.16			
Intestinal type	0.44	0.19-1.03	0.06			
Diffuse type	0.49	0.20-1.20	0.12			
Signet ring type		reference				
Anatomical site			0.64			
EGJ	0.34	0.40-2.15	0.23			
Funds	0.64	0.23-1.53	0.28			
Body	0.88	0.44-1.71	0.68			
Antrum		reference				

Higher TNM stage, older age, lower tumour differentiation grade and miR-140-5p low expression were significantly associated with poorer OS, while patients with response to primary chemotherapy treatment response were associated with better OS. In the DFS analysis (Table 4.3), patients' responses to primary chemotherapy treatment and miR-140-5p status were both independent factors. Chi-square was used to further clarify the association between miR-140-5p suppression and clinical, characteristics (Table 4.4). We found that decreased miR-140-5p significantly correlated with tumour histology, and distant metastasis.

Table 4.3: Cox regression analysis for comparison of gastric cancer patients DFS. Abbreviations: HR, hazard ratio; EGJ, esophagogastric junction.

Parameters	Univariate analysis			Multi variate analysis		
	HR	**95% CI**	**P**	**HR**	**95% CI**	**P**
Primary treatment			**<0.001**			**<0.001**
Non-response	6.83	4.17-11.12		7.23	4.39-11.91	
Response		reference				
miR-140-5p			**0.26**			
High expression	0.76	0.48-1.21		0.60	0.36-0.98	0.04
Low expression		reference				
Stage			**0.09**			**0.51**
Stage I	0.29	0.11-0.78	0.01	0.53	0.18-1.46	0.21
Stage II	0.54	0.26-1.13	0.10	0.80	0.36-1.78	0.59
Stage III	0.59	0.31-1.12	0.11	0.66	0.34-1,28	0.22
Stage IV		reference			reference	
Age			0.53			
< 65	1.16	0.73-1.82				
≥ 65		reference				
Differentiation			0.67			
Well to moderate	0.91	0.57-1.43				
Poor		reference				
Gender			**0.15**			**0.08**
Male	1.44	0.88-2.35		1.57	0.93-2.62	
Female		reference			reference	
Histology			**0.18**			**0.15**
Intestinal type	0.47	0.19-1.18	0.11	0.72	0.27-1.92	0.56
Diffuse type	0.63	0.24-1.67	0.35	1.21	0.43-3.40	0.72
Signet ring type		reference			reference	
Anatomical site			0.30			
EGJ	0.30	0.04-2.32	0.24			
Funds	0.74	0.32-1.67	0.46			
Body	1.10	0.58-2.10	0.77			
Antrum		reference				

Table 4.4: Relationship between miR-140-5p suppression and clinicopathological features in gastric cancer patients.

	miR-140-5p suppression		Chi-square	P[a]
	Positive (%)	Negative (%)		
Gender			0.64	0.52
Male	97(34.6)	183(65.4)		
Female	49(31.6)	106(68.4)		
Age(years)			0.53	0.59
≥65	79(32.0)	168(68.0)		
<65	63(34.4)	120(65.6)		
Tumour location			1.45	0.15
Cardia	30(28.0)	77(72.0)		
Non-cardia	110(35.7)	198(64.3)		
Histology			4.57	0.03
Intestinal	62(33.33)	124(66.67)		
Diffuse	30(41.67)	42(58.33)		
Signet ring type	7(63.6)	4(36.4)		
Differentiation			1.19	0.23
Well-moderate	51(30.7)	115(69.3)		
Poor	91(35.0)	169(65.0)		
Depth of invasion			0.63	0.53
T1-T2	34(29.8)	80(70.2)		
T3–T4	112(36.0)	199(64.0)		
Lymph node involvement			0.57	0.57
No	47(36.4)	82(63.6)		
Yes	97(33.6)	192(66.4)		
Distant metastasis			1.945	0.05
No	131(32.6)	271(67.4)		
Yes	15(50.0)	15(50.0)		
TNM stage			0.70	0.87
I	22(38.6)	35(61.4)		
II	42(32.8)	86(67.2)		
III	62(34.4)	118(65.6)		
IV	16(37.2)	27(62.8)		
Primary treatment response			0.48	0.63
Yes	92(37.7)	152(62.3)		
No	31(34.8)	58(65.2)		

[a]Chi -square test

We then performed Cox univariate and multivariate analyses in intestinal gastric cancer and diffuse gastric cancer separately. Primary treatment response was a critical independent protective factor in all groups. The results of intestinal-type gastric cancer patients' group revealed miR-140-5p expression was an independent prognosis factor in both OS analysis and DFS analysis. Patients with tumour located in the body of the stomach were more likely to have longer DFS survival than gastric cancer patients with tumour located at other sites (Table 4.5 and 4.6). In the Chi-square analysis, miR-140-5p suppression showed a positive trend in a relationship with lymph node involvement, distant metastasis, and tumour stage, but it did not reach statistical significance.

Table 4.5: Cox regression analysis for comparison of the intestinal type of gastric cancer patients OS. Abbreviations: HR, hazard ratio; EGJ, esophagogastric junction.

Parameters	Univariate analysis			Multi variate analysis		
	HR	**95% CI**	**P**	**HR**	**95% CI**	**P**
Primary treatment			**<0.001**			**<0.001**
Non-response	3.08	1.83-5.18		3.261	1.90-5.59	
Response		reference				
miR-140-5p			**0.01**			
High expression	0.52	0.30-0.88		0.57	0.33-0.99	0.05
Low expression		reference				
Stage			**0.02**			**0.01**
Stage I	0.10	0.02-0.43	<0.001	0.08	0.02-0.35	<0.001
Stage II	0.45	0.21-0.96	0.04	0.42	0.19-0.93	0.03
Stage III	0.72	0.39-1.33	0.30	0.57	0.28-1.16	0.12
Stage IV		reference				
Age			**0.03**			**<0.001**
< 65	0.55	0.32-0.93		0.39	0.22-0.68	
≥ 65		reference				
Differentiation			0.61			**0.01**
Well to moderate	0.61	0.38-0.98		0.51	0.31-0.87	
Poor		reference				
Gender			0.40			
Male	0.81	0.50-1.32				
Female		reference				
Anatomical site			0.82			
EGJ	0.61	0.24-1.59	0.31			
Funds	0.75	0.36-1.59	0.46			
Body	0.94	0.58-1.60	0.83			
Antrum		**reference**				

Table 4.6: Cox regression analysis for comparison of the intestinal type of gastric cancer patients DFS. Abbreviations: HR, hazard ratio; EGJ, esophagogastric junction.

Parameters	Univariate analysis			Multi variate analysis		
	HR	**95% CI**	**P**	**HR**	**95% CI**	**P**
Primary treatment			**<0.001**			**<0.001**
Non-response	7.06	3.84-12.95		7.74	3.84-12.95	
Response		reference				
miR-140-5p			**0.15**			**0.03**
High expression	0.66	0.37-1.17		0.52	0.29-0.93	
Low expression		reference				
Stage			**0.09**			0.44
Stage I	0.17	0.05-0.61	<0.001	0.67	0.08-5.41	0.71
Stage II	0.53	0.23-1.24	0.15	0.33	0.09-1.21	0.10
Stage III	0.64	0.31-1.29	0.21	1.08	0.45-2.57	0.87
Stage IV		reference				
Age			0.58			
< 65	1.17	0.68-2.00				
≥ 65		reference				
Differentiation			0.79			
Well to moderate	1.08	0.62-1.89				
Poor		reference				
Gender			0.70			
Male	1.12	0.62-2.02				
Female		reference				
Anatomical site			0.41			
EGJ	0.69	0.28-1.70	0.42			
Funds	0.85	0.39-1.82	0.67			
Body	0.51	0.27-1.00	0.05			
Antrum		reference				

Male patients with diffuse-type gastric cancer had a shorter DFS and OS than female (Table 4.7 and 4.8). Additionally, the analysis also implied that diffuse type of gastric cancer patients with a fundus tumour had a risk of death approximately twice higher compared to those with tumours at other sites. Different from the intestinal type of gastric cancer, miR-140-5p downregulation in the contingency analysis was positively correlated with local infiltration depth of tumour; Similarly, low levels of miR-140-5p were seen in tumours depending on their differentiation and in patients with older age but lacked statistical significance (Table 4.9 and 4.10).

Table 4.7: Cox regression analysis for comparison of diffuse type of gastric cancer patients OS. Abbreviations: HR, hazard ratio; EGJ, esophagogastric junction.

Parameters	Univariate analysis			Multi variate analysis		
	HR	**95% CI**	**P**	**HR**	**95% CI**	**P**
Primary treatment			**<0.001**			**<0.001**
Non-response	4.78	2.05-11.37		4.78	2.01-11.37	
Response		reference				
miR-140-5p			0.93			
High expression	0.97	0.44-2.11				
Low expression		reference				
Stage			**0.11**			0.26
Stage I	0.31	0.07-1.39	0.13	0.53	0.11-2.55	0.43
Stage II	0.19	0.05-0.73	0.02	0.27	0.07-1.03	0.06
Stage III	0.40	0.13-1.24	0.11	0.39	0.13-1.23	0.11
Stage IV		reference				
Age			0.42			
< 65	0.72	0.33-1.59				
≥ 65		reference				
Differentiation			0.27			
Well to moderate	3.20	0.47-25.18				
Poor		reference				
Gender			0.29			
Male	2.05	0.89-4.76				
Female		reference				
Anatomical site			0.90			
EGJ	0.65	0.08-5.03	0.68			
Funds	1.60	0.45-5.67	0.47			
Body	0.98	0.40-2.40	0.97			
Antrum		reference				

Table 4.8: Cox regression analysis for comparison of diffuse type of gastric cancer patients DFS. Abbreviations: HR, hazard ratio; EGJ, esophagogastric junction.

Parameters	Univariate analysis			Multi variate analysis		
	HR	**95% CI**	**P**	**HR**	**95% CI**	**P**
Primary treatment			**<0.001**			**<0.001**
non-response	9.16	3.43-24.42		8.21	3.02-22.32	
response		reference				
Gender			**0.03**			**0.05**
male	2.74	1.08-6.98		2.68	1.02-7.04	
female		reference				
miR-140-5p			0.93			
high expression	1.04	0.47-2.32				
low expression		reference				
Stage			0.36			0.73
Stage I	0.23	0.04-1.40	0.11	0.59	0.09-3.96	0.58.
Stage II	0.35	0.09-1.41	0.14	0.57	0.13-2.44	0.45
Stage III	0.49	0.13-1.78	0.28	0.46	0.12-1.78	0.26
Stage IV		reference				
Age			0.91			
< 65	0.95	0.39-2.30				
≥ 65		reference				
Differentiation			0.54			
well to moderate	1.89	0.24-14.45				
poor		reference				
Anatomical site			0.66			
EGJ	0.77	0.10-6.09	0.81			
Funds	2.33	0.73-7.41	0.15			
Body	1.05	0.40-2.75	0.91			
Antrum		reference				

Table 4.9: Relationship between miR-140-5p suppression and clinicopathological features in gastric cancer patients with intestinal type.

	miR-140-5p suppression		Chi-square	P[a]
	Positive (%)	Negative (%)		
Gender			0.54	0.58
Male	43(34.6)	81(65.4)		
Female	19(31.6)	43(68.4)		
Age(years)			0.42	0.67
≥65	39(32.0)	76(68.0)		
<65	21(34.4)	47(65.6)		
Tumour location			0.53	0.59
Cardia	12(28.0)	28(72.0)		
Non-cardia	49(35.7)	93(64.3)		
Differentiation			0.22	0.82
High-moderate	34(30.7)	67(69.3)		
Poor	26(35.0)	55(65.0)		
Depth of invasion			0.12	0.91
T1-T2	17(29.8)	35(70.2)		
T3–T4	45(36.0)	89(64.0)		
Lymph node involvement			1.14	0.25
No	20(36.4)	30(63.6)		
Yes	41(33.6)	9166.4)		
Distant metastasis			1.38	0.17
No	55(32.6)	117(67.4)		
Yes	7(50.0)	7(50.0)		
TNM stage			2.00	0.15[b]
I	12(38.6)	14(61.4)		
II	16(32.8)	28(67.2)		
III	25(34.4)	64(65.6)		
IV	8(37.2)	16(62.8)		
Primary treatment response			0.12	0.90
Yes	37(34.8)	68(65.2)		
No	14(37.7)	27(62.3)		

[a]Chi-square test. [b]Chi-square test for trend

Table 4.10: Relationship between miR-140-5p suppression and clinicopathological features in gastric cancer patients with diffuse type.

	miR-140-5p suppression		Chi-square	P[a]
	Positive (%)	Negative (%)		
Gender			0.73	0.47
Male	19(45.2)	23(54.8)		
Female	11(36.7)	19(63.3)		
Age(years)			1.14	0.25
≥65	14(50.0)	14(50.0)		
<65	16(36.4)	28(63.6)		
Tumour location			0.35	0.72
Cardia	4(36.4)	7(63.6)		
Non-cardia	24(42.1)	33(57.9)		
Differentiation			0.81	0.23
High-moderate	1(50.0)	1(50.0)		
Poor	28(41.8)	39(58.2)		
Depth of invasion			1.932	**0.05**
T1-T2	4(22.2)	14(77.8)		
T3–T4	26(48.1)	28(51.9)		
Lymph node involvement			0.19	0.85
No	7(43.8)	9(56.2)		
Yes	23(41.1)	33(58.9)		
Distant metastasis			0.51	0.61
No	26(56.3)	38(43.7)		
Yes	4(50.0)	4(50.0)		
TNM stage			0.9183	0.33[b]
I	2(28.6)	5(71.4)		
II	9(42.9)	12(57.1)		
III	15(44.1)	19(55.9)		
IV	4(57.1)	3(42.9)		
Primary treatment response			0.83	0.41
Yes	18(47.3)	20(52.7)		
No	**8(36.4)**	**14(63.6)**		

[a]Chi-square test. [b]Chi-square test for trend

4.3.2 Analysis of miR-140-5p/3p expression in an indication of gastric cancer progression from cohort without neoadjuvant chemotherapy

Further exploration was carried out on the involvement of miR-140-5p/3p in the disease progression of gastric cancer in an independent cohort containing 70 patients who did not receive any treatment before tissue collection. In line with the finding in TCGA analysis, reduced expression of miR-140-5p was observed in tumour tissues compared with adjacent non-tumour samples, especially in Borrmann I-II type of gastric cancer (Table 4.11). A decreased miR-140-5p expression was seen in the relatively localized tumour (Borrmann I-

II) compared with diffuse tumour samples (Borrmann III-IV). Interestingly, higher miR-140-5p expression was found in male patients with Borrmann I-II gastric cancer, but for the Borrmann III-IV patients higher miR-140-5p are more likely happened in female patients. A trend of reduced expression of miR-140-5p was prone in older patients. However, a relatively lower expression of miR-140-5p was seen in the early stage of tumours compared with later stage, which thought showed a reverse trend in Borrmann III-IV type patients, the result was not statistically significant.

We also compared miR-140-3p expression in these gastric cancer patients. Comparing to adjacent non-tumour samples, the level of miR-140-3p showed a decreased trend in paired tumoural tissues and mainly occurred in Borrmann I-II patients. Although no significant correlation was found between miR-140-3p expression and other clinical parameters, similar to miR-140-5p, lower expression of miR-140-5p was more likely to be seen in the early stage of tumours compared with later stage in Borrmann I-II patients, while the opposite in Borrmann III-IV patients.

We further compared patients' OS with different miR-140-5p expression level (Figure 4.6). Patients with lower miR-140-5p in tumour samples compared to paired normal samples was regarded as miR-140-5p low, whereas tumours harbouring a higher or equal level of miR-140-5p was viewed as miR-140-5p high. A higher miR-140-5p was significantly correlated with better OS for the total patients involved in the current study. Subgroup analysis revealed that patients with Borrmann I-II are more likely to benefit from higher miR-140-5p expression. On the contrary, higher miR-140-5p expression indicated an even worse prognosis in gastric cancer patients with Borrmann III-IV subtypes. When both the expression status of miR-140-5p and miR-140-3p was considered, patients with suppression in both miR-140-5p and miR-140-3p showed the poorest survival (Figure 4.7A). The combined analysis of miR-140-5p/3p expression level with tumour Borrmann classification revealed that patients having Borrmann I-II type gastric cancer and having none or one of the low expression of miR-140-5p/3p in the tumour samples had the best OS, however when both miR-140-5p and miR-140-3p were downregulated in tumour tissues, patients would suffer a worse prognosis regardless of their histological types (Figure 4.7 B).

Table 4.11: miR-140-5p expression in non-neoadjuvant chemotherapy cohort from Beijing

	Whole (n=70)			Borrmann I II (n=48)			Borrmann III IV (n=22)		
	N	**Mean ±SEM**	**P value**	**N**	**Mean ± SEM**	**P value**	**N**	**Mean ±SEM**	**P value**
			<0.001			**<0.001**			0.26
Tumour tissue	70	1.73 ± 0.39		48	1.07 ± 0.19		22	3.18 ± 1.14	
Normal tissue	70	3.78 ± 0.44		48	3.42 ± 0.51		22	4.57 ± 0.86	
Gender			0.85			0.47			0.41
Male	53	1.69 ± 0.38		35	1.16 ± 0.24		18	2.73 ± 0.99	
Female	17	1.87 ± 1.14		13	0.84 ± 0.32		4	5.18 ± 4.82	
Age			0.11			0.40			0.22
⩾65	32	1.06 ± 0.26		23	0.90 ± 0.24		9	1.48 ± 0.69	
< 65	38	2.30 ± 0.68		29	1.23 ± 0.30		9	4.35 ± 1.82	
Differentiation			0.17			0.08			0.39
High-Moderate	13	0.59 ± 0.33		9	1.23 ± 0.23		4	3.65 ± 1.36	
Poor	57	1.95 ± 0.47		39	0.38 ± 0.19		18	1.08 ± 1.06	
Histology			**0.01**						
Borrmann I-II	48	1.07 ±0.20							
Borrmann III-IV	22	3.18 ±1.14							
TNM staging			0.36			0.62			0.32
1-2	18	1.12 ± 0.28		14	1.22 ± 0.33		4	0.75 ± 0.47	
3-4	52	1.95 ± 0.52		34	1.01 ± 0.24		18	3.18 ± 1.36	

Table 4.12: miR-140-3p expression in non-neoadjuvant chemotherapy cohort from Beijing

	Whole (n=70)			Borrmann I II (n=48)			Borrmann III IV (n=22)		
	N	**Mean ±SEM**	**P value**	**N**	**Mean ± SEM**	**P value**	**N**	**Mean ±SEM**	**P value**
			0.09			0.08			0.66
Tumour tissue	70	0.12 ± 0.10		48	0.12 ± 0.01		22	0.12 ± 0.02	
Normal tissue	70	0.14 ± 0.08		48	0.14 ± 0.01		22	0.13 ± 0.01	
Gender			0.50			0.58			0.72
Male	53	0.12 ± 0.01		35	0.21 ± 0.02		18	0.12 ± 0.02	
Female	17	0.10 ± 0.02		13	0.10 ± 0.03		4	0.10 ± 0.06	
Age			0.41			0.78			0.28
⩾65	38	0.11 ± 0.02		25	0.12 ± 0.02		13	0.15 ± 0.04	
< 65	32	0.13 ± 0.02		23	0.11 ± 0.02		9	0.10 ± 0.02	
Differentiation			0.88			0.70			0.75
High-Moderate	13	0.12 ± 0.01		9	0.12 ± 0.02		4	0.12 ± 0.03	
Poor	57	0.11 ± 0.03		39	0.10 ± 0.03		18	0.14 ± 0.04	
Histology			0.89						
Borrmann I-II	48	0.12 ± 0.01							
Borrmann III-IV	22	0.12 ± 0.02							
TNM staging			0.33			0.11			0.42
1-2	18	0.14 ± 0.02		14	0.15 ± 0.02		4	0.08 ± 0.04	
3-4	52	0.11 ± 0.01		34	0.10 ± 0.02		18	0.13 ± 0.03	

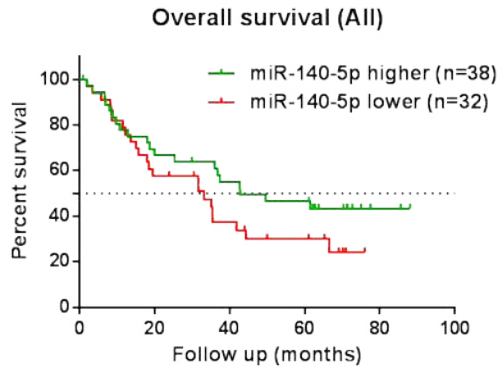

Log-rank (Mantel-Cox) test	
Chi square	2.010
df	1
P value	0.1563

Median survival		
miR-140-5p higher (n=38)	42.87	
miR-140-5p lower (n=32)	33.17	
Ratio (and its reciprocal)	1.292	0.7737
95% CI of ratio	0.7098 to 2.353	0.4250 to 1.409

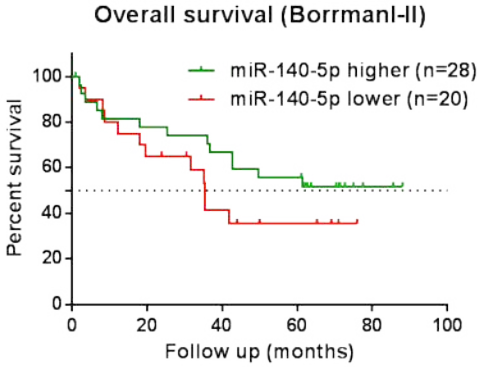

Log-rank (Mantel-Cox) test	
Chi square	1.685
df	1
P value	0.1943

Median survival		
miR-140-5p higher (n=28)	Undefined	
miR-140-5p lower (n=20)	35.47	
Hazard Ratio (log-rank)		
Ratio (and its reciprocal)	0.6022	1.660
95% CI of ratio	0.2548 to 1.309	0.7642 to 3.924

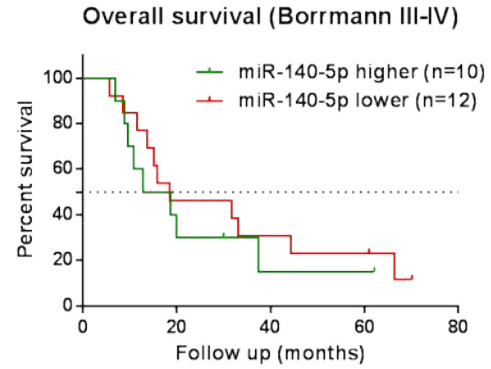

Log-rank (Mantel-Cox) test	
Chi square	0.3966
df	1
P value	0.5288

Median survival		
miR-140-5p higher (n=10)	15.82	
miR-140-5p lower (n=12)	18.50	
Ratio (and its reciprocal)	0.8549	1.170
95% CI of ratio	0.3439 to 2.125	0.4705 to 2.908

Figure 4.6: Kaplan–Meier OS analysis for patients with miR-140-5p high or miR-140-5p low gastric cancer tissues （Beijing cohort）. A. The analysis included total patients showed a trend that patients with high miR-140-5p expression (median survival 42.87 months) are more likely to have better OS versus low miR-140-5p expression in gastric cancer tissues (median survival 33.17 months). **B.** The analysis for patients with relative local disease (Borrmann I-II) showed a similar trend as that in total population, a better clinical outcome for patients with higher miR-140-5p expression (undefined median survival) compared to those with miR-140-5p lower expression (median survival 35.37 months). **C.** For patients with more invasive gastric cancer, higher miR-140-5p (median survival 15.72 months), however, indicated shorter OS; Those patients with lower miR-140-5p exhibited a longer OS (median survival 18.5 months).

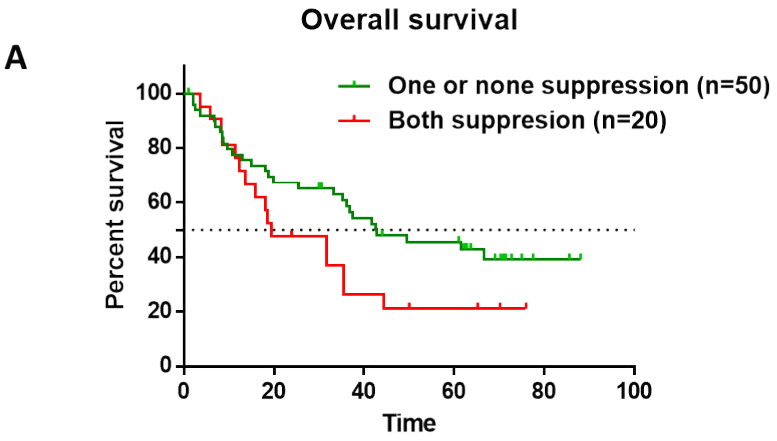

	One or none suppression	Both suppression
Median survival	42.87	19.50
Ratio (and its reciprocal)	2.198	0.4549
95% CI of ratio	1.189 to 4.063	0.2461 to 0.8407
Log-rank (Mantel-Cox) test		
Chi square	3.320	
df	1	
P value	0.0685	

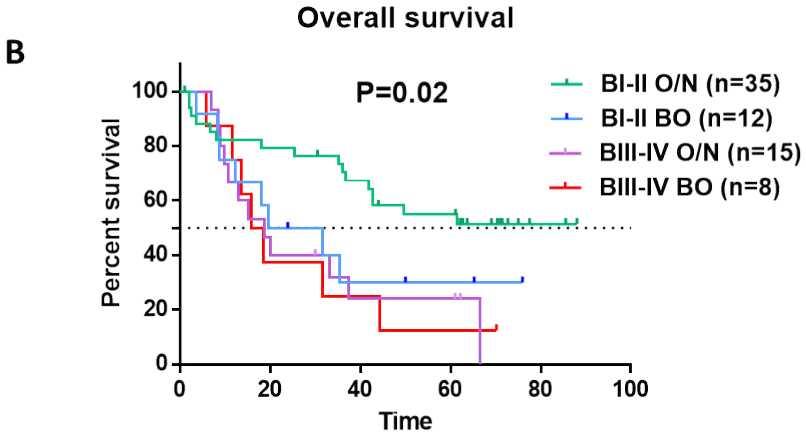

	BI-II O/N	BI-II BO	BIII-IV O/N	BIII-IV BO
Median survival	Undefined	25.615	18.7	17.15
Log-rank (Mantel-Cox) test				
Chi square	9.710			
df	3			
P value	0.0212			
Log-rank (Mantel-Cox) test				
	---	0.0929	0.0086	0.015
		---	0.6093	0.4747
			---	0.9369

Figure 4.7: Kaplan–Meier OS analysis for patients with various miR-140-5p/3p status in gastric cancer tissues. A. The analysis included all the patients, patients with tumour harbouring both suppressing in miR-140-5p and -3p expression showed a trend to have a worse OS than patients with either miR-140-5p suppression or miR-140-3p or with no suppression of neither. **B.** Further analysis based on Borrmann classification showed that the OS significantly declined in the patients, whose tumours were localized but were suppressed in both miR-140-5p/3p. **Abbreviations: BI-II O/N**, one of none suppression of miR-140-5p/3p in Borrmann I-II type; **BI-II BO**, Borrmann I-II type with both suppressed miR-140-5p and miR-140-3p; **BIII-IV O/N**, one of none suppression of miR-140-5p/3p in Borrmann III-IV type; **BIII-IV BO**, Borrmann III-IV type with both suppressed miR-140-5p and miR-140-3p.

Table 4.13: Cox regression analysis for comparison of OS in gastric cancer patients without neoadjuvant chemotherapy. Abbreviations: HR, hazard ratio.

Parameters	Univariate analysis			Multi variate analysis		
	HR	**95% CI**	**p**	**HR**	**95% CI**	**P**
Stage			0.07			**0.05**
Stage I-II	0.41	0.14-1.17		0.40	0.14-1.15	
Stage III-IV			reference			
Age			**<0.001**			**0.01**
< 65	0.36	10.19-0.71		0.37	0.20-0.70	
≥ 65			reference			
Histology			**0.01**			**0.01**
Borrmann I-II	0.40	0.19-0.83		0.40	0.20-0.78	
Borrmann III-IV			reference			
R0 surgical margin			**0.05**			**0.04**
No	2.33	0.99-5.45		2.30	1.03-5.11	
Yes			reference			
Vascular invasion			**0.05**			**0.04**
No	0.43	0.19-1.00		0.45	0.21-0.98	
Yes			reference			
Low miR-140-5p/3p			0.10			0.08
None or one	0.52	0.24-1.14		0.54	0.27-1.07	
Both			reference			
Gender			0.85			
Male	1.09	0.46-2.58				
Female			reference			
Differentiation			0.82			
Well to moderate	1.15	0.43-2.84				
Poor			reference			
Anatomical site						
Cardia						
Non-cardia			reference			

4.3.3 Analysis of miR-140-5p/3p expression related to gastric cancer treatment from cohort with neoadjuvant chemotherapy

A previous microarray-based study enrolling 87 patients diagnosed with metastatic gastric cancer who received fluorouracil and cisplatin chemo treatment, revealed that higher expression of miR-140-5p in pre-treated tumour samples was significantly correlated with a delayed time to progression indicating chemotherapy-related survival benefits. However, miR-140-5p was functionally validated to reduce cell proliferation through G1 and G2 phase arrest mediated in part through the suppression of HDAC4 (Song et al. 2009) and be important in contributing to chemoresistance to 5FU based chemotherapy in colorectal cancer (Yang et al. 2017). Additionally, miR-140-5p was demonstrated to be overexpressed in $CD133^{+Hi}CD44^{+Hi}$ colon cancer stem-like cells and, by reducing its expression, the chemoresistance of $CD133^{+Hi}CD44^{+Hi}$ colon cancer stem-like cells to 5FU treatment can be halted (Ju 2010). This led to a question of how miR-140-5p and miR-140-3p are involved in the chemo response of gastric cancer patients. To answer this, an analysis of miR-140-5p/3p expression in chemosensitive tumour tissues and chemoresistant tumour samples, as well as their corresponding normal stomach tissues, was performed, using another gastric cancer cohort in which tissues samples of patients were collected after 5FU based neoadjuvant chemotherapy from Beijing Cancer Hospital. Neoadjuvant chemotherapy (NAC) is defined as chemotherapy administered before locoregional treatment, such as surgery and/or irradiation. It is well established that NAC plays an important role in downstaging tumours, eliminating micrometastases, and relieving tumour-related symptoms in patients with locally advanced gastric cancer (Yang et al. 2015). NAC increases the surgical resectability rate as well as the quality of surgery if the gastric cancer cell is sensitive to chemotherapy (Chen et al. 2018). As shown in Figure 4.8, among all subjects involved, 30 patients (37.04%) had higher miR-140-5p and miR-140-3p (tumour versus adjacent non-tumour) expressions, and 46 patients had either increased miR-140-5p or increased miR-140-3p. Patients with a pathological complete response or partial response exhibited a higher expression of either miR-140-5p or miR-140-3p in the tumour samples. Patients with pathological complete response or partial response showed a trend to have a better OS compared with patients with stable or progressive disease (Figure 4.9 B HR=0.52, 95% CI: 0.30–0.89, P=0.116), however, it is not an independent indicator for patients' OS (Table 4.13). The Kaplan-Meier analysis, however, demonstrated that patients with at least one alteration in miR-140-5p or miR-140-

3p could have a significantly increased OS (HR=0.56, 95% CI: 0.32-0.93, p=0.018). Furthermore, the Cox analysis also indicated that higher expression of miR-140-5p or miR-140-3p could be a potential independent prognostic factor although it only showed a boundary statistically significance (Figure 4.9 A Table 4.13). Subgroup analysis revealed that if pathological response was achieved, patients with either miR-140-5p or miR-140-3p upregulation and those without alterations had similar survival (P=0.738). In contrast, patients with residual disease (RD) would have worse OS if they did not have any alterations in neither miR-140-5p nor miR-140-3p compared with patients having at least one alteration in them (P < 0.05) (Figure 4.10).

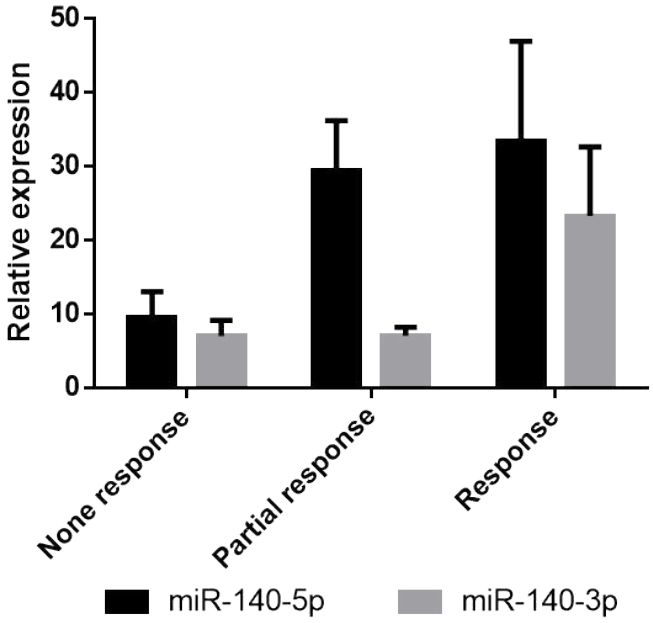

Comparisons of miR-140-5p levels				
Tukey's multiple comparisons test	**Mean Diff.**	**95% CI of diff.**	**Significant**	**Summary**
Non-response vs. Partial response	-19.86	-35.37 to -4.343	Yes	**
Partical response vs. Complete response	-4.136	-51.72 to 43.44	NO	ns
Non-response vs. Complete response	-23.99	-44.07 to -3.912	Yes	*

Figure 4.8: miR-140-5p and miR-140-3p and neoadjuvant treatment response of gastric cancer. The levels of miR-140-5p and miR-140-3p were determined by qPCR in a cohort of gastric cancer patients receiving chemotherapy before surgery. Shown are miR-140-5p and miR-140-3p levels (mean ± standard deviation) and the comparisons of miR-140-5p or miR-140-3p in gastric tumours of complete response, partial response, and non-response from the drug treatment via One-way ANOVA. ** represent P<0.01, * represents P<0.05.

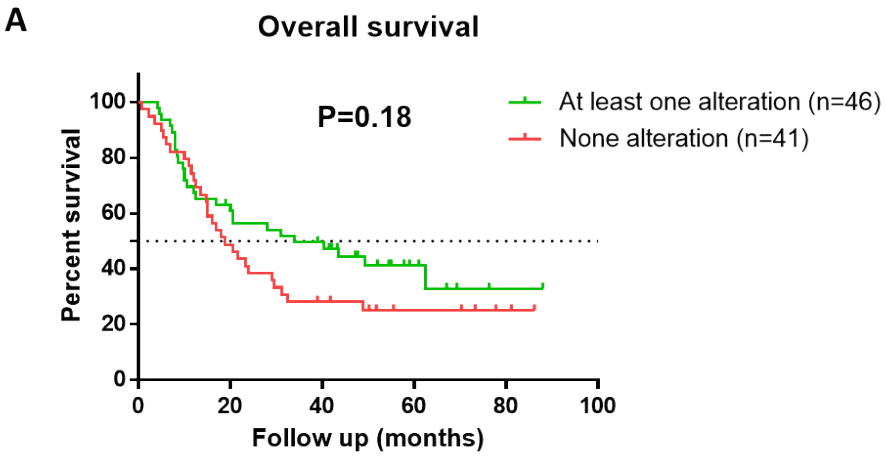

Log-rank (Mantel-Cox) test	
Chi square	1.798
df	1
P value	0.1799

Median survival		
None alteration	18.90	
At least one alteration	34.00	
Ratio (and its reciprocal)	0.5559	1.799
95% CI of ratio	0.3291 to 0.9389	1.065 to 3.039

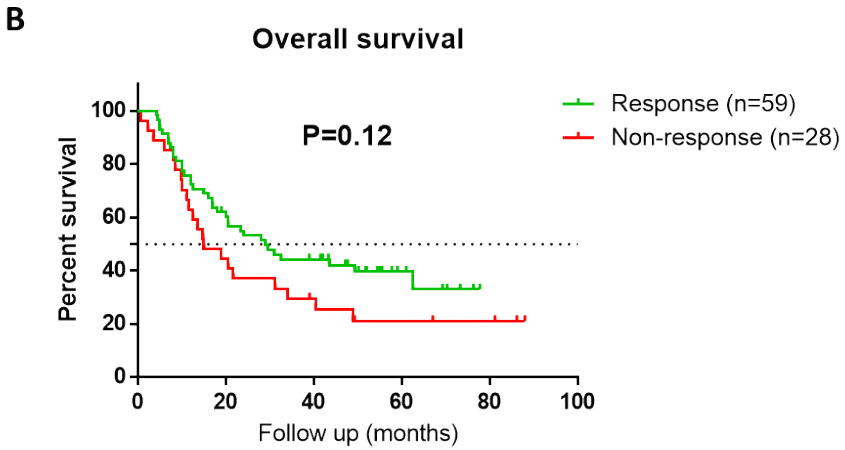

Log-rank (Mantel-Cox) test	
Chi square	2.471
df	1
P value	0.1159

Median survival		
Response (n-59)	29.00	
Non-response (n=28)	15.00	
Ratio (and its reciprocal)	1.933	0.5172
95% CI of ratio	1.126 to 3.321	0.3011 to 0.8885

Figure 4.9: A Kaplan-Meier 5-year OS estimation in patients with different miR-140-5p/3p status. The miRs' expression level was determined according to ROC analysis. Tumours with higher miR-140-5p or miR-140-3p showed a trend to have a better prognosis in comparison with primary tumours without any alterations in neither miR-140-5p nor miR-140-3p (the relative expression was calculated using the expression of tumour sample divided by that of paired normal tissues). However, the difference was not statistically significant (P=0.18). **B. Kaplan-Meier 5-year OS estimation in patients with different responses to chemotherapy.** Neoadjuvant chemotherapy although not statistically significant, may increase long-term survival among patients who showed a complete or partial response (both are defined as a response according to a previous systematic review (Muhich and Boothroyd 1989)).

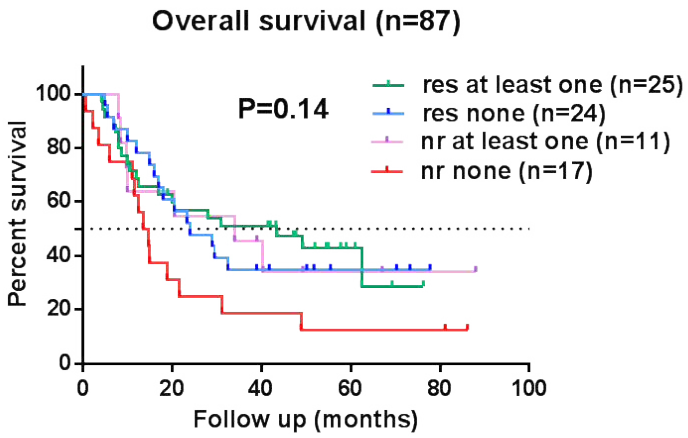

	Res at least one	Res non	Non-res at least one	Non-res non
Median survival	43.5	24	34	14.5
Log-rank (Mantel-Cox) test				
Chi square	9.710			
df	3			
P value	0.139			
Log-rank (Mantel-Cox) test				
	---	0.74 (HR 0.55, 95%CI 0.28-1.08)	0.88 (HR 0.78, 95%CI 0.33-1.85)	0.04 (HR 0.33, 95%CI 0.16-0.64)
		---	0.90 (HR 0.71 95%CI 0.29-1.73)	0.05 (HR 0.59, 95%CI 0.28-1.02)
			---	0.05 (HR 0.41, 95%CI 0.16-1.00)

Figure 4.10: miR-140-5p/3p status and OS in different subtypes of gastric cancer patients. Among the 59 patients with complete response or partial response to NACT, 25 patients had tumours that expressed higher miR-140-5p or -3p, and 24 were alteration negative; their 5-year OS did not significantly differ. In contrast, patients with residual disease (RD) had worse OS if they had no upregulation in miR-140-5p nor miR-140-3p (n=17) compared with patients with increased miR-140-5p or -3p (n=11).

Table 4.14: Cox regression analysis for comparison of OS in gastric cancer patients with neoadjuvant chemotherapy. Abbreviations: HR, hazard ratio.

Parameters	Univariate analysis			Multi variate analysis		
	HR	**95% CI**	**P**	**HR**	**95% CI**	**P**
T stage			**0.01**			**0.01**
T3	2.72	1.23-6.00		2.87	1.38-5.95	
T4	reference					
N stage			0.18			0.08
N0	2.27	0.70-23.82		2.64	0.89-3.89	
N1-N3			reference			
M stage			0.39			
M0	1.66	0.52-5.26				
M1			reference			
Response			0.63			
No	1.18	0.60-2.35				
Yes			reference			
Age			0.12			**0.01**
< 65	0.56	0.28-1.15		0.37	0.20-0.70	
≥ 65			reference			
Gender			0.65			
Male	0.85	0.41-1.73				
Female			reference			
Anatomical site			0.89			
Non-cardia	1.05	0.50-2.21				
Cardia			reference			
Histology			**0.01**			**0.01**
Borrmann I-II	2.43	1.29-4.55		2.23	1.22-4.10	
Borrmann III-IV			reference			
R0 surgical margin			**<0.001**			**<0.001**
No	0.12	0.04-0.40		0.20	0.10-0.38	
Yes			reference			
Vascular invasion			0.11			**0.04**
No	0.53	0.23-1.16		0.58	0.31-1.09	
Yes			reference			
Completed periods			0.26			
No	1.53	0.76-3.19				
Yes			reference			
Differentiation			0.24			
Well to moderate	0.61	0.27-1.39				
Poor			reference			
Higher miR-140-5p/3p			0.09			0.07
None	1.89	0.91-3.93		1.68	0.96-2.93	
At least one			reference			

4.4 Discussion

The roles of miR-140-5p and -3p in maintenance of cartilage tissue, embryonic development, regeneration and repair and in immune response and chronic inflammation have been extensively demonstrated. miR-140-5p and 3p play roles of tumour suppression and have attracted attention as both possible biomarkers and potential therapeutic targets in epithelial-derived carcinoma such as lung cancer, breast cancer, colon cancer and ovarian cancer *et al.*, as well as in other types of malignant tumour, like sarcomas, melanoma, lymphoma, and leukemia. However, higher miR-140-5p expression was significantly associated with poorer OS in anti-EGFR treated chemorefractory metastatic colorectal cancer patients with wild-type KRAS and BRAF (Mosakhani et al. 2012). It was reported the miR-140-5p exhibited significantly higher expression levels in post-neoadjuvant chemotherapy specimens compared with pre-neoadjuvant chemotherapy biopsies in breast cancer and exhibited significantly even higher expression levels in the ineffective group comparing to the effective group after neoadjuvant chemotherapy which indicated a poorer survival in breast cancer patients (Chen et al. 2016). Upregulation of miR-140-3p was found in metastasis nodal tissues comparing to the nonmetastatic oral squamous cell carcinoma (Serrano et al. 2012). Elevated miR-140-3p was also found in the milk of the milk stasis plus breast neoplasm patients and contributed to breast carcinogenesis (Gu et al. 2014). Moreover, highly expressed miR-140-3p was also shown to control stemness of breast cancer cells (Salem et al. 2016). These suggest downregulation of miR-140-5p or-3p or their joint action underlines tumour aggressiveness in a tissue, stage or cell context-dependent manner. To address the specific roles of miR-140-5p and miR-140-3p in gastric cancer, the expression of miR-140-5p in gastric cancer (The Cancer Genome Atlas, https://cancergenome.nih.gov/) was initially analyzed. A slight decrease in miR-140-5p was observed in the whole population (n=435). Interestingly, an ascending trend was noticed in intestinal type of gastric cancer, especially patients with metastasis. In the survival analysis, patients with higher miR-140-5p are more likely to experience longer DFS and OS, particularly in patients with intestinal type. Although patients with intestinal gastric cancer were supposed to have a better survival than those with diffuse type, we did not see that in the TCGA cohort. Moreover, when we compared prognosis considering both their histological subtype and miR-140-5p status, the log-rank analysis revealed that patients with intestinal subtype and higher miR-140-5p expression had the best OS. On the contrary, patients with intestinal subtype but a

downregulated miR-140-5p had even worse OS compared to patients with the diffuse type of gastric cancer. Cox analysis indicated lower miR-140-5p expression status together with later stage, older age, worse differentiation and non-response from primary treatment were independent OS risk factors for the whole cohort of gastric cancer patients and those with intestinal-type gastric cancer patients, it's worth nothing that miR-140-5p downregulation was an independent risk factor for DFS of intestinal gastric cancer patients.

In this study, reduced expression of miR-140-5p and -3p was observed in gastric cancer (n=70) compared with paired adjacent normal gastric tissues (n=70). Consistent with the findings in the TCGA cohort, deregulated miR-140-5p also showed correlation with age, tumour differentiation and tumour growth pattern. Borrmann classification instead of Lauren classification was recorded for these patients, thus Borrmann type I and II tumours were considered the localized type and Borrmann type III and IV were considered infiltrative type in accordance with previous study (Saito et al. 2013). Subgroup analysis based on the Borrmann classification indicated that, in line with the results we found in TCGA cohort, poorer survival is more likely observed in patients with lower miR-140-5p expression, especially in the localized type of gastric cancer. In the infiltrative type of gastric cancer, conversely, lower miR-140-5p may suggest a better survival. The combined analysis of both miR-140-5p and -3p expression and Borrmann's classification indicated that localized type of gastric cancer with none or only one deregulation of either miR-140-5p or miR-140-3p suggested best survival benefit for gastric cancer patients. However, localized type of gastric cancer with both deregulation of miR-140-5p and miR-140-3p expression manifested an OS as poor as an infiltrative type of gastric cancer. Similar results were reported in astrocytoma in which miR-140-5p was significantly lower in the diffuse astrocytoma's tumour samples as compared to the non-neoplastic brain tissues. However, during the spontaneously progress from diffuse astrocytoma of World Health Organization (WHO) grade II to anaplastic astrocytoma WHO grade III or secondary glioblastoma WHO grade IV, miR-140-5p, alongside other 11 miRNAs, was elevated in a progressive manner. In addition, upregulation of its median expression levels was also increased in secondary glioblastomas as compared to low-grade gliomas (Malzkorn et al. 2010). Upregulation of miR-140-5p, along with enriched genes in extracellular matrix (ECM)-receptor interaction, ribosome, and focal adhesion pathways were thought to be important in recurrence of glioblastoma (Bo et al. 2015). Microarrays examination and OS analysis in metastatic colorectal cancer with a genetic

background of wild-type KRAS/BRAF also indicated that increased miR-140-5p significantly correlated with poor OS (Mosakhani et al. 2012). In oestrogen-stimulated breast cancer cells, miR-140 restoration reduced the $CD44^{high}/CD24^{low}$ subpopulation frequency, which is referred to the tumour-initiating cells. However, in the absence of oestrogens, miR-140 overexpression had little to no impact on tumour-initiating cell frequency (Zhang et al. 2012). miR-140-5p expression was elevated in invasive ductal carcinomas (P=0.002), whereas basal-like tumours had decreased expression of miR-140-5p compared to other tumours (P=0.008). Lymph node-positive samples showed an approximately 13-fold increase in miR-140-5p expression compared to lymph node-negative tissue (P=0.049) (Gullu et al. 2015). Samples with no immunohistochemical staining for IGFBP5 showed increased miR-140-5p expression (P=0.009) (Zhang et al. 2012). All of the above evidence again emphasized the context-specific role of miR-140-5p.

Furthermore, we determined the pattern of miR-140-5p and -3p expression in this gastric cancer patient cohort who received 5FU based NAC to evaluate their predictive roles in chemoresponse. We found there was a significantly increased expression of miR-140-5p/3p in malignant tumours compared with adjacent normal tissue, and even higher in responsive tumour tissues. Survival analysis revealed that patients with no response from the NAC treatment but armed with either higher miR-140-5p or miR-140-3p expression (compared to paired normal tissues) could still have a chance for long-term survival.

Taken together, the results suggested that miR-140-5p and miR-140-3p may play specific or even contrasting roles in gastric cancer with different biological background (intestinal vs. diffuse, or Borrmann I-II (localized) vs. Borrmann III-IV (infiltrative)). Generally, miR-140-5p and miR-140-3p played tumour suppressing roles in gastric cancer, and more advanced tumours in the late stage (AJCC Stage III and Stage IV) had a decreased miR-140-5p/3p expression in comparison with tumours at early stages of the disease (Stage I and Stage II). Current cohort analysis also hinted a complementary function for this pair of miRNA duplexes. However, further investigation should be performed to validate this finding in a larger cohort with a well-documented histological description for subgroup analysis. Also, since a big variance was seen in our q-PCR examination, an improvement should be made in optimizing the endogenous reference and enhancing the accuracy for quantitative assessment. Higher expression of miR-140 associated with 5FU chemoresistance was found in small cell lung carcinoma cell lines (Polley et al. 2016), in osteosarcoma tumour xenografts, and in

CD133(+hi) CD44(+hi) colon cancer stem-like cells, probably due to slower proliferating rate (Song et al. 2009). It was also suggested that increased miR-140-5p expression levels up-regulated anticancer drug-induced autophagy in osteosarcoma cells and ameliorated the anticancer drug-induced cell proliferation and viability decrease. Besides, miR-140-5p is highly expressed in erlotinib-resistant cells (mesenchymal type A549) and is predicted to target the TGFβ receptor and Smad2 (Wong and Wang 2015; Bryant et al. 2012). TGFβ may act in a pro-tumourigenic, pro-EMT fashion in erlotinib-resistant cells, but may play an anti-EMT and protective role in erlotinib-sensitive cells (epithelial type PC9) because inhibition of TGFβ did not induce a complete EMT transition in these cells, indicating that the perpetual activation of ERK and AKT signals from active EGFR signalling may rely on basal activation from TGFβRII in order to persist (Krentz Gober et al. 2017). It was not surprising that miR-140-5p, as one of the upstreamers of TGFβ, could play dual roles in the response to cytotoxic stress. The gain of function of K-ras mutations, non-functional p53, as well as deregulated TGFβ are well documented for their roles in the induction and potentiation of tumourigenesis. The definite correlation between miR-140-5p and -3p and these factors contributes to the tumourigenesis of gastric cancer warrant further investigation.

Taken together, these results show that the expression of miR-140-5p and -3p is reduced in specific subtypes of gastric cancer. This is associated with the disease progression and poor prognosis. Current findings from gastric cancer tissue samples led to a further investigation for their functional roles in gastric cancer cells, which is supposed to help to elucidate how and when miR-140-5p and -3p exert their protective roles on gastric cancer progression. This subject is discussed in subsequent chapters.

Chapter 5

The Influence of miR-140-5p and -3p overexpression on the cellular functions of human gastric cancer cell lines

5.1 Chapter Introduction

In the initial investigation, reduced expression of miR-140-5p and -3p was evident in intestinal gastric cancer. The down-regulation of miR-140-5p and -3p may correlate with progression of intestinal gastric cancer during the tumourigenesis, as such a trend was observed in MKN7 with high differentiation, MKN74 with moderate differentiation and AGS with low differentiation. Furthermore, intestinal-type gastric cancer patients with lower expression of miR-140-5p exhibited a shorter OS, suggesting its implication in the prognosis of the disease.

The most fundamental trait of cancer cells involves their ability to sustain chronic proliferation, which is usually sustained by proliferative signaling conveyed in large part by growth factors that bind cell-surface receptors, typically containing intracellular tyrosine kinase domains. In normal cells, the activation of intracellular tyrosine kinase proceeds to emit signals via branched intracellular signaling pathways that regulate progression through the cell cycle as well as cell growth (increases in cell size) in a highly specific and localized fashion properly. However, cancer cells acquire the capability to sustain proliferative signaling in a number of alternative ways, mainly through gaining excessive growth advantages and disruptions of negative-feedback mechanisms that attenuate cell proliferation (Hanahan and Weinberg 2011).

The most virulent form of cancer is not only a disease of uncontrolled cell growth but also a disease of uncontrolled cell migration. Metastasis, viewed as another hallmark of cancer, involves the spread of cancer cells from the primary tumour to surrounding tissues and to distant organs and the remains the leading cause of mortality among cancer patients (Labelle and Hynes 2012; Seyfried and Huysentruyt 2013). Cancer cells must complete several complex sequential steps to metastasize successfully, namely, detachment from the primary tumour, intravasation into the vascular system (whether directly or via lymphatics and lymph nodes), survival while in transit through the circulation, initial arrest, extravasation, initial seeding, and survival and proliferation in the target tissue (Labelle and Hynes 2012). Tumour cells that succeed in forming metastases may have acquired the necessary traits to complete these steps while still in the primary tumour, either autonomously or as a result of changes induced by inflammation, stromal cells or other environmental conditions (e.g., hypoxia,

mechanical forces) present in the primary tumour (Joyce and Pollard 2009).

Deregulated cell migration, along with proliferation, adhesion, and invasion, is an integrated process that is essential for cancer metastasis. Migration takes place throughout embryonic development and also participates in angiogenesis, immune responses, and wound repair (Horwitz and Webb 2003). For example, chondroprogenitors present in the synovium may facilitate their migration into the superficial zone of cartilage in response to articular surface injury (Jayasuriya and Chen 2015). The classic model of cell migration on planar surfaces describes various physicochemical events, including those initiated by a stimulus that activates a set of signalling pathways leading to cell polarization and a rapid reorganization of actin filaments and microtubules. Cells advance by protruding their membrane at their leading cell border, which is followed by dynamic substrate adhesion via integrin adherence to the substrate. Membrane retraction at the lagging cell edge finishes the cycle, which is then repeated in rapid succession. The summation of this process results in cell migration. Cell migration is indeed complex; it requires that events such as those described above, and other allied functions be highly coordinated in time and space to keep the cell moving forward (Morales 2007). Cell invasion, related to cell migration, is not only determined by the cell's ability to change and reorganize its cellular morphology, but also the potential to degrade the extracellular matrix (ECM) (Justus et al. 2014). Scratch assays (or wounding assays), are performed by creating a cell-free gap, or "scratch", on a confluent cell monolayer upon which cells at the edge of the opening move inward to close the scratch (Zaritsky et al. 2015). Cell polarization is correlated with the direction of the maximal principal stress, maximum shear stress drives cell polarity (He et al. 2015; Zaritsky et al. 2015).

Several studies have identified the roles of miR-140-5p and -3p in the regulation of cell functions in various malignancies. Restoration of miR-140-5p induced p53 and p21 expression accompanied with G1 and G2 phase arrest in colon cancer, osteosarcoma (Song et al. 2009), and pancreatic cancer (Liang et al. 2017). Ectopic overexpression of hsa-miR-140-5p in colorectal cancer cell lines decreased Smad2 expression, leading to decreased proliferation and cell invasion, and increased cell cycle arrest *in vitro*, and abolished tumour formation and metastasis *in vivo* (Zhai et al. 2015). Moreover, lower miR-140-5p expression correlated with increased expression of cyclin E which promoted cellular proliferation in non-small cell lung cancer (Xie et al. 2018). E2 phosphorylated oestrogen receptor α (ERα) could suppress miR-140-5p expression, which targets SOX2, leading to enhancement of

breast tumour-initiating cell survival (Vazquez-Martin et al. 2013). Gain-of-function experiments in glioma revealed that miR-140-5p overexpression inhibited proliferation, induced cell cycle arrest at the G0/G1 phase, and enhanced apoptosis (Cui et al. 2017). In gastric cancer, miR-140-5p was reported to inhibit SOX4 directly, which might be one of its mechanisms in suppressing gastric cancer cell proliferation (Zou and Xu 2016). In erlotinib (an EGFR inhibitor) resistant non-small cell lung cancer cells miR-140-5p were highly expressed and might associate with a mesenchymal-like phenotype (Krentz Gober et al. 2017). Transient transfection of miR-140-3p inhibitors showed anti-proliferative effect on chordoma cell lines U-CH1 (retain a wild-type allele of p53 gene, one allele of p53 had a mutation-carrying a C > G substitution at nucleotide residue 412 within exon 4) (Jager et al. 2017; Kato et al. 2011) and U-CH2 (p53 proficient) (Li et al. 2011; Zhang et al. 2017), but had no effect on MUG-Chor1 cell viability. Nevertheless, upregulation of miR-140-3p with miR-140-3p mimics did not affect the cell proliferation or apoptosis (Gulluoglu et al. 2016).

Low expression of miR-140-5p or miR-140-3p was associated with enhanced colony formation, invasion and xenograft formation in biliary tract cancer (Yu et al. 2016), basal-like DCIS (Li et al. 2014a), poorly differentiated gastric cancer (Fang et al. 2017), oesophageal squamous cell carcinoma (Zhang et al. 2018) and lung cancer (Kong et al. 2015).

Considering the paradoxical expression pattern and role in the regulation of the cellular function of miR-140-5p and -3p in different tumour types, we aimed to decipher the expression and function of miR-140-5p and -3p in gastric cancer cells with the different molecular backgrounds. Gain/loss of function assays of miR-140-5p and -3p were employed to compare differences in cell behaviors, including cell proliferation, cell cycle distribution, migration, invasion, and drug-induced cell proliferation of four gastric cancer cell lines AGS, NUGC4, MKN45, and HGC27.

5.2 Materials and methods

5.2.1 Cell lines

Intestinal gastric cancer cell lines AGS (wt*p53*), diffuse gastric cancer cell lines NUGC4 (wt*p53*), and MKN45 (mut*p53*) and HGC27 (mut*p53*) were used in this study. All these cancer cell lines were cultured in DMEM medium with 10% FBS and antibiotics (Chapter 2.1).

5.2.2 Transfection of miR-140-5p and -3p mimics

Overexpression of miR-140-5p and -3p was conducted through chemical transfection of miR-140-5p and -3p mimics with Lipofectamine 3000. Transfection efficiency was confirmed by real-time PCR before cell function assays. All the experiments were performed within 96 hours following transfection (Refer to chapter 2.1).

5.2.3 RNA isolation, cDNA synthesis, RT-PCR, and qPCR

RNA was extracted using a Tri Reagent kit (Sigma-Aldrich, Poole, Dorset, UK), miR-transcription was then converted by the GoScript™ Reverse Transcription System kit separately (Refer to chapter 2.3).

5.2.4 *In vitro* cell proliferation assay

Twelve hours after transfection, cells from the six-well plate were trypsinised and counted as described in chapter 2.10.2. Six replicates were set up for each cell lines with three different transfection groups in one 96-well plate, Thus the cell pellet was resuspended at 1×10^6 cells /36 mL normal media and 100 μL of this suspension/well were seeded in six 96-well plates (Greiner Bio-One Ltd., Gloucestershire, UK). Since serum present in the culture medium can generate background, the outer wells empty were filled with 100 μL normal media but no cells, following the same layout. The plates were incubated for 6h, 12h, 24h, 48h, 72h, and 96h respectively. Following incubation, 10 μL of 5 mg/mL MTT solution was added to each well for both experimental and control plates, which were then left in a normal incubator for 4h. After the purple precipitate was visible, the medium was removed. The remaining purple crystals were dissolved in 100 μL of acidified isopropanol and the absorbance for each plate was read at 540 nm using an ELx800 plate reading spectrophotometer (Bio-Tek, Wolf laboratories, York, UK). The blank plate's absorbance was subtracted from that of the plates which contained cells, to eliminate background interference from the absorbance readings. Cell viability rate was calculated according to the following formula: Cell viability (%) = A540 (sample)/A540 (control) × 100.

5.2.5 *In vitro* cell colony assay

Only a fraction of seeded cells retains the capacity to produce colonies (Franken et al. 2006). Clonogenic assay or colony formation assay is an *in vitro* cell survival assay based on the ability of a single cell to grow into a colony. A colony is defined to consist of at least 50 cells.

Single suspended cells were seeded in six-well plates at 300 cells per well. After one week, the colonies were stained with 800 uL of 0.5% crystal violet for 10 min and washed with tap water carefully. The number of colonies was counted under the microscope.

5.2.6 *In vitro* wound scratch assay

Cells were suspended and seeded into each well of a 6-well plate at a full confluence cell density (1.2-2.0×10^6). After the cells attached to the bottom and formed a monolayer, linear wounds were scratched with a 10 uL pipette tip at the centre of the monolayer and the detached cells were carefully washed off with PBS thrice. Afterward, 2 mL of DMEM (Gibco BRL, USA) containing 2%FBS (Gibco BRL, USA) was added into each well, and the wounds were photographed at 0 and every 2 hours for 24 hours using EVOS® Imaging system and the wound closure area of each scratch wound was measured by Image J (National Institutes of Health, NY, USA).

5.2.7 *In vitro* transwell migration assay

The chemo-stimuli induced migration assay was performed using Transwell chamber (PIEP12R48, Millipore, UK). 2×10^4 cells were seeded into Transwell inserts (pore size, 8μm) in a 24-well plate. After 24-hour incubation, the cells that had migrated through and moved onto the other side of the insert were fixed with 4% formaldehyde and stained with crystal violet. Cells which had migrated were then counted under a microscope.

5.2.8 *In vitro* cell invasion assay

For invasion assay, the chamber was coated with Matrigel, and the following steps were similar to migration assay. 2×10^4 cells were seeded into Transwell inserts (pore size, 8μm). After incubation, cells that had invaded through the Matrigel and migrated on to the other side of the insert were fixed and stained with crystal violet, and then counted under a microscope.

5.2.9 Cell cycle assays for flow cytometry

The analysed cells grown in the logarithmic phase were washed 2 X with PBS, then trypsinised. Cells, cell medium and washed PBS were harvested together and spun at 850 g for 5 minutes and then resuspended in 5 mL of ice cold 70% v/v Ethanol followed by being left at 4°C. Following this, cells were again centrifuged using the same conditions and then

washed twice in PBS. 50 μL of a 100 μg/mL sock of RNase was added to each sample, 200 μL of 50 μg/mL propidium iodide (PI) was added to stain DNA content. Cells were then incubated at room temperature in the dark for 15 minutes. Following this, samples were run on the BD FACSCanto™ II flow cytometer (Becton, Dickinson and Company, UK.) using the FL3 channel (575 nm).

5.2.10 Cell cytotoxic assays

Cells were replanted in 96-well plates at 5 $\times 10^3$ cells/well in hexad in 100 μL of medium. After cell adherence, 5FU (ranging from 2 to 100 μM) was added and incubated for 48 h. The following steps are similar to a proliferation assay. A complete medium control without cells was used to determine background density of serum with drug solvent.

5.3 Results

5.3.1 miR-140-5p, - 3p expression and the overexpression of miR-140-5p, -3p in gastric cancer cell lines

The expression of miR-140-5p and -3p has been detected in six gastric cancer cell lines originated from human carcinoma including intestinal gastric cancer cell lines MKN7, MKN74, and AGS; and diffuse gastric cancer cell lines NUGC4, MKN45, HGC27. Mature miR-140-5p and -3p transcripts were determined using RT-PCR. Overall, miR-140-5p and -3p showed almost equally distribution in all examined gastric cancer cell lines (Figure 5.1). In the intestinal group, the degree of decline of miR-140-5p and -3p was related to the degree of cells' differentiation. Such a trend was not seen in the three diffuse gastric cancer-derived cell lines. AGS, NUGC4, MKN45, and HGC27 were included in preliminary experiments for transient overexpression of miR-140-5p or -3p. Initial tests showed that overexpression of miR-140-5p and -3p was well established in all four of these cell lines by qPCR. (Figure 5.1).

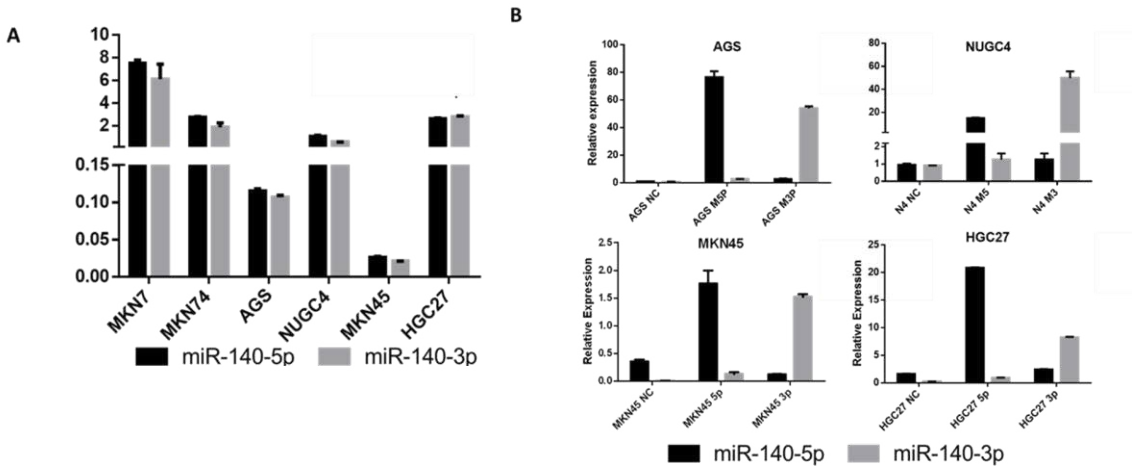

Figure 5.1: miR-140-5p and -3p expression in gastric cancer cell lines and overexpression of miR-140-5p and -3p respectively in AGS, NUGC4, MKN45, and HGC27. (A) Expression of miR-140-5p and -3p in gastric cancer cell lines were examined using qPCR. Reagents used in miRNA reverse transcription step and in real-time PCR step were used as negative controls to exclude any contamination in the PCR reactions, and miR-423-5p was used as an internal control according to the manual direction from TaqMan. **(B)** Expression of miR-140-5p and -3p in AGS, NUGC4, MKN45 and HGC27 gastric cancer cells transfected with miRNAs' mimics were determined using RT-PCR.

5.3.2 Effects of miR-140-5p and -3p on proliferation of gastric cancer cells

Cancer is characterized by abnormal cellular proliferation. Combinations of defined growth-promoting molecules under chemically defined conditions have revealed an important aspect of the molecular events leading to cell proliferation. In particular, the availability of defined mitogenic molecules has opened up the possibility of exploring the molecular and physiological properties of the cellular receptors related to growth control, and the nature of the intracellular signals (e.g. ion fluxes, cyclic nucleotides and cytoskeletal changes) capable of eliciting or modulating a mitogenic response (Phillips 2015). Candidate drugs for solid tumours are commonly evaluated predominantly by their ability to induce tumour shrinkage. Progression in solid cancer is conventionally defined as an increase in tumour size, and, in a superficial sense, the equating of therapeutic efficacy with tumour shrinkage is understandable (Gandalovicova et al. 2017).

To evaluate the influence of miR-140-5p and -3p on proliferation of gastric cancer, we used the MTT assay which examined NAD(P)H-dependent cellular oxidoreductase enzyme activity to reflect the number of viable cells present. Overexpression of miR-140-5p or miR-140-3p led to a distinct result in gastric cancer cell lines' proliferation (Figure 5.2). For *p53* wild-type gastric cancer cell lines AGS and NUGC4, overexpression of miR-140-5p/3p resulted in a significant reduction of proliferation in both cell lines to varying degrees. In AGS, the decrease started from 24 hours after miR-140-5p or miR-140-3p mimic transfection and kept consistent to the end of the assay. For NUGC4, a marginal decrease was only exhibited after two days following transfection compared to the mimic negative control (NC mimic) with the difference statistically significant (Figure 5.2). In reverse, in HGC27 lines, no significant difference in cell proliferation was found during 96 hours' observation, However, for MKN45 cell lines, a significant reduction of cells was only seen at 96 hours (Figure 5.2).

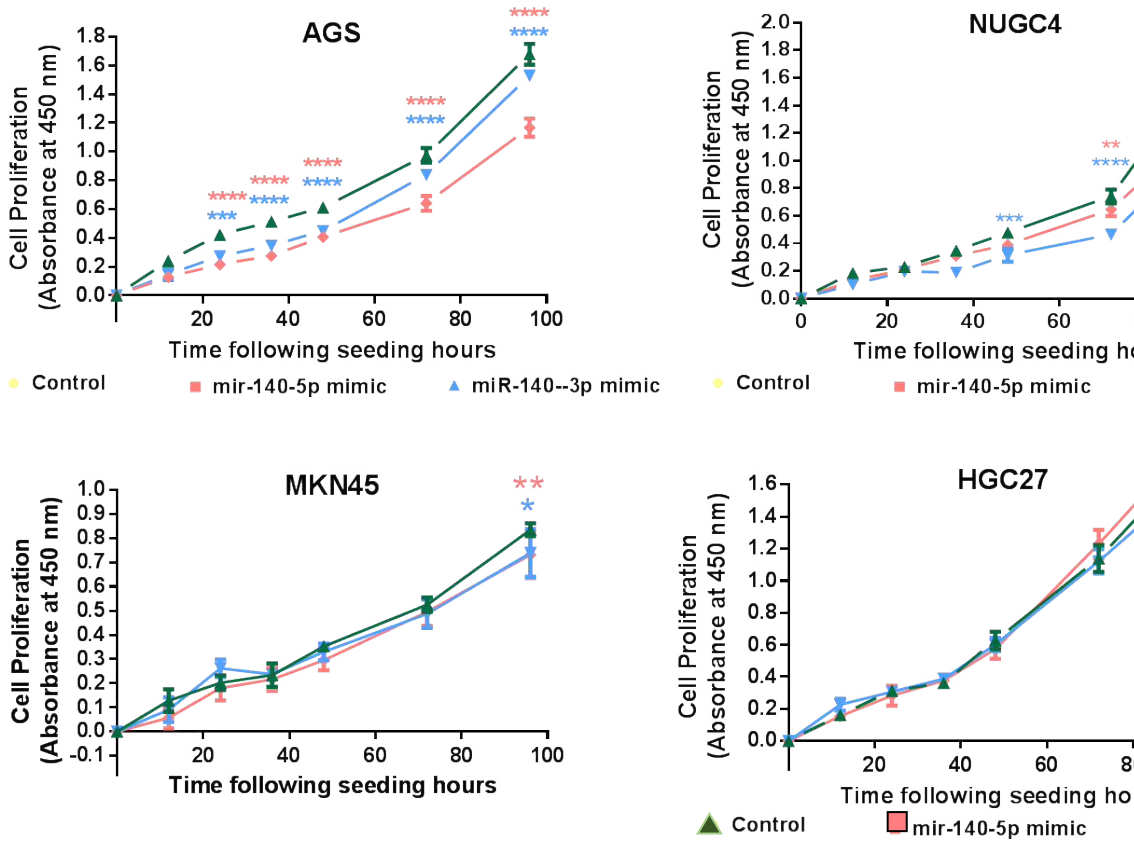

Figure 5.2: Overexpression of miR-140-5p or 3p resulted in a significant reduction of proliferation in AG influence on the growth of in MKN45 and HGC27 cells. Cells were maintained for 6h, 12h, 24h, 48h, 72h, and 96h lines. The proliferation rate (%) was calculated as: Absorbance (Day X) / Absorbance (Day 1) × 100 (%). Shown are representative deviation. **** represent p<0.0001, *** represent p<0.001 and ** represent p<0.01, respectively.

5.3.3 Effect of miR-140-5p/3p on colony formation of gastric cancer cells

The proliferation assay with MTT reflects cells' metabolic state. Colony formation assay, on the other hand, measures the ability to expand and form colonies at a low seeding density, providing a fine visualization in terms of highlighting the pro-survival/pro-apoptosis balance of given perturbations. Clonogenic potential does not necessarily parallel rapid growth, such that prematurely senescent cells do not form colonies but are metabolically active. Since the turnover time of transfected miRNA mimics was thought to be caused by cell division instead of miRNA decay. After considering the possible dilution effect caused by cell division (Jin et al. 2015), the results from the one-week colony formation assay indicated that over-expression of miR-140-5p via mimics transfection significantly suppressed the potential of cell colony formation in NUGC4 cells (doubling time, 2-3 days), but again did not show significant impact on the colony formation on HGC27 and MKN45(Figure 5.3). However, for the AGS cell lines, cells spread out in the dishes instead of forming any colonies.

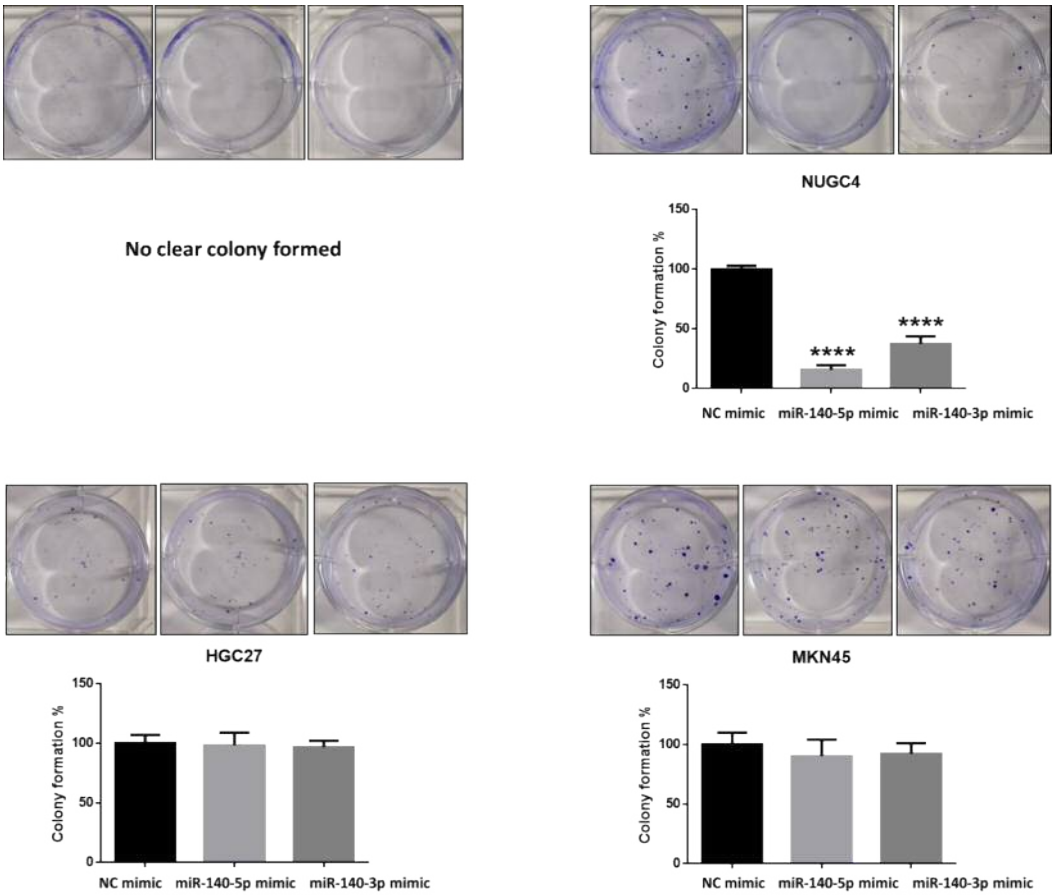

Figure 5.3: Overexpression of miR-140-5p or 3p significantly decrease of colony formation only in NUGC4 cell line. Three hundred cells were maintained for 1 week. The colony formation rate (%) was calculated as: Colony number (miR-140-5p/miR-140-3p mimic) / Colony number

(NC mimic) × 100 (%). Shown are representative results of one experiment out of three performed. Error bars represent standard deviation. **** represent p<0.0001.

5.3.4 Effect of miR-140-5p/3p on cell cycle of gastric cancer cells

To further confirm the proliferation suppression function of miR-140-5p and -3p on gastric cancer cells, the cell cycle progress was investigated of all four gastric cancer cells, and in a pair of colon cancer cell lines, HCT116 p53 Wild-type (WT) and HCT116 p53 Knock-out (KO), by flow cytometric analysis.

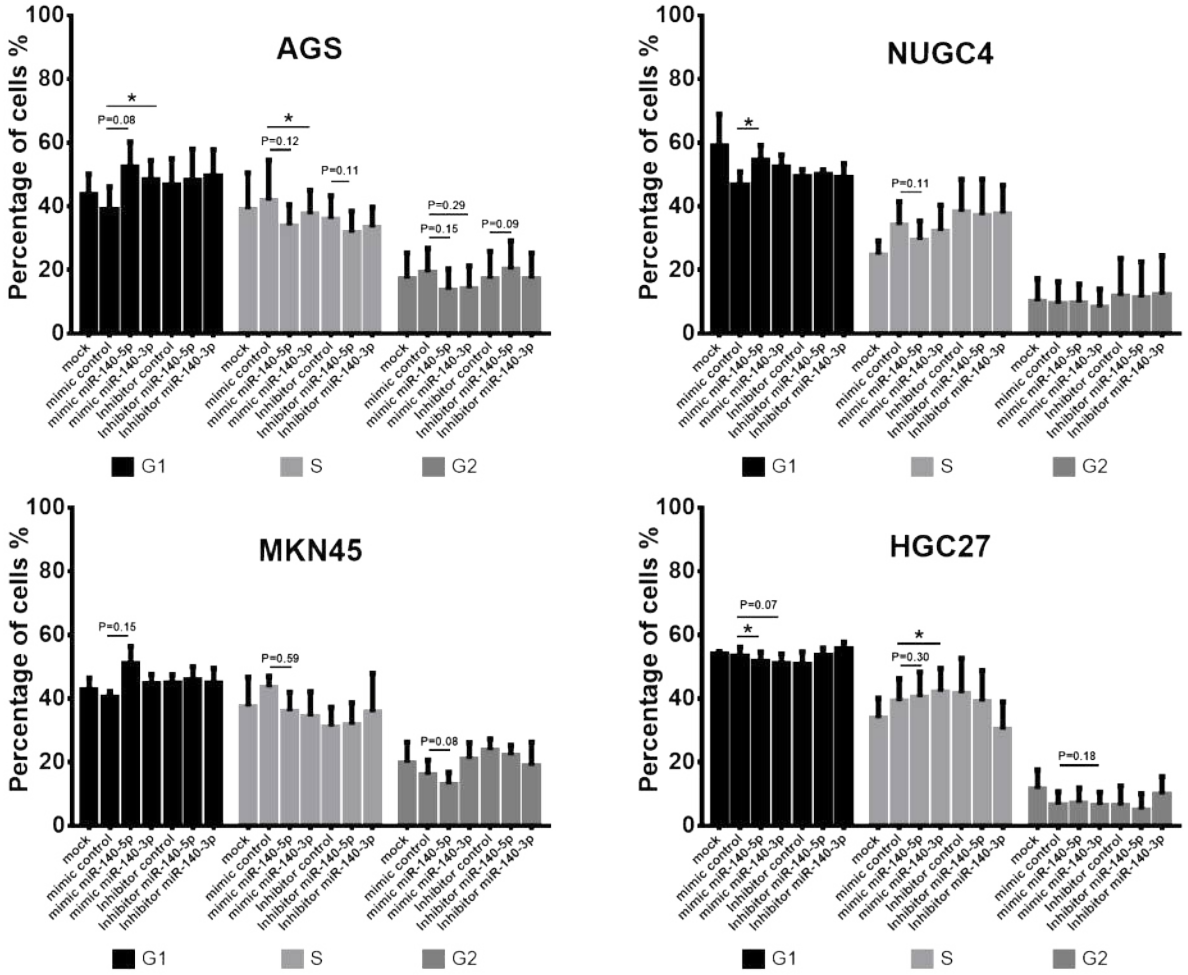

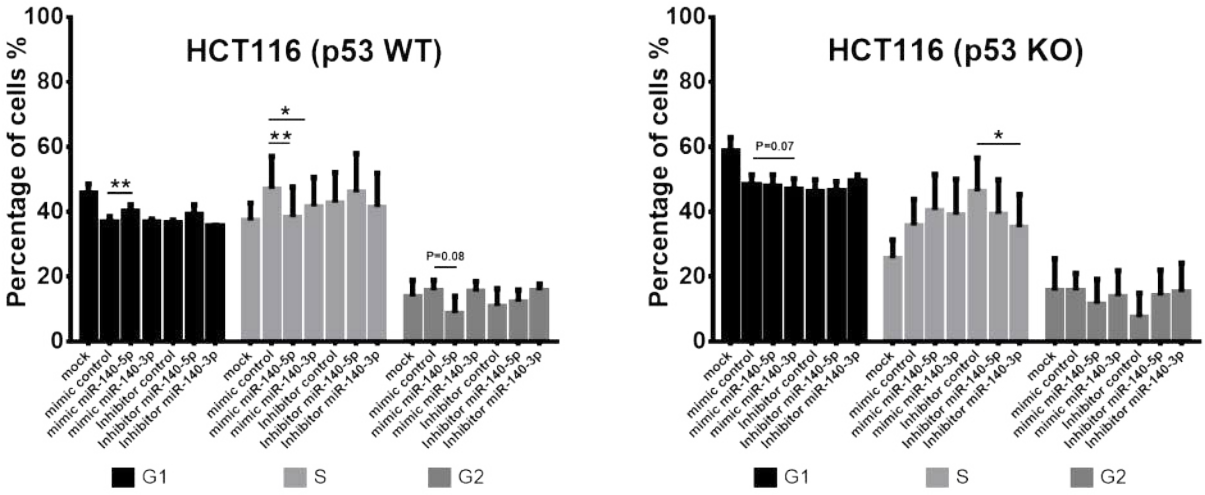

Figure 5.4: Flow cytometric analysis of cell cycle arrest after interfering miR-140-5p/3p expression in gastric and colon cancer cell lines. Mean percentage of cells ± SD were shown. With miR-140-5p overexpression, a slight but significant increase of G1 phase with or without marked decrease in S phase was seen in NUGC4 (p53 wt) and HCT116 (p53 wt) cell line, a similar trend was also seen in AGS cell line (p53 wt) and in MKN45 cell line (p53 missense mutation). Reversely, a decrease of G1 phase but increased trend in S phase was seen in HGC27 cell line. No obvious change was seen in HCT (p53 KO) cell line. Only AGS cells showed increased G1 phase with miR-140-3p overexpression, which showed even more remarkable impact than miR-140-5p overexpression. Error bars represent standard deviation. * represent $p<0.05$, ** represent $p<0.01$.

As shown in Figure 5.4, In wt-p53 cancer cell lines transfected with negative control mimics, around 40% of the cells were in the G0/G1 phase, and 55% and 15% of cells were in S phase and G2/M phase, respectively. While, in cells transfected with miR-140-5p mimics, there was a definite increase in the percentage of cells in G0/G1 phase (about 55%), as well as a decrease in the percentage of cells in S phase (about 40%) and G2/M phase (5-10%). A slight but significant G1/S arrest was also seen MKN45 cells harbouring functional mut-p53. No change was seen in HCT116 KO cells, in HGC27 cells even a decrease in G0/G1 phase was observed. These results imply that overexpression of miR-140-5p or miR-140-3p induced cell cycle arrest at G1/S phase of gastric cancer cells might depend on cells' status and functions of p53.

5.3.5 Effect of miR-140-5p/3p on the migration of gastric cancer cells

During cancer metastasis, cancer cells migrate and spread to distant organs and form a new mass. In the current study, both wound scratch and trans-well migration assays were performed to assess the impact of overexpression of miR-140-5p or -3p on the motility of gastric cancer cells. In the wound scratch assay, a cell-free area is created in a confluent monolayer by physical exclusion. The exposure to the cell-free area induces the cells to

migrate into the gap (Rodriguez et al. 2005). A sequence of representative images from a wound healing assay carried out on the confluent cells' monolayer were captured for analysis. As shown in Figure 5.5, during the 24-hour incubation, miR-140-5p overexpression in AGS and NUGC4 cell lines reduced the cells' migration in comparison with the control cells. Although for AGS cells, significant reduction was seen nearly 12 hours after wounding, for NUGC4 cells, a decreased trend showed at the very beginning of the migration assay. For miR-140-3p overexpression, only NUGC4's motility was weakened. Overexpression of either miR-140-5p or miR-140-3p strengthened the migration of HGC27 cells. No significant difference was found in the MKN45 cell lines.

This result was also in agreement with the other measurement of cell motility using the trans-well migration assay. The ability of cell migration was determined by measuring the number of cells which had migrated to the bottom of the insert from the upper culture chamber over a period of 12 hours. The result showed that significantly decline in motility in AGS and NUGC4 gastric cancer cells as a result of miR-140-5p overexpression. No significant difference was found in the MKN45 cell lines. HGC27, in contrast, showed a higher motility after miR-140-5p overexpression. For miR-140-3p mimic transfection, there was no significant difference shown in all four gastric cancer cells. Furthermore, NUGC4 AND MKN45 two diffuse type originated cell lines exhibited an impaired ability to initiate the migration process. ($P<0.01$) (Figure 5.6).

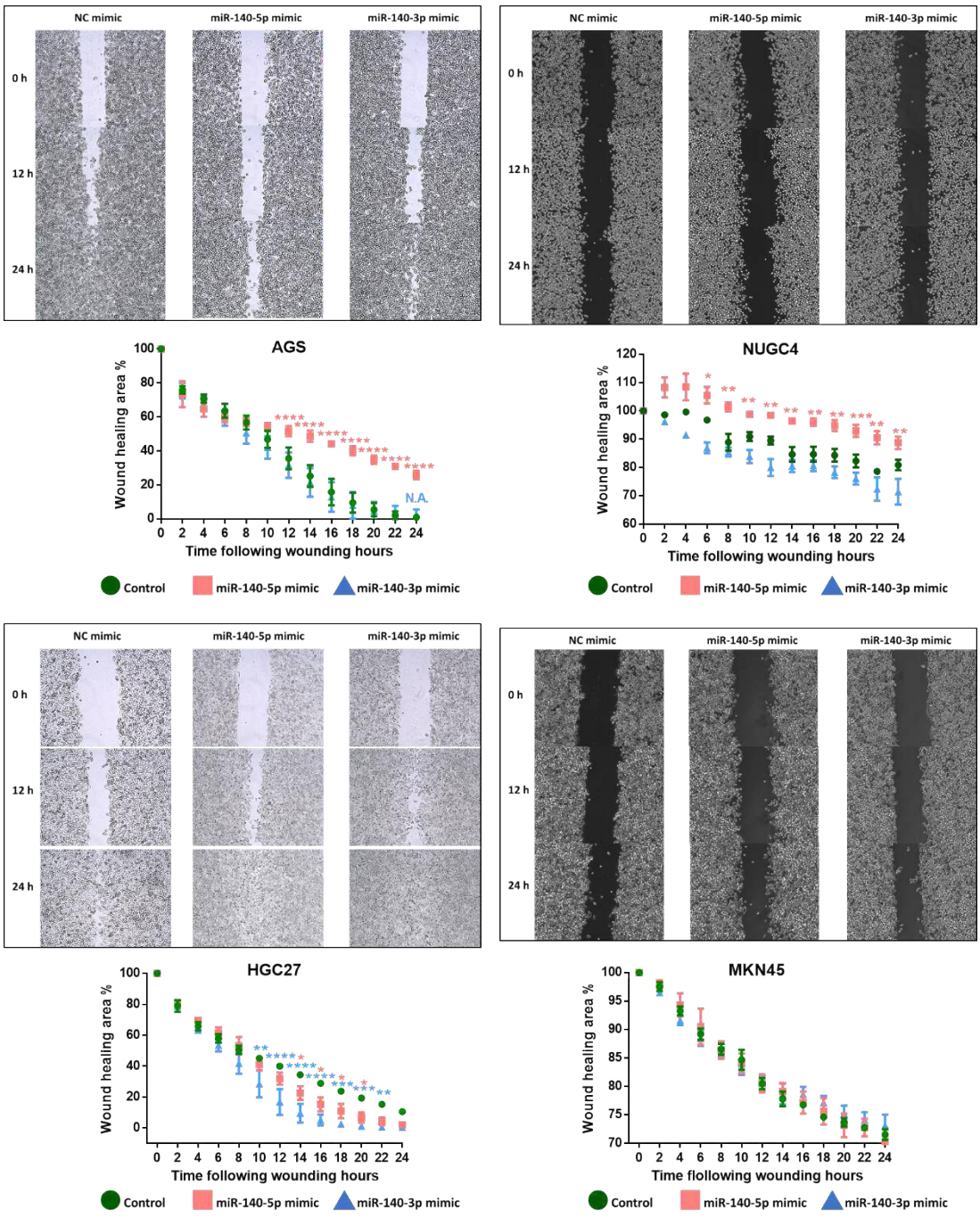

Figure 5.5: Effect of miR-140-5p and -3p on migration of gastric cancer cells. A wound assay was performed using the EVOS live cell analysis system. The migration was measured by the rate of gap closure via Image J software. The wound closure rate (%) was calculated as Gap area (Hour X) / Gap area (Hour 0) × 100 (%). Ten repeats were evaluated for each cell line in each experiment. Shown are the average percentage of the closure of the wounds. Error bars represent standard deviation. **** represent $p<0.0001$, *** represent $p<0.001$ and ** represent $p<0.01$, respectively.

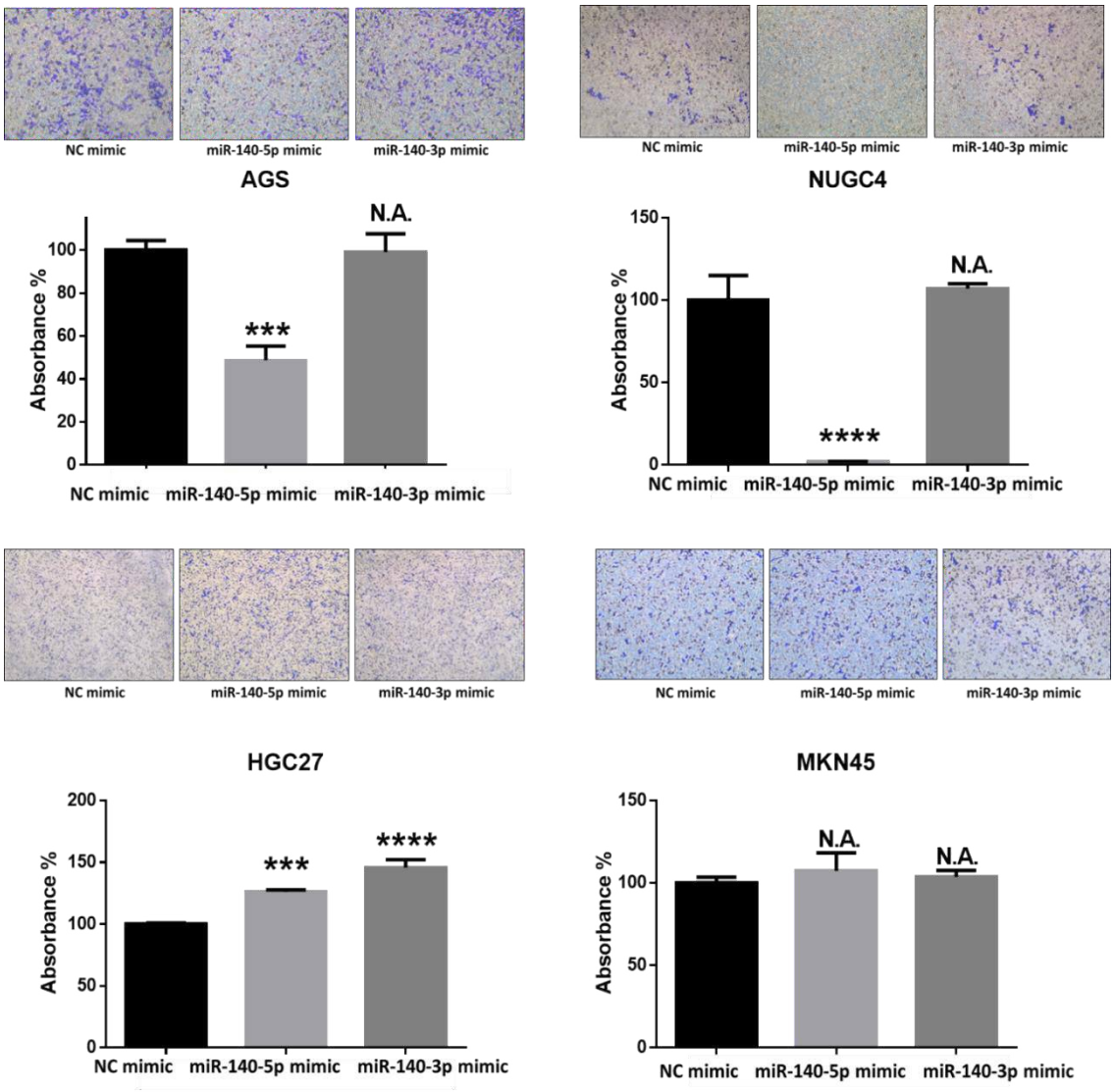

Figure 5.6: Effect of miR-140-5p and -3p overexpression on the migration of gastric cancer cells using trans-well migration assay. Representative images of migrated cells are shown above the bar graph. **** represent p<0.0001, *** represent p<0.001 and ** represent p<0.01, respectively. N.A. stands for no significance. Error bars are the standard deviation.

5.3.6 Effect of miR-140-5p and -3p on invasion of gastric cancer cell

The gain of an invasive phenotype is the most important cancer feature and the one that distinguishes malignant from benign tumours (Lazebnik 2010). *In vitro,* trans-well invasion assay was undertaken to determine whether miR-140-5p/3p is involved in regulation of invasiveness of gastric cancer cells. This assay is similar to the Trans-well migration but with Matrigel coating in the insert. The invasive ability of cells was determined by measuring the number of cells that attached to the matrix, invade into and through the matrix, and migrate towards a chemoattractant. Figure 5.7 shows that AGS, NUGC4, and MKN45 with upregulation of miR-140-5p or miR-140-3p showed significant impairment in their invasiveness. Overexpression of miR-140-5p/3p, however, had no influence on the invasive capacity of HGC27 cancer cells.

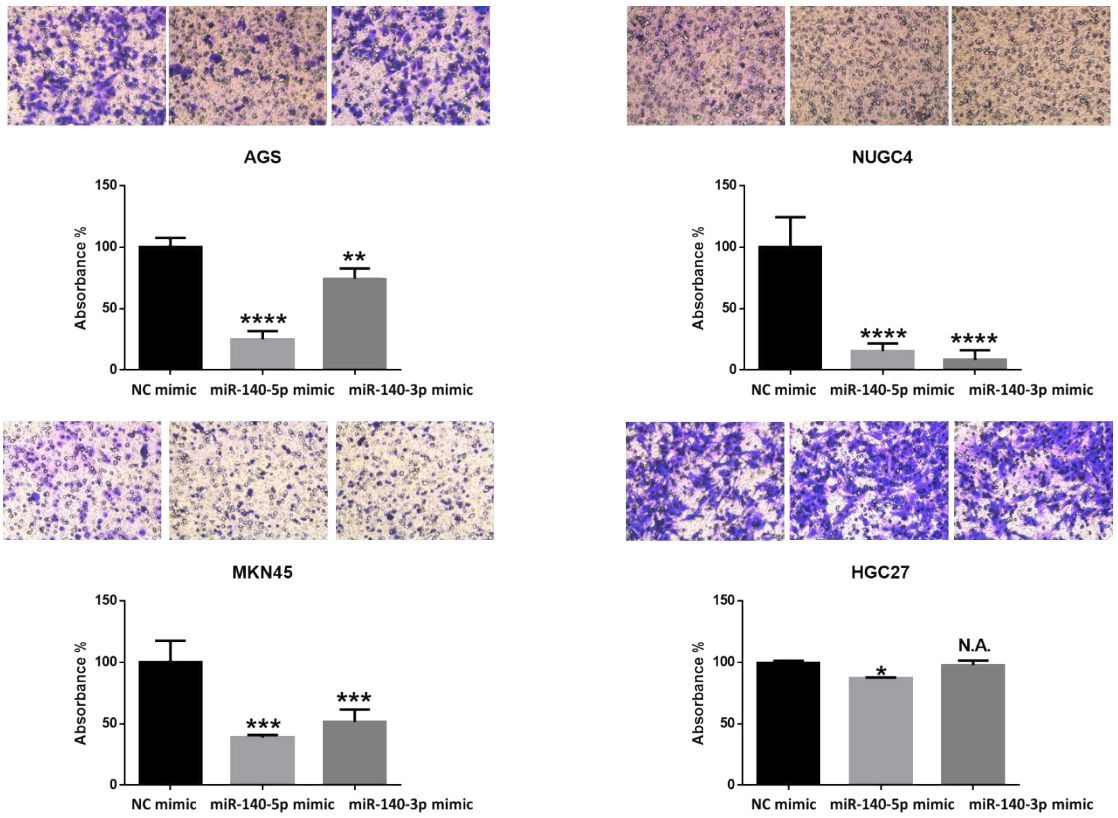

Figure 5.7: Impact of overexpression of miR-140-5p and -3p on invasive capacity of gastric cancer cell lines. Representative images of invade cells after staining and absorbance measured by dissolving the crystal violet stained invaded cells (bar graph). **** represent $p<0.0001$, *** represent $p<0.001$ and ** represent $p<0.01$, respectively. N.A. stands for no significance. Three experiments were performed. Error bars represent standard deviation.

5.3.7 Effect of miR-140-5p and -3p on chemotherapeutic drug-induced cell proliferation inhibition of gastric cancer cells

As previously mentioned, higher miR-140-5p is associated with chemoresistance in patients treated with 5FU based chemotherapy. To investigate the role of miR-140-5p and -3p in anticancer drug-induced apoptosis/autophagy in gastric cancer cells, miRNA expression levels were first analyzed by q-PCR in gastric cancer following treatment with 5FU. Elevated miR-140-5p and -3p were demonstrated in AGS and NUGC4 following treatment with 5FU (Figure 5.8). The cell viability of gastric cancer cells that had been treated with 5FU and transfected with miR-140-5p/3p mimics or inhibitors, was determined using the MTT assay. As shown in Figure 5.8, transfection with miR-140-5p mimic resulted in growing drug resistance in NUGC4 cell line. Upregulation of IC50 with also shown in AGS and MKN45 transfected with miR-140-5p, but it did not reach the statistical significance. However, upregulation of miR-140-5p increased chemosensitivity in the HGC27 cell line. In accordance with these results, miR-140-5p inhibitor gave rise to a marked increase in sensitivity after treatment with 5FU in the AGS and NUGC4 cell lines. As shown in Figure 5.8, miR-140-3p mimic transfection resulted in a dose-dependent amelioration of 5FU induced cell proliferation inhibition in NUGC4 cell lines but had no impact on other three cell lines. Accordingly, miR-140-3p inhibitor decreased chemoresistance in NUGC4 cell line, but not other cells transfected with miR-140-3p inhibitors.

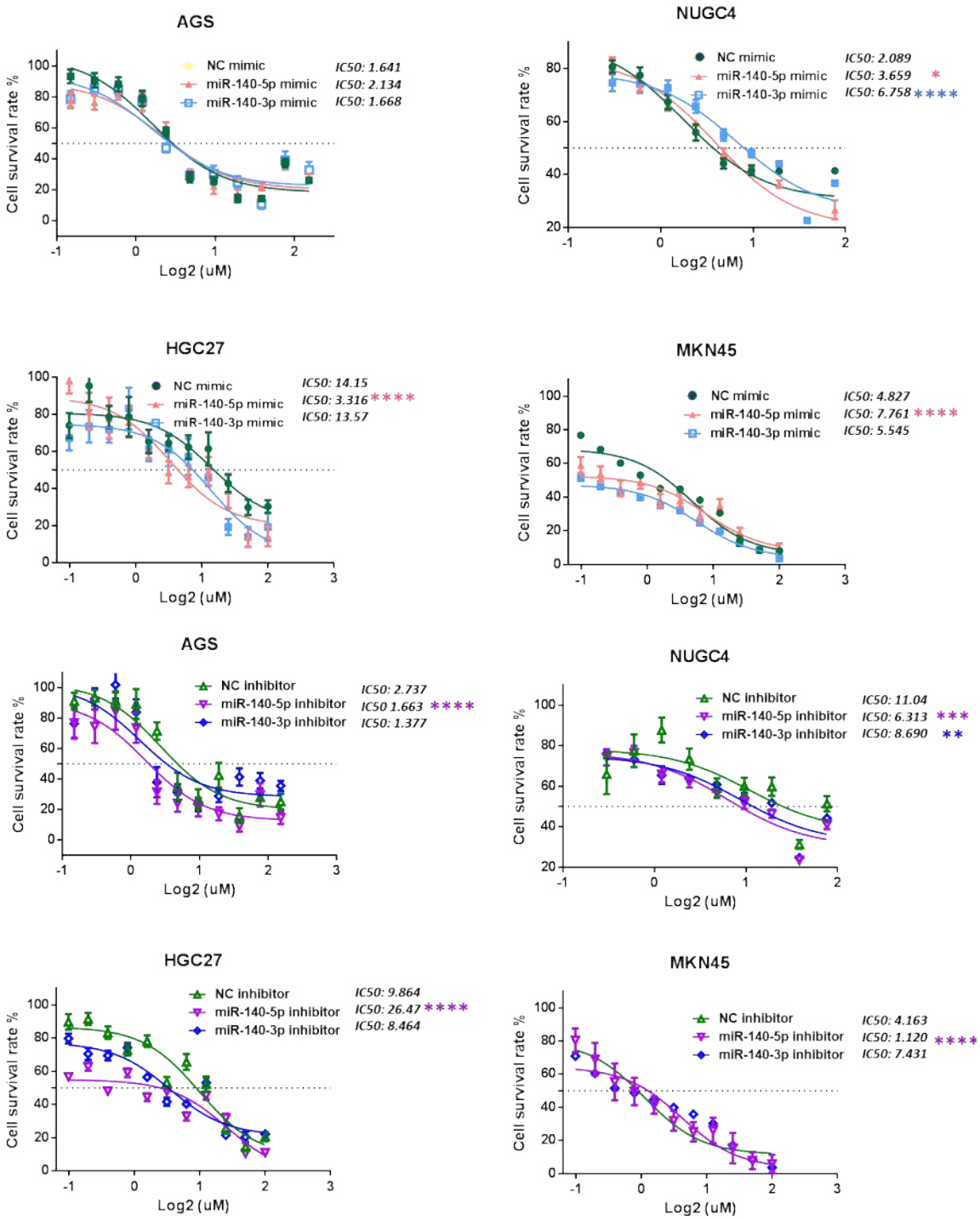

Figure 5.8: Impact of overexpression of miR-140-5p/3p on the drug-induced proliferation inhibition of gastric cancer cell lines. Cells were maintained for 48 hours with a series of gradient concentration 5FU, and the half maximal inhibitory concentration (IC50) for each cell line was determined by multi-proportion dilution method. Six wells were set for each cell lines. Non-linear regression with a sigmoidal fit model was used (GraphPad Prism). Shown are representative results of one experiment out of three being performed. Error bars represent standard deviation. **** represent $p<0.0001$, *** represent $p<0.001$ and ** represent $p<0.01$, respectively.

5.4 Discussion

This chapter has focused on the effect that the expression pattern of miR-140-5p and miR-140-3p has on the phenotypic behaviour of gastric cancer cell lines by proliferation, cell cycle, wound scratch, trans-well migration, invasion and apoptosis assays. Upregulated expression of miR-140-5p indicates a favorable clinical prognosis in patients with the intestinal type of gastric cancer. An *in vitro* assay also suggested the tumour suppressor role of miR-140-5p in intestinal gastric cancer. These are in agreement with the results Fang et al. demonstrated previously (Fang et al. 2017). However, since the current study employed a different method for colony formation (without pre-coated plates by agarose) compare to the previous study, the colony formation assay failed to reflect the miR-140-5p and -3p impacts on AGS cell line. However, in the diffuse type of gastric cancer cell lines, we observed a negative regulating role in cell's aggressiveness played by miR-140-5p in NUGC4 cell line with wild-type of p53 and MKN45 cell lines with mutant but functional p53. Although not much significant results were found in HGC27 cell line transfected with mimic-5p, a significant inhibition of invasion was shown in all examined cell lines, suggesting a strong inhibitory role of miR-140-5p in cells' invasive ability, despite a slight facilitation of the migration of HGC27.

The effect of miR-140-3p on tumourigenesis has previously been only focused in NSCLC and breast cancer. The inhibitory effect of miR-140-3p on cell growth and cell invasion has been demonstrated in NSCLC by downregulating ATP8A1, which participates in the transportation of exposure phosphatidyl-serine, which is a sign of early apoptosis back to the inner layer, and in the formation of membrane ruffles regulating cell motility, via both *in vitro* and *in vivo* assays (Dong et al. 2016). The shorter 3'UTR of its target genes, for example, Ki-67, may play an important role in its function in cancer (Yan et al. 2018). Furthermore, analysis of miRNA-seq data from breast cancer cell lines, identified six pairs of highly expressed miRNAs and associated 5'isomiRs. Among them, hsa-miR-140-3p was of particular interest because its 5'isomiR showed higher expression compared to the canonical miRNA annotated in miRbase. It was found that both the hsa-miR-140-3p and 5'isomiR-140-3p were higher in ER-negative (ER-) patients. Triple negative breast cancer patients showed a trend towards better survival among patients with higher expression levels of both hsa-miR-140-3p and 5'isomiR-140-3p. But it is the 5'isomiR-140-3p but not the hsa-miR-140-3p caused cell cycle arrest in G0/G1-phase, and decreased cell migration. This suggested the highly expressed 5'isomiR of hsa-miR-140-3p contributes to the tumour-suppressive

effects by reducing breast cancer proliferation and migration, and the endogenous canonical hsa-miR-140-3p reflected the expression level of this isomiR (Salem et al. 2016). In the current study, overexpression of miR-140-3p in gastric cancer cells had a similar antiproliferative effect as miR-140-5p overexpression to AGS and NUGC4 cell lines, but no influence on HGC27 and MKN45 cell lines. Also, miR-140-3p exerted an anti-invasive effect on all the cell lines except HGC27 cells. It is noticeable that, both miR-140-5p and miR-140-3p could target ADAMTS-5, one of the matrix-degrading enzymes (Swingler et al. 2012). To be mentioned, interfering expression of miR-140-5p/miR-140-3p with miRNA mimics or inhibitor only showed marginal or no influence on cell cycle analysis assessed by flow cytometry, which could be explained by two possibilities. First, although the proliferation changed greatly by miR-140-5p overexpression based on our MTT assay, the MTT assay measures metabolic activity (mainly succinate dehydrogenase) to reflect cell viability, which could be affected by not cell cycle arrest, but cell senescence and cell apoptosis. Since both miR-140-5p and miR-140-3p are involved in cartilage development and arthritis, the second possibility is that miR-140-5p and miR-140-3p may exert complementary roles in a identical cell signalling pathway, although target different genes.

In conclusion, the downregulation of miR-140-5p and miR-140-3p observed in human gastric intestinal-type cancer suggests its tumour suppressor role in regulating the cellular functions that are acquired by cancer cells during the disease progression, as reported in most other tumours (Wang et al. 2017; Hu et al. 2016; Tan et al. 2011; Kawaguchi et al. 2017; Yan et al. 2008). In contrast, miR-140-5p was upregulated in tumours compared to matched normal tissue in pancreatic cancers, a high expression of miR-140-3p is also reported to be associated with worse progression in clear cell renal cell carcinoma (Guan et al. 2018). These *in vitro* assays demonstrated the complex roles that miR-140-5p and miR-140-3p do exert in tumour development. In addition, the inhibitory role of miR-140-5p overexpression in the cell cycle is possibly the underlying mechanism for chemoresistance, especially for cell cycle-dependent anti-proliferative drug 5FU.

The combination of fluoropyrimidine and platinum is used worldwide for the treatment of patients with advanced or metastatic gastric cancer in both the adjuvant and neoadjuvant setting. Fluoropyrimidines, particularly 5FU, still represent the backbone of gastric cancer chemotherapy, with response rates varying from 31% - 48%. Our results provide data that is

suggestive that this should be taken into account when selecting therapies in chemo-sensitive patients. In order to further determine the role of miR-140-5p and miR-140-3p in gastric cancer, the following chapter will focus on the mechanisms of their inhibitory effect on gastric cancer cells.

Chapter 6.

The Molecular Mechanism Underlying Deregulated miR-140-5p Expression in Human Gastric cancer

6.1 Introduction

The previous chapter has shown that upregulation of miR-140-5p may inhibit proliferation, adhesion, invasion, and migration of AGS and NUGC4 gastric cancer cell lines but had little or no inhibitory effect in MKN45 and HGC27. The diverse outcomes of miR-140-5p *in vitro* assays of gastric cancer cell lines echoed its variable function in gastric cancer tumour tissue analysis. Also, as discussed in Chapter 4, although-140-5p was generally accepted as a tumour suppressor in the tumourigenesis of lung cancer, breast cancer, and colorectal cancer *etc.*, a pro-oncogenic role of miR-140-5p has also been implicated depending on different cell context. Molecules and pathways involved in these different roles played by miR-140-5p in gastric cancer are likely to be subspecies specific but are yet to be investigated. It has been reported that loss of miR-140-5p led to an impairment of chondrocyte proliferation (Song et al. 2009) via upregulation of SP1, a critical transcription factor in the inhibition of the cell cycle via the activation of the p15INK4b and p21Waf1/Clip promoters *in vitro* (Yang et al. 2011). Tumour cells ectopically transfected with miR-140-5p showed upregulation of p53 and p21 expression accompanied with G1 and G2 phase arrest only in cell lines containing wild-type of p53. Furthermore, miR-140-5p suppresses tumour cell migration and invasion by targeting ADAM10-mediated Notch1 signalling pathway in hypopharyngeal squamous cell carcinoma (Jing et al. 2016). Targets of miR-140-5p, SOX9 and ALDH1 were the most significantly activated stem-cell factors in DCIS stem-like cells in breast cancer (Q. Li et al. 2014b; Wolfson et al. 2014; Yan et al. 2008). A decreased level of IGFBP-5, a miR-140-5p target (Tardif et al. 2009), is related to disease recurrence in lung cancer (Shersher et al. 2011) and to tamoxifen resistance in breast cancer. These may link to the restoration of miR-140-5p after releasing from the suppression by ERα. Exosomal levels of miR-140-5p from stem cell populations can be rescued by treatment with sulforaphane (Q. Li et al. 2014b). Moreover, miR-140-5p appeared to be positively controlled by Rb and to antagonize the effect of Rb depletion through targeting IL-6 (Yoshida et al. 2017). Rb depletion or inactivation in soft tissue sarcoma cells exhibited slower proliferation and less efficient BrdU incorporation, but much higher spherogenic activity and aggressive behavior both *in vitro* and *in vivo*. The induction of IL-6 secretion and subsequent autocrine/paracrine activation of STAT3 signalling supports the self-renewal activity of not only cancer cells (Marotta et al. 2011; Korkaya et al. 2012; Sansone et al. 2007), but also embryonic stem cells or induced pluripotent stem cells (Brady et al. 2013; Takahashi and Yamanaka 2016). With regard to

miR-140-5p in gastric cancer progression, there are still relatively few studies available and discrepancy was found between these studies. Plasma miR-140-5p was significantly higher in gastric cancer patients than in healthy controls (Shin et al. 2015). Aberrantly downregulated miR-140-5p in cancer tissue, compared with that in adjacent normal tissues, was determined by both q-PCR and in situ hybridization (ISH) in tissue microarrays (Fang et al. 2017). ISH analysis in 144 gastric cancer tissues revealed 32.6% of the GC tissues showed reduced staining intensities of miR-140-5p. Zhai *et al.* demonstrated that overexpression of miR-140-5p abolished tumour formation and metastasis in gastric cancer cells by directly targeting YES proto-oncogene 1 (YES1) which upregulated Src signalling (Fang et al. 2017). Based on these contrasting reports, the exact mechanism of action for miR-140-5p needs to be further investigated. The aim of this chapter is to explore the pathways activated in miR-140-5p deregulation in gastric cancer progression.

6.2 Materials and methods

6.2.1 Materials

The primers used in this chapter are shown in Table 2.4, including *MDM2*, *p53*, *p21*, *PTEN*, and *GAPDH*. Details of antibodies for detection of MDM2, p53, p21, BAX, and GAPDH are shown in Table 2.5.

6.2.2 Online prediction of miR-140-5p targets.

To identify functionally related pathways and genes that are associated with a miR-140-5p based gastrin cancer phenotype, we associated miR-140-5p expression with transcriptome for patients with accessible RNAseq information from TCGA and the Gene Set Enrichment Analysis (GSEA). This database contains full access to the complete list of gene expression values and was employed to cross-compare prior lists of differentially expressed genes between gastric cancer patients with higher miRNA-140-5p expression (n=17) and lower miRNA-expression (n=54). According to the indicated pathway, the direct targets of both miR-140-3p and miR-140-5p have been investigated by using the bioinformatics approach and *in silico* tools TargetScan, mirTarbase, and miRWalk. The literature review together with the RNA-sequencing and protein array data from transfection with the biotinylated mimics were obtained in a previous study carried out in the host lab (Flamini et al. 2018) and were merged to specify targets of miR-140-5p.

6.2.3 Determining the expression of p53-related signaling molecules using PCR and Western blot.

Since the cell cycle-related pathway was highlighted and MDM2 was indicated as a potential target of miR-140-5p, the p53-related pathway was chosen for further analysis. Both RNA and protein were extracted from gastric cancer cell lines transiently infected with miR-140-5p or miR-140-3p mimic. The samples were analysed using either Western blot or PCR to detect the expression level of these molecules. The methods used were as described in section 2.4 and 2.5.

6.2.4 Statistical analysis

Correlation between miR-140-5p and -3p and other genes in gastric cancer tissue samples was assessed using the Spearman correlation test via GraphPad Prime v 6.0 (GraphPad Software, San Diego, CA).

6.3 Results

6.3.1 Integrative analysis of miRNA and mRNA expression in intestinal versus diffuse miR-140-5p downregulated gastric cancer.

Gene enrichment analysis (GESA) of mRNA expression was obtained using the GAGE package on KEGG pathways. High expression of miR-140-5p strongly indicated an interaction between tumour cells and factors such as immune response, ECM biogenesis and VEGF signaling pathway (Table 6.1). Pathways related to cell biological behaviours assumed absolute superiority, which included autophagy and cell adhesion (Table 6.2). Genes with reversed transcriptional trend in the phenotype with miR-140-5p suppression or not are summarized in Figure 6.1. Given our *in vitro* cell model only showed the loss of miR-140-5p in gastric cancer progression, we focused on the genes specifically activated during miR-140-5p suppression in the analysis. The genes positively regulated in miR-140-5p suppression phenotype included *RTC*, which E6 contributing to the immortalization epithelial cells (Sherman et al. 2002), cell cycle regulator gene *CTNN3* (Mizamtsidi et al. 2018), *Cab39* regulating responses to metabolic stress and promoting survival, in part by activating AMP-activated protein kinase (AMPK) and mTOR pathway(Shackelford and Shaw 2009), cell adhesion-related BVES-AS1 (Xing et al. 2018) and ILK promoting cell survival in a p53-dependent manner (Hausmann et al. 2015). *KIF13B* involved in aberrant cytokinesis (Wu et

al. 2013). The enhanced cell survival associating pathway was the most representative feature in this phenotype.

Table 6.1: The top 20 signalling pathway in gastric cancer associated with miR-140-5p upregulation in GSEA by KEGG.
ES denotes enrichment score, which reflects the degree to which a gene set is overrepresented at the top or bottom of a ranked list of genes. A positive ES indicates gene set enrichment at the top of the ranked list. NES denotes the normalized enrichment score. By normalizing the enrichment score, GSEA accounts for differences in gene set size and in correlations between gene sets and the expression dataset; therefore, the normalized enrichment scores (NES) can be used to compare analysis results across gene sets.

Pathway Name	Size	ES	NES	P
Primary immunodeficiency	35	0.62	1.60	0.07
Glycosaminoglycan biosynthesis chondroitin sulfate	22	0.58	1.56	0.07
Vegf signaling pathway	74	0.33	1.46	0.02
Intestinal immune network for IgA production	43	0.56	1.45	0.16
Ribosome	82	0.64	1.44	0.18
Homologous recombination	28	0.51	1.43	0.14
Complement and coagulation cascades	67	0.40	1.42	0.10
PPAR signaling pathway	69	0.35	1.38	0.07
Phenylalanine metabolism	17	0.44	1.36	0.11
B cell receptor signaling pathway	74	0.38	1.33	0.17
T cell receptor signaling pathway	107	0.35	1.29	0.18
FC epsilon ri signaling pathway	78	0.30	1.26	0.16
Alanine aspartate and glutamate metabolism	32	0.36	1.25	0.18
Spliceosome	122	0.43	1.23	0.30
Fc gamma r mediated phagocytosis	91	0.30	1.17	0.26
Leukocyte transendothelial migration	116	0.28	1.16	0.25
Chemokine signaling pathway	184	0.28	1.12	0.30
DNA replication	36	0.44	1.11	0.41
Cell adhesion molecules cams	128	0.31	1.11	0.34

Table 6.2: The top 20 signalling pathway in gastric cancer associated with miR-140-5p suppression in GESA by KEGG.

Pathway Name	Size	ES	NES	P
Arrhythmogenic right ventricular cardiomyopathy	74	-0.51	-1.70	0.02
Regulation of autophagy	33	-0.43	-1.54	0.03
Hypertrophic cardiomyopathy hcm	83	-0.46	-1.52	0.04
Adherens junction	73	-0.40	-1.51	0.03
Long term depression	68	-0.37	-1.42	0.06
Dilated cardiomyopathy	90	-0.43	-1.39	0.11
Nicotinate and nicotinamide metabolism	21	-0.43	-1.37	0.09
Riboflavin metabolism	16	-0.47	-1.37	0.12
Pantothenate and coa biosynthesis	16	-0.47	-1.35	0.14
Oocyte meiosis	109	-0.34	-1.35	0.12
Vascular smooth muscle contraction	114	-0.38	-1.32	0.18
Vasopressin regulated water reabsorption	44	-0.37	-1.31	0.15
Long term potentiation	69	-0.35	-1.30	0.13
Phosphatidylinositol signalling system	76	-0.36	-1.30	0.15
Erbb signalling pathway	87	-0.33	-1.27	0.16
MAPK signalling pathway	263	-0.28	-1.26	0.11
Focal adhesion	199	-0.33	-1.25	0.21
Fatty acid metabolism	42	-0.42	-1.25	0.21
Linoleic acid metabolism	26	-0.42	-1.22	0.21

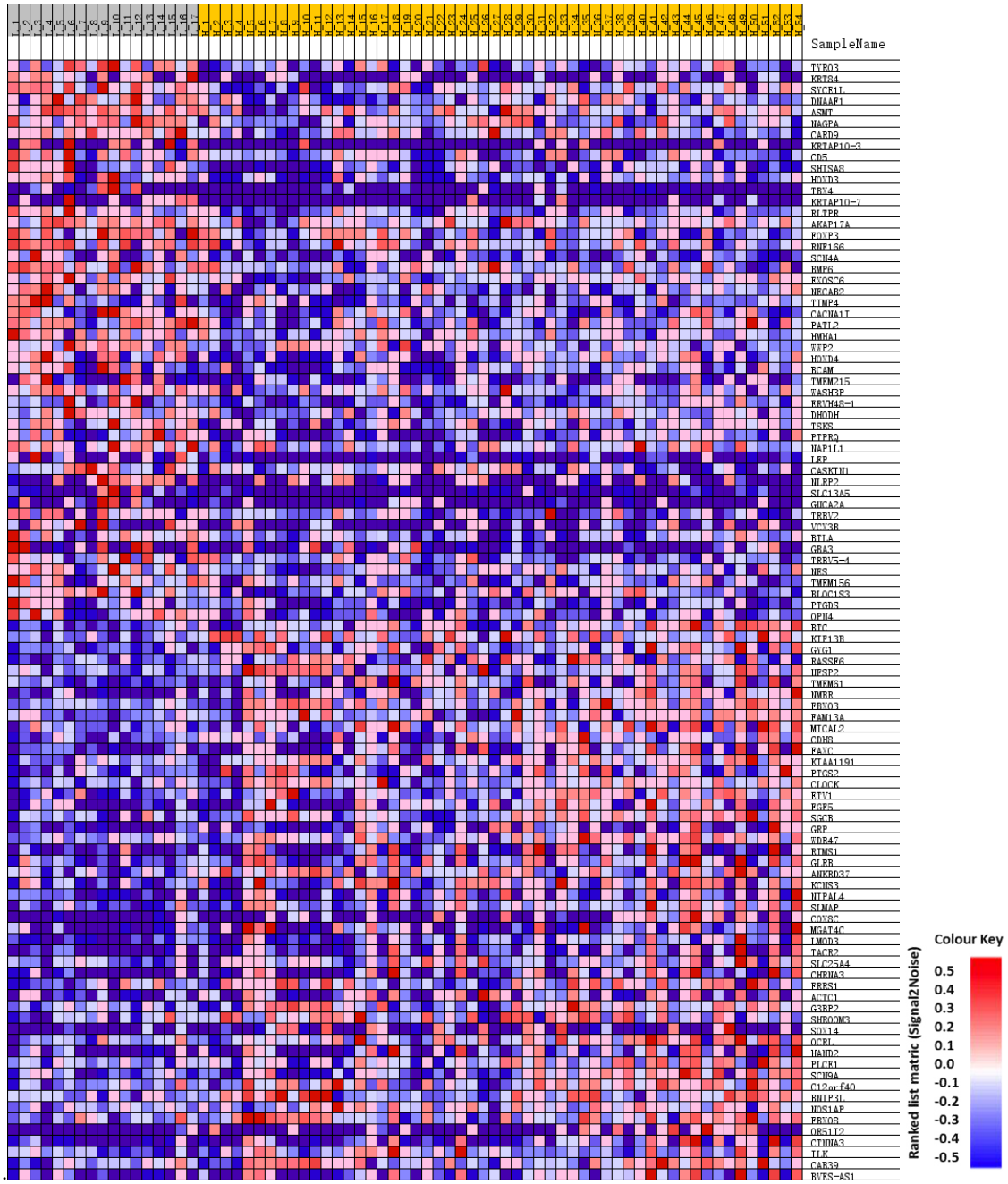

Figure 6.1: Heat Map of the top 50 features for miR-140-5p accumulating or decreasing phenotypes. Red represents positive correlation and blue represents negative correlation. The top row labelled samples enrolled in the analysis. Yellow=those patients' tumours harbouring higher miR-140-5p, Grey=those patients with lower miR-140-5p. The far-right column listed the genes that were positively correlated with higher miR-140-5p expression or lower miR-140-5p expression, respectively.

6.3.2 Target prediction for miR-140-5p

Identifying target mRNAs of miRNAs is an important step in elucidating the function of miRNAs, yet this step has proven computationally difficult due to the complexity of the miRNA–target interactions. Several target prediction programs have been developed, but the overlap between sets of predicted target genes for a given miRNA by different programs is unsatisifacted. Nevertheless, these target prediction programs are very useful to define potential targets that can be validated experimentally. Rather than switching off their targets completely, miRNAs fine-tune their expression thus playing an important role in tumour formation, development, differentiation, metabolism, and disease progression. miRNAs are incorporated into the RNA-induced silencing complex (RISC) and guide this complex to specific mRNAs that contain miRNA target sites, which can fall into three categories. 5'-Dominant canonical target sites show perfect complementarity to the seed sequence of the miRNA (nucleotides 2–8) and extensive base pairing to the rest of the miRNA. 5'-dominant seed only target sites are also perfectly complementary to the seed sequence but have a limited base pairing with the rest of the miRNA. 3'-compensatory target sites do not have a perfect match to the seed sequence but are compensated by extensive base pairing with the 3'-half of the miRNA. Target sites are usually in the 3'-UTR of mRNAs but there are examples of target sites in other regions as well, and their flanking regions can also influence interaction with miRNAs. Translation of mRNAs targeted by miRNAs is repressed and the steady-state level of some but not all mRNA targets is also reduced.

The online prediction with different algorithms generated a list of more than 6000 potential targets of miR-140-5p in total, among which 3593 were predicted by at least two algorithms. However, the commonest predicted targets revealed by all the tools were only 13 (Appendix 11). And we further merged the online predicted genes with the altered transcriptomic and proteomic data from a lung cancer cell line (A549) following the transfection of negative, miR-140-5p and miR-140-3p miRNA mimics (Flamini et al. 2017).

The putative target genes were classified according to the Gene Ontology (GO) categories (Figure. 6.2). Most of the targets were shown related to regulation of growth, cell cycle, cell apoptosis and development. Given the results of our previous cell function assays and GSEA analysis, MDM2, which was predicted by online prediction tools and suggested as a potential target of miR-140-5p in the literature (Nicolas et al. 2008) was further chosen as the object

for further validation.

MDM2 was originally identified as one of three *mdm* genes whose expression is increased more than 50-fold in the spontaneously transformed mouse BALB/c cell line and was later proven to be the reason for the transformation (Fakharzadeh et al. 1991). Via binding to the tumour suppressor p53, MDM2 inhibits p53 transactivation function by engaging its amino-terminal transactivation domain via related N-terminal hydrophobic pockets (Momand et al. 1992; Laurie et al. 2006; Kussie et al. 1996). The wild type p53 is involved in the sensing of cell stress and DNA damage, resulting in regulation of the cell cycle and apoptosis. An interaction between the central acidic domain of MDM2 and the specific DNA-binding domain of p53 is essential for p53 ubiquitination via the RING domain of MDM2 and leads to proteasomal degradation of p53; this keeps p53 levels and activity low in unstressed cells. Mice which do not possess the *mdm2* gene die before embryonic implantation due to inappropriate apoptosis, with a total phenotypic rescue being possible through simultaneous deletion of the *p53* gene. Moreover, mice which express just 30% of the normal levels of MDM2 exhibited decreased body weight and defects in haematopoiesis. These *in vivo* experiments have provided compelling evidence towards the importance of the MDM2/p53 interaction. Of note, this interaction could be disrupted by multiple transcriptional modification. Besides, MDM2 has also been shown to affect translation of p53, by interacting directly with the mRNA encoding p53 itself and by targeting RPL26, which, upon DNA damage, can associate with p53 mRNA and increased its protein expression (Manfredi 2010). The E3 ubiquitin ligase activity of MDM2 depends on an intact carboxy-terminal the really interesting new gene (RING) finger domain. The p53-interaction domain is situated at the amino terminus, which in turn binds to the amino transactivation domain of p53. Although many short MDM2 proteins encoding just the carboxyl terminus of MDM2, without the p53-binding domain, have been identified, in many cases, the frequency of MDM2 deregulation is higher in tumours that retain wild-type p53 (Wade et al. 2013). The p53 protein transcriptionally activates many genes, including the *mdm2* gene. Therefore, p53 is regulated at protein level by MDM2, but once active, p53 activates the transcription of the *mdm2* gene, locking the proteins into a tight negative feedback loop and resulting in oscillation of the cellular levels of the two proteins. Thus, MDM2 and p53 levels plays a crucial role in regulating cell proliferation and apoptosis, loss of MDM2 leads to an active p53 which may determine the vital status of the cell or embryo. Intriguingly, single-nucleotide

polymorphism (SNP) in the MDM2 promoter increased MDM2 expression and altered the oscillation relationship. Similarly, point mutations in the two p53-binding sites of the Mdm2 promoter that were introduced into the endogenous Mdm2 locus resulted in increased response to DNA damage, although p53 degradation kinetics in various tissues remained similar to the wild-type control. This highlights the importance of understanding the distinct roles of MDM2 in different tissues (Karni-Schmidt et al. 2016). Apart from its involvement in p53-dependent activities, MDM2 has p53-independent activities, including induction of stemness by supporting polycomb repressor functions and K48-linked ubiquitination of the Notch antagonist Numb (Todoric et al. 2017). A study of human sarcomas and bladder cancers found tumours which overexpressed MDM2 and mutant *p53* and the patients possessing both of these abnormalities had a poorer prognosis than those with just one (Onel and Cordon-Cardo 2004; Cordon-Cardo et al. 1994). Given its role as a negative regulator of p53, as well as its overexpression in human tumours, the notion of Mdm2 as an oncogene is quite reasonable. Nevertheless, as reviewed by Manfredi (2010), there is a growing body of evidence to suggest that Mdm2 may also exert effects as a tumour suppressor in certain experimental conditions. In gastric cancer, *MDM2* promoter polymorphism is associated with both an increased susceptibility to gastric carcinoma and poor prognosis (Ohmiya et al. 2006). Amplified *MDM2* gene is associated with chromosomal instability (Lee et al. 2014).

The previous chapter has shown that miR-140-5p restoration resulted in inhibition of in vitro cell cycle progress and proliferation of gastric cancer cells. Together with the role of MDM2-p53 interaction in the regulation of cell cycle and apoptosis, we hypothesised that one of the mechanisms by which miR-140-5p influence the growth rate of gastric cancer cells is via the suppression of MDM2 and activation of p53.

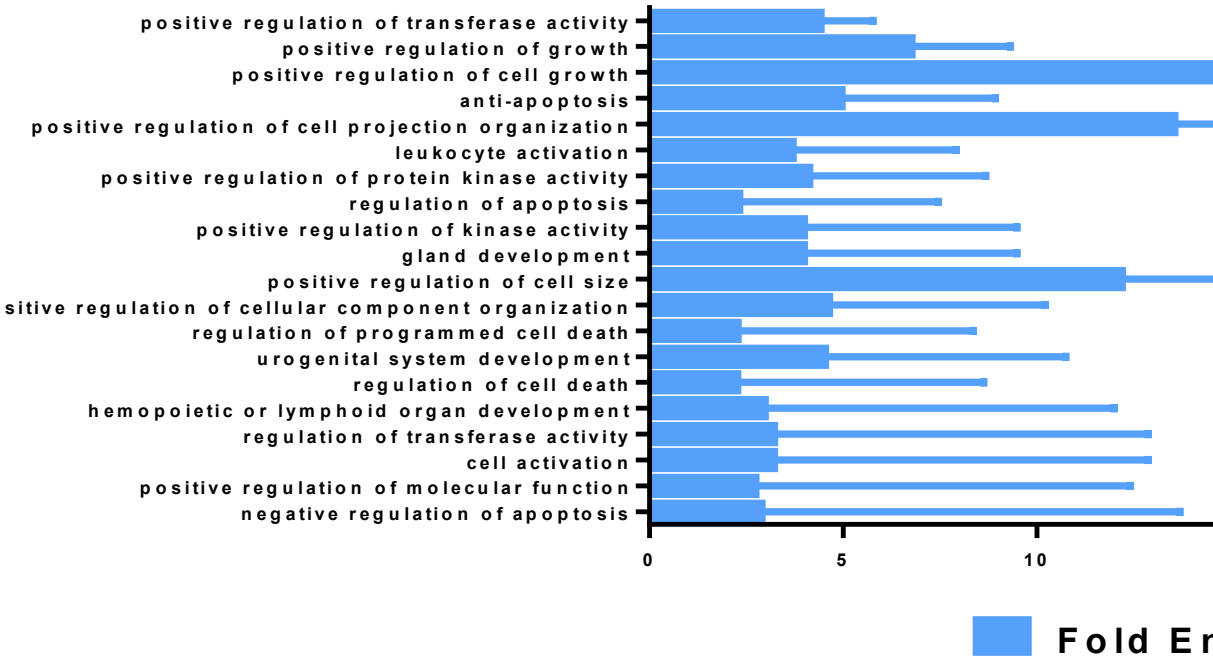

Figure 6.2: The Gene Ontology (GO) category analysis of merged predicted targets of miR-140-5p from Protein array data. The relative expression was adopted from the RNA seq results by Nicolas (Nicolas et al. 2011).

6.3.3 Possible link between miR-140-5p and *MDM2* in gastric cancer tumour tissues

The possible correlation between miR-140-5p and *MDM2* was first evaluated in gastric cancer patients' transcriptome data from TGCA using the Spearman correlation test. A significant negative correlation was seen between miR-140-5p and *MDM2* (Figure 6.3).

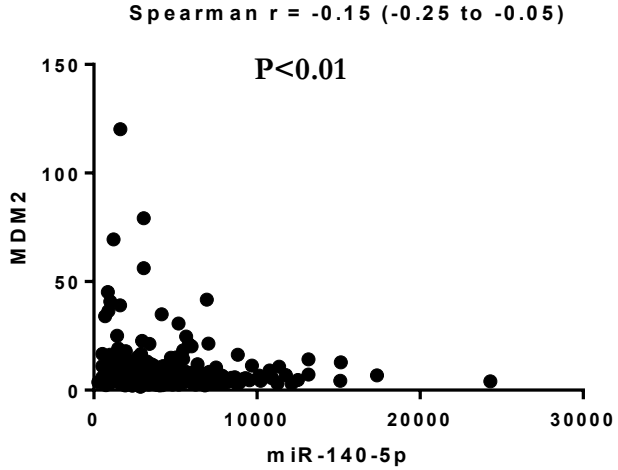

Figure 6.3: Correlation between miR-140-5p and MDM2 in gastric cancer (TCGA).

To validate this discovery, a similar correlation analysis was performed in the gastric cancer patients' cohort from Beijing Cancer Hospital. The negative correlations between miR-140-5p and *MDM2*, and between miR-140-3p and *MDM2* was also observed but did not reach statistical significance. Interestingly, miR-140-5p and miR-140-3p showed significant co-expression pattern in our analysis (Table 6.3).

Table 6.3: Correlation between miR-140-5p/3p and MDM2 in gastric cancer (Beijing cohort). Note: Cor = Correlation coefficient. N= Number of samples

	mir-140-3p	**MDM2**
miR-140-5p	Cor=0.54 P<0.00 N=75	Cor=-0.11 P=0.34 N=76
miR-140-3p		Cor=-0.14 P=0.22 N=81

6.3.4 miR-140-5p and miR-140-3p overexpression and p53 signaling

The negative correlation between miR-140-5p and *MDM2* was observed in tumour tissue analysis in both cohorts of gastric cancer. We then used qPCR and Western blots to address whether the correlation is associated with deregulation of downstream genes and signaling pathways.

The expression of *MDM2*, its direct target *p53* and the downstream effector *p21* were firstly determined by qPCR in gastric cancer cell lines under normal conditions. The results showed increased *p21* expression at the transcriptional level. There was no significant difference at the mRNA level in the expression of *MDM2* or p53 in miR-140-5p overexpressed cells compared with corresponding negative control. (Figure 6.4).

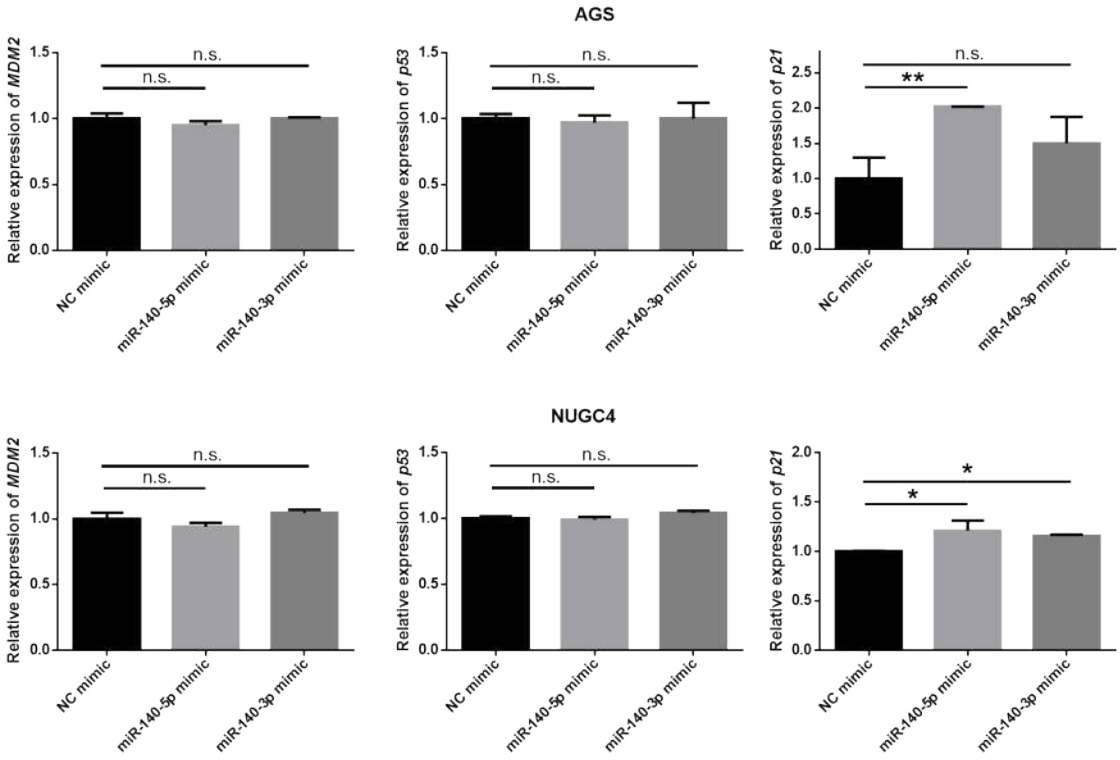

Figure 6.4: One-way ANOVA comparations of relative expression of MDM2, p53, and p21 in miR-140-5p and miR-140-3p overexpression gastric cancer cell lines. Shown are representative results n=3. Error bars represent standard deviation. ** represent $p<0.01$, respectively.

To detect whether miR-140-5p affects the expression of MDM2 at the protein level, we examined the expression of MDM2 and its object of action using Western blot. A decreased MDM2 expression was seen in miR-140-5p or -3p overexpressing cells compared to

corresponding transient transcription of the negative control. Conversely, the increased protein level of p53 was seen in all examined gastric cancer cell lines following miR-140-5p or -3p expression. In the examination of p21 expression, increased p21 was only seen in AGS and NUGC4 cell lines which harbored wild-type p53, suggesting that miR-140-5p or miR-140-3p may have a role in MDM2/p53/p21 signaling (Figure 6.5).

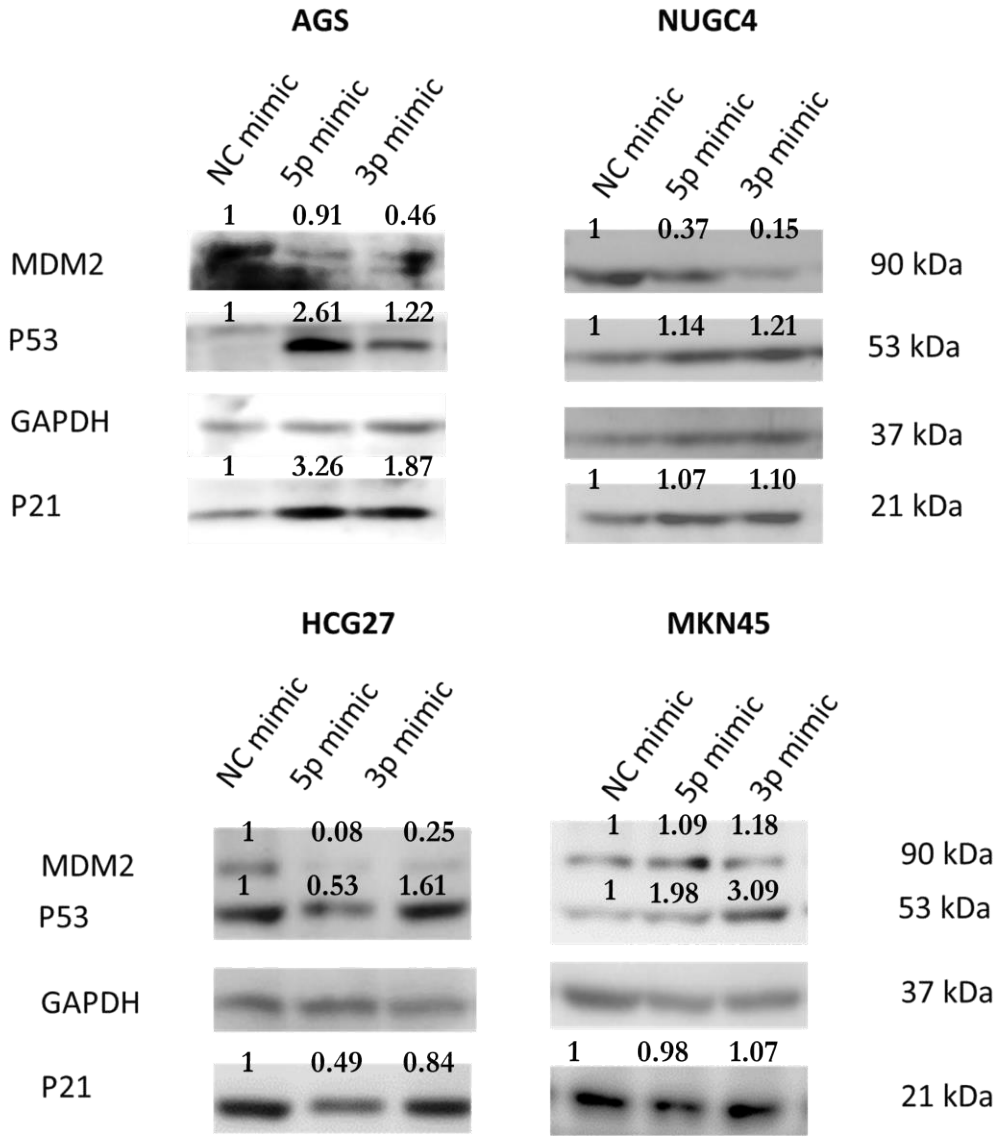

Figure 6.5: The expression of MDM2, p53, and p21 in the miR-140-5p and miR-140-3p overexpression gastric cancer cell lines. Quantification of immunoblots was performed using the ImageJ software, after densitometric analysis of the corresponding bands detected upon revelation with a peroxidase-coupled secondary antibody.

MDM2, as a chief negative regulator of p53 (Bond et al. 2005), restrains p53 activity by firstly binding and cutting off p53 from p53 target gene promoters (Momand et al. 1992). It contains a RING domain with E3 ubiquitin ligase activity which can ubiquitinate p53, resulting in p53 degradation through a negative feedback loop (Chen et al. 1995). Thus, MDM2 can induce a rapid tumour growth by inhibiting p53 signaling pathways, which is in agreement with our cell proliferation assay. However, the cytotoxic assay in our study suggested an augmented cell resistance to 5FU treatment in gastric cancer cell lines with wild-type p53. To clarify the role of p53 in drug-induced apoptosis, we explored the apoptosis-related genes' expression in NUGC4 and AGS cell lines. Western blots showed a relative mildly reduced MDM2 in the miR-140-5p overexpressing cells after treating with 5FU. Induced p53 was observed in all the cell lines with 5FU treatment, but comparison in different transfection groups did not differ. However, the proapoptotic factor BAX showed a slightly decrease in AGS miR-140-5p overexpressing cells and a significantly decline in NUGC4 miR-140-5p overexpression cells. (Figure 6.6).

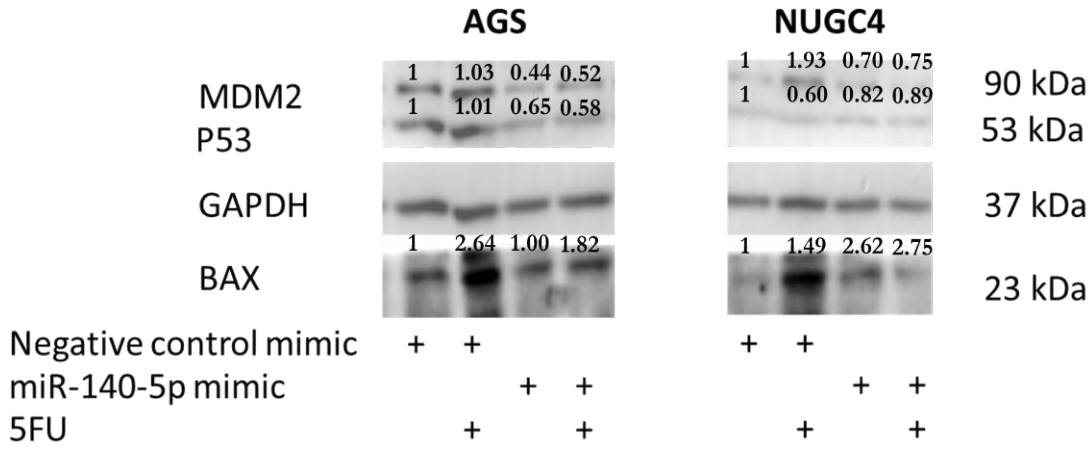

Figure 6.6: Abated activation of MDM2/p53/BAX signaling in miR-140-5p overexpression cells was determined using Western blot.

The inconsistency shown from the tissue sample analysis, where miR-140-5p upregulation indicated a chemosensitive promoting role in NACT gastric cancer cohort, provoked further analysis to compare the miR-140-5p expression status in negative control transfected cells and in miR-140-5p mimic transfected cells after 5FU stimulating. The qPCR result demonstrated that a high-level miR-140-5p showed a relatively slower and lesser upregulation of miR-140-5p compared to the upregulated level of miR-140-5p in negative control transfected cells, pre- and post-treated with 5FU (Figure 6.7).

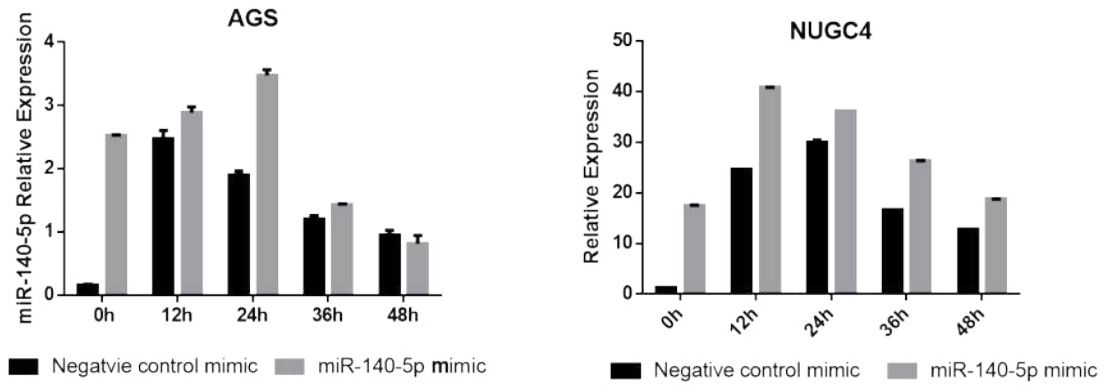

Figure 6.7: 5FU induced miR-140-5p upregulation in cells with higher miR-140-5p before treatment. Results are triplicated analysis from two independent experiments.

6.4 Discussion

Generally, malignant cells acquire the ability to undergo de-regulated mitogenesis, to resist proapoptotic insults, and to invade through tissue boundaries during progression. Several aberrant cellular signalling pathways orchestrate these malignant traits in any particular type of cancer tissues (Giancotti 2014). MDM2, as well as its homolog MDMX, is best understood as a negative regulator of the p53 tumour suppressor to exert oncogenic activity, although it has additional p53-independent roles (Karni-Schmidt et al. 2016). The p53 protein consists of two N-terminal transactivation domains followed by a conserved proline-rich domain, a central DNA binding domain, and a C terminus encoding its nuclear localization signals and an oligomerization domain needed for the transcriptional activity. In normal and unstressed cells, p53 protein is maintained at low levels by a series of regulators including MDM2 (Kubbutat et al. 1997; Haupt et al. 1997). However, p53 is stabilized in response to various cellular stresses. For instance, DNA damage promotes p53 phosphorylation, blocking MDM2-mediated degradation (Shieh et al. 1997). Largely through its function as a sequence-specific transcriptional factor, p53 regulates a plethora of genes whose products mediate a variety of cellular pathways. The best-understood functions of p53 focus on its ability to promote cell cycle arrest and apoptosis. Indeed, from the early 1990s, seminal studies showed that p53 is crucial for a reversible G1 phase checkpoint, which is mediated, in part, by its ability to transcriptionally activate the *p21* cyclin-dependent kinase inhibitor gene. p53 can also promote apoptosis, relying on the induction of pro-apoptotic BCL-2 family members whose action facilitates caspase activation and cell death. An ever-growing body of work suggests that p53 also controls additional "non-canonical" programs

that contribute to its effects. As examples, p53 can modulate autophagy, alter metabolism, repress pluripotency and cellular plasticity, and facilitate an iron-dependent form of cell death known as ferroptosis. The p53 response is remarkably flexible and depends on the cell type, its differentiation state, stress conditions, and collaborating environmental signals. Approximately 30% of gastric cancers have been found to have *p53* mutation or deletion. MDM2 expression is positively regulated by p53 transactivation by a feedback loop. Amplified MDM2 has been reported in more than 10% of gastric cancers.

Our initial analysis via GESA and online prediction tool to determine the cellular signaling pathways that are altered in gastric cancer according to miR-140-5p status found an enrichment of cell cycle pathway related transcriptome alteration, which was in line with the omics-based findings in a previous study of miR-140-5p in lung cancer. Especially, *MDM2* was suggested as a potential target of miR-140-5p.

In this study, we aimed to investigate changes in MDM2 and its downstream signalling in gastric cancer cell lines with miR-140-5p overexpression. The co-expression analysis in the TCGA cohort and the Beijing cohort of samples revealed a negative correlation between miR-140-5p expression and *MDM2* in both cohorts. It was initially indicated that downregulation of miR-140-5p might contribute to disease progression of gastric cancer via increasing MDM2 expression. We then showed that forced miR-140-5p expression by transient transfection of mimic did not influence MDM2 expression at the transcriptional level in gastric cancer cells, but we saw a significant reduction of MDM2 at translational levels. Due to the possible limitation in recapitulating the actions of endogenous miRNAs via transfection of miRNA mimic (Jin et al. 2015), whether miR-140-5p directly suppresses MDM2 expression is yet to be elucidated. Meanwhile, p53 was upregulated, as was the p21, but only in cells with an intact p53 function. This suggested that miR-140-5p was involved in the transcriptional regulation of MDM2 via a direct or indirect way. Additionally, such a regulation may lead to different cell response, at least partly depending on p53 status. For example, miR-140-5p overexpression leading to a slight but significant cell cycle arrest in both AGS and NUGC4 cell lines which harbour wild-type p53. Although both AGS and NUGC4 are p53 functional cell lines, there is some difference in the cell functions and protein alterations between these two cell lines after miR-140-5p transfection. This may be explained by the fact that most miRNAs exert mild repression on many targets and act as rheostats, fine-tuning the expression of hundreds of genes to reinforce cell fate decisions

brought about through other mechanisms (Vidigal and Ventura 2015); Secondly, there is an emerging paradigm that miRNA can be not only cell-type or tissue-specific "signatures" for certain normal or cancerous tissues, but also functional or inoperative to certain genes depending on the molecular and cellular context (Zhang et al. 2015). For example, AGS is a TGF-β/Smad/cMyc activated cell line other than NUGC4 cell line (Periasamy et al. 2014) and TGF-β receptor I and SMAD3 were experimentally validated as miR-140-5p's direct targets (Pais et al. 2010; Zhang et al. 2015). Interestingly, accumulation of miR-140 could also be transiently suppressed by TGF-β (Pais et al. 2010; Tardif et al. 2013).

We then focused on whether regulation of miR-140-5p on MDM2 still conserved during cells' response to 5FU, a cell-cycle-dependent cytotoxic drug. We found that 5FU treatment resulted in lower MDM2 expression and upregulated p53. However, miR-140-5p upregulated cells did not induce as much p53 accumulation as paired control cells without miR-140-5p overexpression before drug treatment. Moreover, a decreased BAX was shown in cells with upregulated miR-140-5p. Although current analysis supported *MDM2* as a possible target of miR-140-5p, this requires further work to determine the direct target site(s) and confirmed with an intervention such as a dual-luciferase reporter gene system. A rescue analysis could be considered in a miR-140-5p stably transfected cell model which could provide more evidence about the interaction between miR-140-5p and MDM2 and its downstream effectors. The correlation between miR-140-5p/3p expression and protein expression and activation of MDM2/P53 in human gastric cancer tissues collecting before and after drug treatment should be further examined using immunochemical or other techniques. Morover qPCR analysis suggested that miR-140-5p did not increase after 5FU treatment in an already higher miR-140-5p cell type. However, this was only implied in an *in vitro* cell model with a transient transfection. Further evaluation in a stable transfection situation and *in vivo* mice model should be investigated to evaluate this reaction following treatment with 5FU. In addition, ectopic expression in the current study addressed the question of whether miR-140-5p can exert a specific function on cell cycle-related genes, while loss-of-function studies are still required to test whether it is also necessary for these functions.

During cytotoxic-induced cellular stress, p53-mediated processes can be antagonistic: cancer cell growth in G1 phase may lead to an impairment of 5FU which exerts its anticancer effects through inhibition of thymidylate synthase (TS) and incorporation of its

metabolites into RNA and DNA mainly in S (synthesis) phase (Focaccetti et al. 2015). Additionally p53 could also modulate autophagy which has the potential to delay apoptosis (Thorburn et al. 2014), However, it was reported that in situations where p53 failed to repress glycolysis, apoptosis would be favoured (Duan et al. 2015). Thus, the molecular interaction between distinct biochemical processes controlled by p53, as well as its translocation sites (Park et al. 2016; S. Wang et al. 2017) might be explored to elicit different biological outcomes.

Taken together, our study provided evidence that miR-140-5p regulated the cell cycle through an MDM2/p53 regulatory feedback loop, which may contribute to the promotion of cell proliferation and anti-apoptosis, although further investigations remain necessary.

Chapter 7.

General Discussion

Extensive evidence has suggested that miRNAs are crucial regulators of gastric carcinogenesis and progression via alteration of cell growth, cell cycles, apoptosis, and cell migration. Several groups have analyzed the global miRNA content in gastric cancer with the use of varying amounts of tumour samples, diverse reference samples as well as various types of large-scale methods. Current progress in understanding the role of specific miRNAs recognized as deregulated in gastric cancer cells has been reviewed (Pan et al. 2013; Liang et al. 2017; Hao et al. 2017). The comprehensive multi-platform genomics data generated by TCGA provides a large-scale miRNA profiling of gastric cancer for both tumour and adjacent normal samples, and is the largest of its type worldwide (Chu et al. 2016). As shown in the TCGA analysis, integrative miRNA expression analyses could be useful for the identification of subclasses and subtype-specific drivers of expression changes of gastric cancer (Cancer Genome Atlas Research 2014; Liu et al. 2018).

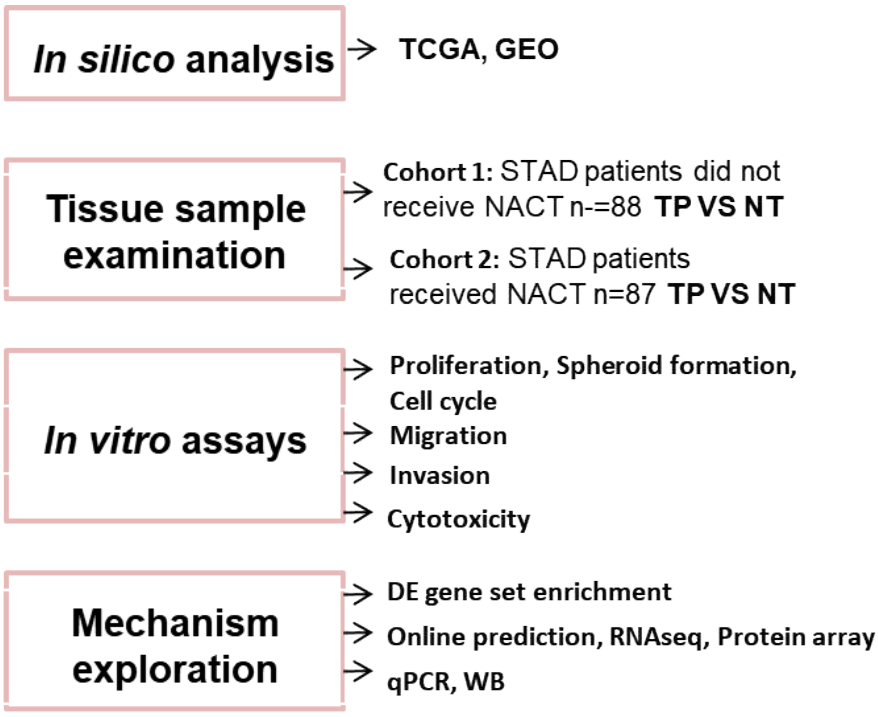

Figure 7.1: The techniques used in this study

In this study (Figure 7.1 Technical Route), we investigated the genome-wide miRNA expression pattern in gastric cancer from TCGA database. Three analytical approaches (linear model fitting, unpaired and paired t-test) were performed for analysis of differentially expressed miRNAs in gastric cancer tissues and adjacent to tumour stomach samples. Moreover, we conducted both the generalized linear model and the linear model in order to discover potential gastric cancer biomarkers, not only to distinguish gastric cancer tissues from normal stomach, but also to provide therapeutic or prognostic biomarkers. We identified 16 potentially novel prognostic miRNA biomarkers of gastric cancer, out of which ten were negatively correlated, and six were positively correlated with OS of gastric cancer patients. Although their expression and role in gastric cancer need further experimental investigation, computational analysis indicated that these miRNAs seemed to be potential prognostic biomarkers for gastric cancer. miR-140 in particular, seemed to be interesting in terms of its downregulation in tumour tissues compared to normal samples, but higher expression in advanced gastric cancer tissues, reflecting its multiple identities in gastric cancer progression. Very few studies have taken into account the different histological subtypes of gastric cancer, miR-140-5p although generally accepted as a tumour suppressor in many cancers, including non-small cell lung cancer (Wang et al. 2017; Tang et al. 2017; Flamini et al. 2017; Zhang et al. 2016; Dong et al. 2016; Tan et al. 2011; Hu et al. 2016; Yuan et al. 2013), primary breast cancer (Yan et al. 2008; Kawaguchi et al. 2017; Yan et al. 2018; Q. Li et al. 2014a; Wolfson et al. 2014; Gullu et al. 2015; Gernapudi et al. 2015), colorectal cancer (Song et al. 2009; Zhai et al. 2015; J. Li et al. 2018; L. Yu et al. 2016; Piepoli et al. 2012) gastric cancer (Fang et al. 2017), oesophageal cancer (Li et al. 2014), epithelial ovarian cancer (Su et al. 2016; Lan et al. 2015; Iorio et al. 2007), basal cell carcinoma of the skin (Sand et al. 2012b), cutaneous squamous cell carcinoma (Sand et al. 2012a), hepatocellular carcinoma (Yang et al. 2013) osteosarcoma (Song et al. 2009; Xiao et al. 2017; Wei et al. 2016; Gu et al. 2016), gliomas (Malzkorn et al. 2010; Zhao et al. 2016), glioblastoma (Bo et al. 2015), and T-cell acute lymphoblastic leukaemia (Correia et al. 2016). By targeting various targets, miR-140-5p has shown to critically involved in tumour cell proliferation, apoptosis, vascularization, migration, and invasion. These previously confirmed targets include *HDAC4*, *Sp1*, *IGF1R*, *MMD*, *TGFBR1*, *Smad2*, *Smad3*, *FGF9*, *BMP2*, *SOX2*, *SOX9*, *Slug*, and *ADAMTS5* (Summarized in Table 7.1).

However, miR-140-5p has also been implicated as having a possible oncogenic role in splenic

hemangiosarcoma (Grimes et al. 2016), chordomas (Bayrak et al. 2013), clear cell renal cell carcinoma (Guan et al. 2018), and Hodgkin lymphoma (Khare et al. 2017). Moreover, its upregulation was correlated with malignant progression of gliomas (Malzkorn et al. 2010), disease recurrence in lung cancer (Shersher et al. 2011), and to chemoresistance in breast cancer (Ahn et al. 2010; Chen et al. 2016). A miRNA profiling study on salivary gland tumours showed that miR-140-5p was downregulated in tumour subtypes with low malignant potential but showed an upregulation trend in histological subtypes with high malignant potential (Bostjancic et al. 2017).

miR-140-5p/3p is encoded within intron 16 of *Wnp2*, an E3 ubiquitin ligase on chromosome 16q22.1 (Inui et al. 2018). Extensive studies have demonstrated its role in mediating embryonic development and regeneration, especially in cartilage development (Miyaki et al. 2010; Araldi and Schipani 2010; Papaioannou et al. 2015; Mahboudi et al. 2018; Plociennikowska et al. 2015), such as by targeting *CXCL12* (Thorpe et al. 2010), *IGF-I*(Pando et al. 2014), *TLR-4* (Sun et al. 2017), and *FGF9* (Yin et al. 2015). MiR-140-deficient mice manifested a mild skeletal phenotype, with short stature and low body weight, as well as craniofacial deformities characterized by a short snout and domed skull, supporting the notion that miR-140 is a tissue-specific miRNA significant in chondrocyte development and maintenance and ECM synthesis (Miyaki et al. 2010; Araldi and Schipani 2010; Papaioannou et al. 2015; Papaioannou et al. 2013). miR-140-5p also play an important role in various inflammatory diseases, such as osteoarthritis (Iliopoulos et al. 2008; Gabay and Clouse 2016), asthma (Guedes et al. 2015), pulmonary arterial hypertension (Rothman et al. 2016) and chronic inflammation induced oxidative stress injury such as coronary artery disease (Marques et al. 2016) and type 2 diabetes (Ortega et al. 2014). *In vivo* studies of miR-140-deficient mice showed age-related osteoarthritis-like changes characterized by proteoglycan loss and fibrillation of articular cartilage, and by 12 months, miR-140-deficient mice showed severe structural cartilage defects, while transgenic mice with overexpressed miR-140 in cartilage were resistant to antigen-induced arthritis, which indicates suppression of miR-140 expression and plays an important role in diseases associated with cartilage destruction (Miyaki et al. 2010). Targets of miR-140-5p, *HDAC4*, *BMP2*, *SMAD3*, *IGFBP5,* and *Adamts-5,* were all responsible for enhanced cartilage destruction (Tardif et al. 2013; Clemmons et al. 2002). In this present study, the role played by miR-140-5p/3p in gastric cancer was examined.

7.1 Deregulated miRNAs in gastric cancer

With the latest released TCGA data, we utilized distinct analysing algorithms (DESeq2, glm and lm) compared to existing research (Shrestha et al. 2014; Ding et al. 2017) and identified a new group of DEMs and prognostic related DEMs in primary gastric cancer. In all 207 differentially expressed miRNAs were determined in this study, among which 65 miRNAs were downregulated and 142 miRNAs were upregulated.

Almost simultaneously, Ding et al. (2017) explored dysregulated miRNAs in gastric cancer by using the raw counts of miRNA expression data of 41 paired tumour and normal tissues cancer from TCGA. miRNA expression was normalized by the R/Bioconductor package edgeRv. Their results discovered 138 differentially expressed miRNAs ($\log FC > 1$ or $\log FC < -1$, $P < 0.05$ after FDR adjustment). We compared results and found 100 miRNAs which are consistently deregulated in both analyses (Appendix 8). There is no optimal pipeline for the variety of different applications and analysis scenarios in which RNA-seq can be used. Independent comparison studies have demonstrated that the choice of method (or even the version of a software package) can markedly affect the outcome of the analysis and that no single method is likely to perform favourably for all datasets. Repetition of important analyses using more than one package should be considered to improve the reliability of differential gene expression analysis (Conesa et al. 2016).

According to the system review by Shrestha *et al.* (2014) a total of 352 differentially expressed microRNAs were reported in 14 miRNA expression profiling studies which compared gastric cancer tissues with normal tissues. 120 microRNAs were reported in at least in two studies, which is similar to the comparative analysis between Ding *et al.*'s (2017) work and ours. Among the 120 differentially expressed miRNAs, 69 miRNAs had a consistent direction of expression, in which 41 were reported to be upregulated and 28 down-regulated. The review indicated that in the group of consistently reported miRNAs from 14 various publications, miR-21 was reported upregulated in 10 studies followed by miR-25, miR-92, and miR-223 upregulated in eight studies. miR-375 and miR-148a were found downregulated in six and five studies, respectively, followed by miR-638 in four studies. Of note, miR-107 and miR-103 were reported in nine and eight studies, respectively, but their expression was inconsistent (Shrestha et al. 2014). We further overlapped this vote ranking results with our analysis and Ding *et al.'s*, and 18 and 17 consistently deregulated miRNAs were found

respectively (Appendix 8). 12 miRNAs were reported in all three analyses (Table 3.3). Among these, downregulation of miRNA-100 and upregulation of miR-188 were demonstrated on TCGA data, however, they represented a contrary tendency in the review analysis. The unsatisfactory agreement between results obtained from different tools might be due to different parameter settings, especially for genes that are expressed at low levels. As RNA-seq has become the standard method for transcriptome analysis, but the technology and tools are continuing to evolve. The heterogeneity of tumour characteristics between tumours is equally deserving of attention.

Lymph node metastasis (LNM) is one of the most important risk factors of gastric cancer recurrence after curative surgery. The 5-year survival rates of pathological N stages were as follows: N0 (83.5%), N1 (57.8%), N2 (27.4%), and N3 (11.4%). As a result, pathological N stage is one of the independent prognostic factors of gastric cancer (Fang et al. 2011). Moreover, the occurrence of lymph node metastases after endoscopic submucosal dissection (ESD) in patients with gastric cancer leads to a poor prognosis. Using logistic regression, Liu *et al.* identified miR-100 and other 3 miRNAs (miR-27b, miR-128, and miR-214) which were associated with LNM in GC patients. Expression of miR-27b, miR-128, miR-100, and miR-214 were down-regulated in GC samples with LNM (Liu et al. 2017). Similarly, miRNA microarray analyses were performed for 5 patients with LNM and 5 patients without LNM and found that miR-188-5p as well as miR-451, miR-497, miR-1207-5p, miR-30a-5p, let-7e, let-7g, let-7f, miR-96, and let-7a significantly dysregulated between patients with or without LNM. However, further confirmation demonstrated that, with the exception of miR-1207-5p, there was no significant correlation between lymph node metastasis and the expression of other miRNAs (Huang et al. 2015).

In Yepes *et al.*'s (2016) study aimed to characterize miRNA expression profiles and identify key miRNAs related to gastric carcinogenesis and histopathological traits, using co-expression networks and supervised analysis, miR-100 together with miR-195, let-7c, miR-140, miR-99a, and miR-125b, was determined to be highly correlated with the diffuse subtype. Despite the evident morphological differences that allow classification of tissues into intestinal and diffuse subtypes, the expression patterns that differentiate these subtypes are subtle. This may become much clearer when the correlations between genes and progression characteristics, such as TNM staging are analyzed.

Another aspect of this study on DEMs of TCGA gastric cancer subgroups (Appendix 9) also as well demonstrated such variability. A large proportion of DEMs distributed across four subtypes of gastric cancer (EBV, MSI, GS, and CIN). Some of them exhibited distinct expression in specific subgroups. For example, EBV subgroup exhibited suppressed miR-193a-5p downregulation and upregulated miR-181a-2-3p, miR-134-5p, miR-199b-5p miR-199a-5p/3p and miR-217. Decreased miR-143-5p, miR-125b-5p, miR-26a-5p, miR-140-3p, miR-30d-5p and increased miR-135b-5p were only characterized in the CIN subgroup. The GS subgroup featured a lack of miR-582-3p, miR-10a-5p, but gain of let7f-5p, miR-361-3p, let-7d-3p, miR-15b-3p, and miR-155-5p expressions. In the MSI group, non-downregulated miRNA but unique upregulation of miR-16-5p, miR-29b-3p, miR-24-3p, miR-484, miR-128-3p, let-7i-5p, miR-223-3p and miR-200b-5p were detected.

With regard to prognosis related miRNAs, except for miR-21, we discovered 15 more miRNAs related to gastric cancer patients' outcome based on current analysis methods. Among 6 downregulated miRNAs, miR-5683 has been reported to be implicated in maintaining the differentiated state of muscle cells (Doerrenberg et al. 2017) and was also pinpointed to be one of down-regulated miRNAs in TCGA based gastric cancer analysis by Huo (Doerrenberg et al. 2017). Down-regulated miR-28 in gastric cancer samples compared with normal stomach tissue samples was also found by Kim *et al.* (Kim et al. 2011). A former study defined that miR-28-5p and miR-28-3p had distinct effects on colorectal cancer cells (Almeida et al. 2012). However, their roles in gastric cancer were not yet demonstrated. miR-193a (Lujambio et al. 2007; Ando et al. 2009), and miR-129 are reported in methylation associated gastric cancer, their low expression was associated with poor clinicopathological features (Tsai et al. 2011), miR 34b was also distinguished as a methylation-associated miRNA (Tsai et al. 2011), but in our study, it was upregulated and had a negative relationship with gastric cancer outcomes. Upregulated miR-328 is widely underexpressed in many cancers and contributes to tumour resistance to chemotherapy (Li et al. 2010). Macrophage-derived reactive oxygen species play a role in suppressing miR-328 targeting CD44 in cancer cells and promote redox adaptation (Ishimoto et al. 2014). High miR-140-5p levels have been detected in the plasma of gastric cancer patients (Shin et al. 2015), whereas low miR-140-5p level was found in cancerous tissues compared with that in adjacent gastric mucosa tissues (Zou and Xu 2016). Lower expression of miRNA-140-5p is associated with decreased chemosensitivity, but no significant change was found between tumour and non-tumour

tissue samples (Kim et al. 2011). A recent study also demonstrated that downregulated miR-140-5p in gastric cancer was significantly correlated with reduced OS of these patients (Fang et al. 2017).

Amongst the ten upregulated miRNAs, increased hsa-miR-671-5p in gastric cancer tissues was found in a microarray-based analysis (Zhang et al. 2015), and miR 671 5p played as an onco-miR in epithelioid sarcoma (Papp et al. 2014). However, decreased expression of miR-671-5p was reported in invasive ductal carcinoma (IDC) compared to normal in microdissected formalin-fixed, paraffin-embedded (FFPE) tissues (Tan et al. 2016). Hansen *et al.* (2013) also reported that miR-671-directed cleavage of ciRS-7 results in prompt and efficient repression of miR-7 targets and acted as a tumour suppressor in such cases. High levels of miR-455-3p in gastric cancer tissues compared to their matching references has been confirmed by qPCR (Su et al. 2012). Nonetheless, miR-455-5p was found to act as a tumour suppressor in gastric cancer by down-regulating RAB18 (Liu et al. 2016). The role of miR-1255a seems to be double-sided. It presented contrary expression trends in different bladder cancer cell lines (Tatarano et al. 2011), and it was downregulated by Atorvastatin in PC3 prostate cancer cells (Peng et al. 2013). As for miR-493, although Zhou *et al.* found that expression levels of miR-493 were strongly down-regulated in gastric cancer, and its downregulation was associated with clinical stage and the presence of LNM (Zhou et al. 2015). Tambe *et al.* (2016) demonstrated that high miR-493-3p levels were associated with reduced survival of ovarian and breast cancer patients with aggressive tumours, especially in the paclitaxel therapy arm. Upregulation of miR-4326 was also reported in Li *et al.*'s (2017) study, and they further demonstrated miR-4326 might be associated with race, with a lower level of miR-4326 more common in Asian patients. In metastatic renal cell carcinoma, upregulated miR–4326, was among a group of miRNAs that could define patients not only associated with short PFS and OS, but also with a poor response to tyrosine kinase inhibitors (TKI) (Garcia-Donas et al. 2016). miR-514a was found to be an EMT-inducing miRNA in gastric cancer (Yanaka et al. 2015). Upregulated miR-514a targeted the tumour suppressor NF1 and modulated BRAFi sensitivity in melanoma (Stark et al. 2015). Conversely, miR-514a-3p served as a tumour suppressor which could inhibit cell proliferation and EMT was demonstrated in clear cell renal carcinoma (Ke et al. 2017) and human testicular germ cell tumours (Ozata et al. 2017). Upregulation of miR-549 was associated with colorectal carcinogenesis (Hamfjord et al. 2012) and oral cancer developed from oral leucoplakia (Zhu

et al. 2015) and may indicate tumours of glial origin if discovered in patients' serum (Drusco et al. 2018).

In the integrative analysis of prognostic related DEMs, it is inappropriate to interpret the variation of a continuous variable in the same way as the variation of a binary variable. Different modelling assumptions need to be taken into consideration. We applied the framework introduced by Mo *et al.* (2013). Categorical observations are modelled as multivariate binomial or multinomial random variables. Count data are modelled as multivariate Poisson variables, and continuous measures such as miRNAs' expression are modelled as multivariate normal. Given the proper distributional assumptions for these diverse types of bioinformatic variables, glm for a non-linear relationship for the distribution of these variables and lm for the linear relationship were performed to identify those DEMs representing distinct roles in gastric cancer patients' survival. Like previous studies, increased levels of miR-21 in both blood and tumour tissues indicate a significantly worse prognosis in OS, as well as DFS, than those with decreased expression levels (Xu et al. 2012; Komatsu et al. 2013).

Bioinformatic analysis of DEMs, potential and validated targets of miRNA and the subsequent analysis of activation of downstream pathways clustered by target genes are promising strategies for gaining insights into plausible biomarkers and key events involved in cancer development and progression. However, both biological factors and analytical factors could affect the actual performance of the DEMs analysis. In this study, we did not set exclusion criteria so some tissues samples without completed data and cases of other malignancies were enrolled. Therefore, it is essential to interrogate these candidate genes subsequently with other pathological features and validate them systematically by PCR or other independent experimental approaches before utilizing them as useful clinical biomarkers.

7.2 Deregulated miR-140-5p expression in gastric cancer is associated with disease progression in gastric cancer

To determine the role of miR-140-5p in gastric cancer, the expression of miR-140-5p was conducted by detailed analysis from TCGA. The result showed a significantly reduced expression of miR-140-5p in gastric cancers compared with adjacent non-tumour tissues,

especially in intestinal gastric cancer. This result was in line with the observations from a qPCR examination conducted on paired gastric tumour tissue samples from the Beijing cohort which presented a reduced expression of miR-140-5p in gastric cancers, particularly the less infiltrative gross type (Borrmann I-II) of tumour samples with a predominantly intestinal histological type (Chen et al. 2016). A decreased miR-140-5p expression was also observed in relatively localized tumour (Borrmann I-II) compared with that in more infiltrative tumour samples (Borrmann III-IV). Univariate and multivariate analysis have suggested that miR-140-5p could serve as a prognostic biomarker in gastric cancer. Decreased miR-140-5p and miR-140-3p expression in tumour tissues may be linked to a shorter life expectancy for gastric cancer patients even those with earlier disease and/or lower malignant potential subtypes.

In our further analysis of the role of miR-140-5p/3p in the cohort of gastric cancer tissue samples having been treated with 5FU based NAC, it was demonstrated that reduced expression of miR-140-5p/3p in treated tumour tissues compared with that in treated normal tissues was associated with drug resistance of gastric cancer. Further analyses showed that even in the no response group, gastric cancer patients with a higher level of miR-140-5p in treated tumour samples could still have a relatively better OS. The findings of this study have demonstrated that miR-140-5p/3p may act as tumour suppressor in intestinal gastric cancer in comparison with diffuse type. This again highlights that miR-140-5p/3p plays different roles in different malignancies which might be cancer specific and even cell specific. Despite data indicating that miR-140-5p/3p can, in principle, control a wide variety of biological processes, the physiological settings in which one or more processes predominate are incompletely understood and deserve more systematic study. The exact molecular and cellular events associated with the deregulated expression of miR-140-5p/3p in gastric cancer are yet to be identified.

7.3 Overexpression of miR-140-5p/3p inhibited malignant traits of gastric cancer cells based on specific cell context

To understand how altered expression of miR-140-5p/3p in gastric cancer is associated with tumourigenesis, disease progression and prognosis, its impact on cellular function of gastric cancer cells was examined in this study. Expression of miR-140-5p and -3p was determined in six gastric cancer cell lines, as described in section 5.2.1. In the intestinal group of cancer

cell lines, decreased expression of miR-140-5p/3p was noted, which was in agreement with the findings we had on cohort analysis. Overexpression of miR-140-5p or 3p in four cell lines (AGS, NUGC4, MKN45 and HGC27) resulted in decreased proliferation and colony formation only in cell lines harbouring wild-type p53: AGS and NUGC4. Cell cycle analysis revealed an increased G1 phase but decreased S phase in AGS, NUGC4 and human colorectal cancer cell lines with wild type p53 (HCT116 p53 wt), which suggests a G1/S cell cycle arrest. Interestingly MKN45 with a missense mutation in *p53* gene but was demonstrated to have a functional p53 (Chen et al. 2016) also showed cell cycle arrest at the G1/S as well. These observations were consistent with the results from a study on human osteosarcoma and colon cancer cells (

Song et al. 2009).

Besides its inhibition role on cell growth, overexpression of miR-140-5p/3p had a prohibiting impact on cell migration in AGS and NUGC4. However, an interesting finding was seen in HGC27 cell lines, which reflected an oncomiR role of miR-140-5p in this specific cell type. Notably, significantly restrained invasive ability was observed in all the examined cell lines, considering the inconsistent role of miR-140-5p on cell motility, this may indicate a profound part of miR-140-5p in curbing ECM degradation ability in gastric cancer cells. It is interesting, but may not be surprising, that miR-140 is regarded as a cartilage-specific miRNA. Knockout studies have revealed miR-140 to be an essential factor in osteoarthritis development, as miR-140-/- mice showed osteoarthritis-like changes such as accelerated proteoglycan loss and ECM degradation, while mice overexpressing miR-140 were protected against degradation of proteoglycans and COL2 in a model of antigen-induced arthritis (Miyaki et al. 2010). In the same study, the aggrecanase ADAMTS5 was shown to be a target of miR-140, and it was suggested that this could explain the protective role of miR-140 in ECM degradation.

7.4 Effective chemotherapy response is accompanied by enhanced expression of miR-140-5p and -3p in gastric cancer

In the tissue analysis, elevated expression of miR-140-5p or miR-140-3p was detected in tumours with complete or partial response to 5FU based NAC treatment compared to their corresponding normal stomach tissues. The augmented expression of miR-140-5p or miR-

140-3p was associated with favourable prognosis even in the non-responsive patients. However, in the gastric cancer cell models, a pre-overexpressed miR-140-5p induced significant chemoresistance in NUGC4 and MKN45 cells, and an increased IC50 was shown in AGS cells but did not reach a statistical significance. In the mechanism exploring analysis, we found that a pre-upregulated miR-140-5p before drug treatment did not result in enough p53 upregulation comparing to the control cells, which may partly explain the abatement in cell apoptosis. Our results indicated a quantity dependent p53 induced apoptosis during cytotoxic stress in gastric cancer cells. Further *in vitro* and *in vivo* apoptosis assay, as well as corresponding mechanism examination, are required to elucidate this particular aspect, which may provide a new potential strategy for the stratification of patients who can benefit from specific drug treatment and also candidate targets to increase chemosensitivity.

7.5 Reduced miR-140-5p/3p is associated with enhanced MDM2 signalling through upregulation of its protein expression

P53 is the most frequently mutated gene in human cancer (Kastenhuber and Lowe 2017). Half of the gastric cancer patients were reported to show *p53* somatic mutations. MDM2 functions as an oncogene mainly due to its major negative regulator role of p53. Studies have repeated the central importance of MDM2 as a p53 regulator, demonstrating that very early embryonic lethality of Mdm2-null mice was fully rescued in a p53-null background (Fakharzadeh et al. 1991; Montes de Oca Luna et al. 1995; Jones et al. 1995). A recent study investigating the role of MARCH7, a RING domain-containing ubiquitin E3 ligase, in interacting and maintaining the stability of MDM2, also strengthened the concept that direct or indirect MDM2 destabilization could enhance p53 accumulation and p21 induction in normal cells and in DNA-damage treated cells (Zhao et al. 2018). In addition, MDM2 is involved in a number of pathways that regulate cell proliferation and apoptosis, playing a p53-independent role. MDM2. In a study of Cao *et al.* (2019), MDM2 was proven to promote genome instability by ubiquitinating the transcription factor HBP1. Overexpression-induced cell death following ionizing radiation could be abolished by overexpression of HBP1, which delays DNA break repair and causes cell death in a p53-independent manner. However, MDM2 has also been shown to regulate the expression of the anti-apoptotic protein XIAP by binding to its mRNA that enhances XIAP translation, leading to the increased expression of XIAP, which led to an MDM2-dependent prevention of cell death via caspase-mediated

apoptosis (Gu et al. 2009).

By using n gastric cancer cell lines, we showed that overexpression of miR-140-5p decreased protein but not mRNA levels of MDM2. Corresponding changes of p53 and downstream p21, if a functional p53 existed, were also seen in the miR-140-5p overexpression cell lines. Upon being treated with 5FU, the miR-140-5p overexpressing cells presented a less enhanced activation of p53, and lacked BAX, compared with cells transfected with negative control mimics. Intriguingly, we also observed an increased apoptosis in HGC27 cell line with nonsense mutation of p53, suggesting a MDM2-mediated apoptosis in a p53-independent manner. Involvement of MDM2/p53 in the miR-140-5p and -3p overexpressing cells resulted in cell cycle arrest and suppression of proliferation. Metastatic potential is yet to be elucidated, for example via eliminating p53 by siRNA or CRISPR/Cas9 system. On the other hand, targets of miR-140-5p participating migration should be investigated in a p53 dependent manner as well.

7.6 Conclusion and perspectives

In this study, reduced expression of miR-140-5p was observed in gastric cancer tissues and was associated with advanced disease progression, those with distant metastases and poor prognosis, especially in intestinal histological gastric cancer. *In vitro* function assays through miR-140-5p and miR-140-3p overexpression demonstrated the inhibitory roles of miR-140-5p and -3p in proliferation, migration and invasion of gastric cancer cells with wild-type p53. However, its overexpression may cause an increased migration ability in HGC27 cells with mutant p53. Although this association between mutant p53 and aggressive phenotype needs further clarification, this suggests that miR-140-5p/3p exhibited a putative tumour suppressor in some cases of gastric cancer. Elevated chemoresistance was also observed in the miR-140-5p overexpressing gastric cancer cell lines with wild-type p53 and following 5FU treatment. Accordingly, miR-140-5p depletion by miR-140-5p inhibitor promoted chemosensitivity. Further examination showed that pre upregulated miR-140-5p resulted in a less effective activation in accelerating p53 and BAX expression. This study again highlighted that miR-140-5p and -3p may have multiple cell identities based on cellular context or specific molecular subgroups.

Questions raised by this study include;

1. Through what mechanism is miR-140 expression controlled in different types of gastric cancer?

2. What is the functional significance of miR-140 in gastric cancer *in vivo*? Does miR-140 alter cancer cells phenotype? Does miR-140 play a role in communication between gastric cancer cells and cells in their surrounding microenvironment, such as stromal cells or immune cells?

3. If gastric cancer cells express miR-140 to protect against apoptosis, can this be reversed by other drugs that are not cycle-dependent?

4. What is the association between different mutant *p53* type and aggressive phenotype of gastric cancer?

It is yet to be revealed if miR-140 or p53 alone are sufficient to influence cell fate in response to chemotherapy. We have shown that miR-140-5p provides a mechanism through MDM2 which p53 can be manipulated; however, there are many other factors which influence p53 expression and function and need to be explored. We have identified constitutional MDM2 decreasing along with miR-140-5p upregulation in gastric cancer cells, the direct interacting target site, or interacting approach and where this modulation occurs are yet unexplored.

Like many other potentially exciting therapies in cancer, the efficiency of therapy between individuals differs for unexplained reasons and declines over time. The relevance of miRNA functional heterogeneity and variants of its effector protein may help to understanding differences in disease patterns between otherwise identical patients and even provide potential therapeutic strategy or targets.

References

ABELSON, J. F. et al. 2005. Sequence variants in SLITRK1 are associated with Tourette's syndrome. *Science,* 310, 317-20.

ABNET, C. C. et al. 2015. Diet and upper gastrointestinal malignancies. *Gastroenterology,* 148, 1234-1243 e4.

ADJEI, A. A. 1999. A review of the pharmacology and clinical activity of new chemotherapy agents for the treatment of colorectal cancer. *Br J Clin Pharmacol,* 48, 265-77.

AHMED, K. A. and XIANG, J. 2011. Mechanisms of cellular communication through intercellular protein transfer. *J Cell Mol Med,* 15, 1458-73.

AHN, B. Y. et al. 2010. Genetic screen identifies insulin-like growth factor binding protein 5 as a modulator of tamoxifen resistance in breast cancer. *Cancer Res,* 70, 3013-9.

AHN, S. et al. 2017. High-throughput Protein and mRNA Expression-based Classification of Gastric Cancers Can Identify Clinically Distinct Subtypes, Concordant With Recent Molecular Classifications. *Am J Surg Pathol,* 41, 106-115.

AIRD, I. et al. 1953. A relationship between cancer of stomach and the ABO blood groups. *Br Med J,* 1, 799-801.

AL-BATRAN, S. E. et al. 2008. Phase III trial in metastatic gastroesophageal adenocarcinoma with fluorouracil, leucovorin plus either oxaliplatin or cisplatin: a study of the Arbeitsgemeinschaft Internistische Onkologie. *J Clin Oncol,* 26, 1435-42.

AL-BATRAN, S. E. et al. 2016. Histopathological regression after neoadjuvant docetaxel, oxaliplatin, fluorouracil, and leucovorin versus epirubicin, cisplatin, and fluorouracil or capecitabine in patients with resectable gastric or gastro-oesophageal junction adenocarcinoma (FLOT4-AIO): results from the phase 2 part of a multicentre, open-label, randomised phase 2/3 trial. *Lancet Oncol,* 17, 1697-1708.

ALISON, M. R. et al. 2012. Cancer stem cells: in the line of fire. *Cancer Treat Rev,* 38, 589-98.

ALMEIDA, M. I. et al. 2012. Strand-specific miR-28-5p and miR-28-3p have distinct effects in colorectal cancer cells. *Gastroenterology,* 142, 886-896 e9.

ALTINI, C. et al. 2015. 18F-FDG PET/CT role in staging of gastric carcinomas: comparison with conventional contrast enhancement computed tomography. *Medicine (Baltimore),* 94, e864.

AMBROS, V. 2003. MicroRNA pathways in flies and worms: growth, death, fat, stress, and timing. *Cell,* 113, 673-6.

AMBROS, V. et al. 2003. A uniform system for microRNA annotation. *RNA,* 9, 277-9.

AMIEVA, M. and PEEK, R. M., JR. 2016. Pathobiology of Helicobacter pylori-Induced Gastric Cancer. *Gastroenterology,* 150, 64-78.

AMIRI, M. et al. 2011. The decline in stomach cancer mortality: exploration of future trends in seven European countries. *Eur J Epidemiol,* 26, 23-8.

ANDERSON, W. F. et al.. 2010. Age-specific trends in incidence of noncardia gastric cancer in US adults. *JAMA,* 303, 1723-8.

ANDO, T. et al. 2009. DNA methylation of microRNA genes in gastric mucosae of gastric cancer patients: its possible involvement in the formation of epigenetic field defect. *Int J Cancer,* 124, 2367-74.

ANG, T. L. and FOCK, K. M. 2014. Clinical epidemiology of gastric cancer. *Singapore Med J,* 55, 621-8.

ARALDI, E. and SCHIPANI, E. 2010. MicroRNA-140 and the silencing of osteoarthritis. *Genes Dev,* 24, 1075-80.

ARAVIN, A. A. et al. 2003. The small RNA profile during Drosophila melanogaster development. *Dev Cell,* 5, 337-50.

ASCHENBRENNER, L. et al. 2004. Uncoated endocytic vesicles require the unconventional myosin, Myo6, for rapid transport through actin barriers. *Mol Biol Cell,* 15, 2253-63.

BADER, A. G. 2012. miR-34 - a microRNA replacement therapy is headed to the clinic. *Front Genet,* 3, 120.

BANG, Y. J. et al. 2010. Trastuzumab in combination with chemotherapy versus chemotherapy alone for treatment of HER2-positive advanced gastric or gastro-oesophageal junction cancer (ToGA): a phase 3, open-label, randomised controlled trial. *Lancet,* 376, 687-97.

BARTEL, D. P. 2009. MicroRNAs: target recognition and regulatory functions. *Cell,* 136, 215-33.

BARTER, M. J. et al. 2015. Genome-Wide MicroRNA and Gene Analysis of Mesenchymal Stem Cell Chondrogenesis Identifies an Essential Role and Multiple Targets for miR-140-5p. *Stem Cells,* 33, 3266-80.

BAYRAK, O. F. et al. 2013. MicroRNA expression profiling reveals the potential function of microRNA-31 in chordomas. *J Neurooncol,* 115, 143-51.

BEG, M. S. et al. 2017. Phase I study of MRX34, a liposomal miR-34a mimic, administered twice weekly in patients with advanced solid tumours. *Invest New Drugs,* 35, 180-188.

BEIER, U. H. and GOROGH, T. 2005. Implications of galactocerebrosidase and galactosylcerebroside metabolism in cancer cells. *Int J Cancer,* 115, 6-10.

BENCUROVA, P. et al. 2017. MicroRNA and mesial temporal lobe epilepsy with hippocampal sclerosis: Whole miRNome profiling of human hippocampus. *Epilepsia,* 58, 1782-1793.

BENJAMINI, Y., HOCHBERG, Y. 1995. Controlling the false discovery rate: a practical and powerful approach to multiple testing. Journal of the Royal Statistical Society, Series B. 57 (1): 289–300.

BERINDAN-NEAGOE, I. et al. A. 2014. MicroRNAome genome: a treasure for cancer diagnosis and therapy. *CA Cancer J Clin,* 64, 311-36.

BERLTH, F. et al. 2014. Pathohistological classification systems in gastric cancer: diagnostic relevance and prognostic value. *World J Gastroenterol,* 20, 5679-84.

BERNAL, M. et al. 2012. Implication of the beta2-microglobulin gene in the generation of tumour escape phenotypes. *Cancer Immunol Immunother,* 61, 1359-71.

BERTUCCIO, P. et al. 2009. Recent patterns in gastric cancer: a global overview. *Int J Cancer,* 125, 666-73.

BHATTACHARYYA, A. et al. 2014. Oxidative stress: an essential factor in the pathogenesis of gastrointestinal mucosal diseases. *Physiol Rev,* 94, 329-54.

BIASCO, G. et al. 1993. Serum pepsinogen I and II concentrations and IgG antibody to Helicobacter pylori in dyspeptic patients. *J Clin Pathol,* 46, 826-8.

BITTONI, A. et al. 2015. Three drugs vs two drugs first-line chemotherapy regimen in advanced gastric cancer patients: a retrospective analysis. *Springerplus,* 4, 743.

BO, L. J. et al. 2015. Bioinformatics analysis of miRNA expression profile between primary and recurrent glioblastoma. *Eur Rev Med Pharmacol Sci,* 19, 3579-86.

BOBRIE, A. et al. 2011. Exosome secretion: molecular mechanisms and roles in immune responses. *Traffic,* 12, 1659-68.

BOKU, N. et al. 2009. Fluorouracil versus combination of irinotecan plus cisplatin versus S-1 in metastatic gastric cancer: a randomised phase 3 study. *Lancet Oncol,* 10, 1063-9.

BOLAND, C. R. and YURGELUN, M. B. 2017. Historical Perspective on Familial Gastric Cancer. *Cell Mol Gastroenterol Hepatol,* 3, 192-200.

BOLKE, E. et al. 2008. Capecitabine and oxaliplatin for advanced esophagogastric cancer. *N Engl J Med,* 358, 1965; author reply 1965.

BOND, G. L. et al. 2005. MDM2 is a central node in the p53 pathway: 12 years and counting. *Curr Cancer Drug Targets,* 5, 3-8.

BORCH, K.,et al. 2000. Changing pattern of histological type, location, stage and outcome of surgical treatment of gastric carcinoma. *Br J Surg,* 87, 618-26.

BORRMANN, R. 1926 Geschwülste des Magens and Duodenums. In: Borchardt, H., Borrmann, R. and Christeller, E., Eds., Verdauungsschlauch: Erster Teil Rachenund Tonsillen, Speiserohre Magen und Darm, Bauchfell, Springer, Vienna, 812-1054.

BOSTJANCIC, E. et al. 2017. Expression, Mutation, and Amplification Status of EGFR and Its Correlation with Five miRNAs in Salivary Gland Tumours. *Biomed Res Int,* 2017, 9150402.

BRADY, C. A. et al. 2011. Distinct p53 transcriptional programs dictate acute DNA-damage responses and tumour suppression. *Cell,* 145, 571-83.

BRADY, J. J. et al. 2013. Early role for IL-6 signalling during generation of induced pluripotent stem cells revealed by heterokaryon RNA-Seq. *Nat Cell Biol,* 15, 1244-52.

BRYANT, J. L.,et al. 2012. A microRNA gene expression signature predicts response to erlotinib in epithelial cancer cell lines and targets EMT. *Br J Cancer,* 106, 148-56.

BUTZ, H. et al. 2011. MicroRNA profile indicates downregulation of the TGFbeta pathway in sporadic non-functioning pituitary adenomas. *Pituitary,* 14, 112-24.

CALDAS, C. et al. 1999. Familial gastric cancer: overview and guidelines for management. *J Med Genet,* 36, 873-80.

CALIN, G. A. et al. 2007. Ultraconserved regions encoding ncRNAs are altered in human leukemias and carcinomas. *Cancer Cell,* 12, 215-29.

CAMARGO, M. C. et al. 2011. Divergent trends for gastric cancer incidence by anatomical subsite in US adults. *Gut,* 60, 1644-9.

CAMILLERI, M. et al. 2017. Gastrointestinal Complications of Obesity. *Gastroenterology,* 152, 1656-1670.

CANCER GENOME ATLAS RESEARCH, N. 2014. Comprehensive molecular characterization of gastric adenocarcinoma. *Nature,* 513, 202-9.

CANCER REARCH. 2016a. Stomach cancer mortality statistics. Available at: https://www.cancerresearchuk.org/health-professional/cancer-statistics/statistics-by-cancer-type/stomach-cancer/mortality [Accessed: 4 March 2018].

CANCER RESEARCH. 2016b. Survival by stage. Avilable at: http://about-cancer.cancerresearchuk.org/about-cancer/stomach-cancer/survival [Accessed 20 June 2019]

CAO, D. et al. 2002. Uridine phosphorylase (-/-) murine embryonic stem cells clarify the key role of this enzyme in the regulation of the pyrimidine salvage pathway and in the activation of fluoropyrimidines. *Cancer Res,* 62, 2313-7.

Cao Z. et al. 2019. MDM2 promotes genome instability by ubiquitinating the transcription factor HBP1. *Oncogene*. 38, 4835-4855

CARNEIRO, F. et al. 1994. T (Thomsen-Friedenreich) antigen and other simple mucin-type carbohydrate antigens in precursor lesions of gastric carcinoma. *Histopathology,* 24, 105-13.

CARNEIRO, F. et al. 1995. New elements for an updated classification of the carcinomas of the stomach. *Pathol Res Pract,* 191, 571-84.

CARNINCI, P. et al. 2005. The transcriptional landscape of the mammalian genome. *Science,* 309, 1559-63.

CARVALHO, J. et al. 2012. Lack of microRNA-101 causes E-cadherin functional deregulation through EZH2 up-regulation in intestinal gastric cancer. *J Pathol,* 228, 31-44.

Cha Y. et al. 2018. MicroRNA-140-5p suppresses cell proliferation and invasion in gastric cancer by targeting WNT1 in the WNT/beta-catenin signaling pathway. *Oncology letters*. 16, 6369-6376.

CHAN, J. A. et al. S. 2005. MicroRNA-21 is an antiapoptotic factor in human glioblastoma cells. *Cancer Res,* 65, 6029-33.

CHAN, J. J. and TAY, Y. 2018. Noncoding RNA:RNA Regulatory Networks in Cancer. *Int J Mol Sci,* 19.

CHANG, H. et al. 2015. Different microRNA expression levels in gastric cancer depending on Helicobacter pylori infection. *Gut Liver,* 9, 188-96.

CHANG, J. T. et al. 2016. Identification of MicroRNAs as Breast Cancer Prognosis Markers through the Cancer Genome Atlas. *PLoS One,* 11, e0168284.

CHEN, J. et al. 1995. Regulation of transcription functions of the p53 tumour suppressor by the mdm-2 oncogene. *Mol Med,* 1, 142-52.

CHEN, M. H. et al. 2016. A Phase II Study of Sequential Capecitabine Plus Oxaliplatin Followed by Docetaxel Plus Capecitabine in Patients With Unresectable Gastric Adenocarcinoma: The TCOG 3211 Clinical Trial. *Medicine (Baltimore),* 95, e2565.

CHEN, X. et al. 2016. The role of miRNAs in drug resistance and prognosis of breast cancer formalin-fixed paraffin-embedded tissues. *Gene,* 595, 221-226.

CHEN, Y. et al. 2018. Survival benefit of neoadjuvant chemotherapy for resectable breast cancer: A meta-analysis. *Medicine (Baltimore),* 97, e10634.

CHEN, Y. C. et al. 2016. Clinicopathological Variation of Lauren Classification in Gastric Cancer. *Pathol Oncol Res,* 22, 197-202.

CHEUNG, D. Y. 2017. Atrophic Gastritis Increases the Risk of Gastric Cancer in Asymptomatic Population in Korea. *Gut Liver,* 11, 575-576.

CHEUNG, K. S. et al. 2018. Long-term proton pump inhibitors and risk of gastric cancer development after treatment for Helicobacter pylori: a population-based study. *Gut,* 67, 28-35.

CHIARAVALLI, A. M. et al. 2012. Histotype-based prognostic classification of gastric cancer. *World J Gastroenterol,* 18, 896-904.

CHIHARA, K.,et al. 2009. Increased vulnerability of hippocampal pyramidal neurons to the toxicity of kainic acid in OASIS-deficient mice. *J Neurochem,* 110, 956-65.

CHOI, Y. J. et al. 2018. Correction: The relationship between drinking alcohol and esophageal, gastric or colorectal cancer: A nationwide population-based cohort study of South Korea. *PLoS One,* 13, e0197765.

CHOWDHURY, U. R. et al. 2009. Emerging role of nuclear protein 1 (NUPR1) in cancer biology. *Cancer Metastasis Rev,* 28, 225-32.

CHU, A. et al. 2016. Large-scale profiling of microRNAs for The Cancer Genome Atlas. *Nucleic Acids Res,* 44, e3.

CHU, E. et al. 1993. Regulation of thymidylate synthase in human colon cancer cells treated with 5-fluorouracil and interferon-gamma. *Mol Pharmacol,* 43, 527-33.

CLEMMONS, D. R. et al. 2002. Inhibition of insulin-like growth factor binding protein 5 proteolysis in articular cartilage and joint fluid results in enhanced concentrations of insulin-like growth factor 1 and is associated with improved osteoarthritis. *Arthritis Rheum,* 46, 694-703.

COATI, I. et al. 2015. Autoimmune gastritis: Pathologist's viewpoint. *World J Gastroenterol,* 21, 12179-89.

COBURN, N. et al. 2018. Staging and surgical approaches in gastric cancer: A systematic review. *Cancer Treat Rev,* 63, 104-115.

COCCOLINI, F. et al. 2014. Intraperitoneal chemotherapy in advanced gastric cancer. Meta-analysis of randomized trials. *Eur J Surg Oncol,* 40, 12-26.

COKKINIDES, V. E. et al. 2012. Cancer-related risk factors and preventive measures in US Hispanics/Latinos. *CA Cancer J Clin,* 62, 353-63.

COLLABORATORS, G. B. D. R. F. 2016. Global, regional, and national comparative risk assessment of 79 behavioural, environmental and occupational, and metabolic risks or clusters of risks, 1990-2015: a systematic analysis for the Global Burden of Disease Study 2015. *Lancet,* 388, 1659-1724.

COLLARES, C. V. et al. 2013. Identifying common and specific microRNAs expressed in peripheral blood mononuclear cell of type 1, type 2, and gestational diabetes mellitus patients. *BMC Res Notes,* 6, 491.

COLQUHOUN, A. et al. 2015. Global patterns of cardia and non-cardia gastric cancer incidence in 2012. *Gut,* 64, 1881-8.

CONESA, A. et al. 2016. A survey of best practices for RNA-seq data analysis. *Genome Biol,* 17, 13.

CONTEDUCA, V. et al. 2013. H. pylori infection and gastric cancer: state of the art (review). *Int J Oncol,* 42, 5-18.

COPUR, S. et al. 1995. Thymidylate synthase gene amplification in human colon cancer cell lines resistant to 5-fluorouracil. *Biochem Pharmacol,* 49, 1419-26.

CORDON-CARDO, C. et al. 1994. Molecular abnormalities of mdm2 and p53 genes in adult soft tissue sarcomas. *Cancer Res,* 54, 794-9.

CORREA, P. 1992. Human gastric carcinogenesis: a multistep and multifactorial process--First American Cancer Society Award Lecture on Cancer Epidemiology and Prevention. *Cancer Res,* 52, 6735-40.

CORREA, P. 2011. Gastric cancer: two epidemics? *Dig Dis Sci,* 56, 1585-6; author reply 1586.

CORREA, P. and PIAZUELO, M. B. 2011. Helicobacter pylori Infection and Gastric Adenocarcinoma. *US Gastroenterol Hepatol Rev,* 7, 59-64.

CORREA, P. and PIAZUELO, M. B. 2012. The gastric precancerous cascade. *J Dig Dis,* 13, 2-9.

CORREIA, N. C. et al. 2016. microRNAs regulate TAL1 expression in T-cell acute lymphoblastic leukemia. *Oncotarget,* 7, 8268-81.

CORTEZ, M. A. et al. 2011. MicroRNAs in body fluids--the mix of hormones and biomarkers. *Nat Rev Clin Oncol,* 8, 467-77.

CORTEZ, M. A. et al. 2016. PDL1 Regulation by p53 via miR-34. *J Natl Cancer Inst,* 108.

CRAIG, P. M. et al. W. 2014. Profiling hepatic microRNAs in zebrafish: fluoxetine exposure mimics a fasting response that targets AMP-activated protein kinase (AMPK). *PLoS One,* 9, e95351.

CRICK, F. 1970. Central dogma of molecular biology. *Nature,* 227, 561-3.

CRISTESCU, R. et al. 2015. Molecular analysis of gastric cancer identifies subtypes associated with distinct clinical outcomes. *Nat Med,* 21, 449-56.

CROWE, N. et al. 2016. Detecting new microRNAs in human osteoarthritic chondrocytes identifies miR-3085 as a human, chondrocyte-selective, microRNA. *Osteoarthritis Cartilage,* 24, 534-43.

CUI, Y. et al. 2017. Long Noncoding RNA HOXA11-AS Functions as miRNA Sponge to Promote the Glioma Tumourigenesis Through Targeting miR-140-5p. *DNA Cell Biol,* 36, 822-828.

CUNNINGHAM, D. et al. 2006. Perioperative chemotherapy versus surgery alone for resectable gastroesophageal cancer. *N Engl J Med,* 355, 11-20.

CUNNINGHAM, D. et al. 2008. Capecitabine and oxaliplatin for advanced esophagogastric cancer. *N Engl J Med,* 358, 36-46.

CZOPEK, J. P. et al. 2003. EBV-positive gastric carcinomas in Poland. *Pol J Pathol,* 54, 123-8.

DAI, Y. and WANG, W. H. 2006. Non-steroidal anti-inflammatory drugs in prevention of gastric cancer. *World J Gastroenterol,* 12, 2884-9.

DANAEI, G. et al. 2005. Causes of cancer in the world: comparative risk assessment of nine behavioural and environmental risk factors. *Lancet,* 366, 1784-93.

DANN, C. E. et al. 2001. Insights into Wnt binding and signalling from the structures of two Frizzled cysteine-rich domains. *Nature*. 412, 86-90.

DAVIDSON-MONCADA, J.,et al. 2010. MicroRNAs of the immune system: roles in inflammation and cancer. *Ann N Y Acad Sci,* 1183, 183-94.

DAWSON, M. A. et al. 2009. Clinical and immunohistochemical features associated with a response to bortezomib in patients with multiple myeloma. *Clin Cancer Res,* 15, 714-22.

DE ANGELIS, R. et al. 2014. Cancer survival in Europe 1999-2007 by country and age: results of EUROCARE--5-a population-based study. *Lancet Oncol,* 15, 23-34.

DE MARTEL, C. et al. 2012. Global burden of cancers attributable to infections in 2008: a review and synthetic analysis. *Lancet Oncol,* 13, 607-15.

DE ROZIERES, S. et al. 2000. The loss of mdm2 induces p53-mediated apoptosis. *Oncogene,* 19, 1691-7.

DE VRIES, A. C. et al. 2008. Gastric cancer risk in patients with premalignant gastric lesions: a nationwide cohort study in the Netherlands. *Gastroenterology,* 134, 945-52.

DEMICCO, E. G. et al. 2011. The dichotomy in carcinogenesis of the distal esophagus and esophagogastric junction: intestinal-type vs cardiac-type mucosa-associated adenocarcinoma. *Mod Pathol,* 24, 1177-90.

DERAKHSHAN, M. H. et al. 2015. In healthy volunteers, immunohistochemistry supports squamous to columnar metaplasia as mechanism of expansion of cardia, aggravated by central obesity. *Gut,* 64, 1705-14.

DESVIGNES, T. et al. 2015. miRNA Nomenclature: A View Incorporating Genetic Origins, Biosynthetic Pathways, and Sequence Variants. *Trends Genet,* 31, 613-626.

DIASIO, R. B. and HARRIS, B. E. 1989. Clinical pharmacology of 5-fluorouracil. *Clin Pharmacokinet,* 16, 215-37.

DILEEPAN, M. et al. 2016. MicroRNA Mediated Chemokine Responses in Human Airway Smooth Muscle Cells. *PLoS One,* 11, e0150842.

DING, B. et al. 2017. A novel microRNA signature predicts survival in stomach adenocarcinoma. *Oncotarget,* 8, 28144-28153.

DING, L. et al. 2010. MiR-375 frequently downregulated in gastric cancer inhibits cell proliferation by targeting JAK2. *Cell Res,* 20, 784-93.

DINIS-RIBEIRO, M. et al. 2012. Management of precancerous conditions and lesions in the stomach (MAPS): guideline from the European Society of Gastrointestinal Endoscopy (ESGE), European Helicobacter Study Group (EHSG), European Society of Pathology (ESP), and the Sociedade Portuguesa de Endoscopia Digestiva (SPED). *Endoscopy,* 44, 74-94.

DJEBALI, S. et al. 2012. Landscape of transcription in human cells. *Nature,* 489, 101-8.

DOERRENBERG, M. et al. 2017. T-cell acute lymphoblastic leukemia in infants has distinct genetic and epigenetic features compared to childhood cases. *Genes Chromosomes Cancer,* 56, 159-167.

DONEHOWER, L. A. 2014. Insights into wild-type and mutant p53 functions provided by genetically engineered mice. *Hum Mutat,* 35, 715-27.

DONG, W. et al. 2016. MiR-140-3p suppressed cell growth and invasion by downregulating the expression of ATP8A1 in non-small cell lung cancer. *Tumour Biol,* 37, 2973-85.

DRUSCO A. et al. 2018. Circulating Micrornas Predict Survival of Patients with Tumours of Glial Origin. *EBioMedicine,* 30, 105-112.

DUAN, L. et al. 2015. p53-regulated autophagy is controlled by glycolysis and determines cell fate. *Oncotarget,* 6, 23135-56.

DULAK, A. M. et al. 2013. Exome and whole-genome sequencing of esophageal adenocarcinoma identifies recurrent driver events and mutational complexity. *Nat Genet,* 45, 478-86.

DURU, N. et al. 2016. Loss of miR-140 is a key risk factor for radiation-induced lung fibrosis through reprogramming fibroblasts and macrophages. *Sci Rep,* 6, 39572.

EL-OMAR, E. M. 2001. The importance of interleukin 1beta in Helicobacter pylori associated disease. *Gut,* 48, 743-7.

ERICKSEN, R. E. et al. 2014. Obesity accelerates Helicobacter felis-induced gastric carcinogenesis by enhancing immature myeloid cell trafficking and TH17 response. *Gut,* 63, 385-94.

FABBRI, M. et al. 2012. MicroRNAs bind to Toll-like receptors to induce prometastatic inflammatory response. *Proc Natl Acad Sci U S A,* 109*,* E2110-6.

Fakharzadeh, S. S. et al. 1991. Tumourigenic potential associated with enhanced expression of a gene that is amplified in a mouse tumour cell line. *EMBO J,* 10*,* 1565–1569.

FANG, W. L. et al. 2011. Comparison of the survival difference between AJCC 6th and 7th editions for gastric cancer patients. *World J Surg,* 35*,* 2723-9.

FANG, Z. et al. 2017. miR-140-5p suppresses the proliferation, migration and invasion of gastric cancer by regulating YES1. *Mol Cancer,* 16, 139.

FERLAY J, S. I. et al. 2013. *GLOBOCAN 2012 v 1.0, Cancer incidence and mortality worldwide: IARC CancerBase No. 11 [Internet]. Lyon: International Agency for Research on Cancer; 2013]. Available from: http://globocan.iarc.fr.* [Online]. 2018].

FERLAY, J. et al. 2015. Cancer incidence and mortality worldwide: sources, methods and major patterns in GLOBOCAN 2012. *Int J Cancer,* 136, E359-86.

FERRO, A. et al. 2018a. Tobacco smoking and gastric cancer: meta-analyses of published data versus pooled analyses of individual participant data (StoP Project). *Eur J Cancer Prev,* 27, 197-204.

FERRO, A. et al. 2018b. Alcohol intake and gastric cancer: Meta-analyses of published data versus individual participant data pooled analyses (StoP Project). *Cancer Epidemiol,* 54, 125-132.

FERRO, A. et al. 2014. Worldwide trends in gastric cancer mortality (1980-2011), with predictions to 2015, and incidence by subtype. *Eur J Cancer,* 50*,* 1330-44.

FLAMINI, V. et al. 2018. Distinct mechanisms by which two forms of miR-140 suppress the malignant properties of lung cancer cells. *Oncotarget,* 9*,* 36474-36491.

FLAMINI, V., et al 2017. Therapeutic Role of MiR-140-5p for the Treatment of Non-small Cell Lung Cancer. *Anticancer Res,* 37*,* 4319-4327.

FOCACCETTI, C. et al. 2015. Effects of 5-fluorouracil on morphology, cell cycle, proliferation, apoptosis, autophagy and ROS production in endothelial cells and cardiomyocytes. *PLoS One,* 10*,* e0115686.

FOCK, K. M. et al. 2009. Second Asia-Pacific Consensus Guidelines for Helicobacter pylori infection. *J Gastroenterol Hepatol,* 24*,* 1587-600.

FONTHAM, E. T. 2009. Infectious diseases and global cancer control. *CA Cancer J Clin,* 59, 5-7.

FORD, A. C. et al. 2014. Helicobacter pylori eradication therapy to prevent gastric cancer in healthy asymptomatic infected individuals: systematic review and meta-analysis of randomised controlled trials. *BMJ,* 348*,* g3174.

FORD, H. E. et al. 2014. Docetaxel versus active symptom control for refractory oesophagogastric adenocarcinoma (COUGAR-02): an open-label, phase 3 randomised controlled trial. *Lancet Oncol,* 15*,* 78-86.

FOX, J. G. and WANG, T. C. 2007. Inflammation, atrophy, and gastric cancer. *J Clin Invest,* 117, 60-9.

FRANKEN, N. A. et al. 2006. Clonogenic assay of cells in vitro. *Nat Protoc,* 1, 2315-9.

FUCHS, C. S. et al. 2014. Ramucirumab monotherapy for previously treated advanced gastric or gastro-oesophageal junction adenocarcinoma (REGARD): an international, randomised, multicentre, placebo-controlled, phase 3 trial. *Lancet,* 383, 31-39.

GABAY, O. and CLOUSE, K. A. 2016. Epigenetics of cartilage diseases. *Joint Bone Spine,* 83, 491-4.

GALIATSATOS, P. et al. 2017. Low yield of gastroscopy in patients with Lynch syndrome. *Turk J Gastroenterol,* 28, 434-438.

GANDALOVICOVA, A. et al. 2017. Migrastatics-Anti-metastatic and Anti-invasion Drugs: Promises and Challenges. *Trends Cancer,* 3, 391-406.

GARCIA-DONAS, J. et al. 2016. Deep sequencing reveals microRNAs predictive of antiangiogenic drug response. *JCI Insight,* 1, e86051.

GAT-YABLONSKI, G. et al. 2013. Nutritional catch-up growth. *World Rev Nutr Diet,* 106, 83-9.

GERNAPUDI, R. et al. 2015. Targeting exosomes from preadipocytes inhibits preadipocyte to cancer stem cell signaling in early-stage breast cancer. *Breast Cancer Res Treat,* 150, 685-95.

GIANCOTTI, F. G. 2014. Deregulation of cell signaling in cancer. *FEBS Lett,* 588, 2558-70.

GIBSON, G. and ASAHARA, H. 2013. microRNAs and cartilage. *J Orthop Res,* 31, 1333-44.

GLAZER, R. I. and LLOYD, L. S. 1982. Association of cell lethality with incorporation of 5-fluorouracil and 5-fluorouridine into nuclear RNA in human colon carcinoma cells in culture. *Mol Pharmacol,* 21, 468-73.

GLOBAL BURDEN OF DISEASE CANCER COLLABORATION. 2017. Global, Regional, and National Cancer Incidence, Mortality, Years of Life Lost, Years Lived With Disability, and Disability-Adjusted Life-years for 32 Cancer Groups, 1990 to 2015: A Systematic Analysis for the Global Burden of Disease Study. *JAMA Oncol,* 3, 524-548.

GASTRIC (Global Advanced/Adjuvant Stomach Tumour Research International Collaboration) Group. 2013. Role of chemotherapy for advanced/recurrent gastric cancer: an individual-patient-data meta-analysis. Eur J Cancer, 49, 1565-77.

Goel, H.L. and Mercurio, A. M. 2013. VEGF targets the tumour cell. *Nature reviews Cancer.* 13, 871-882.

GONG, E. J. et al. 2018. Characteristics of non-cardia gastric cancer with a high serum anti-Helicobacter pylori IgG titer and its association with diffuse-type histology. *PLoS One,* 13, e0195264.

GONZALEZ, C. A. et al. 2012. Fruit and vegetable intake and the risk of gastric adenocarcinoma: a reanalysis of the European Prospective Investigation into Cancer and Nutrition (EPIC-EURGAST) study after a longer follow-up. *Int J Cancer,* 131, 2910-9.

GONZALEZ, C. A. et al. 2003. Smoking and the risk of gastric cancer in the European Prospective Investigation Into Cancer and Nutrition (EPIC). *Int J Cancer,* 107, 629-34.

GOSEKI, N. et al. 1992. Differences in the mode of the extension of gastric cancer classified by histological type: new histological classification of gastric carcinoma. *Gut,* 33, 606-12.

GREEN, P. H. and O'TOOLE, K. M. 1982. Early gastric cancer. *Ann Intern Med,* 97, 272-3.

GRIFFITHS-JONES, S. et al. 2006. miRBase: microRNA sequences, targets and gene nomenclature. *Nucleic Acids Res,* 34, D140-4.

GRIMES, J. A. et al. 2016. A comparison of microRNA expression profiles from splenic hemangiosarcoma, splenic nodular hyperplasia, and normal spleens of dogs. *BMC Vet Res,* 12, 272.

Gu L. et al. 2009. Regulation of XIAP translation and induction by MDM2 following irradiation. *Cancer cell*. 15, 363-375.

GU, R. et al. 2016. Biological roles of microRNA-140 in tumour growth, migration, and metastasis of osteosarcoma in vivo and in vitro. *Tumour Biol,* 37, 353-60.

GU, Y. Q. et al. 2014. miRNA profiling reveals a potential role of milk stasis in breast carcinogenesis. *Int J Mol Med,* 33, 1243-9.

GUAN, L. et al. 2018. Biomarker identification in clear cell renal cell carcinoma based on miRNA-seq and digital gene expression-seq data. *Gene,* 647, 205-212.

GUEDES, A. G. et al. 2015. CD38 and airway hyper-responsiveness: studies on human airway smooth muscle cells and mouse models. *Can J Physiol Pharmacol,* 93, 145-53.

GUILFORD, P. et al. 1998. E-cadherin germline mutations in familial gastric cancer. *Nature,* 392, 402-5.

GULLU, G. et al. 2015. Clinical significance of miR-140-5p and miR-193b expression in patients with breast cancer and relationship to IGFBP5. *Genet Mol Biol,* 38, 21-9.

GULLUOGLU, S. et al. 2016. The potential function of microRNA in chordomas. *Gene,* 585, 76-83.

HA, M. et al. 2012. A case of Cowden syndrome diagnosed from multiple gastric polyposis. *World J Gastroenterol,* 18, 861-4.

HAMFJORD, J. et al. 2012. Differential expression of miRNAs in colorectal cancer: comparison of paired tumour tissue and adjacent normal mucosa using high-throughput sequencing. *PLoS One,* 7, e34150.

HANAHAN, D. and WEINBERG, R. A. 2011. Hallmarks of cancer: the next generation. *Cell,* 144, 646-74.

HANSEN, T. B. et al. 2013. Circular RNA and miR-7 in cancer. *Cancer Res,* 73, 5609-12.

HANSON, B. J. and HONG, W. 2003. Evidence for a role of SNX16 in regulating traffic between the early and later endosomal compartments. *J Biol Chem,* 278, 34617-30.

HANSSON, G. K. 2005. Inflammation, atherosclerosis, and coronary artery disease. *N Engl J Med,* 352, 1685-95.

HANSSON, L. E. et al. 1996. The risk of stomach cancer in patients with gastric or duodenal ulcer disease. *N Engl J Med,* 335, 242-9.

HAO, N. B.et al. 2017. The role of miRNA and lncRNA in gastric cancer. *Oncotarget,* 8, 81572-81582.

HAUPT, Y. et al. 1997. Mdm2 promotes the rapid degradation of p53. *Nature,* 387, 296-9.

HAUSMANN, C. et al. 2015. ILKAP, ILK and PINCH1 control cell survival of p53-wildtype glioblastoma cells after irradiation. *Oncotarget,* 6, 34592-605.

HE, S. et al. 2015. Dissecting Collective Cell Behavior in Polarization and Alignment on Micropatterned Substrates. *Biophys J,* 109, 489-500.

HELICOBACTER and CANCER COLLABORATIVE, G. 2001. Gastric cancer and Helicobacter pylori: a combined analysis of 12 case control studies nested within prospective cohorts. *Gut,* 49, 347-53.

HILL, B. T. and BASERGA, R. 1975. The cell cycle and its significance for cancer treatment. *Cancer Treat Rev,* 2, 159-75.

HONG, E. and REDDI, A. H. 2013. Dedifferentiation and redifferentiation of articular chondrocytes from surface and middle zones: changes in microRNAs-221/-222, -140, and -143/145 expression. *Tissue Eng Part A,* 19, 1015-22.

HORIE, N. et al. 1995. Functional analysis and DNA polymorphism of the tandemly repeated sequences in the 5'-terminal regulatory region of the human gene for thymidylate synthase. *Cell Struct Funct,* 20, 191-7.

HORWITZ, R. and WEBB, D. 2003. Cell migration. *Curr Biol,* 13, R756-9.

HOUGHTON, J. A. et al. 1995. Ratio of 2'-deoxyadenosine-5'-triphosphate/thymidine-5'-triphosphate influences the commitment of human colon carcinoma cells to thymineless death. *Clin Cancer Res,* 1, 723-30.

HSU, P. I. et al. 1997. Correlation of serum immunoglobulin G Helicobacter pylori antibody titers with histologic and endoscopic findings in patients with dyspepsia. *J Clin Gastroenterol,* 25, 587-91.

HU, B.et al. 2012. Gastric cancer: Classification, histology and application of molecular pathology. *J Gastrointest Oncol,* 3, 251-61.

HU, L. et al. 2016. Integrative microRNA and gene profiling data analysis reveals novel biomarkers and mechanisms for lung cancer. *Oncotarget,* 7, 8441-54.

HUANG, K. H.et al. 2015. The correlation between miRNA and lymph node metastasis in gastric cancer. *Biomed Res Int,* 2015, 543163.

HUANG, Q. et al. 2015. Differences in Clinicopathology of Early Gastric Carcinoma between Proximal and Distal Location in 438 Chinese Patients. *Sci Rep,* 5, 13439.

HUANG, X.et al. 2016. Transcriptional Profiles from Paired Normal Samples Offer Complementary Information on Cancer Patient Survival--Evidence from TCGA Pan-Cancer Data. *Sci Rep,* 6, 20567.

HUANG, X. Z. et al. 2017. Aspirin and non-steroidal anti-inflammatory drugs use reduce gastric cancer risk: A dose-response meta-analysis. *Oncotarget,* 8, 4781-4795.

HUO, Q. 2017. Analysis of expression profile of miRNA in stomach adenocarcinoma. *J BUON,* 22, 1154-1159.

HUSZNO, J. et al. 2012. Mucin secretion activity of gastric cancer as a prognostic factor: a clinicopathological analysis. *Contemp Oncol (Pozn),* 16, 159-64.

HUTVAGNER, G. et al. 2001. A cellular function for the RNA-interference enzyme Dicer in the maturation of the let-7 small temporal RNA. *Science,* 293, 834-8.

HWANG, S. W.et al. 2010. Preoperative staging of gastric cancer by endoscopic ultrasonography and multidetector-row computed tomography. *J Gastroenterol Hepatol,* 25, 512-8.

INTERNATIONAL AGENCY FOR RESEARCH ON CANCER. 1994a. IARC working group on the evaluation of carcinogenic risks to humans: some industrial chemicals. Lyon, 15-22 February 1994. IARC Monogr Eval Carcinog Risks Hum, 60, 1-560.

INTERNATIONAL AGENCY FOR RESEARCH ON CANCER. 1994b. Schistosomes, liver flukes and Helicobacter pylori. IARC Working Group on the Evaluation of Carcinogenic Risks to Humans. Lyon, 7-14 June 1994. IARC Monogr Eval Carcinog Risks Hum, 61, 1-241.

IGUCHI, H. et al. 2010. Secretory microRNAs as a versatile communication tool. *Commun Integr Biol,* 3, 478-81.

IHRE, B. J. et al. 1964. Ulcer-Cancer of the Stomach. A Follow-up Study of 473 Cases of Gastric Ulcer. *Gastroenterologia,* 102, 78-91.

IIZASA, H. et al. 2012. Epstein-Barr Virus (EBV)-associated gastric carcinoma. *Viruses,* 4, 3420-39.

IKOMA, N. et al. 2018. Evaluation of the American Joint Committee on Cancer 8th edition staging system for gastric cancer patients after preoperative therapy. *Gastric Cancer,* 21, 74-83.

IKUSHIMA, H. and MIYAZONO, K. 2010. TGFbeta signalling: a complex web in cancer progression. *Nat Rev Cancer,* 10, 415-24.

ILIOPOULOS, D. et al. 2008. Integrative microRNA and proteomic approaches identify novel osteoarthritis genes and their collaborative metabolic and inflammatory networks. *PLoS One,* 3, e3740.

IMAI, S. et al. 1994. Gastric carcinoma: monoclonal epithelial malignant cells expressing Epstein-Barr virus latent infection protein. *Proc Natl Acad Sci U S A,* 91, 9131-5.

INSTITUTE, N. C. 2017. *Survival by Stage, Cancer Stat Facts: Stomach Cancer [Online]* [Online]. [Accessed 5th April 2018].

INSTITUTE, N. C. 2018. *Cancer Stat Facts: Stomach Cancer [Online].* [Online]. Available: Available at: https://seer.cancer.gov/statfacts/html/stomach.html [Accessed 15 Augest 2018].

INUI, M. et al, H. 2018. Dissecting the roles of miR-140 and its host gene. *Nat Cell Biol,* 20, 516-518.

IORIO, M. V. et al. 2007. MicroRNA signatures in human ovarian cancer. *Cancer Res,* 67, 8699-707.

ISHIMOTO, T. et al. 2014. Macrophage-derived reactive oxygen species suppress miR-328 targeting CD44 in cancer cells and promote redox adaptation. *Carcinogenesis,* 35, 1003-11.

ISHIOKA, K. et al. 2018. Association between ALDH2 and ADH1B polymorphisms, alcohol drinking and gastric cancer: a replication and mediation analysis. *Gastric Cancer,* 21, 936-945.

ISOBE, T. et al. 2015. Characteristics and prognosis of mucinous gastric carcinoma. *Mol Clin Oncol,* 3, 44-50.

JACKSON, C. et al. 2007. Therapeutic options in gastric cancer: neoadjuvant chemotherapy vs postoperative chemoradiotherapy. *Oncology (Williston Park),* 21, 1084-7; discussion 1090, 1096-8, 1101.

JACKSON, L. M. et al. 2000. Cyclooxygenase (COX) 1 and 2 in normal, inflamed, and ulcerated human gastric mucosa. *Gut,* 47, 762-70.

JAGER, D. et al. 2017. HOXA7, HOXA9, and HOXA10 are differentially expressed in clival and sacral chordomas. *Sci Rep,* 7, 2032.

JANSSEN, H. L. et al. 2013. Treatment of HCV infection by targeting microRNA. *N Engl J Med,* 368, 1685-94.

JAPANESE GASTRIC CANCER Association. 2011. Japanese classification of gastric carcinoma: 3rd English edition. *Gastric Cancer,* 14, 101-12.

JAYASURIYA, C. T. and CHEN, Q. 2015. Potential benefits and limitations of utilizing chondroprogenitors in cell-based cartilage therapy. *Connect Tissue Res,* 56, 265-71.

JEMAL, A. et al. 2011. Global cancer statistics. *CA Cancer J Clin,* 61, 69-90.

JEMAL, A. et al. 2006. Cancer statistics, 2006. *CA Cancer J Clin,* 56, 106-30.

JEURNINK, S. M. et al. 2012. Variety in vegetable and fruit consumption and the risk of gastric and esophageal cancer in the European Prospective Investigation into Cancer and Nutrition. *Int J Cancer,* 131, E963-73.

JIMENEZ FONSECA, P. et al. 2017. Lauren subtypes of advanced gastric cancer influence survival and response to chemotherapy: real-world data from the AGAMENON National Cancer Registry. *Br J Cancer,* 117, 775-782.

Jin H.Y. et al. 2015. Transfection of microRNA Mimics Should Be Used with Caution. *Frontiers in genetics*. 6, 340.

JING, P. et al. 2016. MicroR-140-5p suppresses tumour cell migration and invasion by targeting ADAM10-mediated Notch1 signaling pathway in hypopharyngeal squamous cell carcinoma. *Exp Mol Pathol,* 100, 132-8.

JOHNSTON, P. G. and KAYE, S. 2001. Capecitabine: a novel agent for the treatment of solid tumours. *Anticancer Drugs,* 12, 639-46.

JONES, S. N. et al. 1995. Rescue of embryonic lethality in Mdm2-deficient mice by absence of p53. *Nature,* 378, 206-8.

JORGENSEN, J. T. 2010. Targeted HER2 treatment in advanced gastric cancer. *Oncology,* 78, 26-33.

JOYCE, J. A. and POLLARD, J. W. 2009. Microenvironmental regulation of metastasis. *Nat Rev Cancer,* 9, 239-52.

JU, J. 2010. miRNAs as biomarkers in colorectal cancer diagnosis and prognosis. *Bioanalysis,* 2, 901-6.

JUNG, K. W. et al. 2017. Cancer Statistics in Korea: Incidence, Mortality, Survival, and Prevalence in 2014. *Cancer Res Treat,* 49, 292-305.

JUSTUS, C. R. et al. 2014. In vitro cell migration and invasion assays. *J Vis Exp*.

KAKIUCHI, M. et al. 2014. Recurrent gain-of-function mutations of RHOA in diffuse-type gastric carcinoma. *Nat Genet,* 46, 583-7.

KAMOSHIDA, S. et al. 2005. Immunohistochemical demonstration of fluoropyrimidine-metabolizing enzymes in various types of cancer. *Oncol Rep,* 14, 1223-30.

KAMPSCHOER, G. H. et al. 1989. Changing patterns in gastric adenocarcinoma. *Br J Surg,* 76, 914-6.

KANDOTH, C. et al. 2013. Mutational landscape and significance across 12 major cancer types. *Nature,* 502, 333-339.

KANEKO, S. and YOSHIMURA, T. 2001. Time trend analysis of gastric cancer incidence in Japan by histological types, 1975-1989. *Br J Cancer,* 84, 400-5.

KANG, G. H. et al. 2002. Epstein-barr virus-positive gastric carcinoma demonstrates frequent aberrant methylation of multiple genes and constitutes CpG island methylator phenotype-positive gastric carcinoma. *Am J Pathol,* 160, 787-94.

KANG, J. H. et al. 2012. Salvage chemotherapy for pretreated gastric cancer: a randomized phase III trial comparing chemotherapy plus best supportive care with best supportive care alone. *J Clin Oncol,* 30, 1513-8.

KANG, J. Y. et al. 2002. Risk of gastric carcinoma in patients with atrophic gastritis and intestinal metaplasia. *Gut,* 51, 899.

KARAKAS, M. et al. 2017. Circulating microRNAs strongly predict cardiovascular death in patients with coronary artery disease-results from the large AtheroGene study. *Eur Heart J,* 38, 516-523.

KARIMI, P. et al. 2014. Gastric cancer: descriptive epidemiology, risk factors, screening, and prevention. *Cancer Epidemiol Biomarkers Prev,* 23, 700-13.

KARLSEN, T. A. et al. 2014. microRNA-140 targets RALA and regulates chondrogenic differentiation of human mesenchymal stem cells by translational enhancement of SOX9 and ACAN. *Stem Cells Dev,* 23, 290-304.

Karni-Schmidt O. et al. 2016. The Roles of MDM2 and MDMX in Cancer. A*nnual review of pathology*. 11, 617-644

KASTENHUBER, E. R. and LOWE, S. W. 2017. Putting p53 in Context. *Cell,* 170, 1062-1078.

KATADA, T. et al. 2009. microRNA expression profile in undifferentiated gastric cancer. *Int J Oncol,* 34, 537-42.

KATO, I. et al. 1992. Atrophic gastritis and stomach cancer risk: cross-sectional analyses. *Jpn J Cancer Res,* 83, 1041-6.

KATO, T. A. et al. 2011. In vitro characterization of cells derived from chordoma cell line U-CH1 following treatment with X-rays, heavy ions and chemotherapeutic drugs. *Radiat Oncol,* 6, 116.

KATTAN, M. W. et al. 2003. Postoperative nomogram for disease-specific survival after an R0 resection for gastric carcinoma. *J Clin Oncol,* 21, 3647-50.

KAURAH, P. et al. 2007. Founder and recurrent CDH1 mutations in families with hereditary diffuse gastric cancer. *JAMA,* 297, 2360-72.

KAWAGUCHI, T. et al. 2017. Overexpression of suppressive microRNAs, miR-30a and miR-200c are associated with improved survival of breast cancer patients. *Sci Rep,* 7, 15945.

KAWAMURA, H. et al. 2001. A clinicopathologic study of mucinous adenocarcinoma of the stomach. *Gastric Cancer,* 4, 83-6.

KE, X.et al. 2017. MiR-514a-3p inhibits cell proliferation and epithelial-mesenchymal transition by targeting EGFR in clear cell renal cell carcinoma. *Am J Transl Res,* 9, 5332-5346.

KENYON, J. D. et al. 2019. Analysis of -5p and -3p Strands of miR-145 and miR-140 During Mesenchymal Stem Cell Chondrogenic Differentiation. *Tissue Eng Part A,* 25, 80-90.

KEUM, N. et al. 2016. Association of Physical Activity by Type and Intensity With Digestive System Cancer Risk. *JAMA Oncol,* 2, 1146-53.

KHARE, D. et al. 2017. Plasma microRNA profiling: Exploring better biomarkers for lymphoma surveillance. *PLoS One,* 12, e0187722.

KIM, C. H. et al. 2011. miRNA signature associated with outcome of gastric cancer patients following chemotherapy. *BMC Med Genomics,* 4, 79.

KIM, G. H. et al. 2016. Screening and surveillance for gastric cancer in the United States: Is it needed? *Gastrointest Endosc,* 84, 18-28.

KOIZUMI, W. et al. 2008. S-1 plus cisplatin versus S-1 alone for first-line treatment of advanced gastric cancer (SPIRITS trial): a phase III trial. *Lancet Oncol,* 9, 215-21.

KOMATSU, S. et al. 2013. Prognostic impact of circulating miR-21 in the plasma of patients with gastric carcinoma. *Anticancer Res,* 33, 271-6.

KONG, X. M. et al. 2015. MicroRNA-140-3p inhibits proliferation, migration and invasion of lung cancer cells by targeting ATP6AP2. *Int J Clin Exp Pathol,* 8, 12845-52.

KORKAYA, H. et al. 2012. Activation of an IL6 inflammatory loop mediates trastuzumab resistance in HER2+ breast cancer by expanding the cancer stem cell population. *Mol Cell,* 47, 570-84.

KOWALSKI, M. L. et al. 2008. Increased responsiveness to toll-like receptor 4 stimulation in peripheral blood mononuclear cells from patients with recent onset rheumatoid arthritis. *Mediators Inflamm,* 2008, 132732.

KRENTZ GOBER, M. et al. 2017. A microRNA signature of response to erlotinib is descriptive of TGFbeta behaviour in NSCLC. *Sci Rep,* 7, 4202.

KUBBUTAT, M. H. et al. 1997. Regulation of p53 stability by Mdm2. *Nature,* 387, 299-303.

KUFE, D. W. and MAJOR, P. P. 1981. 5-Fluorouracil incorporation into human breast carcinoma RNA correlates with cytotoxicity. *J Biol Chem,* 256, 9802-5.

KUMAR, R. D. et al. 2016. Unsupervised detection of cancer driver mutations with parsimony-guided learning. *Nat Genet,* 48, 1288-94.

KUNISAKI, C.et al. 2006. Clinicopathologic characteristics and surgical outcomes of mucinous gastric carcinoma. *Ann Surg Oncol,* 13, 836-42.

KUO, W. T. et al. 2015. Bioinformatic Interrogation of 5p-arm and 3p-arm Specific miRNA Expression Using TCGA Datasets. *J Clin Med,* 4, 1798-814.

KUSSIE, P. H. et al. 1996. Structure of the MDM2 oncoprotein bound to the p53 tumour suppressor transactivation domain. *Science,* 274, 948-53.

KWAK, H. W. et al. 2014. Characteristics of gastric cancer according to Helicobacter pylori infection status. *J Gastroenterol Hepatol,* 29, 1671-7.

LA VECCHIA, C. et al. 1992. Family history and the risk of stomach and colorectal cancer. *Cancer,* 70, 50-5.

LABELLE, M. and HYNES, R. O. 2012. The initial hours of metastasis: the importance of cooperative host-tumour cell interactions during hematogenous dissemination. *Cancer Discov,* 2, 1091-9.

LADNER, R. D. 2001. The role of dUTPase and uracil-DNA repair in cancer chemotherapy. *Curr Protein Pept Sci,* 2, 361-70.

LAN, H. et al. 2015. miR-140-5p inhibits ovarian cancer growth partially by repression of PDGFRA. *Biomed Pharmacother,* 75, 117-22.

LANDGRAF, P. et al. 2007. A mammalian microRNA expression atlas based on small RNA library sequencing. *Cell,* 129, 1401-14.

LARSSON, S. C. et al. 2006. Folate intake, MTHFR polymorphisms, and risk of esophageal, gastric, and pancreatic cancer: a meta-analysis. *Gastroenterology,* 131, 1271-83.

LAUREN, P. 1965. The Two Histological Main Types of Gastric Carcinoma: Diffuse and So-Called Intestinal-Type Carcinoma. An Attempt at a Histo-Clinical Classification. *Acta Pathol Microbiol Scand,* 64, 31-49.

LAURIE, N. A. et al. 2006. Inactivation of the p53 pathway in retinoblastoma. *Nature,* 444, 61-6.

LAZEBNIK, Y. 2010. What are the hallmarks of cancer? *Nat Rev Cancer,* 10, 232-3.

LE, L. T. et al. 2013. Review: the role of microRNAs in osteoarthritis and chondrogenesis. *Arthritis Rheum,* 65, 1963-74.

LEE, J. H. et al. 2018. Body mass index and mortality in patients with gastric cancer: a large cohort study. *Gastric Cancer,* 21, 913-924.

LEE, Y. C. et al. 2016. Association Between Helicobacter pylori Eradication and Gastric Cancer Incidence: A Systematic Review and Meta-analysis. *Gastroenterology,* 150, 1113-1124 e5.

LEE, Y. S. et al. 2014. Genomic profile analysis of diffuse-type gastric cancers. *Genome Biol,* 15, R55.

LEHMANN, S. M. et al. 2012. An unconventional role for miRNA: let-7 activates Toll-like receptor 7 and causes neurodegeneration. *Nat Neurosci,* 15, 827-35.

LEHTOLA, J. 1978. Family study of gastric carcinoma; With special reference to histological types. *Scand J Gastroenterol Suppl,* 50, 3-54.

LEVI, Z. et al. 2018. Body mass index at adolescence and risk of noncardia gastric cancer in a cohort of 1.79 million men and women. *Cancer,* 124, 356-363.

LI, C. et al. 2013. MiRNA-199a-3p: A potential circulating diagnostic biomarker for early gastric cancer. *J Surg Oncol,* 108, 89-92.

LI, C. Y. et al. 2017. Identification and functional characterization of microRNAs reveal a potential role in gastric cancer progression. *Clin Transl Oncol,* 19, 162-172.

LI, H. et al. 2017. MiR-140-5p inhibits synovial fibroblasts proliferation and inflammatory cytokines secretion through targeting TLR4. *Biomed Pharmacother,* 96, 208-214.

LI, J. et al. 2018. MicroRNA-140 Inhibits the Epithelial-Mesenchymal Transition and Metastasis in Colorectal Cancer. *Mol Ther Nucleic Acids,* 10, 426-437.

LI, M. et al. 2013. Helicobacter pylori infection synergizes with three inflammation-related genetic variants in the GWASs to increase risk of gastric cancer in a Chinese population. *PLoS One,* 8, e74976.

LI, M. et al. 2017. Time trends of esophageal and gastric cancer mortality in China, 1991-2009: an age-period-cohort analysis. *Sci Rep,* 7, 6797.

LI, Q. et al. 2014a. Characterization of a stem-like subpopulation in basal-like ductal carcinoma in situ (DCIS) lesions. *J Biol Chem,* 289, 1303-12.

LI, Q. et al. 2014b. Downregulation of miR-140 promotes cancer stem cell formation in basal-like early stage breast cancer. *Oncogene,* 33, 2589-600.

LI, T. et al. 2018. Identification of hub genes with prognostic values in gastric cancer by bioinformatics analysis. *World J Surg Oncol,* 16, 114.

LI, W. and HE, F. 2014. Monocyte to macrophage differentiation-associated (MMD) targeted by miR-140-5p regulates tumour growth in non-small cell lung cancer. *Biochem Biophys Res Commun,* 450, 844-50.

LI, W. et al. 2014. Down-regulation of miR-140 induces EMT and promotes invasion by targeting Slug in esophageal cancer. *Cell Physiol Biochem,* 34, 1466-76.

LI, W. Q. et al. 2010. Downregulation of ABCG2 expression in glioblastoma cancer stem cells with miRNA-328 may decrease their chemoresistance. *Med Sci Monit,* 16, HY27-30.

LI, X. et al. 2011a. Identification of new aberrantly expressed miRNAs in intestinal-type gastric cancer and its clinical significance. *Oncol Rep,* 26, 1431-9.

LI, X. et al. 2011b. miRNA-223 promotes gastric cancer invasion and metastasis by targeting tumour suppressor EPB41L3. *Mol Cancer Res,* 9, 824-33.

LI, X. et al. 2010. Survival prediction of gastric cancer by a seven-microRNA signature. *Gut,* 59, 579-85.

LI, X. D. et al. 2017. Elevated plasma miRNA-122, -140-3p, -720, -2861, and -3149 during early period of acute coronary syndrome are derived from peripheral blood mononuclear cells. *PLoS One,* 12, e0184256.

LI, Z. et al. 2011. Differential DNA damage responses in p53 proficient and deficient cells: cisplatin-induced nuclear import of XPA is independent of ATR checkpoint in p53-deficient lung cancer cells. *Int J Biochem Mol Biol,* 2, 138-145.

LIANG, L. et al. 2017. Identification of the key miRNAs associated with survival time in stomach adenocarcinoma. *Oncol Lett,* 14, 4563-4572.

LIANG, S. et al. 2017. The lncRNA XIST interacts with miR-140/miR-124/iASPP axis to promote pancreatic carcinoma growth. *Oncotarget,* 8, 113701-113718.

LIANG, Y. X. et al. 2013. Characteristics and prognosis of gastric cancer in patients aged >/= 70 years. *World J Gastroenterol,* 19, 6568-78.

LIAO, Y. L. et al. 2012. Transcriptional regulation of miR-196b by ETS2 in gastric cancer cells. *Carcinogenesis,* 33, 760-9.

LIM, J. Y. et al. 2013. Overexpression of miR-196b and HOXA10 characterize a poor-prognosis gastric cancer subtype. *World J Gastroenterol,* 19, 7078-88.

LINDAHL, T. 1974. An N-glycosidase from Escherichia coli that releases free uracil from DNA containing deaminated cytosine residues. *Proc Natl Acad Sci U S A,* 71, 3649-53.

LINDBLAD, M. et al. 2005. Nonsteroidal anti-inflammatory drugs and risk of esophageal and gastric cancer. *Cancer Epidemiol Biomarkers Prev,* 14, 444-50.

LINDOW, M. and KAUPPINEN, S. 2012. Discovering the first microRNA-targeted drug. *J Cell Biol,* 199, 407-12.

LINK, A. et al. 2012. Macro-role of microRNA in gastric cancer. *Dig Dis,* 30, 255-67.

LIU, H. T. et al. 2017. Prognostic Value of microRNA Signature in Patients with Gastric Cancers. *Sci Rep,* 7, 42806.

LIU, H. Z. et al. 2016. Pioglitazone up-regulates long non-coding RNA MEG3 to protect endothelial progenitor cells via increasing HDAC7 expression in metabolic syndrome. *Biomed Pharmacother,* 78, 101-109.

LIU, J. et al. 2018. Identification of key miRNAs and genes associated with stomach adenocarcinoma from The Cancer Genome Atlas database. *FEBS Open Bio,* 8, 279-294.

LIU, J. et al. 2016. MiR-455-5p acts as a novel tumour suppressor in gastric cancer by down-regulating RAB18. *Gene,* 592, 308-15.

LIU, T. et al. 2009. MicroRNA-27a functions as an oncogene in gastric adenocarcinoma by targeting prohibitin. *Cancer Lett,* 273, 233-42.

LIU, X. and MELTZER, S. J. 2017. Gastric Cancer in the Era of Precision Medicine. *Cell Mol Gastroenterol Hepatol,* 3, 348-358.

LIU, Y. et al. 2014. TLR2 and TLR4 in autoimmune diseases: a comprehensive review. *Clin Rev Allergy Immunol,* 47, 136-47.

LIU, Y. et al. 2013 MicroRNA-140 promotes adipocyte lineage commitment of C3H10T1/2 pluripotent stem cells via targeting osteopetrosis-associated transmembrane protein 1. *The Journal of biological chemistry*. 288, 8222-8230.

LORDICK, F. et al. 2014. Unmet needs and challenges in gastric cancer: the way forward. *Cancer Treat Rev,* 40, 692-700.

LORDICK, F. et al. 2013. Capecitabine and cisplatin with or without cetuximab for patients with previously untreated advanced gastric cancer (EXPAND): a randomised, open-label phase 3 trial. *Lancet Oncol,* 14, 490-9.

LUJAMBIO, A. et al. 2007. Genetic unmasking of an epigenetically silenced microRNA in human cancer cells. *Cancer Res,* 67, 1424-9.

LUO, H. et al. 2009. Down-regulated miR-9 and miR-433 in human gastric carcinoma. *J Exp Clin Cancer Res,* 28, 82.

LUTZ, M. P. et al. 2012. Highlights of the EORTC St. Gallen International Expert Consensus on the primary therapy of gastric, gastroesophageal and oesophageal cancer - differential treatment strategies for subtypes of early gastroesophageal cancer. *Eur J Cancer,* 48, 2941-53.

MA, J. et al. 2016. Lauren classification and individualized chemotherapy in gastric cancer. *Oncol Lett,* 11, 2959-2964.

MA, X. et al. 2018. Clinicopathological Characteristics and Prognoses of Elderly Gastric Cancer Patients after R0 Resection: A Multicenter Study in China. *J Environ Pathol Toxicol Oncol,* 37, 81-91.

MACDONALD, J. S. et al. 2001. Chemoradiotherapy after surgery compared with surgery alone for adenocarcinoma of the stomach or gastroesophageal junction. *N Engl J Med,* 345, 725-30.

MACHADO, A. M. et al. 2009. Helicobacter pylori infection induces genetic instability of nuclear and mitochondrial DNA in gastric cells. *Clin Cancer Res,* 15, 2995-3002.

MACHADO, J. C. et al. 1999. E-cadherin gene mutations provide a genetic basis for the phenotypic divergence of mixed gastric carcinomas. *Lab Invest,* 79, 459-65.

MACKINTOSH, C. E. and KREEL, L. 1977. Anatomy and radiology of the areae gastricae. *Gut,* 18, 855-64.

MAEHARA, Y. 2003. S-1 in gastric cancer: a comprehensive review. *Gastric Cancer,* 6 Suppl 1, 2-8.

MAEHARA, Y. et al. 1992. Prognosis for surgically treated gastric cancer patients is poorer for women than men in all patients under age 50. *Br J Cancer,* 65, 417-20.

MAHBOUDI, H. et al. 2018. Enhanced chondrogenesis differentiation of human induced pluripotent stem cells by MicroRNA-140 and transforming growth factor beta 3 (TGFbeta3). *Biologicals,* 52, 30-36.

MALFERTHEINER, P. et al. 2007. Current concepts in the management of Helicobacter pylori infection: the Maastricht III Consensus Report. *Gut,* 56, 772-81.

MALZKORN, B. et al. 2010. Identification and functional characterization of microRNAs involved in the malignant progression of gliomas. *Brain Pathol,* 20, 539-50.

MARCHET, A. et al. 2011. Validation of the new AJCC TNM staging system for gastric cancer in a large cohort of patients (n = 2,155): focus on the T category. *Eur J Surg Oncol,* 37, 779-85.

MARIETTE, C. et al. 2011. Oesophagogastric junction adenocarcinoma: which therapeutic approach? *Lancet Oncol,* 12, 296-305.

Manfredi, J. J. et al. The Mdm2-p53 relationship evolves: Mdm2 swings both ways as an oncogene and a tumour suppressor. 2010. *Genes & development*, 24, 1580-1589

MAROTTA, L. L. et al. 2011. The JAK2/STAT3 signaling pathway is required for growth of CD44(+)CD24(-) stem cell-like breast cancer cells in human tumours. *J Clin Invest,* 121, 2723-35.

MARQUES, F. Z. et al. 2016. The transcardiac gradient of cardio-microRNAs in the failing heart. *Eur J Heart Fail,* 18, 1000-8.

MARSH, S. et al. 2001. Polymorphism in the thymidylate synthase promoter enhancer region in colorectal cancer. *Int J Oncol,* 19, 383-6.

MARSHALL, B. J. and WARREN, J. R. 1984. Unidentified curved bacilli in the stomach of patients with gastritis and peptic ulceration. *Lancet,* 1, 1311-5.

MARSHALL, B. J. and WINDSOR, H. M. 2005. The relation of Helicobacter pylori to gastric adenocarcinoma and lymphoma: pathophysiology, epidemiology, screening, clinical presentation, treatment, and prevention. *Med Clin North Am,* 89, 313-44, viii.

MATSUDA, T. et al. 2011. Population-based survival of cancer patients diagnosed between 1993 and 1999 in Japan: a chronological and international comparative study. *Jpn J Clin Oncol,* 41, 40-51.

MATSUZAKA, M. et al. 2016. High Mortality Rate of Stomach Cancer Caused Not by High Incidence but Delays in Diagnosis in Aomori Prefecture, Japan. *Asian Pac J Cancer Prev,* 17, 4723-4727.

MCCREDIE, M. et al. 1999. Cancer mortality in migrants from the British Isles and continental Europe to New South Wales, Australia, 1975-1995. *Int J Cancer,* 83, 179-85.

MENG Y. et al. 2017. MicroRNA-140-5p regulates osteosarcoma chemoresistance by targeting HMGN5 and autophagy. *Scientific reports.* 7, 416.

MEYN, R. E. et al. 1980. Cycle-dependent anticancer drug cytotoxicity in mammalian cells synchronized by centrifugal elutriation. *J Natl Cancer Inst,* 64, 1215-9.

MEZHIR, J. J et al. 2011. Positive peritoneal cytology in patients with gastric cancer: natural history and outcome of 291 patients. *Indian J Surg Oncol,* 2, 16-23.

MIN, Z. et al. 2015. MicroRNAs associated with osteoarthritis differently expressed in bone matrix gelatin (BMG) rat model. *Int J Clin Exp Med,* 8, 1009-17.

MING, S. C. 1977. Gastric carcinoma. A pathobiological classification. *Cancer,* 39, 2475-85.

MIWA, M. et al. 1998. Design of a novel oral fluoropyrimidine carbamate, capecitabine, which generates 5-fluorouracil selectively in tumours by enzymes concentrated in human liver and cancer tissue. *Eur J Cancer,* 34, 1274-81.

MIYAKI, S. et al. 2009. MicroRNA-140 is expressed in differentiated human articular chondrocytes and modulates interleukin-1 responses. *Arthritis Rheum,* 60, 2723-30.

MIYAKI, S. et al. 2010. MicroRNA-140 plays dual roles in both cartilage development and homeostasis. *Genes Dev,* 24, 1173-85.

MIZAMTSIDI, M. et al. 2018. Diagnosis, management, histology and genetics of sporadic primary hyperparathyroidism: old knowledge with new tricks. *Endocr Connect,* 7, R56-R68.

MO, Q. et al. 2013. Pattern discovery and cancer gene identification in integrated cancer genomic data. *Proc Natl Acad Sci U S A,* 110, 4245-50.

MOCELLIN, S. and PASQUALI, S. 2015. Diagnostic accuracy of endoscopic ultrasonography (EUS) for the preoperative locoregional staging of primary gastric cancer. *Cochrane Database Syst Rev*, CD009944.

MOEHLER, M. et al. 2015. International comparison of the German evidence-based S3-guidelines on the diagnosis and multimodal treatment of early and locally advanced gastric cancer, including adenocarcinoma of the lower esophagus. *Gastric Cancer,* 18, 550-63.

MOMAND, J. et al. 1992. The mdm-2 oncogene product forms a complex with the p53 protein and inhibits p53-mediated transactivation. *Cell,* 69, 1237-45.

MONTES DE OCA LUNA, R. et al. 1995. Rescue of early embryonic lethality in mdm2-deficient mice by deletion of p53. *Nature,* 378, 203-6.

MOORE, S. C. et al. 2016. Association of Leisure-Time Physical Activity With Risk of 26 Types of Cancer in 1.44 Million Adults. *JAMA Intern Med,* 176, 816-25.

MORALES, T. I. 2007. Chondrocyte moves: clever strategies? *Osteoarthritis Cartilage,* 15, 861-71.

MOSAKHANI, N. et al. 2012. MicroRNA profiling predicts survival in anti-EGFR treated chemorefractory metastatic colorectal cancer patients with wild-type KRAS and BRAF. *Cancer Genet,* 205, 545-51.

MOTTET D. et al. 2009. HDAC4 represses p21(WAF1/Cip1) expression in human cancer cells through a Sp1-dependent, p53-independent mechanism. *Oncogene*.28, 243-256.

MUHICH, M. L. and BOOTHROYD, J. C. 1989. Synthesis of trypanosome hsp70 mRNA is resistant to disruption of trans-splicing by heat shock. *J Biol Chem,* 264, 7107-10.

MUTA, H. et al. 1996. E-cadherin gene mutations in signet ring cell carcinoma of the stomach. *Jpn J Cancer Res,* 87, 843-8.

NAKAMURA, K. et al. 1992. Pathology and prognosis of gastric carcinoma. Findings in 10,000 patients who underwent primary gastrectomy. *Cancer,* 70, 1030-7.

NAUMANN, M. and CRABTREE, J. E. 2004. Helicobacter pylori-induced epithelial cell signalling in gastric carcinogenesis. *Trends Microbiol,* 12, 29-36.

NEMATI, A. et al. 2012. Case-control study of dietary pattern and other risk factors for gastric cancer. *Health Promot Perspect,* 2, 20-7.

NEWCOMB, D. C. and PEEBLES, R. S., JR. 2013. Th17-mediated inflammation in asthma. *Curr Opin Immunol,* 25, 755-60.

NGUYEN, T. L. et al. 2013. Autoimmune gastritis mediated by CD4+ T cells promotes the development of gastric cancer. *Cancer Res,* 73, 2117-26.

NICOLAS, F. E. et al. 2008. Experimental identification of microRNA-140 targets by silencing and overexpressing miR-140. *RNA,* 14, 2513-20.

NICOLAS, F. E. et al. 2011. mRNA expression profiling reveals conserved and non-conserved miR-140 targets. *RNA Biol,* 8, 607-15.

NISHIKAWA, J. et al. 2017. The Role of Epigenetic Regulation in Epstein-Barr Virus-Associated Gastric Cancer. *Int J Mol Sci,* 18.

NOH, S. H. et al. 2014. Adjuvant capecitabine plus oxaliplatin for gastric cancer after D2 gastrectomy (CLASSIC): 5-year follow-up of an open-label, randomised phase 3 trial. *Lancet Oncol,* 15, 1389-96.

NOMURA, A. M. et al. 2003. Case-control study of diet and other risk factors for gastric cancer in Hawaii (United States). *Cancer Causes Control,* 14, 547-58.

NOONE AM, H. N. et al. 2017 *SEER Cancer Statistics Review, 1975-2015* [Online]. National Cancer Institute. Bethesda, MD. Available: https://seer.cancer.gov/csr/1975_2015 [Accessed 5 May 2018].

O'DOHERTY, M. G. et al. 2012. A prospective cohort study of obesity and risk of oesophageal and gastric adenocarcinoma in the NIH-AARP Diet and Health Study. *Gut,* 61, 1261-8.

O'NEILL, L. A. et al. 2011. MicroRNAs: the fine-tuners of Toll-like receptor signalling. *Nat Rev Immunol,* 11, 163-75.

OFFERHAUS, G. J. et al. 1988. Mortality caused by stomach cancer after remote partial gastrectomy for benign conditions: 40 years of follow up of an Amsterdam cohort of 2633 postgastrectomy patients. *Gut,* 29, 1588-90.

OH, H. K. et al. 2011. Genomic loss of miR-486 regulates tumour progression and the OLFM4 antiapoptotic factor in gastric cancer. *Clin Cancer Res,* 17, 2657-67.

OHMIYA, N. et al. 2006. MDM2 promoter polymorphism is associated with both an increased susceptibility to gastric carcinoma and poor prognosis. *J Clin Oncol,* 24, 4434-40.

OKINES, A. et al. 2010. Gastric cancer: ESMO Clinical Practice Guidelines for diagnosis, treatment and follow-up. *Ann Oncol,* 21 Suppl 5, v50-4.

OLIVEIRA, C. et al. 2015. Familial gastric cancer: genetic susceptibility, pathology, and implications for management. *Lancet Oncol,* 16, e60-70.

ONEL, K. and CORDON-CARDO, C. 2004. MDM2 and prognosis. *Mol Cancer Res,* 2, 1-8.

ONODERA, H. et al. 2004. Surgical outcome of 483 patients with early gastric cancer: prognosis, postoperative morbidity and mortality, and gastric remnant cancer. *Hepatogastroenterology,* 51, 82-5.

ORTEGA, F. J. et al. 2014. Profiling of circulating microRNAs reveals common microRNAs linked to type 2 diabetes that change with insulin sensitization. *Diabetes Care,* 37, 1375-83.

OSAWA, S. et al. 2011. MicroRNA profiling of gastric cancer patients from formalin-fixed paraffin-embedded samples. *Oncol Lett,* 2, 613-619.

OZATA, D. M. et al. 2017. Loss of miR-514a-3p regulation of PEG3 activates the NF-kappa B pathway in human testicular germ cell tumours. *Cell Death Dis,* 8, e2759.

PACHOLEWSKA, A. et al. 2017. Differential Expression of Serum MicroRNAs Supports CD4(+) T Cell Differentiation into Th2/Th17 Cells in Severe Equine Asthma. *Genes (Basel),* 8.

PAIS, H. et al. 2010. Analyzing mRNA expression identifies Smad3 as a microRNA-140 target regulated only at protein level. *RNA,* 16, 489-94.

PAN, H. W. et al. 2013. MicroRNA dysregulation in gastric cancer. *Curr Pharm Des,* 19, 1273-84.

PAN, K. F. et al. 2016. A large randomised controlled intervention trial to prevent gastric cancer by eradication of Helicobacter pylori in Linqu County, China: baseline results and factors affecting the eradication. *Gut,* 65, 9-18.

PANDO, R. et al. 2014. A serum component mediates food restriction-induced growth attenuation. *Endocrinology,* 155, 932-40.

PAPAIOANNOU, G. et al. 2013. let-7 and miR-140 microRNAs coordinately regulate skeletal development. *Proc Natl Acad Sci U S A,* 110, E3291-300.

PAPAIOANNOU, G. et al. 2015. MicroRNA-140 Provides Robustness to the Regulation of Hypertrophic Chondrocyte Differentiation by the PTHrP-HDAC4 Pathway. *J Bone Miner Res,* 30, 1044-52.

PAPP, G. et al. 2014. SMARCB1 expression in epithelioid sarcoma is regulated by miR-206, miR-381, and miR-671-5p on Both mRNA and protein levels. *Genes Chromosomes Cancer,* 53, 168-76.

PARK, J. H. et al. 2016. p53 as guardian of the mitochondrial genome. *FEBS Lett,* 590, 924-34.

PARSONNET, J. et al. 1991. Helicobacter pylori infection in intestinal- and diffuse-type gastric adenocarcinomas. *J Natl Cancer Inst,* 83, 640-3.

PEEK, R. M. et al. 2010. Role of innate immunity in Helicobacter pylori-induced gastric malignancy. *Physiol Rev,* 90, 831-58.

PEGTEL, D. M. et al. 2010. Functional delivery of viral miRNAs via exosomes. *Proc Natl Acad Sci U S A,* 107, 6328-33.

PELETEIRO, B. et al. 2011. Salt intake and gastric cancer risk according to Helicobacter pylori infection, smoking, tumour site and histological type. *Br J Cancer,* 104, 198-207.

PENG, J. S. et al. 2016. Amelioration of Experimental Autoimmune Arthritis Through Targeting of Synovial Fibroblasts by Intraarticular Delivery of MicroRNAs 140-3p and 140-5p. *Arthritis Rheumatol,* 68, 370-81.

PENG, X. et al. 2013. Inhibition of proliferation and induction of autophagy by atorvastatin in PC3 prostate cancer cells correlate with downregulation of Bcl2 and upregulation of miR-182 and p21. *PLoS One,* 8, e70442.

PERIASAMY, J. et al. 2014. Stratification and delineation of gastric cancer signaling by in vitro transcription factor activity profiling and integrative genomics. *Cell Signal,* 26, 880-94.

PERRONE, F. et al. 2010. TP53 mutations and pathologic complete response to neoadjuvant cisplatin and fluorouracil chemotherapy in resected oral cavity squamous cell carcinoma. *J Clin Oncol,* 28, 761-6.

PETERSON, S. M. et al. 2014. Common features of microRNA target prediction tools. *Front Genet,* 5, 23.

PETRELLI, F. et al. 2017. Prognostic value of diffuse versus intestinal histotype in patients with gastric cancer: a systematic review and meta-analysis. *J Gastrointest Oncol,* 8, 148-163.

PETROCCA, F. et al. 2008. E2F1-regulated microRNAs impair TGFbeta-dependent cell-cycle arrest and apoptosis in gastric cancer. *Cancer Cell,* 13, 272-86.

PHILLIPS, B. 2015. Towards evidence based medicine for paediatricians. *Arch Dis Child,* 100, 713.

PIEPOLI, A. et al. 2012. Mirna expression profiles identify drivers in colorectal and pancreatic cancers. *PLoS One,* 7, e33663.

PLEBANI, M. et al. 1996. Helicobacter pylori serology in patients with chronic gastritis. *Am J Gastroenterol,* 91, 954-8.

PLOCIENNIKOWSKA, A. et al. 2015. Co-operation of TLR4 and raft proteins in LPS-induced pro-inflammatory signaling. *Cell Mol Life Sci,* 72, 557-581.

POLLEY, E. et al. 2016. Small Cell Lung Cancer Screen of Oncology Drugs, Investigational Agents, and Gene and microRNA Expression. *J Natl Cancer Inst,* 108.

POULSEN, A. H. et al. 2009. Proton pump inhibitors and risk of gastric cancer: a population-based cohort study. *Br J Cancer,* 100, 1503-7.

PULLARKAT, S. T. et al. 2001. Thymidylate synthase gene polymorphism determines response and toxicity of 5-FU chemotherapy. *Pharmacogenomics J,* 1, 65-70.

QIU, M. Z. et al. 2013. Clinicopathological characteristics and prognostic analysis of Lauren classification in gastric adenocarcinoma in China. *J Transl Med,* 11, 58.

QUANTE, M. et al. 2013. The rapid rise in gastroesophageal junction tumours: is inflammation of the gastric cardia the underwater iceberg? *Gastroenterology,* 145, 708-11.

RANI, S. et al. 2011. Isolation of exosomes for subsequent mRNA, MicroRNA, and protein profiling. *Methods Mol Biol,* 784, 181-95.

REINHART, B. J. et al. 2000. The 21-nucleotide let-7 RNA regulates developmental timing in Caenorhabditis elegans. *Nature,* 403, 901-6.

RENNERT, O. M. and ANKER, H. S. 1963. On the Incorporation of 5',5',5'-Trifluoroleucine into Proteins of E. Coli. *Biochemistry,* 2, 471-6.

ROBERTSON, E. V. et al. 2013. Central obesity in asymptomatic volunteers is associated with increased intrasphincteric acid reflux and lengthening of the cardiac mucosa. *Gastroenterology,* 145, 730-9.

ROCCO, A. et al. 2012. Cancer stem cell hypothesis and gastric carcinogenesis: Experimental evidence and unsolved questions. *World J Gastrointest Oncol,* 4, 54-9.

RODRIGUEZ, L. G. et al. 2005. Wound-healing assay. *Methods Mol Biol,* 294, 23-9.

ROLLAG, A. and JACOBSEN, C. D. 1984. Gastric ulcer and risk of cancer. A five-year follow-up study. *Acta Med Scand,* 216, 105-9.

RONELLENFITSCH, U. et al. 2013. Perioperative chemo(radio)therapy versus primary surgery for resectable adenocarcinoma of the stomach, gastroesophageal junction, and lower esophagus. *Cochrane Database Syst Rev*, CD008107.

ROTHMAN, A. M. et al. 2016. MicroRNA-140-5p and SMURF1 regulate pulmonary arterial hypertension. *J Clin Invest,* 126, 2495-508.

RUGGE, M. et al. 1994. Gastric epithelial dysplasia in the natural history of gastric cancer: a multicenter prospective follow-up study. Interdisciplinary Group on Gastric Epithelial Dysplasia. *Gastroenterology,* 107, 1288-96.

RUGGE, M. et al. 2016. Chronicles of a cancer foretold: 35 years of gastric cancer risk assessment. *Gut,* 65, 721-5.

SABROE, I. et al. 2003. Toll-like receptors in health and disease: complex questions remain. *J Immunol,* 171, 1630-5.

SAITO, H. et al. 2013. Clinicopathologic characteristics and prognosis of advanced gastric cancer simulating early gastric cancer. *Yonago Acta Med,* 56, 73-8.

SAITO, M. et al. 2013. Role of DNA methylation in the development of Epstein-Barr virus-associated gastric carcinoma. *J Med Virol,* 85, 121-7.

SAKAGUCHI, T. et al. 1998. Characteristics and clinical outcome of proximal-third gastric cancer. *J Am Coll Surg,* 187, 352-7.

SAKAI, T. et al. 2003. Simultaneous early adenocarcinoma and mucosa-associated lymphoid tissue (MALT) lymphoma of the stomach associated with Helicobacter pylori infection. *Gastric Cancer,* 6, 191-6.

SALEM, O. et al. 2016. The highly expressed 5'isomiR of hsa-miR-140-3p contributes to the tumour-suppressive effects of miR-140 by reducing breast cancer proliferation and migration. *BMC Genomics,* 17, 566.

SALIH, B. A. 2009. Helicobacter pylori infection in developing countries: the burden for how long? *Saudi J Gastroenterol,* 15, 201-7.

SALMENA, L. et al. 2011. A ceRNA hypothesis: the Rosetta Stone of a hidden RNA language? *Cell,* 146, 353-8.

SAND, M. et al. 2012a. Microarray analysis of microRNA expression in cutaneous squamous cell carcinoma. *J Dermatol Sci,* 68, 119-26.

SAND, M. et al. 2012b. Expression of microRNAs in basal cell carcinoma. *Br J Dermatol,* 167, 847-55.

SANO, T. et al. 2004. Gastric cancer surgery: morbidity and mortality results from a prospective randomized controlled trial comparing D2 and extended para-aortic lymphadenectomy--Japan Clinical Oncology Group study 9501. *J Clin Oncol,* 22, 2767-73.

SANSONE, P. et al. 2007. IL-6 triggers malignant features in mammospheres from human ductal breast carcinoma and normal mammary gland. *J Clin Invest,* 117, 3988-4002.

SASAKO, M. et al. 2006. Left thoracoabdominal approach versus abdominal-transhiatal approach for gastric cancer of the cardia or subcardia: a randomised controlled trial. *Lancet Oncol,* 7, 644-51.

SASTRE, J. et al. 2006. Chemotherapy for gastric cancer. *World J Gastroenterol,* 12, 204-13.

SERRANO, N. A. et al. 2012. Integrative analysis in oral squamous cell carcinoma reveals DNA copy number-associated miRNAs dysregulating target genes. *Otolaryngol Head Neck Surg,* 147, 501-8.

SETHI, A. et al. 2013. Role of miRNAs in CD4 T cell plasticity during inflammation and tolerance. *Front Genet,* 4, 8.

SEYFRIED, T. N. and HUYSENTRUYT, L. C. 2013. On the origin of cancer metastasis. *Crit Rev Oncog,* 18, 43-73.

SHACKELFORD, D. B. and SHAW, R. J. 2009. The LKB1-AMPK pathway: metabolism and growth control in tumour suppression. *Nat Rev Cancer,* 9, 563-75.

SHAH, M. A. et al. 2011. Phase II study of modified docetaxel, cisplatin, and fluorouracil with bevacizumab in patients with metastatic gastroesophageal adenocarcinoma. *J Clin Oncol,* 29, 868-74.

SHEN, J. et al. 2015. Epigenetic silencing of miR-490-3p reactivates the chromatin remodeler SMARCD1 to promote Helicobacter pylori-induced gastric carcinogenesis. *Cancer Res,* 75, 754-65.

SHERMAN, L. et al. 2002. Inhibition of serum- and calcium-induced terminal differentiation of human keratinocytes by HPV 16 E6: study of the association with p53 degradation, inhibition of p53 transactivation, and binding to E6BP. *Virology,* 292, 309-20.

SHERSHER, D. D. et al. 2011. Biomarkers of the insulin-like growth factor pathway predict progression and outcome in lung cancer. *Ann Thorac Surg,* 92, 1805-11; discussion 1811.

SHIBUE, T. and WEINBERG, R. A. 2017. EMT, CSCs, and drug resistance: the mechanistic link and clinical implications. *Nat Rev Clin Oncol,* 14, 611-629.

SHIEH, S. Y. et al. 1997. DNA damage-induced phosphorylation of p53 alleviates inhibition by MDM2. *Cell,* 91, 325-34.

SHIMOKAWA, T. et al. 1998. Hypocholesterolemic effects of the LDL receptor gene transcriptional upregulator CP-230821. *J Biochem,* 123, 596-601.

SHIN, V. Y. et al. 2015. A three-miRNA signature as promising non-invasive diagnostic marker for gastric cancer. *Mol Cancer,* 14, 202.

SHRESTHA, S. et al. 2014. A systematic review of microRNA expression profiling studies in human gastric cancer. *Cancer Med,* 3, 878-88.

SIDONI, A. et al. 1989. Changing patterns in gastric carcinoma. *Tumouri,* 75, 605-8.

SIEWERT, J. R. and STEIN, H. J. 1998. Classification of adenocarcinoma of the oesophagogastric junction. *Br J Surg,* 85, 1457-9.

SITARZ, R. et al. 2012. Gastroenterostoma after Billroth antrectomy as a premalignant condition. *World J Gastroenterol,* 18, 3201-6.

SITARZ, R. et al. 2018. Gastric cancer: epidemiology, prevention, classification, and treatment. *Cancer Manag Res,* 10, 239-248.

SMALLEY, S. R. et al. 2012. Updated analysis of SWOG-directed intergroup study 0116: a phase III trial of adjuvant radiochemotherapy versus observation after curative gastric cancer resection. *J Clin Oncol,* 30, 2327-33.

SMYTH, E. C. et al. 2016. Gastric cancer: ESMO Clinical Practice Guidelines for diagnosis, treatment and follow-up. *Ann Oncol,* 27, v38-v49.

SOGAARD, K. K. et al. 2016. Long-term risk of gastrointestinal cancers in persons with gastric or duodenal ulcers. *Cancer Med,* 5, 1341-51.

SOHN, B. H. et al. 2017. Clinical Significance of Four Molecular Subtypes of Gastric Cancer Identified by The Cancer Genome Atlas Project. *Clin Cancer Res*.

SOLCIA, E. et al. 2009. A combined histologic and molecular approach identifies three groups of gastric cancer with different prognosis. *Virchows Arch,* 455, 197-211.

SOMMER, H. and SANTI, D. V. 1974. Purification and amino acid analysis of an active site peptide from thymidylate synthetase containing covalently bound 5-fluoro-2'-deoxyuridylate and methylenetetrahydrofolate. *Biochem Biophys Res Commun,* 57, 689-95.

SONG, B. et al. 2009. Mechanism of chemoresistance mediated by miR-140 in human osteosarcoma and colon cancer cells. *Oncogene,* 28, 4065-74.

SONG, H. et al. 2015. Incidence of gastric cancer among patients with gastric precancerous lesions: observational cohort study in a low risk Western population. *BMJ,* 351, h3867.

SONG, J. H. et al. 2017. Risk Factors for Gastric Tumourigenesis in Underlying Gastric Mucosal Atrophy. *Gut Liver,* 11, 612-619.

SONG, J. H. and MELTZER, S. J. 2012. MicroRNAs in pathogenesis, diagnosis, and treatment of gastroesophageal cancers. *Gastroenterology,* 143, 35-47 e2.

SONG, M. Y. et al. 2012. Identification of serum microRNAs as novel non-invasive biomarkers for early detection of gastric cancer. *PLoS One,* 7, e33608.

SONGUN, I. et al. 2010. Surgical treatment of gastric cancer: 15-year follow-up results of the randomised nationwide Dutch D1D2 trial. *Lancet Oncol,* 11, 439-49.

SONNENBERG, A. 2011. Time trends of mortality from gastric cancer in Europe. *Dig Dis Sci,* 56, 1112-8.

SPICER D. 2009. FGF9 on the move. *Nature genetics*. 41, 272-273.

STARK, M. S. et al. 2015. miR-514a regulates the tumour suppressor NF1 and modulates BRAFi sensitivity in melanoma. *Oncotarget,* 6, 17753-63.

STEEVENS, J. et al. 2010. Alcohol consumption, cigarette smoking and risk of subtypes of oesophageal and gastric cancer: a prospective cohort study. *Gut,* 59, 39-48.

SU, Y. et al. 2012. Aberrant expression of microRNAs in gastric cancer and biological significance of miR-574-3p. *Int Immunopharmacol,* 13, 468-75.

SU, Y. et al. 2016. MicroRNA-140-5p targets insulin like growth factor 2 mRNA binding protein 1 (IGF2BP1) to suppress cervical cancer growth and metastasis. *Oncotarget,* 7, 68397-68411.

SUN, D. G. et al. 2017. miR-140-5p-mediated regulation of the proliferation and differentiation of human dental pulp stem cells occurs through the lipopolysaccharide/toll-like receptor 4 signaling pathway. *Eur J Oral Sci,* 125, 419-425.

SUN, M. et al. 2012. MiR-196a is upregulated in gastric cancer and promotes cell proliferation by downregulating p27(kip1). *Mol Cancer Ther,* 11, 842-52.

SUN J, et al. 2016. miR1405p regulates angiogenesis following ischemic stroke by targeting VEGFA. *Molecular medicine reports*. 13, 4499-4505.

SUZUKI, H. et al. 2016. High rate of 5-year survival among patients with early gastric cancer undergoing curative endoscopic submucosal dissection. *Gastric Cancer,* 19, 198-205.

SUZUKI, K. et al. 2006. Global DNA demethylation in gastrointestinal cancer is age dependent and precedes genomic damage. *Cancer Cell,* 9, 199-207.

SWAIN, S. M. et al. 1989. Fluorouracil and high-dose leucovorin in previously treated patients with metastatic breast cancer. *J Clin Oncol,* 7, 890-9.

SWINGLER, T. E. et al. 2012. The expression and function of microRNAs in chondrogenesis and osteoarthritis. *Arthritis Rheum,* 64, 1909-19.

SZKARADKIEWICZ, A. et al. 2006. Epstein-Barr virus (EBV) infection and p53 protein expression in gastric carcinoma. *Virus Res,* 118, 115-9.

TAKADA, K. 2000. Epstein-Barr virus and gastric carcinoma. *Mol Pathol,* 53, 255-61.

TAKAHASHI, K. and YAMANAKA, S. 2016. A decade of transcription factor-mediated reprogramming to pluripotency. *Nat Rev Mol Cell Biol,* 17, 183-93.

TAKATA, A. et al. 2011. MicroRNA-22 and microRNA-140 suppress NF-kappaB activity by regulating the expression of NF-kappaB coactivators. *Biochem Biophys Res Commun,* 411, 826-31.

TAKE, S. et al. 2007. Baseline gastric mucosal atrophy is a risk factor associated with the development of gastric cancer after Helicobacter pylori eradication therapy in patients with peptic ulcer diseases. *J Gastroenterol,* 42 Suppl 17, 21-7.

TAKE, S. et al. 2005. The effect of eradicating helicobacter pylori on the development of gastric cancer in patients with peptic ulcer disease. *Am J Gastroenterol,* 100, 1037-42.

TAMBE, M. et al. 2016. Novel Mad2-targeting miR-493-3p controls mitotic fidelity and cancer cells' sensitivity to paclitaxel. *Oncotarget,* 7, 12267-85.

TAMURA, G. et al. 1996. Inactivation of the E-cadherin gene in primary gastric carcinomas and gastric carcinoma cell lines. *Jpn J Cancer Res,* 87, 1153-9.

TAN, I. B. et al. 2011. Intrinsic subtypes of gastric cancer, based on gene expression pattern, predict survival and respond differently to chemotherapy. *Gastroenterology,* 141, 476-85, 485 e1-11.

TAN, X. et al. 2016. miR-671-5p inhibits epithelial-to-mesenchymal transition by downregulating FOXM1 expression in breast cancer. *Oncotarget,* 7, 293-307.

TAN, X. et al. 2011. A 5-microRNA signature for lung squamous cell carcinoma diagnosis and hsa-miR-31 for prognosis. *Clin Cancer Res,* 17, 6802-11.

TANG, Y. et al. 2017. lncRNA XIST interacts with miR-140 to modulate lung cancer growth by targeting iASPP. *Oncol Rep,* 38, 941-948.

TANNER, M. et al. 2005. Amplification of HER-2 in gastric carcinoma: association with Topoisomerase IIalpha gene amplification, intestinal type, poor prognosis and sensitivity to trastuzumab. *Ann Oncol,* 16, 273-8.

TAO, S. C. et al. 2017. Exosomes derived from miR-140-5p-overexpressing human synovial mesenchymal stem cells enhance cartilage tissue regeneration and prevent osteoarthritis of the knee in a rat model. *Theranostics,* 7, 180-195.

TARDIF, G. et al. 2009. Regulation of the IGFBP-5 and MMP-13 genes by the microRNAs miR-140 and miR-27a in human osteoarthritic chondrocytes. *BMC Musculoskelet Disord,* 10, 148.

TARDIF, G. et al. 2013. NFAT3 and TGF-beta/SMAD3 regulate the expression of miR-140 in osteoarthritis. *Arthritis Res Ther,* 15, R197.

TATARANO, S. et al. 2011. miR-218 on the genomic loss region of chromosome 4p15.31 functions as a tumour suppressor in bladder cancer. *Int J Oncol,* 39, 13-21.

TATEMICHI, M. et al. 2008. Different etiological role of Helicobacter pylori (Hp) infection in carcinogenesis between differentiated and undifferentiated gastric cancers: a nested case-control study using IgG titer against Hp surface antigen. *Acta Oncol,* 47, 360-5.

TAURINO, C. et al. 2010. Gene expression profiling in whole blood of patients with coronary artery disease. *Clin Sci (Lond),* 119, 335-43.

TCHERNITSA, O. et al. 2010. Systematic evaluation of the miRNA-ome and its downstream effects on mRNA expression identifies gastric cancer progression. *J Pathol,* 222, 310-9.

TERSMETTE, A. C. et al. 1990. Meta-analysis of the risk of gastric stump cancer: detection of high risk patient subsets for stomach cancer after remote partial gastrectomy for benign conditions. *Cancer Res,* 50, 6486-9.

TESTINO, G. 2011. The burden of cancer attributable to alcohol consumption. *Maedica (Buchar),* 6, 313-20.

TEY, J. et al. 2017. Palliative radiotherapy for gastric cancer: a systematic review and meta-analysis. *Oncotarget,* 8, 25797-25805.

The American Society for Gastrointestinal Endoscopy. 1988. The role of endoscopy in the surveillance of premalignant conditions of the upper gastrointestinal tract. Guidelines for clinical application. *Gastrointest Endosc,* 34, 18S-20S.

THORBURN, J. et al. 2014. Autophagy controls the kinetics and extent of mitochondrial apoptosis by regulating PUMA levels. *Cell Rep,* 7, 45-52.

THORPE, S. D. et al. 2010. The response of bone marrow-derived mesenchymal stem cells to dynamic compression following TGF-beta3 induced chondrogenic differentiation. *Ann Biomed Eng,* 38, 2896-909.

TIVNAN, A. et al. 2012. Inhibition of neuroblastoma tumour growth by targeted delivery of microRNA-34a using anti-disialoganglioside GD2 coated nanoparticles. *PLoS One,* 7, e38129.

TODORIC, J. et al. 2017. Stress-Activated NRF2-MDM2 Cascade Controls Neoplastic Progression in Pancreas. *Cancer Cell,* 32, 824-839 e8.

TORRE, L. A. et al. 2015. Global cancer statistics, 2012. *CA Cancer J Clin,* 65, 87-108.

TREECE, A. L. et al. 2016. Gastric adenocarcinoma microRNA profiles in fixed tissue and in plasma reveal cancer-associated and Epstein-Barr virus-related expression patterns. *Lab Invest,* 96, 661-71.

TSAI, K. W. et al. 2012. Aberrant expression of miR-196a in gastric cancers and correlation with recurrence. *Genes Chromosomes Cancer,* 51, 394-401.

TSAI, K. W. et al. 2011. Epigenetic regulation of miR-34b and miR-129 expression in gastric cancer. *Int J Cancer,* 129, 2600-10.

TSUJIURA, M. et al. 2015. Circulating miR-18a in plasma contributes to cancer detection and monitoring in patients with gastric cancer. *Gastric Cancer,* 18, 271-9.

TU, H. et al. 2014. Serum anti-Helicobacter pylori immunoglobulin G titer correlates with grade of histological gastritis, mucosal bacterial density, and levels of serum biomarkers. *Scand J Gastroenterol,* 49, 259-66.

UEDA, T. et al. 2010. Relation between microRNA expression and progression and prognosis of gastric cancer: a microRNA expression analysis. *Lancet Oncol,* 11, 136-46.

UEMURA, N. et al. 2001. Helicobacter pylori infection and the development of gastric cancer. *N Engl J Med,* 345, 784-9.

UNO, K. et al. 2016. Gastric cancer development after the successful eradication of Helicobacter pylori. *World J Gastrointest Oncol,* 8, 271-81.

USHIJIMA, T. and SASAKO, M. 2004. Focus on gastric cancer. *Cancer Cell,* 5, 121-5.

VALENZUELA-MUNOZ, V. et al. 2017. Modulation of Atlantic salmon miRNome response to sea louse infestation. *Dev Comp Immunol,* 76, 380-391.

VAN CUTSEM, E. et al. 2015. HER2 screening data from ToGA: targeting HER2 in gastric and gastroesophageal junction cancer. *Gastric Cancer,* 18, 476-84.

VAN CUTSEM, E. et al. 2011. The diagnosis and management of gastric cancer: expert discussion and recommendations from the 12th ESMO/World Congress on Gastrointestinal Cancer, Barcelona, 2010. *Ann Oncol,* 22 Suppl 5, v1-9.

VAN CUTSEM, E. et al. 2006. Phase III study of docetaxel and cisplatin plus fluorouracil compared with cisplatin and fluorouracil as first-line therapy for advanced gastric cancer: a report of the V325 Study Group. *J Clin Oncol,* 24, 4991-7.

VAN CUTSEM, E. et al. 2016. Gastric cancer. *Lancet,* 388, 2654-2664.

VAN CUTSEM, E. et al. 2008. Expert opinion on management of gastric and gastro-oesophageal junction adenocarcinoma on behalf of the European Organisation for Research and Treatment of Cancer (EORTC)-gastrointestinal cancer group. *Eur J Cancer,* 44, 182-94.

VAN LIER, M. G. et al. 2011. High cancer risk and increased mortality in patients with Peutz-Jeghers syndrome. *Gut,* 60, 141-7.

VASUDEVAN, S. et al. 2007. Switching from repression to activation: microRNAs can up-regulate translation. *Science,* 318, 1931-4.

VAZQUEZ-MARTIN, A. et al. 2013. Reprogramming of non-genomic estrogen signaling by the stemness factor SOX2 enhances the tumour-initiating capacity of breast cancer cells. *Cell Cycle,* 12, 3471-7.

VELLANKI, R. N. et al. 2010. OASIS/CREB3L1 induces expression of genes involved in extracellular matrix production but not classical endoplasmic reticulum stress response genes in pancreatic beta-cells. *Endocrinology,* 151, 4146-57.

VIDIGAL, J. A. and VENTURA, A. 2015. The biological functions of miRNAs: lessons from in vivo studies. *Trends Cell Biol,* 25, 137-47.

VINCENT, A. J. et al. 2012. Cytoplasmic translocation of p21 mediates NUPR1-induced chemoresistance: NUPR1 and p21 in chemoresistance. *FEBS Lett,* 586, 3429-34.

VOLINIA, S. et al. 2006. A microRNA expression signature of human solid tumours defines cancer gene targets. *Proc Natl Acad Sci U S A,* 103, 2257-61.

WADDELL, T. et al. 2013. Epirubicin, oxaliplatin, and capecitabine with or without panitumumab for patients with previously untreated advanced oesophagogastric cancer (REAL3): a randomised, open-label phase 3 trial. *Lancet Oncol,* 14, 481-9.

WADDELL, T. et al. 2014. Gastric cancer: ESMO-ESSO-ESTRO Clinical Practice Guidelines for diagnosis, treatment and follow-up. *Radiother Oncol,* 110, 189-94.

WADE, M. et al. 2013. MDM2, MDMX and p53 in oncogenesis and cancer therapy. *Nat Rev Cancer,* 13, 83-96.

WAGNER, A. D. et al. 2006. Chemotherapy in advanced gastric cancer: a systematic review and meta-analysis based on aggregate data. *J Clin Oncol,* 24, 2903-9.

WAGNER, A. D. et al. 2017. Chemotherapy for advanced gastric cancer. *Cochrane Database Syst Rev,* 8, CD004064.

WANG, K. et al. 2017. Analysis of microRNA (miRNA) expression profiles reveals 11 key biomarkers associated with non-small cell lung cancer. *World J Surg Oncol,* 15, 175.

WANG, M. et al. 2013. miR-17-5p/20a are important markers for gastric cancer and murine double minute 2 participates in their functional regulation. *Eur J Cancer,* 49, 2010-21.

WANG, Q. et al. 2014. Consumption of fruit, but not vegetables, may reduce risk of gastric cancer: results from a meta-analysis of cohort studies. *Eur J Cancer,* 50, 1498-509.

WANG, S. et al. 2017. Overaccumulation of p53-mediated autophagy protects against betulinic acid-induced apoptotic cell death in colorectal cancer cells. *Cell Death Dis,* 8, e3087.

WANG, W. H. et al. 2003. Non-steroidal anti-inflammatory drug use and the risk of gastric cancer: a systematic review and meta-analysis. *J Natl Cancer Inst,* 95, 1784-91.

WANG, X. et al. 2018. Exosomes Serve as Nanoparticles to Deliver Anti-miR-214 to Reverse Chemoresistance to Cisplatin in Gastric Cancer. *Mol Ther,* 26, 774-783.

WANG, Y. Y. et al. 2013. Clinicopathologic significance of miR-10b expression in gastric carcinoma. *Hum Pathol,* 44, 1278-85.

WANG, Z. et al. 2014. Predictive factors for lymph node metastasis in early gastric cancer with signet ring cell histology and their impact on the surgical strategy: analysis of single institutional experience. *J Surg Res,* 191, 130-3.

WATANABE, M. et al. 2012. Development of gastric cancer in nonatrophic stomach with highly active inflammation identified by serum levels of pepsinogen and Helicobacter pylori antibody together with endoscopic rugal hyperplastic gastritis. *Int J Cancer,* 131, 2632-42.

WEBLEY, S. D. et al. 2000. Deoxyuridine triphosphatase (dUTPase) expression and sensitivity to the thymidylate synthase (TS) inhibitor ZD9331. *Br J Cancer,* 83, 792-9.

WEI, D. Z. et al. 2017. Ellagic acid promotes ventricular remodeling after acute myocardial infarction by up-regulating miR-140-3p. *Biomed Pharmacother,* 95, 983-989.

WEI, R. et al. 2016. miR-140-5p attenuates chemotherapeutic drug-induced cell death by regulating autophagy through inositol 1,4,5-trisphosphate kinase 2 (IP3k2) in human osteosarcoma cells. *Biosci Rep,* 36.

WEN, Y. Y. et al. 2014. Association of the IL-1B +3954 C/T polymorphism with the risk of gastric cancer in a population in Western China. *Eur J Cancer Prev,* 23, 35-42.

WILKE, H. et al. 2014. Ramucirumab plus paclitaxel versus placebo plus paclitaxel in patients with previously treated advanced gastric or gastro-oesophageal junction adenocarcinoma (RAINBOW): a double-blind, randomised phase 3 trial. *Lancet Oncol,* 15, 1224-35.

WILLIAMS, B. et al. 1988. Do young patients with dyspepsia need investigation? *Lancet,* 2, 1349-51.

WOHLHUETER, R. M. et al. 1980. Facilitated transport of uracil and 5-fluorouracil, and permeation of orotic acid into cultured mammalian cells. *J Cell Physiol,* 104, 309-19.

WOLFSON, B. et al. 2014. Roles of microRNA-140 in stem cell-associated early stage breast cancer. *World J Stem Cells,* 6, 591-7.

WONG, N. and WANG, X. 2015. miRDB: an online resource for microRNA target prediction and functional annotations. *Nucleic Acids Res,* 43, D146-52.

WONG, S. S. et al. 2014. Genomic landscape and genetic heterogeneity in gastric adenocarcinoma revealed by whole-genome sequencing. *Nat Commun,* 5, 5477.

Wu K. et al. 2019. MicroRNA-140-5p inhibits cell proliferation, migration and promotes cell apoptosis in gastric cancer through the negative regulation of THY1-mediated Notch signaling. Bioscience reports. 39.

WU, J. et al. 2013. Up-regulation of microRNA-1290 impairs cytokinesis and affects the reprogramming of colon cancer cells. *Cancer Lett,* 329, 155-63.

XIAO, Q. et al. 2017. Overexpression of miR-140 Inhibits Proliferation of Osteosarcoma Cells via Suppression of Histone Deacetylase 4. *Oncol Res,* 25, 267-275.

XIE, M. et al. 2018. MicroRNA-1 acts as a tumour suppressor microRNA by inhibiting angiogenesis-related growth factors in human gastric cancer. *Gastric Cancer,* 21, 41-54.

XIE, W. B. et al. 2018. MiR-140 Expression Regulates Cell Proliferation and Targets PD-L1 in NSCLC. *Cell Physiol Biochem,* 46, 654-663.

XING, Y. et al. 2018. Comprehensive analysis of differential expression profiles of mRNAs and lncRNAs and identification of a 14-lncRNA prognostic signature for patients with colon adenocarcinoma. *Oncol Rep,* 39, 2365-2375.

XIONG, B. H. et al. 2014. An updated meta-analysis of randomized controlled trial assessing the effect of neoadjuvant chemotherapy in advanced gastric cancer. *Cancer Invest,* 32, 272-84.

XU, H. and EL-GEWELY, M. R. 2001. P53-responsive genes and the potential for cancer diagnostics and therapeutics development. *Biotechnol Annu Rev,* 7, 131-64.

XU, X. et al. 2013. miRNA: The nemesis of gastric cancer (Review). *Oncol Lett,* 6, 631-641.

XU, Y. et al. 2012. miR-21 Is a Promising Novel Biomarker for Lymph Node Metastasis in Patients with Gastric Cancer. *Gastroenterol Res Pract,* 2012, 640168.

XU, Z. Y. et al. 2015. 5-Fluorouracil chemotherapy of gastric cancer generates residual cells with properties of cancer stem cells. *Int J Biol Sci,* 11, 284-94.

YAMAGATA, H. et al. 2005. Impact of fasting plasma glucose levels on gastric cancer incidence in a general Japanese population: the Hisayama study. *Diabetes Care,* 28, 789-94.

YAMAMOTO, E. et al. 2011. Role of DNA methylation in the development of diffuse-type gastric cancer. *Digestion,* 83, 241-9.

YAMAMOTO, N. et al. 1994. Epstein-Barr virus and gastric remnant cancer. *Cancer,* 74, 805-9.

YAMASAKI, M. et al. 2010. p53 genotype predicts response to chemotherapy in patients with squamous cell carcinoma of the esophagus. *Ann Surg Oncol,* 17, 634-42.

YAN, C. et al. 2011. MicroRNA regulation associated chondrogenesis of mouse MSCs grown on polyhydroxyalkanoates. *Biomaterials,* 32, 6435-44.

YAN, H. et al. 2018. Aberrant Ki-67 expression through 3'UTR alternative polyadenylation in breast cancers. *FEBS Open Bio,* 8, 332-338.

YAN, L. X. et al. 2008. MicroRNA miR-21 overexpression in human breast cancer is associated with advanced clinical stage, lymph node metastasis and patient poor prognosis. *RNA,* 14, 2348-60.

YANAKA, Y. et al. 2015. miR-544a induces epithelial-mesenchymal transition through the activation of WNT signaling pathway in gastric cancer. *Carcinogenesis,* 36, 1363-71.

YANG, H. et al. 2013. MicroRNA-140-5p suppresses tumour growth and metastasis by targeting transforming growth factor beta receptor 1 and fibroblast growth factor 9 in hepatocellular carcinoma. *Hepatology,* 58, 205-17.

YANG, J. et al. 2017. Expression analysis of microRNA as prognostic biomarkers in colorectal cancer. *Oncotarget,* 8, 52403-52412.

YANG, J. et al. 2011. MiR-140 is co-expressed with Wwp2-C transcript and activated by Sox9 to target Sp1 in maintaining the chondrocyte proliferation. *FEBS Lett,* 585, 2992-7.

YANG, M. et al. 2011. Microvesicles secreted by macrophages shuttle invasion-potentiating microRNAs into breast cancer cells. *Mol Cancer,* 10, 117.

YANG, S. M. et al. 2013. miR-21 confers cisplatin resistance in gastric cancer cells by regulating PTEN. *Toxicology,* 306, 162-8.

YANG, Y. et al. 2015. Perioperative chemotherapy more of a benefit for overall survival than adjuvant chemotherapy for operable gastric cancer: an updated Meta-analysis. *Sci Rep,* 5, 12850.

YAO, Y. et al. 2009. MicroRNA profiling of human gastric cancer. *Mol Med Rep,* 2, 963-70.

YASUDA, K. et al. 2000. Papillary adenocarcinoma of the stomach. *Gastric Cancer,* 3, 33-38.

YCHOU, M. et al. 2011. Perioperative chemotherapy compared with surgery alone for resectable gastroesophageal adenocarcinoma: an FNCLCC and FFCD multicenter phase III trial. *J Clin Oncol,* 29, 1715-21.

YEH, J. M. et al. 2016. Gastric adenocarcinoma screening and prevention in the era of new biomarker and endoscopic technologies: a cost-effectiveness analysis. *Gut,* 65, 563-74.

YEPES, S. et al. 2016. Co-expressed miRNAs in gastric adenocarcinoma. *Genomics,* 108, 93-101.

YIN, Y. et al. 2015. Fibroblast Growth Factor 9 Regulation by MicroRNAs Controls Lung Development and Links DICER1 Loss to the Pathogenesis of Pleuropulmonary Blastoma. *PLoS Genet,* 11, e1005242.

YOO, J. K. et al. 2014. Discovery and characterization of miRNA during cellular senescence in bone marrow-derived human mesenchymal stem cells. *Exp Gerontol,* 58, 139-45.

YOSHIDA, A. et al 2017. MicroRNA-140 mediates RB tumour suppressor function to control stem cell-like activity through interleukin-6. *Oncotarget,* 8, 13872-13885.

YOSHIDA, S. and SAITO, D. 1996. Gastric premalignancy and cancer screening in high-risk patients. *Am J Gastroenterol,* 91, 839-43.

YOSHIOKA, A. et al. 1987. Deoxyribonucleoside triphosphate imbalance. 5-Fluorodeoxyuridine-induced DNA double strand breaks in mouse FM3A cells and the mechanism of cell death. *J Biol Chem,* 262, 8235-41.

YOU, W. C. et al. 1999. Evolution of precancerous lesions in a rural Chinese population at high risk of gastric cancer. *Int J Cancer,* 83, 615-9.

YOUN, H. G. et al. 2010. Recurrence after curative resection of early gastric cancer. *Ann Surg Oncol,* 17, 448-54.

YOUNG, K. H. et al. 2008. Structural profiles of TP53 gene mutations predict clinical outcome in diffuse large B-cell lymphoma: an international collaborative study. *Blood,* 112, 3088-98.

YU, J. et al. 2016. Septin 2 accelerates the progression of biliary tract cancer and is negatively regulated by mir-140-5p. *Gene,* 589, 20-26.

Yu J. et al. 2019. SNHG20/miR-140-5p/NDRG3 axis contributes to 5-fluorouracil resistance in gastric cancer. Oncology letters. 18,1337-1343.

YU, L. et al. 2016. microRNA -140-5p inhibits colorectal cancer invasion and metastasis by targeting ADAMTS5 and IGFBP5. *Stem Cell Res Ther,* 7, 180.

YUAN, Y. et al. 2013. miR-140 suppresses tumour growth and metastasis of non-small cell lung cancer by targeting insulin-like growth factor 1 receptor. *PLoS One,* 8, e73604.

ZALI, H. et al. 2011. Gastric cancer: prevention, risk factors and treatment. *Gastroenterol Hepatol Bed Bench,* 4, 175-85.

ZANGHIERI, G. et al. 1990. Familial occurrence of gastric cancer in the 2-year experience of a population-based registry. *Cancer,* 66, 2047-51.

ZARITSKY, A. et al. 2015. Seeds of Locally Aligned Motion and Stress Coordinate a Collective Cell Migration. *Biophys J,* 109, 2492-2500.

ZENG, Y. K. et al. 2012. Laparoscopy-assisted versus open distal gastrectomy for early gastric cancer: evidence from randomized and nonrandomized clinical trials. *Ann Surg,* 256, 39-52.

ZERTAL-ZIDANI, S. et al. 2007. Regulation of pancreatic endocrine cell differentiation by sulphated proteoglycans. *Diabetologia,* 50, 585-95.

ZHAI, H. et al. 2015. Inhibition of colorectal cancer stem cell survival and invasive potential by hsa-miR-140-5p mediated suppression of Smad2 and autophagy. *Oncotarget,* 6, 19735-46.

ZHANG, C. et al. 2017. Radioresistance of chordoma cells is associated with the ATM/ATR pathway, in which RAD51 serves as an important downstream effector. *Exp Ther Med,* 14, 2171-2179.

ZHANG, J. et al. 2018. The prognostic value of age in non-metastatic gastric cancer after gastrectomy: a retrospective study in the U.S. and China. *J Cancer,* 9, 1188-1199.

ZHANG, J. et al. 2015. Circulating MiR-16-5p and MiR-19b-3p as Two Novel Potential Biomarkers to Indicate Progression of Gastric Cancer. *Theranostics,* 5, 733-45.

ZHANG, K. et al. 2018. SNHG16/miR-140-5p axis promotes esophagus cancer cell proliferation, migration and EMT formation through regulating ZEB1. *Oncotarget,* 9, 1028-1040.

ZHANG, W. et al. 2015. MicroRNA-140-5p inhibits the progression of colorectal cancer by targeting VEGFA. *Cell Physiol Biochem,* 37, 1123-33.

ZHANG, X. et al. 2015. miR-140-5p regulates adipocyte differentiation by targeting transforming growth factor-beta signaling. *Sci Rep,* 5, 18118.

ZHANG, Y. et al. 2012. Estrogen receptor alpha signaling regulates breast tumour-initiating cells by down-regulating miR-140 which targets the transcription factor SOX2. *J Biol Chem,* 287, 41514-22.

ZHANG, Y. X. et al. 2016. Smad3-related miRNAs regulated oncogenic TRIB2 promoter activity to effectively suppress lung adenocarcinoma growth. *Cell Death Dis,* 7, e2528.

ZHAO, H. et al. 2016. The lncRNA H19 interacts with miR-140 to modulate glioma growth by targeting iASPP. *Arch Biochem Biophys,* 610, 1-7.

Zhao K, et al. 2018. Regulation of the Mdm2-p53 pathway by the ubiquitin E3 ligase MARCH7. *EMBO reports*. 19, 305-319.

ZHENG, H. C. et al. 2010. The pathobiological behaviors and prognosis associated with Japanese gastric adenocarcinomas of pure WHO histological subtypes. *Histol Histopathol,* 25, 445-52.

ZHOU, W. et al. 2015. MiR-493 suppresses the proliferation and invasion of gastric cancer cells by targeting RhoC. *Iran J Basic Med Sci,* 18, 1027-33.

ZHU, C. et al. 2014. A five-microRNA panel in plasma was identified as potential biomarker for early detection of gastric cancer. *Br J Cancer,* 110, 2291-9.

ZHU, G. et al. 2015. Identification of Gene and MicroRNA Signatures for Oral Cancer Developed from Oral Leukoplakia. *Biomed Res Int,* 2015, 841956.

ZHU, J. et al. 2016. Establishment of a miRNA-mRNA regulatory network in metastatic renal cell carcinoma and screening of potential therapeutic targets. *Tumour Biol*.

ZOMER, A. et al. 2010. Exosomes: Fit to deliver small RNA. *Commun Integr Biol,* 3, 447-50.

ZONG, L. et al. 2016. The challenge of screening for early gastric cancer in China. *Lancet,* 388, 2606.

ZOU, G. M. 2008. Cancer initiating cells or cancer stem cells in the gastrointestinal tract and liver. *J Cell Physiol,* 217, 598-604.

ZOU, J. and XU, Y. 2016. MicroRNA-140 Inhibits Cell Proliferation in Gastric Cancer Cell Line HGC-27 by Suppressing SOX4. *Med Sci Monit,* 22, 2243-52.

ZOU, M. X. et al. 2014. Identification of miR-140-3p as a marker associated with poor prognosis in spinal chordoma. *Int J Clin Exp Pathol,* 7, 4877-85.

ZUR HAUSEN, A. et al. 2004. Epstein-Barr virus in gastric carcinomas and gastric stump carcinomas: a late event in gastric carcinogenesis. *J Clin Pathol,* 57, 487-91.

Appendix

Appendix 1: Peking University Cancer Hospital Patients in Consent Information

Peking University Cancer Hospital
Patients in Consent Information

Name: Gender: Date of Birth: Department:

Dear patients,

In order to make your disease further understood, guarantee scientific research quality and improve the level of medical research, we would like to introduce how we use the Patient Sample to do medical research.

1. The importance of your specimens in medical research

1.1 For the benefit of your diagnosis and treatment, we would like to collect your specimens and blood in order to do necessary clinical examine through bioscopy or surgery.

1.2 If you permit, we would like to reserve the rest of your specimens and blood to do further medical research in order to make a full understanding of cancer and other diseases, and provide more evidence to medicine and treatment.

1.3 We hereby guarantee that we use the rest of your specimens and blood for medical research. This will not affect your examine, treatment and health.

1.4 The medical research is fully confidential. The research reports will not inform you and your doctor, and at the same time, it will not be saved in your personal healthy file.

2. Problems to be considered

2.1 We respect your decision, whether you agree or disagree to preserve your specimens, which will not affect your treatment.

2.2 You can make a decision now, and change your mind at any time. Please keep in touch with us and let us know your decision.

2.3 Your specimens will be used in the study of hereditary diseases; however, results will not be saved in your personal healthy file.

2.4 Your specimens may greatly contribute to research. However, you may not get benefit from them.

3. Benefits and Risks

3.1 The purpose of medical research is to make a contribution to all patients, and you will not get any financial benefit and welfare from them.

3.2 Your specimens and blood are important resources for the understanding of the development of diseases and exploration of effective methods of treatment.

[Date] 1

3.3 Your specimens and information will be preserved in the tissue bank of Peking University Cancer Hospital. All of your information will be coded with uniform numbers, and the basic information will be stored in electronic files in the computer. Only involvement of researchers, ethics committees and government officer of departments in charge can get access to your information, researchers and other staff collecting the clinical data will not know your information.

3.4 The risk of your participation in this study is that, within the progress of research, you and your health-related information may be accessible by other people besides researchers, ethics committees and government departments, but researchers will try to avoid it.

4. Please read the above information carefully and make your owe choice. If you have any questions, please feel free to contact our doctors and nurses or ethics committees.

My specimens are used for cancer prevention, diagnostics and scientific research, and at the same time, my clinical data can be associated with my specimens.

A. Agree **B. Disagree**

Patient's name: Date:

Doctor's name: Date:

Appendix 2: General compounds used in this study and their sources.

Material/Reagent	Supplier
Acetic acid	Fisher Scientific, Leicestershire, UK
Acrylamide mix (30%)	Sigma-Aldrich, Poole, Dorset, UK
Agarose	Melford Laboratories Ltd, Suffolk, UK
Ammonium Persulphate (APS)	Sigma-Aldrich, Poole, Dorset, UK
Ampicillin	Sigma-Aldrich, Poole, Dorset, UK
Bio-Rad DC™ Protein Assay	Bio-Rad Laboratories, Hercules, CA, USA
Bovine serum albumin (BSA)	Sigma-Aldrich, Poole, Dorset, UK
Calcium chloride ($CaCl_2$)	Sigma-Aldrich, Poole, Dorset, UK
Chloroform	Sigma-Aldrich, Poole, Dorset, UK
Crystal violet	Sigma-Aldrich, Poole, Dorset, UK
Diethylpyrocarbonate (DEPC)	Sigma-Aldrich, Poole, Dorset, UK
Dimethylsulphoxide (DMSO)	Sigma-Aldrich, Poole, Dorset, UK
Dulbecco's Modified Eagles' Medium/Nutrient mixture F12	Sigma-Aldrich, Poole, Dorset, UK
Ethylenediaminetetraacetic acid (EDTA)	Duchefa Biochemie, Haarlem, Netherlands
Ethanol	Fisher Scientific, Leicestershire, UK
10% Fetal calf serum (FCS)	PAA Laboratories, Coelbe, Germany
Formalin	Sigma-Aldrich Ltd, Dorset, UK
GoTaq® Green Master Mix	Promega
G418	
Hydrochloric acid (HCl)	Sigma-Aldrich, Poole, Dorset, UK
Isopropyl alcohol/isopropanol/2-propanol	Sigma-Aldrich, Poole, Dorset, UK
Matrigel®	BD Biosciences, Oxford, UK
Methanol	Fisher Scientific, Leicestershire, UK
Penicillin	Sigma-Aldrich, Poole, Dorset, UK
Peroxidase-conjugated goat anti-rabbit IgG	Sigma-Aldrich, Poole, Dorset, UK
Peroxidase-conjugated rabbit anti-mouse IgG	Sigma-Aldrich, Poole, Dorset, UK
Phenylmethyl sulfonyl fluoride (PMSF)	Sigma-Aldrich, Poole, Dorset, UK
Precision qScript™ RT PCR kit	Primerdesign Ltd, Southampton, UK
REDTaq® ReadyMix™ PCR Reaction Mix	Sigma-Aldrich, Poole, Dorset, UK
RPMI-1640	Sigma-Aldrich, Poole, Dorset, UK

Serum bovine albumin	Sigma-Aldrich, Poole, Dorset, UK
Sodium dodecyl sulphate (SDS)	Melford Laboratories Ltd, Suffolk, UK
Streptomycin	Sigma-Aldrich, Poole, Dorset, UK
SYBR®Safe DNA gel stain	Life Technologies Ltd, Paisley, UK
Tetramethylelthylenediamine (TEMED)	Sigma-Aldrich, Poole, Dorset, UK
TRI Reagent	Sigma-Aldrich, Poole, Dorset, UK
Tris-Cl	Melford Laboratories Ltd, Suffolk, UK
Triton X-100	Sigma-Aldrich, Poole, Dorset, UK
Trypsin	Sigma-Aldrich, Poole, Dorset, UK
Tween 20	Melford Laboratories Ltd, Suffolk, UK

Appendix 3: General plastic consumables, hardware, and software used in this study and their sources

Hardware/Software	Supplier
0.2 μm filtration unit	Sigma-Aldrich Co, Poole, Dorset, UK
$25cm^2$ and $75cm^2$ culture flasks	Cell Star, Germany
Image J	National Institute of Health
Lecia DM IRB microscope	Lecia GmbH, Bristol, UK
R software	http://www.r-project.org/
GraphPad Prism 6.0	San Diego, CA Software, La Jolla, CA
SPSS version 23.0	IBM Corporation, Armonk, NY, USA
Microsoft Excel	Microsoft In., Redmond, WA, USA
Neubauer hemocytometer counting chamber	Reichert, Austria
Protein spectrophotometer	BIO-TEK, Wolf Laboratories, York, UK
RNA spectrophotometer	BIO-TEK, Wolf Laboratories, York, UK
UV light chamber	Germix

Appendix 4: Amplifluor™ Universal detection system using UniPrimer™.

Source: The Scientist: https://www.the-scientist.com/.

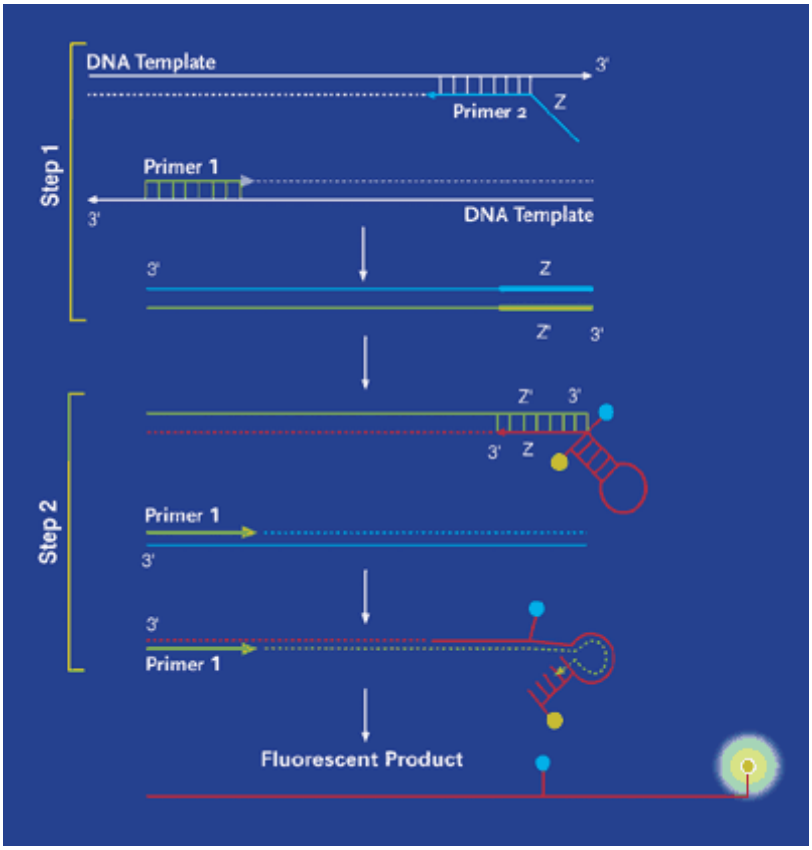

Appendix 5: Amplification plot and standard curve produced using qPCR.

A. Amplification plot showing an exponential increase in transcript copy number with cycle number B. Standard curve produced by plotting starting copy number against the cycle threshold (Ct). Source: The Scientist: https://www.the-scientist.com/

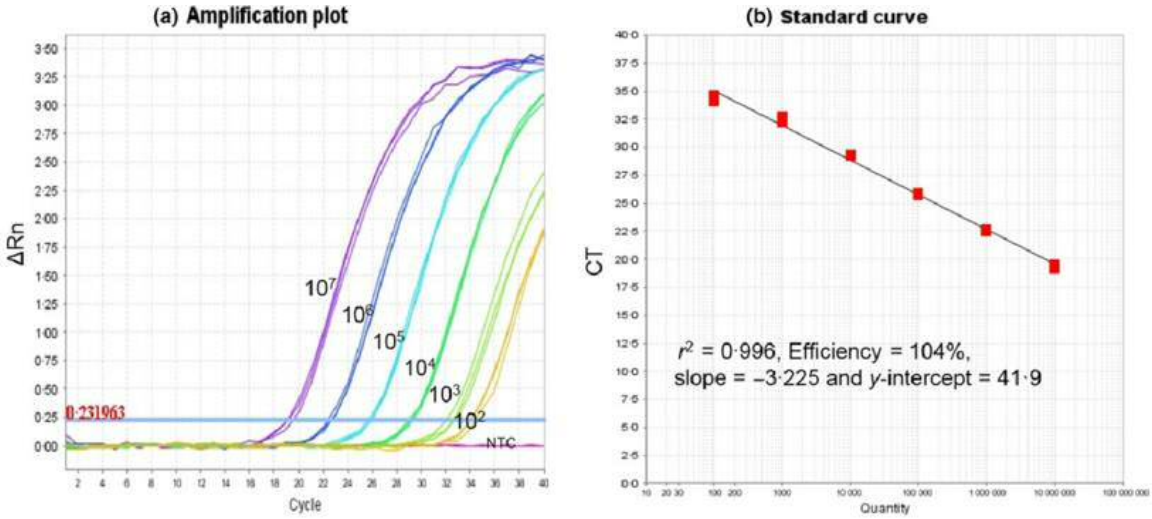

Appendix 6: Gastric Cancer Treatment Regimens.

[1]Category 2A: Based upon lower-level evidence, there is uniform NCCN consensus that the intervention is appropriate. [2]Category 1: Based upon the high-level evidence, there is uniform NCCN consensus that the intervention is appropriate. [3]Category 2B: Based upon lower-level evidence, there is NCCN consensus that the intervention is appropriate. Source: Gastrointestinal cancer advisor available at https://www.cancertherapyadvisor.com/gastrointestinal-cancers/gastric-cancer-treatment-regimens/article/218159/.

Preoperative Chemoradiation (esophagogastric junction and gastric cardia)[1]	
Note: All recommendations are Category 2A[1] unless otherwise indicated.	
Preferred Regimens	
REGIMEN	**DOSING**
Paclitaxel + carboplatin (Category 1)	**Day 1:** Paclitaxel 50mg/m^2 IV + carboplatin AUC 2mg·min/mL IV. Repeat cycle weekly for 5 weeks.
Cisplatin + 5FU (Category 1)	**Days 1 and 29:** Cisplatin 75–100mg/m^2 IV **Days 1–4 and 29–32:** 5FU 750–1000mg/m^2 continuous IV infusion over 24 hours daily. **Or** **Days 1–5:** Cisplatin 15mg/m^2 IV once daily + 5FU 800mg/m^{2}continuous IV infusion over 24 hours daily. Repeat cycle every 21 days for 2 cycles.
Oxaliplatin + 5FU (Category 1)	**Day 1:** Oxaliplatin 85mg/m^2 + leucovorin 400mg/m^2 + 5FU 400mg/m^{2}IV push **followed by** **Days 1–2:** 5FU 800mg/m^2 24-hour continuous infusion. Repeat cycle every 14 days for 3 cycles with radiation and 3 cycles after radiation.
Cisplatin + capecitabine	**Day 1:** Cisplatin 30mg/m^2 IV **Days 1–5:** Capecitabine 800mg/m^2 orally twice daily. Repeat cycle weekly for 5 weeks.
Oxaliplatin + capecitabine	**Days 1, 15, and 29:** Oxaliplatin 85mg/m^2 IV **Days 1–5:** Capecitabine 625mg/m^2 orally twice daily for 5 weeks.
Other Regimens	
Paclitaxel + 5FU (Category 2B)	**Day 1:** Paclitaxel 45–50mg/m^2 IV weekly **Days 1–5:** 5FU 300mg/m^2 IV continuous infusion. Repeat cycle weekly for 5 weeks.
Paclitaxel + capecitabine (Category 2B)	**Day 1:** Paclitaxel 45–50mg/m^2 IV **Days 1–5:** Capecitabine 625-825mg/m^2 orally twice daily. Repeat cycle weekly for 5 weeks.
Perioperative Chemotherapy (including esophagogastric junction)[1]	
Epirubicin + cisplatin + 5FU (ECF) (Category 2B)	**Day 1:** Epirubicin 50mg/m^2 IV bolus + cisplatin 60mg/m^2 IV **Days 1–21:** 5FU 200mg/m^2/day IV continuous infusion over 24 hours daily. Repeat cycle every 21 days for 3 cycles preoperatively and 3 cycles postoperatively.
ECF modification: epirubicin + oxaliplatin + 5FU (Category 2B)	**Day 1:** Epirubicin 50mg/m^2 IV + oxaliplatin 130mg/m^2 IV **Days 1–21:** 5FU 200mg/m^2/day IV continuous infusion over 24 hours. Repeat cycle every 21 days for 3 cycles preoperatively and 3 cycles postoperatively

ECF modification: epirubicin + cisplatin + capecitabine (Category 2B)	**Day 1:** Epirubicin 50mg/m^2 IV + cisplatin 60mg/m^2 IV **Days 1–21:** Capecitabine 625mg/m^2 orally twice daily. Repeat cycle every 21 days for 3 cycles preoperatively and 3 cycles postoperatively.
ECF modification: epirubicin + oxaliplatin + capecitabine (Category 2B)	**Day 1:** Epirubicin 50mg/m^2 IV + oxaliplatin 130mg/m^2 IV **Days 1–21:** Capecitabine 625mg/m^2 orally twice daily. Repeat cycle every 21 days for 3 cycles preoperatively and 3 cycles postoperatively.
5FU + cisplatin (Category 1)	**Day 1:** Cisplatin 75–80mg/m^2 IV **Days 1–5:** 5FU 800mg/m^2 IV continuous infusion over 24 hours daily. Repeat cycle every 28 days for 2–3 cycles preoperatively and 3–4 cycles postoperatively for a total of 6 cycles.
5FU + leucovorin + oxaliplatin	**Day 1:** Oxaliplatin 85mg/m^2 IV + leucovorin 400mg/m^2 + 5FU 400mg/m^2 IV push **followed by**: **Days 1–2:** 5FU 1200mg/m^2 continuous IV daily over 24 hours. **Or** **Day 1:** Oxaliplatin 85mg/m^2 + leucovorin 200mg/m^2 + 5FU 2600mg/m^2 continuous IV infusion over 24 hours. Repeat cycle every 14 days.
Capecitabine + oxaliplatin	**Day 1:** Oxaliplatin 130mg/m^2 IV **Days 1–14:** Capecitabine 1000mg/m^2 orally twice daily. Repeat cycle every 21 days.
Postoperative Chemoradiation (including esophagogastric junction)1	
5FU + leucovorin (Category 1)	**Cycles 1, 3, and 4 (before and after radiation)** **Days 1–5:** Leucovorin 20mg/m^2 IV push + 5FU 425mg/m^2/day IV push Repeat cycle every 28 days. **Cycle 2 (with radiation)** **Days 1–4 and 31–33:** Leucovorin 20mg/m^2 IV push **Days 1–4:** 5FU 400mg/m^2/day IV push. Repeat cycle every 35 days. The NCCN panel acknowledges that the Intergroup 0116 Trial formed the basis for postoperative adjuvant chemoradiation strategy. However, the panel does not recommend the above-specified doses or schedule of cytotoxic agents because of concerns regarding toxicity. The panel recommends one of the following modifications instead.
Capecitabine	**Days 1–14:** Capecitabine 750–1000mg/m^2 orally twice daily. Repeat cycle every 28 days; 1 cycle before and 2 cycles after chemoradiation.
5FU + leucovorin	**Days 1, 2, 15, and 16:** Leucovorin 400mg/m^2 IV followed by 5FU 400mg/m^2 IV push and a 24-hour infusion of 5FU 1200mg/m^2; 1 cycle before and 2 cycles after chemoradiation. Repeat cycle every 28 days.
5FU with radiation	**Days 1–5 OR Days 1–7:** 5FU 200–250mg/m^2 IV continuous infusion over 24 hours once daily; weekly for 5 weeks.
Capecitabine with radiation	**Days 1–5 OR Days 1–7:** Capecitabine 625–825mg/m^2 orally twice daily; weekly for 5 weeks.

Postoperative Chemotherapy (for patients who have undergone primary D2 lymph node dissection)	
Capecitabine + oxaliplatin (Category 1)	**Days 1–14:** Capecitabine 1000mg/m^2 orally twice daily **Day 1:** Oxaliplatin 130mg/m^2 IV. Repeat cycle every 21 days for 8 cycles.
Unresectable Locally Advanced, Recurrent or Metastatic Disease (where local therapy is not indicated)[1]	
First-line Therapy	
Trastuzumab + chemotherapy (NOTE: for HER2-neu overexpressing adenocarcinoma)	**Day 1:** Trastuzumab 8mg/kg IV loading dose (Cycle 1 only); **followed by** trastuzumab 6mg/kg IV every 3 weeks, plus chemotherapy **Or** **Day 1 of Cycle 1:** Trastuzumab 6mg/kg IV loading dose, then 4mg/kg IV every 14 days. **Chemotherapy:** **Day 1:** Cisplatin 80mg/m^2 IV, **plus** **Days 1–14:** Capecitabine 1000mg/m^2 orally twice daily. (Category 1) **Or** **Days 1–5:** 5FU 800mg/m^2 continuous IV infusion. (Category 2B) Repeat cycle every 21 days for 6 cycles.
Preferred Regimens	
Fluoropyrimidine and cisplatin (5FU + cisplatin) (Category 1)	**Day 1:** Cisplatin 75−100mg/m^2 IV **Days 1–4:** 5FU 750−1,000mg/m^2 IV continuous infusion over 24 hours daily.
Fluoropyrimidine and cisplatin (5FU + cisplatin + leucovorin) (Category 1)	**Day 1:** Cisplatin 50mg/m^2 IV + leucovorin 200mg/m^2 IV + 5FU 2,000mg/m^2 IV continuous infusion over 24 hours. Repeat cycle every 14 days.
Fluoropyrimidine and cisplatin (capecitabine + cisplatin) (Category 1)	**Day 1:** Cisplatin 80mg/m^2 IV **Days 1–14:** Capecitabine 1000mg/m^2 orally twice daily. Repeat cycle every 3 weeks.
Fluoropyrimidine and oxaliplatin (oxaliplatin + capecitabine)	**Day 1:** Oxaliplatin 130mg/m^2 IV **Days 1–14:** Capecitabine 1000mg/m^2 orally twice daily. Repeat cycle every 21 days.
Fluoropyrimidine and oxaliplatin (oxaliplatin + leucovorin + 5FU)	**Day 1:** Oxaliplatin 85mg/m^2 IV + leucovorin 400mg/m^2 IV + 5FU 400mg/m^2 IVP **Days 1−2:** 5FU 1200mg/m^2 IV continuous infusion over 24 hours daily. Repeat cycle every 14 days. **Or** **Day 1:** Oxaliplatin 85mg/m^2 IV + leucovorin 200mg/m^2 IV + 5FU 2,600mg/m^2 IV continuous infusion over 24 hours. Repeat cycle every 14 days.
Other Regimens	
Modified DCF (docetaxel + cisplatin + leucovorin + 5FU)	**Day 1:** Docetaxel 40mg/m^2 IV + leucovorin 400mg/m^2 IV + 5FU 400mg/m^2 IV **Days 1−2:** 5FU 1000mg/m^2 IV continuous infusion over 24 hours **Day 3:** Cisplatin 40mg/m^2 IV. Repeat cycle every 14 days.

Modified DCF (docetaxel + oxaliplatin + 5FU)	**Day 1:** Docetaxel 50mg/m^2 IV + oxaliplatin 85mg/m^2 IV **Days 1−2:** 5FU 1,200mg/m^2 IV continuous infusion over 24 hours. Repeat cycle every 14 days.
Modified DCF (docetaxel + carboplatin + 5FU) (Category 2B)	**Day 1:** Docetaxel 75mg/m^2 IV **Day 2:** Carboplatin AUC 6mg·min/mL IV **Days 1–3:** 5FU 1,200mg/m^2 IV continuous infusion over 24 hours daily. Repeat cycle every 21 days.
ECF (Category 2B)	**Day 1:** Epirubicin 50mg/m^2 IV bolus + cisplatin 60mg/m^2 IV **Days 1–21:** 5FU 200mg/m^2 IV continuous infusion over 24 hours daily. Repeat cycle every 21 days.
ECF modifications (epirubicin + oxaliplatin + 5FU) (Category 2B)	**Day 1:** Epirubicin 50mg/m^2 IV + oxaliplatin 130mg/m^2 IV **Days 1–21:** 5FU 200mg/m^2 IV continuous infusion over 24 hours. Repeat cycle every 21 days.
ECF modifications (epirubicin + cisplatin + capecitabine) (Category 2B)	**Day 1:** Epirubicin 50mg/m^2 IV + cisplatin 60mg/m^2 IV **Days 1–21:** Capecitabine 625mg/m^2 orally twice daily. Repeat cycle every 21 days.
ECF modifications (epirubicin + oxaliplatin + capecitabine) (Category 2B)	**Day 1:** Epirubicin 50mg/m^2 IV + oxaliplatin 130mg/m^2 IV **Days 1–21:** Capecitabine 625mg/m^2 IV orally twice daily. Repeat cycle every 21 days.
Fluorouracil and irinotecan (irinotecan + leucovorin + 5FU)	**Day 1:** Irinotecan 180mg/m^2 IV + leucovorin 400mg/m^2 IV + 5FU 400mg/m^2 IV push **followed by** **Day 1−2:** 5FU 1200mg/m^2 IV continuous infusion over 24 hours daily. Repeat cycle every 14 days.
Paclitaxel + cisplatin or carboplatin	**Day 1:** Paclitaxel 135–200mg/m^2 IV **Day 2:** Cisplatin 75mg/m^2 IV. Repeat cycle every 21 days. **Or** **Day 1:** Paclitaxel 90mg/m^2 IV + cisplatin 50mg/m^2 IV. Repeat cycle every 14 days. **Or** **Day 1:** Paclitaxel 200mg/m^2 IV + carboplatin AUC 5mg·min/mL IV. Repeat cycle every 21 days.
Docetaxel + cisplatin	**Day 1:** Docetaxel 70–85mg/m^2 IV + cisplatin 70–75mg/m^2 IV. Repeat cycle every 21 days.
Fluoropyridimine	**Day 1:** Leucovorin 400mg/m^2 IV + 5FU 400mg/m^2 IV push **Days 1−2:** 5FU 1200mg/m^2 IV continuous infusion over 24 hours daily. Repeat cycle every 14 days. **Or** **Days 1–5:** 5FU 800mg/m^2 IV continuous infusion over 24 hours daily. Repeat cycle every 28 days. **Or** **Days 1–14:** Capecitabine 1000–1250mg/m^2 orally twice daily. Repeat cycle every 21 days.
Taxane	**Day 1:** Docetaxel 75–100mg/m^2 IV. Repeat cycle every 21 days. **Or**

	Day 1: Paclitaxel 135–250mg/m^2 IV. Repeat cycle every 21 days. **Or** **Days 1, 8, 15 and 22:** Paclitaxel 80mg/m^2 IV once weekly. Repeat cycle every 28 days.
Second-line Therapy and Subsequent Therapy	
Preferred Regimens	
Ramucirumab (Category 1[2])	**Day 1:** Ramucirumab 8mg/kg IV. Repeat cycle every 14 days.
Ramucirumab + paclitaxel (Category 1)	**Day 1 and 15:** Ramucirumab 8mg/kg IV **Day 1, 8, and 15:** Paclitaxel 80mg/m^2. Repeat cycle every 28 days.
Docetaxel (Category 1)	**Day 1:** Docetaxel 75–100mg/m^2 IV. Repeat cycle every 21 days.
Paclitaxel (Category 1)	**Day 1:** Paclitaxel 135–250mg/m^2 IV. Repeat cycle every 21 days. **Or** **Day 1:** Paclitaxel 80mg/m^2 IV once weekly. Repeat cycle every 28 days. **Or** **Days 1, 8, and 15:** Paclitaxel 80mg/m^2 IV. Repeat cycle every 28 days.
Irinotecan (Category 1)	**Day 1:** Irinotecan 250–350mg/m^2 IV. Repeat cycle every 21 days. **Or** **Day 1:** Irinotecan 150–180mg/m^2 IV. Repeat cycle every 14 days. **Or** **Days 1 and 8:** Irinotecan 125mg/m^2 IV. Repeat cycle every 21 days.
5FU + irinotecan (if not previously used in first-line therapy)	**Day 1:** Irinotecan 180mg/m^2 IV + leucovorin 400mg/m^2 IV + 5FU 400mg/m^2 IV push **followed by** **Day 1 and 2:** 5FU 1200mg/m^2 IV continuous infusion over 24 hours daily. Repeat cycle every 14 days.
Other Regimens	
Irinotecan + cisplatin	**Days 1 and 8:** Irinotecan 65mg/m^2 IV + cisplatin 25–30mg/m^2 IV. Repeat cycle every 21 days.
Docetaxel + irinotecan (Category 2B[3])	**Days 1 and 8:** Docetaxel 35mg/m^2 IV + irinotecan 50mg/m^2 IV. Repeat cycle every 21 days.
Pembrolizumab (for second-line or subsequent therapy for MSI-H/dMMR tumours; for third-line or subsequent therapy for PD-L1-positive adenocarcinoma)	**Days 1:** Pembrolizumab 200 mg IV. Repeat cycle every 21 days.

Appendix 7: Characteristics of miRNA datasets in human gastric cancer.

Modified from A systematic review of microRNA expression profiling studies in human gastric cancer(Shrestha et al. 2014). miRNAs over twofold change provided [1] Formalin-fixed, paraffin-embedded tissues of H. pylori-positive (n=8) or H. pylori-negative (n=8) patients with an intestinal type of gastric cancer. GNCA, gastric non-cardia adenocarcinoma; GCI, gastric cancer intestinal; GCD, gastric cancer diffused, NR, not reported.

Dataset	Year	Region	Tumour type	No. of samples (cancer/normal)	Platform (manufacturer)	Total miRNA	Differentially expressed miRNAs			
							Criteria	Up	Down	Total
Wang (Y. Y. Wang et al. 2013)	2013	China	NR	17 Tissue specimen	miRCURY LNA Array (v.16.0; Exiqon, Vedbaek, Denmark)	564	FC > 2, FC < 1.5	49	39	154
Katada (Katada et al. 2009)	2009	Japan	GCD	84 (42/42)	TaqMan PCR kit protocol on an Applied Biosystems 7500 real-time PCR System	72	FC > 2, FC < 0.5	3	3	72
Hyun (Chang et al. 2015)	2015	Korea	GCI	16 (8/8)[1] Tissue specimen	Microarray (Agilent Technologies, Palo Alto, CA, USA); TaqMan miRNA assays.	3523	FC > 2, $P < 0.05$	18	19	219
KAZUHIRO (Osawa et al. 2011)	2011	Japan	NR	74 (37/37)	Toray 3D-Gene® miRNA oligo chip (Toray Industries)	885	T/N ratio >1.40, <0.85, $P < 0.05$	30	11	41
Zhu (Zhu et al. 2014)	2014	China	GNCA	80 (40/40)	TaqMan low density array (TLDA) chips (V2.0; Applied Biosystems, Foster city, CA, USA)	667	FC > 4	5	NR	NR

Carvalho (Carvalho et al. 2012)	2012	Netherlands	GCI	47 (37/10) Tissue specimen	miRNAChip_human_v2 (National DNA-Microarray Facility, University of Aveiro, Portugal)	703	$P < 0.05$, FDR < +0.05	5	5	70
Kim (Kim et al. 2011)	2011	Korea	GCI, GCD	124 (90/34) Tissue specimen	LMT miRNA microarray (Agilent technologies)	1667	$P < 0.005$	62	63	125
Li (X. Li et al. 2011a)	2011	China	GCI	12 (6/6) Tissue specimen	miRCURY Array LNA microRNA Chip (v.14.0) (Exiqon)	904	$P < 0.01$ FC > 2	40	36	76
Li (X. Li et al. 2011b)	2011	China	NR	20 (10/10) Tissue specimen	TaqMan Human miRNA Array v1.0 (Applied Biosystems)	365	$P < 0.05$	16	6	22
Oh (Oh et al. 2011)	2011	Singapore	GCI, GCD	80 (40/40) Tissue specimen	Agilent Human miRNA Microarrays (V2, Agilent)	723	FDR < 0.01	40	40	146
Tchernitsa (Tchernitsa et al. 2010)	2010	Germany	GCI	12 (6/6) Tissue specimen	NCode TM MultiSpecies miRNA Microarray V1 (Invitrogen)	373	Significance of class comparison = 0.05	20	2	22
Ding (Ding et al. 2010)	2010	China	GCI, GCD	12 (6/6) Tissue specimen	μParaflo microfluidic chip (LC Sciences)	NR	$P < 0.05$	8	7	15
Tsukamoto	2010	Japan	GCI, GCD	27 (22/5) Tissue specimen	G4470A Human MiRNA Microarray (Agilent technologies)	470	$P < 0.05$	33	6	102
Ueda (Ueda et al. 2010)	2010	Japan	GCI, GCD	353 (184/169) Tissue specimen	microRNA microarray chip (OSU_CCC version 3.0, ArrayExpress)	326	$P < 0.01$	22	13	35

Yao (Yao et al. 2009)	2009	China	NR	6 (3/3) Tissue specimen	miRCURY LNA microarray Array (v.11.0) (Exiqon)	847	FC > 2	59	46	326
Luo (Luo et al. 2009)	2009	China	NR	27 (24/3) Tissue specimen	NR	328	$P < 0.05$	7	19	26
Liu (Liu et al. 2009)	2009	China	NR	8 (4/4) Tissue specimen	microRNA Microarray (Packard Biochip Technologies ScanArray Express microarray)	243	$P < 0.05$	4	5	9
Petrocca (Petrocca et al. 2008)	2008	Italy	GCI	40 (20/20) Tissue specimen	second generation miRNA microarray chips (V2) (Amersham BioScience Codelink)	250	Significance analysis of microarray (SAM)	14	5	19
Volinia (Volinia et al. 2006)	2006	USA	NR	41 (20/21) Tissue specimen	miRNA microarray (Amersham BioScience Codelink)	190	FDR=0.06	22	6	28

Appendix 8: List of overlapping differentially expressed miRNAs in gastric cancer.

MicroRNAs in blue denote the overlapped miRNAs in current and Bowen *et al.* 's analysis (Conesa et al. 2016). * denotes that the microRNAs were reported in Sirjana *et al.*'s vote ranking review as well. ^ denotes deregulated miRNA in the same trend in both Ding *et al.*'s analysis (Ding et al. 2017) and Shrestha *et al.*'s (Shrestha et al. 2014). # denotes differentially expressed. miRNAs with an opposite change pattern between current analysis and Sirjana *et al.*'s.

DESeq2 et al. based analysis in the current study			
miRNA	**Base Mean**	**log2 Fold Change**	**P value**
hsa-mir-490*	96.4754	-3.3	4.38E-15
hsa-mir-133a-2	333.696	-3.2	1.53E-24
hsa-mir-133a-1	365.503	-3.1	1.70E-24
hsa-mir-944	8.48945	-3	4.17E-15
hsa-mir-1-1	261.397	-3	1.35E-22
hsa-mir-1-2	277.487	-3	1.76E-22
hsa-mir-5683	16.0219	-2.9	5.11E-20
hsa-mir-133b*	95.3475	-2.8	5.22E-19
hsa-mir-383	4.61665	-2.5	1.67E-12
hsa-mir-205	779.212	-2.5	4.49E-05
hsa-mir-145	22605.5	-2.4	1.30E-29
hsa-mir-139*	253.038	-2.3	1.62E-42
hsa-mir-143	1118321	-2.1	1.41E-22
hsa-mir-551b	6.17111	-2	1.09E-16
hsa-mir-204	27.1713	-1.9	1.75E-10
hsa-mir-29c*	17565.9	-1.8	3.17E-23
hsa-mir-1258	4.319	-1.7	6.25E-10
hsa-mir-6720	6.07512	-1.6	5.16E-12
hsa-mir-129-1	17.087	-1.6	1.10E-08
hsa-mir-129-2	20.1071	-1.6	2.35E-08
hsa-mir-195	167.322	-1.6	1.23E-24
hsa-mir-486-2	236.69	-1.6	1.31E-15
hsa-mir-486-1	241.67	-1.6	1.94E-15
hsa-mir-605	1.29341	-1.5	2.24E-11

edgeRv based analysis in Bowen's study					
miRNA	**logFC**	**logCPM**	**LR**	**P value**	**FDR**
hsa-mir-490*	-4.8051	5.883648	227.3672	2.24E-51	3.37E-49
hsa-mir-1-2	-3.52462	8.462458	179.2811	6.96E-41	5.24E-39
hsa-mir-133a-1	-3.47009	7.686724	189.3515	4.40E-43	4.98E-41
hsa-mir-133b*	-3.43591	4.882301	180.3691	4.03E-41	3.64E-39
hsa-mir-133a-2	-3.28029	2.878416	142.2048	8.77E-33	3.60E-31
hsa-mir-383	-2.58313	1.372154	65.92232	4.69E-16	1.18E-14
hsa-mir-139*	-2.56445	6.924574	144.909	2.25E-33	1.02E-31
hsa-mir-1-1	-2.5258	-0.29066	42.01943	9.04E-11	1.10E-09
hsa-mir-204	-2.51743	3.768183	101.6399	6.66E-24	2.32E-22
hsa-mir-145	-2.43625	13.4502	68.19737	1.48E-16	4.18E-15
hsa-mir-129-1	-2.37581	3.5062	86.67324	1.28E-20	4.13E-19
hsa-mir-137	-2.17364	0.549852	39.20199	3.82E-10	4.11E-09
hsa-mir-187	-2.15428	3.835279	61.5645	4.28E-15	9.22E-14
hsa-mir-9-3	-2.10139	0.276495	41.2004	1.37E-10	1.55E-09
hsa-mir-129-2	-2.0211	3.623788	64.84779	8.09E-16	1.92E-14
hsa-mir-885	-1.99205	-0.00875	29.71627	5.00E-08	3.37E-07
hsa-mir-486	-1.98119	7.630246	78.75621	7.03E-19	2.12E-17
hsa-mir-1258	-1.91162	1.044307	41.40072	1.24E-10	1.44E-09
hsa-mir-9-2	-1.86005	8.839239	58.76241	1.78E-14	3.66E-13
hsa-mir-9-1	-1.84622	8.838711	57.91596	2.74E-14	5.38E-13
hsa-mir-143	-1.8152	19.02113	26.76652	2.30E-07	1.30E-06
hsa-mir-206	-1.79548	0.553828	28.00989	1.21E-07	7.18E-07
hsa-mir-605	-1.70801	-0.18536	24.60363	7.04E-07	3.42E-06
hsa-mir-23c	-1.65737	0.656976	33.62034	6.70E-09	5.41E-08

hsa-mir-202	2.27267	-1.5	5.92E-07
hsa-mir-365b	253.656	-1.5	3.01E-38
hsa-mir-365a	253.876	-1.5	3.12E-38
hsa-mir-203a	47749.9	-1.5	9.50E-10
hsa-mir-30a	75745.6	-1.5	5.11E-19
hsa-mir-149	75.7773	-1.4	9.85E-12
hsa-mir-187	44.3908	-1.3	0.00051
hsa-mir-218-2	65.653	-1.3	1.04E-12
hsa-mir-218-1	69.2889	-1.3	1.84E-12
hsa-mir-451a	1881.71	-1.3	6.28E-10
hsa-let-7c	9049.56	-1.3	3.37E-08
hsa-mir-100#	20309.1	-1.3	4.07E-09
hsa-mir-378d-2	2.39748	-1.2	2.04E-08
hsa-mir-504	2.67883	-1.2	2.67E-06
hsa-mir-6511b-2	3.468	-1.2	9.24E-13
hsa-mir-144	428.623	-1.2	7.41E-08
hsa-mir-28	21953.9	-1.2	9.13E-25
hsa-mir-3199-2	2.55187	-1.1	2.09E-11
hsa-mir-4786	3.44811	-1.1	1.19E-07
hsa-mir-363	32.9539	-1.1	6.54E-07
hsa-mir-378c	48.7569	-1.1	4.40E-14
hsa-mir-193a	624.346	-1.1	8.69E-21
hsa-mir-125b-1	1025.14	-1.1	7.99E-09
hsa-mir-125b-2	1076.54	-1.1	8.85E-09
hsa-mir-125a	1597.74	-1.1	1.27E-20
hsa-mir-378a	3824.24	-1.1	1.71E-15
hsa-let-7e	4583.89	-1.1	5.29E-11
hsa-mir-23b	10354	-1.1	5.05E-20
hsa-mir-27b	13371.1	-1.1	4.86E-26
hsa-mir-378d-1	1.80983	-1	6.40E-06
hsa-mir-1262	3.89914	-1	2.39E-09
hsa-mir-153-1	8.8946	-1	4.45E-05

hsa-mir-30a	-1.65228	14.39009	35.24595	2.91E-09	2.58E-08
hsa-mir-144	-1.6373	7.165103	56.44918	5.77E-14	1.09E-12
hsa-mir-363	-1.6186	3.370372	46.60951	8.66E-12	1.22E-10
hsa-mir-202	-1.60021	0.505004	26.81042	2.24E-07	1.28E-06
hsa-mir-149	-1.56676	4.789035	49.14688	2.37E-12	3.70E-11
hsa-mir-99a	-1.53989	9.092692	39.06369	4.10E-10	4.21E-09
hsa-mir-100#	-1.5395	12.16728	30.5749	3.21E-08	2.30E-07
hsa-mir-551b	-1.50979	2.030806	29.24939	6.36E-08	4.17E-07
hsa-mir-20b^	-1.4901	4.066006	39.32045	3.60E-10	3.96E-09
hsa-mir-365-1	-1.45572	4.578685	47.35135	5.93E-12	8.94E-11
hsa-mir-29c*	-1.45217	12.17281	31.27397	2.24E-08	1.63E-07
hsa-mir-218-2	-1.43116	5.544884	44.19166	2.98E-11	3.85E-10
hsa-mir-451	-1.41848	9.482372	31.30019	2.21E-08	1.63E-07
hsa-mir-365-2	-1.4117	4.593021	44.94708	2.02E-11	2.69E-10
hsa-mir-195	-1.38402	6.196652	46.34211	9.93E-12	1.36E-10
hsa-let-7c	-1.37102	11.10562	25.06968	5.53E-07	2.75E-06
hsa-mir-378^	-1.3524	9.977656	33.84618	5.96E-09	4.90E-08
hsa-mir-378c	-1.34841	3.995761	37.56583	8.84E-10	8.68E-09
hsa-mir-504	-1.34318	0.518477	21.00924	4.57E-06	1.93E-05
hsa-mir-1247	-1.31901	4.444355	32.06739	1.49E-08	1.14E-07
hsa-mir-802	-1.30525	2.120566	8.819754	0.00298	0.006907
hsa-mir-101-2	-1.238	5.831003	37.49146	9.18E-10	8.83E-09
hsa-mir-125b-1	-1.22699	9.332394	25.33243	4.83E-07	2.49E-06
hsa-mir-125b-2	-1.19928	4.172908	25.12644	5.37E-07	2.70E-06
hsa-mir-1262	-1.19894	0.628874	18.60011	1.61E-05	6.12E-05
hsa-mir-1224	-1.1755	4.110555	13.78066	0.000205	0.000611
hsa-mir-28	-1.16295	12.74368	20.38194	6.34E-06	2.61E-05
hsa-mir-23b	-1.14816	10.70065	23.39329	1.32E-06	6.22E-06
hsa-mir-218-1	-1.13081	0.310216	12.81953	0.000343	0.001
hsa-mir-125a	-1.12163	8.957969	26.09095	3.26E-07	1.77E-06
hsa-mir-328	-1.08873	4.505851	25.32157	4.85E-07	2.49E-06
hsa-mir-3678	-1.06929	-0.46024	9.381958	0.002191	0.005297

hsa-mir-326			
hsa-mir-328	23.785	-1	2.55E-09
hsa-mir-497	66.3037	-1	4.19E-12
hsa-mir-381	85.8655	-1	4.83E-12
hsa-mir-30c-2	193.556	-1	7.00E-14
hsa-mir-99a	1442.18	-1	2.50E-20
hsa-mir-140	2829.08	-1	0.00011
hsa-mir-26a-1	3622.47	-1	3.36E-20
hsa-mir-26a-2	3747.54	-1	2.76E-25
hsa-mir-4640	3762.93	-1	1.58E-24
hsa-mir-3664	0.93441	1	0.00215
hsa-mir-4709	1.78673	1	0.00128
hsa-mir-219b	1.82011	1	5.84E-05
hsa-mir-4660	1.88076	1	0.00011
hsa-mir-3117	2.13797	1	0.00031
hsa-mir-3922	2.54896	1	9.46E-05
hsa-mir-550a-3	2.55428	1	0.00014
hsa-mir-616	5.6589	1	6.82E-07
hsa-mir-323b	11.9804	1	1.58E-05
hsa-mir-421	12.6471	1	5.90E-05
hsa-mir-34c	12.839	1	1.97E-10
hsa-mir-95	15.742	1	1.06E-08
hsa-mir-500b	26.4724	1	1.14E-06
hsa-mir-362	68.0902	1	2.29E-13
hsa-mir-222	68.414	1	9.27E-12
hsa-mir-106b*	386.191	1	3.26E-13
hsa-mir-181a-1	2069.48	1	8.98E-22
hsa-mir-532	2251.98	1	4.21E-20
hsa-mir-200c	4282.56	1	5.06E-16
hsa-mir-548k	33728.2	1	1.49E-09
hsa-mir-3680-1	0.90486	1.1	0.00063
hsa-mir-5703	0.94644	1.1	0.00098

hsa-mir-193a					
hsa-mir-497	-1.06783	7.615196	26.51488	2.62E-07	1.46E-06
hsa-mir-381	-1.05245	4.887338	25.87917	3.63E-07	1.96E-06
hsa-mir-30c-2	-1.04833	5.898908	27.794	1.35E-07	7.92E-07
hsa-mir-3199-2	-1.01405	9.079368	21.95033	2.80E-06	1.22E-05
hsa-mir-579	-1.01231	0.049924	11.01296	0.000905	0.00242
hsa-mir-500b	1.003594	0.173085	10.04165	0.00153	0.003864
hsa-mir-1301	1.01082	2.853586	19.51406	9.99E-06	3.96E-05
hsa-mir-19b-1	1.013281	2.662935	19.28604	1.13E-05	4.42E-05
hsa-mir-3690	1.017658	2.760713	19.80815	8.56E-06	3.46E-05
hsa-mir-33b	1.019013	-0.45859	7.58355	0.00589	0.012157
hsa-mir-200c	1.06251	2.191573	17.20339	3.36E-05	0.000119
hsa-mir-181b-2	1.123707	12.62303	13.92546	0.00019	0.000573
hsa-mir-3682	1.131267	1.465516	18.29105	1.90E-05	7.08E-05
hsa-mir-1304	1.133584	0.095028	13.76865	0.000207	0.000611
hsa-mir-19a*	1.158205	0.530508	14.85341	0.000116	0.000378
hsa-mir-4326	1.169756	4.440135	29.28147	6.26E-08	4.16E-07
hsa-mir-1537	1.178167	2.60476	22.28298	2.35E-06	1.03E-05
hsa-mir-335*	1.196737	-0.57095	8.840801	0.002946	0.006863
hsa-mir-3127	1.200402	5.660871	34.92476	3.43E-09	2.98E-08
hsa-mir-222	1.205502	1.919227	25.61662	4.16E-07	2.19E-06
hsa-mir-550a-1	1.229276	6.354788	34.67439	3.90E-09	3.32E-08
hsa-mir-3677	1.230369	1.765377	24.84935	6.20E-07	3.05E-06
hsa-mir-3194	1.233403	2.618829	28.11401	1.14E-07	6.99E-07
hsa-mir-940	1.245561	-0.22182	12.65948	0.000374	0.001069
hsa-mir-142	1.252802	1.526729	23.16899	1.48E-06	6.69E-06
hsa-mir-147b	1.26474	11.22242	21.86826	2.92E-06	1.25E-05
hsa-mir-556	1.268672	1.916673	17.66322	2.64E-05	9.53E-05
hsa-mir-1228	1.284855	0.331394	16.9532	3.83E-05	0.000134
hsa-mir-577	1.285879	0.054366	15.80262	7.03E-05	0.000237
hsa-mir-639	1.286575	4.265989	23.98078	9.73E-07	4.63E-06
hsa-mir-1266	1.309998	-0.29025	14.34584	0.000152	0.000477

hsa-mir-3691	1.13193	1.1	0.00064
hsa-mir-3942	1.38189	1.1	0.00063
hsa-mir-4797	1.49245	1.1	0.00047
hsa-mir-559	1.49388	1.1	0.00031
hsa-mir-548o	1.52738	1.1	0.00133
hsa-mir-4766	1.54383	1.1	8.28E-05
hsa-mir-548s	1.56175	1.1	0.00028
hsa-mir-3194	1.57248	1.1	0.00061
hsa-mir-3682	1.93347	1.1	0.00058
hsa-mir-3652	3.23956	1.1	4.18E-07
hsa-mir-5586	3.84742	1.1	7.63E-05
hsa-mir-940	7.84255	1.1	1.41E-09
hsa-mir-550a-2	10.075	1.1	6.07E-08
hsa-mir-3934	12.0803	1.1	1.35E-09
hsa-mir-320b-1	15.2677	1.1	1.73E-10
hsa-mir-4677	21.6989	1.1	2.45E-09
hsa-mir-3677	25.4845	1.1	3.16E-18
hsa-mir-320b-2	27.5123	1.1	2.80E-09
hsa-mir-130b	35.5248	1.1	5.73E-10
hsa-mir-203b	113.421	1.1	8.95E-13
hsa-mir-223*	386.682	1.1	1.53E-05
hsa-mir-1307	1625.73	1.1	3.04E-08
hsa-mir-141	5186.86	1.1	1.10E-17
hsa-mir-3684	5850.09	1.1	3.54E-09
hsa-mir-4645	1.04176	1.2	0.0001
hsa-mir-7854	1.11731	1.2	0.00019
hsa-mir-1229	1.43001	1.2	8.95E-05
hsa-mir-3150b	2.82291	1.2	8.75E-05
hsa-mir-3200	7.16886	1.2	0.00023
hsa-mir-217	12.7464	1.2	2.14E-06
hsa-mir-708	186.445	1.2	2.66E-08
hsa-mir-181b-2	283.501	1.2	1.38E-11

hsa-mir-130b	1.31746	3.625128	30.40361	3.51E-08	2.44E-07
hsa-mir-503	1.334593	4.434231	34.33792	4.63E-09	3.88E-08
hsa-mir-3944	1.339988	2.37236	28.07584	1.17E-07	7.03E-07
hsa-mir-501	1.359005	-0.58497	12.04175	0.00052	0.001451
hsa-mir-1292	1.364548	4.953196	42.87447	5.84E-11	7.33E-10
hsa-mir-509-3	1.372709	-0.40602	14.58476	0.000134	0.000433
hsa-mir-184	1.375675	-0.11822	12.50652	0.000406	0.001153
hsa-mir-141	1.434392	3.704775	15.82452	6.95E-05	0.000236
hsa-mir-182	1.461218	10.07376	27.45664	1.61E-07	9.31E-07
hsa-mir-509-2	1.483654	12.73574	25.78177	3.82E-07	2.03E-06
hsa-mir-935	1.484827	-0.22201	13.70959	0.000213	0.000626
hsa-mir-877	1.490044	1.558525	25.22209	5.11E-07	2.59E-06
hsa-mir-200b*	1.490746	1.090363	30.53817	3.27E-08	2.31E-07
hsa-mir-301b	1.515505	10.36933	28.65058	8.67E-08	5.60E-07
hsa-mir-21*	1.517523	0.565191	24.26225	8.41E-07	4.04E-06
hsa-mir-429	1.524249	17.07657	28.22467	1.08E-07	6.78E-07
hsa-mir-7-3	1.550224	8.159935	35.86425	2.12E-09	1.95E-08
hsa-mir-937	1.551694	0.962984	28.57573	9.01E-08	5.74E-07
hsa-mir-3651	1.566361	0.824561	28.12699	1.14E-07	6.99E-07
hsa-mir-146b	1.56792	0.552446	23.31423	1.38E-06	6.35E-06
hsa-mir-188*	1.571159	8.577653	50.55111	1.16E-12	1.94E-11
hsa-mir-1254	1.584507	2.062049	41.67226	1.08E-10	1.28E-09
hsa-mir-551a	1.594923	-0.15366	21.86838	2.92E-06	1.25E-05
hsa-mir-215^	1.646534	-0.21254	18.34646	1.84E-05	6.94E-05
hsa-mir-200a	1.685801	10.59604	23.36748	1.34E-06	6.24E-06
hsa-mir-192^	1.69807	10.43228	36.13127	1.84E-09	1.74E-08
hsa-mir-105-2	1.719582	14.41716	22.35297	2.27E-06	1.01E-05
hsa-mir-96	1.771443	3.833691	19.13901	1.22E-05	4.74E-05
hsa-mir-18a*	1.771828	3.458154	50.32947	1.30E-12	2.10E-11
hsa-mir-767	1.797128	4.26354	64.10104	1.18E-15	2.67E-14
hsa-mir-3648	1.813376	3.790524	23.19221	1.47E-06	6.69E-06
hsa-mir-194-1	1.822511	1.564576	39.0819	4.06E-10	4.21E-09

hsa-mir-181b-1	443.857	1.2	2.41E-18
hsa-mir-200b*	470.55	1.2	3.38E-19
hsa-mir-93*	6719.84	1.2	3.80E-12
hsa-mir-3174	20498.4	1.2	2.01E-16
hsa-mir-4461	0.89233	1.3	0.00012
hsa-mir-643	2.3604	1.3	2.51E-05
hsa-mir-548v	2.94041	1.3	6.55E-08
hsa-mir-550a-1	5.93127	1.3	1.01E-06
hsa-mir-3127	12.2797	1.3	1.27E-13
hsa-mir-1301	19.0495	1.3	1.56E-14
hsa-mir-4326	33.1328	1.3	3.47E-17
hsa-mir-20a*	33.3916	1.3	3.99E-08
hsa-mir-210	1653.88	1.3	3.90E-14
hsa-mir-500a	1838.62	1.3	1.85E-07
hsa-mir-17*	2145.32	1.3	1.85E-22
hsa-mir-194-1	5960.17	1.3	2.25E-19
hsa-mir-5698	23296.8	1.3	7.99E-11
hsa-mir-618	1.65549	1.4	1.37E-05
hsa-mir-7702	2.06486	1.4	1.99E-05
hsa-mir-4746	4.67635	1.4	5.00E-06
hsa-mir-7-2	9.18916	1.4	4.83E-13
hsa-mir-503	12.891	1.4	2.90E-09
hsa-mir-200a	30.0206	1.4	7.63E-14
hsa-mir-194-2	7398.47	1.4	5.51E-14
hsa-mir-6783	26030.3	1.4	4.32E-12
hsa-mir-1254-1	1.09785	1.5	1.45E-05
hsa-mir-4449	1.54109	1.5	1.96E-06
hsa-mir-3131	2.69368	1.5	4.91E-05
hsa-mir-188*	8.22796	1.5	0.00012
hsa-mir-3187	19.8367	1.5	1.06E-18
hsa-mir-1292	1.3466	1.6	4.04E-05
hsa-mir-1228	2.1785	1.6	4.04E-08
hsa-mir-194-2	1.827376	11.98643	31.70942	1.79E-08	1.35E-07
hsa-mir-3662	1.858527	12.10746	32.49045	1.20E-08	9.33E-08
hsa-mir-183	1.887278	-0.58133	20.02632	7.64E-06	3.11E-05
hsa-mir-592	1.943658	11.47269	47.08264	6.81E-12	9.92E-11
hsa-mir-1911	2.046905	1.778939	55.78928	8.07E-14	1.46E-12
hsa-mir-3176	2.127434	0.854113	20.84261	4.99E-06	2.09E-05
hsa-mir-105-1	2.160355	-0.58701	26.15449	3.15E-07	1.74E-06
hsa-mir-615	2.170972	3.821292	29.73005	4.97E-08	3.37E-07
hsa-mir-3687	2.176016	1.402284	53.00359	3.33E-13	5.79E-12
hsa-mir-509-1	2.324626	0.222873	38.23519	6.27E-10	6.30E-09
hsa-mir-549	2.430465	-0.2549	32.75796	1.04E-08	8.28E-08
hsa-mir-135b*	2.68146	-0.48982	35.57181	2.46E-09	2.22E-08
hsa-mir-552	3.186272	4.944869	171.6598	3.21E-39	2.07E-37
hsa-mir-196a-2	3.718047	4.015132	117.9429	1.78E-27	6.72E-26
hsa-mir-548f-1	3.993711	2.400791	162.9158	2.61E-37	1.47E-35
hsa-mir-196b	4.040168	-0.00399	67.67345	1.93E-16	5.13E-15
hsa-mir-196a-1	4.826419	7.887649	348.1235	1.09E-77	2.45E-75
hsa-mir-1269	5.173649	6.457087	393.0208	1.82E-87	8.23E-85
	5.24766	4.896873	153.8731	2.47E-35	1.24E-33

hsa-mir-3651	3.69614	1.6	9.65E-12
hsa-mir-7-3	5.68695	1.6	3.24E-09
hsa-mir-19a*	12.5505	1.6	2.17E-10
hsa-mir-675	151.942	1.6	1.22E-23
hsa-mir-335*	153.6	1.6	1.26E-06
hsa-mir-584	387.919	1.6	3.39E-21
hsa-mir-182	462.292	1.6	1.36E-14
hsa-mir-4777	43270.4	1.6	1.07E-18
hsa-mir-2115	1.13096	1.7	8.33E-08
hsa-mir-3944	1.17655	1.7	5.05E-06
hsa-mir-3690-1	1.90094	1.7	6.73E-07
hsa-mir-1304	2.36746	1.7	8.46E-08
hsa-mir-501	6.56631	1.7	3.11E-08
hsa-mir-3176	205.564	1.7	2.85E-31
hsa-mir-514a-3	1.2533	1.8	8.32E-07
hsa-mir-6854	1.89751	1.8	3.26E-05
hsa-mir-7705	2.31974	1.8	4.53E-10
hsa-mir-96	4.21949	1.8	6.94E-12
hsa-mir-146b	63.2816	1.8	4.32E-21
hsa-mir-1254-2	2678.81	1.8	1.75E-40
hsa-mir-551a	1.55107	1.9	9.71E-09
hsa-mir-301b	2.66212	1.9	1.59E-07
hsa-mir-877	6.99953	1.9	3.63E-13
hsa-mir-21*	11.0106	1.9	8.82E-18
hsa-mir-3189	974537	1.9	1.64E-76
hsa-mir-4661	1.50429	2	1.19E-07
hsa-mir-508	18.7893	2	6.09E-16
hsa-mir-183	20.5662	2	1.01E-11
hsa-mir-514a-2	17272.3	2	1.01E-24
hsa-mir-514a-1	1.86496	2.1	1.56E-06
hsa-mir-4728	1.90098	2.1	1.11E-06
hsa-mir-18a*	10.1128	2.1	3.08E-10

hsa-mir-592	207.313	2.1	5.96E-26
hsa-mir-509-1	20.7431	2.2	1.81E-17
hsa-mir-615	3.36674	2.3	2.98E-08
hsa-mir-184	13.2415	2.3	6.79E-16
hsa-mir-7974	9.13882	2.4	3.47E-08
hsa-mir-937	2.95907	2.5	2.68E-11
hsa-mir-483	11.4755	2.5	7.84E-20
hsa-mir-4664	29.6098	2.5	2.88E-12
hsa-mir-934	2.76805	2.6	5.11E-14
hsa-mir-509-2	6.86696	2.6	5.89E-07
hsa-mir-509-3	3.46509	2.7	1.71E-10
hsa-mir-3662	3.79058	2.7	4.34E-11
hsa-mir-935	2.85484	2.8	1.07E-13
hsa-mir-549a	24.3065	2.9	1.47E-21
hsa-mir-135b*	2.29748	3	9.07E-14
hsa-mir-196b	214.13	3.3	1.01E-45
hsa-mir-196a-1	1928.06	4.5	3.16E-52
hsa-mir-196a-2	350.082	4.7	1.69E-67
hsa-mir-105-1	392.763	4.7	1.51E-66
hsa-mir-552	117.22	5.7	4.56E-24
hsa-mir-1269a	189.267	5.8	2.60E-40
hsa-mir-105-2	98.0023	5.9	2.86E-23
hsa-mir-767	116.387	5.9	6.40E-26
miRNA	144.592	5.9	9.33E-26

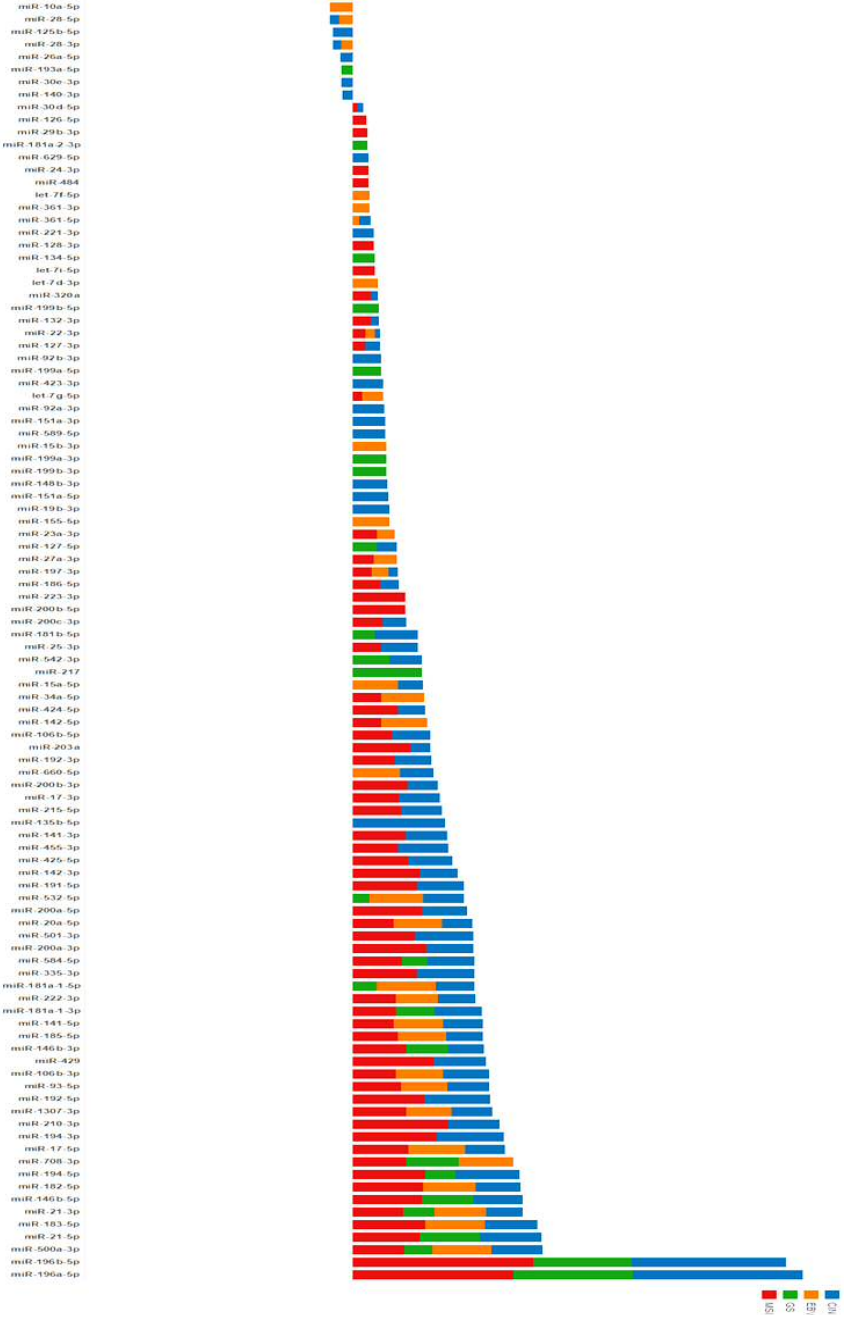
miR-10a-5p
miR-28-5p
miR-125b-5p
miR-28-3p
miR-26a-5p
miR-193a-5p
miR-30e-3p
miR-140-3p
miR-30d-5p
miR-126-5p
miR-29b-3p
miR-181a-2-3p
miR-629-5p
miR-24-3p
miR-484
let-7f-5p
miR-361-3p
miR-361-5p
miR-221-3p
miR-128-3p
miR-134-5p
let-7i-5p
let-7d-3p
miR-320a
miR-199b-5p
miR-132-3p
miR-22-3p
miR-127-3p
miR-92b-3p
miR-199a-5p
miR-423-3p
let-7g-5p
miR-92a-3p
miR-151a-3p
miR-589-5p
miR-15b-3p
miR-199a-3p
miR-199b-3p
miR-148b-3p
miR-151a-5p
miR-19b-3p
miR-155-5p
miR-23a-3p
miR-127-5p
miR-27a-3p
miR-197-3p
miR-186-5p
miR-223-3p
miR-200b-5p
miR-200c-3p
miR-181b-5p
miR-25-3p
miR-542-3p
miR-217
miR-15a-5p
miR-34a-5p
miR-424-5p
miR-142-5p
miR-106b-5p
miR-203a
miR-192-3p
miR-660-5p
miR-200b-3p
miR-17-3p
miR-215-5p
miR-135b-5p
miR-141-3p
miR-455-3p
miR-425-5p
miR-142-3p
miR-191-5p
miR-532-5p
miR-200a-5p
miR-20a-5p
miR-501-3p
miR-200a-3p
miR-584-5p
miR-335-3p
miR-181a-1-5p
miR-222-3p
miR-181a-1-3p
miR-141-5p
miR-185-5p
miR-146b-3p
miR-429
miR-106b-3p
miR-93-5p
miR-192-5p
miR-1307-3p
miR-210-3p
miR-194-3p
miR-17-5p
miR-708-3p
miR-194-5p
miR-182-5p
miR-146b-5p
miR-21-3p
miR-183-5p
miR-21-5p
miR-500a-3p
miR-196b-5p
miR-196a-5p
MS
GS
EB
CM

Appendix 10: Summary of miRNA target prediction tools.

Bold are tools used in the current study. Adopted from common features of microRNA target prediction tools by Peterson *et al.* (Peterson et al. 2014)

Method	Type of Method	Ref	Resource
Stark et. al	Complementary	(Stark et. al., 2003)	http://www.russell.embl.de/miRNAs
miRanda	Complementary	(John et al., 2004)	http://www.microrna.org
miRanda mirSVR	Complementary	(Enright et al., 2003)	http://microrna.sanger.ac.uk
miRWalk	-	-	http://www.umm.uni-heidelberg.de/apps/zmf/mirwalk/index.html
Target Scan	Seed Complementary	(Lewis et al., 2005)	http://www.targetscan.org
DIANA	Thermodynamics	(Kirakidou et al., 2004)	http://diana.cslab.ece.ntua.gr/
PicTar	Thermodynamics	(Krek et al., 2005)	http://pictar.mdc-berlin.de/
RNAHybrid	Thermodynamics & Statistical model	(Rehmsmeier et al., 2004)	http://bibiserv.techfak.uni-bielefeld.de/rnahybrid
miRGen++	Baynesian Inference	(Huang et al., 2007b)	http://www.psi.toronto.edu/genmir
MiTarget	Support Vector Machine	(Kim et al. 2006)	http://cbit.snu.ac.kr/~miTarget
MiRtaget2	Support Vector Machine	(Wang and El Naqa, 2008)	http://mirdb.org
TarBase	Experimentally Validated Targets	(Sethupathy et al., 2006)	http://diana.cslab.ece.ntua.gr/tarbase/
MiRTarbase	Experimentally validated	(Chou CH et al., 2011)	http://miRTarBase.mbc.nctu.edu.tw/

Appendix 11: Overlapping results of targets prediction of miR-140-5p from online tools.

Gene	Description	Validated evidence as miR-140-5p target
SNX16	Play a role in protein transportation from endosome to lysosome (Hanson and Hong 2003)	Not available
GALC	The enzyme responsible for the lysosomal catabolism of galactosyl ceramide (Beier and Gorogh 2005)	Barter *et al*. (2015)
MYO6	Motor protein of the actin cytoskeleton (Aschenbrenner et al. 2004)	Not available
VEGFA	Angiogenesis and tumourigenesis （Goel et al. 2013）	Zhang *et al.* (2015), Sun *et al.* (2016)
FZD6	Negative regulator of the canonical Wnt/beta-catenin signalling cascade, thereby inhibiting the processes that trigger the oncogenic transformation, cell proliferation, and inhibition of apoptosis. (Dann and Mercurio 2001)	Barter *et al*. (2015)
FGF9	An FGF family member possessing broad mitogenic and cell survival activities (Spicer 2009)	Yang *et al.* (2013)
HMGN5	A nucleosomal binding and transcriptional activating protein	Meng *et al.* (2017)
PRDM1	Transcription factor that mediates a transcriptional program in various innate and adaptive immune	Not available
HDAC4	Chromatin remodelling and negative regulation of transcription by RNA polymerase II (Mottet 2009)	Xiao *et al.* (2017), Papaioannou *et al.* (2015), Song *et al.* (2009)
STRADB	A pseudokinase, induce cell cycle arrest but protect against apoptosis.	Not available
OSTM1	Osteoclast differentiation and ion transmembrane transport	Liu *et al.* (2013), Gernapudi *et al.* (2015)
MRPS10	Help in protein synthesis within the mitochondrion	Not available
PHACTR2	Platelet activation, signalling and aggregation	Not available